Biomedical Textiles for Orthopaedic and Surgical Applications

Related titles

Diamond-based materials for biomedical applications
(ISBN 978-0-85709-340-0)

Bone substitute biomaterials
(ISBN 978-0-85709-497-1)

Porous silicon for biomedical applications
(ISBN 978-0-85709-711-8)

Woodhead Publishing Series in Biomaterials: Number 93

Biomedical Textiles for Orthopaedic and Surgical Applications

Fundamentals, Applications and Tissue Engineering

Edited by

Todd Blair

AMSTERDAM • BOSTON • CAMBRIDGE • HEIDELBERG
LONDON • NEW YORK • OXFORD • PARIS • SAN DIEGO
SAN FRANCISCO • SINGAPORE • SYDNEY • TOKYO
Woodhead Publishing is an imprint of Elsevier

Woodhead Publishing is an imprint of Elsevier
80 High Street, Sawston, Cambridge, CB22 3HJ, UK
225 Wyman Street, Waltham, MA 02451, USA
Langford Lane, Kidlington, OX5 1GB, UK

British Library Cataloguing in Publication Data
A catalogue record for this book is available from the British Library.

Library of Congress Control Number: 2014957601

ISBN 978-1-78242-017-0 (print)
ISBN 978-1-78242-026-2 (online)

For information on all Woodhead Publishing publications visit our website at http://store.elsevier.com/

Typeset by SPi Global
www.spi-global.com

Printed and bound in the United Kingdom

List of contributors

Tuija Annala Scaffdex Oy, Tampere, Finland

A.C. Breier Leibniz-Institut für Polymerforschung Dresden e. V., Dresden, Germany

E.R. Durham University of Leeds, Leeds, UK

Ville Ellä BioMediTech, Tampere, Finland, and Tampere University of Technology, Tampere, Finland

R. Guidoin Laval University, Québec, Québec, Canada

C. Holland Department of Materials Science and Engineering, The University of Sheffield, Sheffield, UK

Minna Kellomäki BioMediTech, Tampere, Finland, and Tampere University of Technology, Tampere, Finland

Frank Ko University of British Columbia, Vancouver, BC, Canada

M. Laflamme Laval University, Québec, Québec, Canada

Kaisa Laine BioMediTech, Tampere, Finland, and Tampere University of Technology, Tampere, Finland

J. Lamontagne Laval University, Québec, Québec, Canada

Victor Leung University of British Columbia, Vancouver, BC, Canada

Kevin D. Nelson TissueGen, Inc., Dallas, TX, USA

S.J. Russell University of Leeds, Leeds, UK

G. Tronci University of Leeds, Leeds, UK

D.J. Wood University of Leeds, Leeds, UK

A. Woods Department of Zoology, University of Oxford, Oxford, UK

Heejae Yang University of British Columbia, Vancouver, BC, Canada

X. Yang University of Leeds, Leeds, UK

Woodhead Publishing Series in Biomaterials

1 **Sterilisation of tissues using ionising radiations**
Edited by J. F. Kennedy, G. O. Phillips and P. A. Williams
2 **Surfaces and interfaces for biomaterials**
Edited by P. Vadgama
3 **Molecular interfacial phenomena of polymers and biopolymers**
Edited by C. Chen
4 **Biomaterials, artificial organs and tissue engineering**
Edited by L. Hench and J. Jones
5 **Medical modelling**
R. Bibb
6 **Artificial cells, cell engineering and therapy**
Edited by S. Prakash
7 **Biomedical polymers**
Edited by M. Jenkins
8 **Tissue engineering using ceramics and polymers**
Edited by A. R. Boccaccini and J. Gough
9 **Bioceramics and their clinical applications**
Edited by T. Kokubo
10 **Dental biomaterials**
Edited by R. V. Curtis and T. F. Watson
11 **Joint replacement technology**
Edited by P. A. Revell
12 **Natural-based polymers for biomedical applications**
Edited by R. L. Reiss et al
13 **Degradation rate of bioresorbable materials**
Edited by F. J. Buchanan
14 **Orthopaedic bone cements**
Edited by S. Deb
15 **Shape memory alloys for biomedical applications**
Edited by T. Yoneyama and S.Miyazaki
16 **Cellular response to biomaterials**
Edited by L. Di Silvio
17 **Biomaterials for treating skin loss**
Edited by D. P. Orgill and C. Blanco
18 **Biomaterials and tissue engineering in urology**
Edited by J.Denstedt and A. Atala
19 **Materials science for dentistry**
B. W. Darvell

20 **Bone repair biomaterials**
Edited by J. A. Planell, S. M. Best, D. Lacroix and A. Merolli
21 **Biomedical composites**
Edited by L. Ambrosio
22 **Drug–device combination products**
Edited by A. Lewis
23 **Biomaterials and regenerative medicine in ophthalmology**
Edited by T. V. Chirila
24 **Regenerative medicine and biomaterials for the repair of connective tissues**
Edited by C. Archer and J. Ralphs
25 **Metals for biomedical devices**
Edited by M. Ninomi
26 **Biointegration of medical implant materials: Science and design**
Edited by C. P. Sharma
27 **Biomaterials and devices for the circulatory system**
Edited by T. Gourlay and R. Black
28 **Surface modification of biomaterials: Methods analysis and applications**
Edited by R. Williams
29 **Biomaterials for artificial organs**
Edited by M. Lysaght and T. Webster
30 **Injectable biomaterials: Science and applications**
Edited by B. Vernon
31 **Biomedical hydrogels: Biochemistry, manufacture and medical applications**
Edited by S. Rimmer
32 **Preprosthetic and maxillofacial surgery: Biomaterials, bone grafting and tissue engineering**
Edited by J. Ferri and E. Hunziker
33 **Bioactive materials in medicine: Design and applications**
Edited by X. Zhao, J. M. Courtney and H. Qian
34 **Advanced wound repair therapies**
Edited by D. Farrar
35 **Electrospinning for tissue regeneration**
Edited by L. Bosworth and S. Downes
36 **Bioactive glasses: Materials, properties and applications**
Edited by H. O. Ylänen
37 **Coatings for biomedical applications**
Edited by M. Driver
38 **Progenitor and stem cell technologies and therapies**
Edited by A. Atala
39 **Biomaterials for spinal surgery**
Edited by L. Ambrosio and E. Tanner
40 **Minimized cardiopulmonary bypass techniques and technologies**
Edited by T. Gourlay and S. Gunaydin
41 **Wear of orthopaedic implants and artificial joints**
Edited by S. Affatato
42 **Biomaterials in plastic surgery: Breast implants**
Edited by W. Peters, H. Brandon, K. L. Jerina, C. Wolf and V. L. Young
43 **MEMS for biomedical applications**
Edited by S. Bhansali and A. Vasudev

44 **Durability and reliability of medical polymers**
Edited by M. Jenkins and A. Stamboulis
45 **Biosensors for medical applications**
Edited by S. Higson
46 **Sterilisation of biomaterials and medical devices**
Edited by S. Lerouge and A. Simmons
47 **The hip resurfacing handbook: A practical guide to the use and management of modern hip resurfacings**
Edited by K. De Smet, P. Campbell and C. Van Der Straeten
48 **Developments in tissue engineered and regenerative medicine products**
J. Basu and J. W. Ludlow
49 **Nanomedicine: Technologies and applications**
Edited by T. J. Webster
50 **Biocompatibility and performance of medical devices**
Edited by J-P. Boutrand
51 **Medical robotics: Minimally invasive surgery**
Edited by P. Gomes
52 **Implantable sensor systems for medical applications**
Edited by A. Inmann and D. Hodgins
53 **Non-metallic biomaterials for tooth repair and replacement**
Edited by P. Vallittu
54 **Joining and assembly of medical materials and devices**
Edited by Y. (Norman) Zhou and M. D. Breyen
55 **Diamond-based materials for biomedical applications**
Edited by R.Narayan
56 **Nanomaterials in tissue engineering: Fabrication and applications**
Edited by A. K. Gaharwar, S. Sant, M. J. Hancock and S. A. Hacking
57 **Biomimetic biomaterials: Structure and applications**
Edited by A. J. Ruys
58 **Standardisation in cell and tissue engineering: Methods and protocols**
Edited by V. Salih
59 **Inhaler devices: Fundamentals, design and drug delivery**
Edited by P. Prokopovich
60 **Bio-tribocorrosion in biomaterials and medical implants**
Edited by Y. Yan
61 **Microfluidic devices for biomedical applications**
Edited by X-J. James Li and Y. Zhou
62 **Decontamination in hospitals and healthcare**
Edited by J. T. Walker
63 **Biomedical imaging: Applications and advances**
Edited by P. Morris
64 **Characterization of biomaterials**
Edited by M. Jaffe, W. Hammond, P. Tolias and T. Arinzeh
65 **Biomaterials and medical tribology**
Edited by J. Paolo Davim
66 **Biomaterials for cancer therapeutics: Diagnosis, prevention and therapy**
Edited by K. Park
67 **New functional biomaterials for medicine and healthcare**
E.P. Ivanova, K.Bazaka and R. J. Crawford

68 **Porous silicon for biomedical applications**
Edited by H. A. Santos
69 **A practical approach to spinal trauma**
Edited by H. N. Bajaj and S. Katoch
70 **Rapid prototyping of biomaterials: Principles and applications**
Edited by R.Narayan
71 **Cardiac regeneration and repair Volume 1: Pathology and therapies**
Edited by R-K. Li and R. D. Weisel
72 **Cardiac regeneration and repair Volume 2: Biomaterials and tissue engineering**
Edited by R-K. Li and R. D. Weisel
73 **Semiconducting silicon nanowires for biomedical applications**
Edited by J.L. Coffer
74 **Silk biomaterials for tissue engineering and regenerative medicine**
Edited by S. Kundu
75 **Biomaterials for bone regeneration: Novel techniques and applications**
Edited by P.Dubruel and S. Van Vlierberghe
76 **Biomedical foams for tissue engineering applications**
Edited by P. Netti
77 **Precious metals for biomedical applications**
Edited by N. Baltzer and T. Copponnex
78 **Bone substitute biomaterials**
Edited by K. Mallick
79 **Regulatory affairs for biomaterials and medical devices**
Edited by S. F. Amato and R. Ezzell
80 **Joint replacement technology Second edition**
Edited by P. A. Revell
81 **Computational modelling of biomechanics and biotribology in the musculoskeletal system: Biomaterials and tissues**
Edited by Z. Jin
82 **Biophotonics for medical applications**
Edited by I. Meglinski
83 **Modelling degradation of bioresorbable polymeric medical devices**
Edited by J. Pan
84 **Perspectives in total hip arthroplasty: Advances in biomaterials and their tribological interactions**
S. Affatato
85 **Tissue engineering using ceramics and polymers Second edition**
Edited by A. R. Boccaccini and P. X. Ma
86 **Biomaterials and medical-device associated infections**
Edited by L. Barnes and I. R. Cooper
87 **Surgical techniques in total knee arthroplasty (TKA) and alternative procedures**
Edited by S. Affatato
88 **Lanthanide oxide nanoparticles for molecular imaging and therapeutics**
G. H. Lee
89 **Surface modification of magnesium and its alloys for biomedical applications Volume 1: Biological interactions, mechanical properties and testing**
Edited by T .S. N. Sankara Narayanan, I. S. Park and M. H. Lee

90 **Surface modification of magnesium and its alloys for biomedical applications Volume 2: Modification and coating techniques**
Edited by T .S. N. Sankara Narayanan, I. S. Park and M. H. Lee
91 **Medical modelling: the application of advanced design and rapid prototyping techniques in medicine Second Edition**
Edited by R. Bibb, D. Eggbeer and A. Paterson
92 **Switchable and responsive surfaces for biomedical applications**
Edited by Z.Zhang
93 **Biomedical textiles for orthopaedic and surgical applications: fundamentals, applications and tissue engineering**
Edited by T. Blair
94 **Surface coating and modification of metallic biomaterials**
Edited by C. Wen
95 **Hydroxyapatite (HAP) for biomedical applications**
Edited by M. Mucalo
96 **Implantable neuroprostheses for restoring function**
Edited by K.Kilgore
97 **Shape memory polymers for biomedical applications**
Edited by L.Yahia

Biomechanical testing and the development of silk-based textiles for regenerative medicine and surgery

1

A. Woods[1], *C. Holland*[2]
[1]University of Oxford, Oxford, UK; [2]The University of Sheffield, Sheffield, UK

1.1 Introduction

This chapter is written for the medical researcher, with an aim toward shifting our current paradigm of tissue engineering. Currently, tissue engineering efforts are geared toward assessing a material's cell compatibility and toxicity, which is understandably so given the requirements for medical approval. Hardly a day goes by without the appearance of some new form of scaffolding material that shows biocompatibility, but this biochemical focus often detracts attention from the mechanical properties of the material, a key factor in its ultimate application. This has led to our current situation in which important feedback for implantable devices' material performance often occurs far down a long and expensive production line and is often nonquantitative (i.e., it just doesn't work inside a person; patients have pain or don't even notice the device has failed). Hence, there is a clear need to introduce means to ascertain the mechanical performance of a new biomaterial and its suitability for application prior to animal and patient-level trials.

This chapter introduces the current status of tissue engineering and our new approach and its application to silk-based textiles under the paradigm of compliance matching and material property led engineering technologies (CoMMPLETe). The approach that we propose brings tools developed within biological and physical sciences to bear on medical problems. Introducing basic science approaches to defined medical and surgical problems and integrating them with clinical experience, we aim to redefine the way in which clinicians think about musculoskeletal pathologies.

This approach better informs both prognosis and diagnosis, improving predictive capabilities for clinicians, which is essential when developing management plans with individual patients and for better understanding best practice. The ultimate goal of the approach extends beyond diagnosis and prognosis to allow engineering of novel, or improved, management options. Hence, for the first time and through the application of CoMMPLETe, we will be able to develop quantitative criteria to use in deriving this information and then to provide an evidence base for assessing its benefits.

Biomedical Textiles for Orthopaedic and Surgical Applications. http://dx.doi.org/10.1016/B978-1-78242-017-0.00001-5

1.2 Current landscape

Why is there a need for tissue engineering? Simply put, normal bodies fail. The economic burden of musculoskeletal disease is significant, with present costs (% of GDP) of 4% and 7.4% in the UK and US, respectively. Moreover, it is expected that this burden will escalate over the next 10–20 years due to demography and lifestyle (Chaudhury et al., 2012). Although some excellent interventions, such as joint replacement, are available, they are not suitable for younger patients, nor do they currently match the ethos of regenerative medicine (i.e., temporary relief and complete healing with the body's own materials). This is a particular problem as diseases such as osteoarthritis are being targeted by physicians and surgeons at earlier stages. Furthermore, results for some operations, such as surgical repair of tendon and cartilage, have been largely unsuccessful. In many cases, although anatomical reconstruction is adequate, subsequent healing does not occur, a result often attributed to either biochemical or biomechanical incompatibility.

In keeping with the themes of this book, we have chosen to focus our discussion on textile-based implantable devices for regenerative medicine, specifically tendon; however, our general approach and the techniques used are readily transferrable to the entire gamut of musculoskeletal tissue.

A range of polymeric materials are currently used in textile-based devices, ranging from naturally sourced to the completely synthetic (Table 1.1). Most of the more commonly used nontoxic materials have been shown to be both mechanically stable and elastic, as well as having the desired stability in regard to degradation (Hersel et al., 2003). However, when a material comes into contact with biological systems, initial events are dominated by protein adsorption and cell adhesion. The major problem of most deployed materials is that they show inadequate interaction between material and cells, which can lead to *in vivo* host immune responses, inflammation, infections, aseptic loosening, and implant encapsulation, as well as thrombus formation and mobilisation (Hersel et al., 2003; Thull, 2001). Therefore, by reducing the time required for adequate binding between an implant and surrounding tissue, the clinician may be able to reduce the length of recovery in the hospital, reduce the level of disability before function is restored, decrease morbidity, increase function, and potentially increase the number of patients who could receive the treatment (Healy et al., 1999; Niu et al., 2005). Recent approaches to developing improved biomaterials for tissue engineering applications have focused on the use of biomimetic materials that are able to interact with surrounding tissues by biomolecular recognition (Langer and Tirrell, 2004). This approach could help to reduce nonspecific protein adsorption, so called 'nonfouling properties', as well as enhance adsorption of specific proteins (Hersel et al., 2003). Furthermore, materials are being modified through the addition of immobilised cell recognition motives on their surface to obtain controlled interaction between cells and the material surfaces (LeBaron and Athanasiou, 2000).

Yet, even if the biochemical compatibility of an implantable device is optimised, the issue of biomechanical compatibility remains. Hence, there is a clear need to better understand the basic science behind the material properties of both natural and implanted material in order to develop successful regenerative solutions.

Table 1.1 Overview of the range of polymeric materials currently used in textile-based devices for regenerative medicine

Type	Subtype		Reference
Biological	Human (autograft)	Tendon (e.g., Biceps tendon)	Cho et al. (2009), Rhee et al. (2008)
	Human (allograft)	Dermis (e.g., GraftJacket (Wright medical))	Barber and Aziz-Jacobo (2009), Burkhead et al. (2007), Bond et al. (2007), Snyder and Bond (2007)
		Fascia lata (e.g., AlloPatch (Musculoskeletal Transplant Foundation))	Agrawal (2012), Barber and Aziz-Jacobo (2009)
	Animal (xenograft)	Bovine dermis (e.g., TissueMend (Stryker))	Derwin et al. (2006)
		Porcine dermis (e.g., Zimmer Collagen Repair (Zimmer) – crosslinked)	Badhe et al. (2008), Yao et al. (2005)
		Porcine small intestine submucosa (e.g., CuffPatch (Arthrotek) – multilayered, Restore (DePuy) – multi-layered)	Iannotti et al. (2006), Metcalf et al. (2002), Sclamberg et al. (2004), Zheng et al. (2005)
		Equine pericardium (e.g., OrthADAPT (Synovis/ Pegasus))	DePaolo and Burton (2009)
Biopolymers	Collagen		Dunn et al. (1995), Mafi et al. (2012)
	Silks		Altman et al. (2002), Hennecke et al. (2013), Horan et al. (2009)
Synthetic	Polyethylene (Mersilene Mesh)		Audenaert et al. (2006)
	Polyglycolic acid (PLGA)		Cooper et al. (2007), Lu et al. (2005), Moffat et al. (2009)
	Poly-L-lactide (e.g., X-Repair (Synthasome))		Derwin et al. (2009) McCarron et al. (2010)
	Poly-*N*-acetyl-D-glucosamine (i.e., chitin)		Sato et al. (2000)
	Polycarbonate poly(urethane urea) (e.g., Biomerix RCR Patch (Biomerix), SportMesh (Biomet))		Barber and Aziz-Jacobo (2009), Cole et al. (2007), Encalada-Diaz et al. (2011)
	Dacron		Nada et al. (2010)

Biomedical engineering aims to understand the complex interactions of the body's form and function, and it relies ever more on insights into the structure–property relationships of the huge variety of materials that make up our bodies. Yet, surprisingly little is known about these materials beyond anatomical description. For example, how

do the mechanical properties of a 'diseased' tendon deviate from those of a healthy one? How, if at all, do the mechanical properties change with age? Indeed, why do these differences exist; are they due to material-inherent modifications (such as fatigue, fibrillation, denaturation, plasticising) or are they essentially extraneous (i.e., introduced by interactions with neighbouring tissues or by ingress of foreign cells)? Thus, there is a need to understand the mechanical properties of tendon repair patches and how well these compare to natural tendons; if the patches are too weak, they may fail prematurely, and if they are too strong, they may prevent tissue ingrowth due to stress shielding (Burkhart et al., 1997, 2014; Lewis, 2009), or failure could be the combination of both, as a result of tension mismatch (Baring et al., 2011; Davidson and Rivenburgh, 2000).

It is our firm belief that a more complete understanding of the material properties of human tissues, as well as the materials used to repair them, will form the basis for many important aspects of healthcare. And it is our belief that at present this complete understanding is missing. Yet, mechanobiology tells us that cells are inherently sensitive to physical stress fields, and tissue engineers point to the importance of environmental conditions such as mechanical forces in aspects of cell proliferation and differentiation. Clearly, the iterative process of diagnosis, interpretation, and treatment often lacks fundamental information to allow informed diagnosis leading to evidence-based interpretation followed by the appropriate treatment.

1.3 A new paradigm: Compliance Matching and Material Property Led Engineering Technologies

Clearly there exist disconnects between the basic science and the clinical success of implantable devices that our current approach to tissue engineering is unable to address effectively. To resolve this we propose a new paradigm in regenerative tissue engineering: CoMMPLETe, a framework designed to ensure early design-led feedback and to bridge the gaps in knowledge transfer from lab to factory to clinic (Figure 1.1).

Broadly speaking, CoMMPLETe is split into three parallel routes that seek to (1) property map the tissue and its pathology, (2) assess current solutions, and (3) develop novel materials and devices matched specifically to the repair.

1.3.1 Phase 1: Understanding natural tissue

In order to obtain a comprehensive understanding of a specific tissue engineering challenge, we must first fully characterise the system in question, using consistent and comparable techniques. Combined with expert modelling capabilities, this wealth of data informs quantitatively the structure–property relationships of human tissues, both healthy and diseased, and thus will allow the clinician to effectively link diagnosis and treatment. To truly understand the effects of 'disease' on a tissue, however, we must first understand what constitutes 'normal'. It has been well reported that

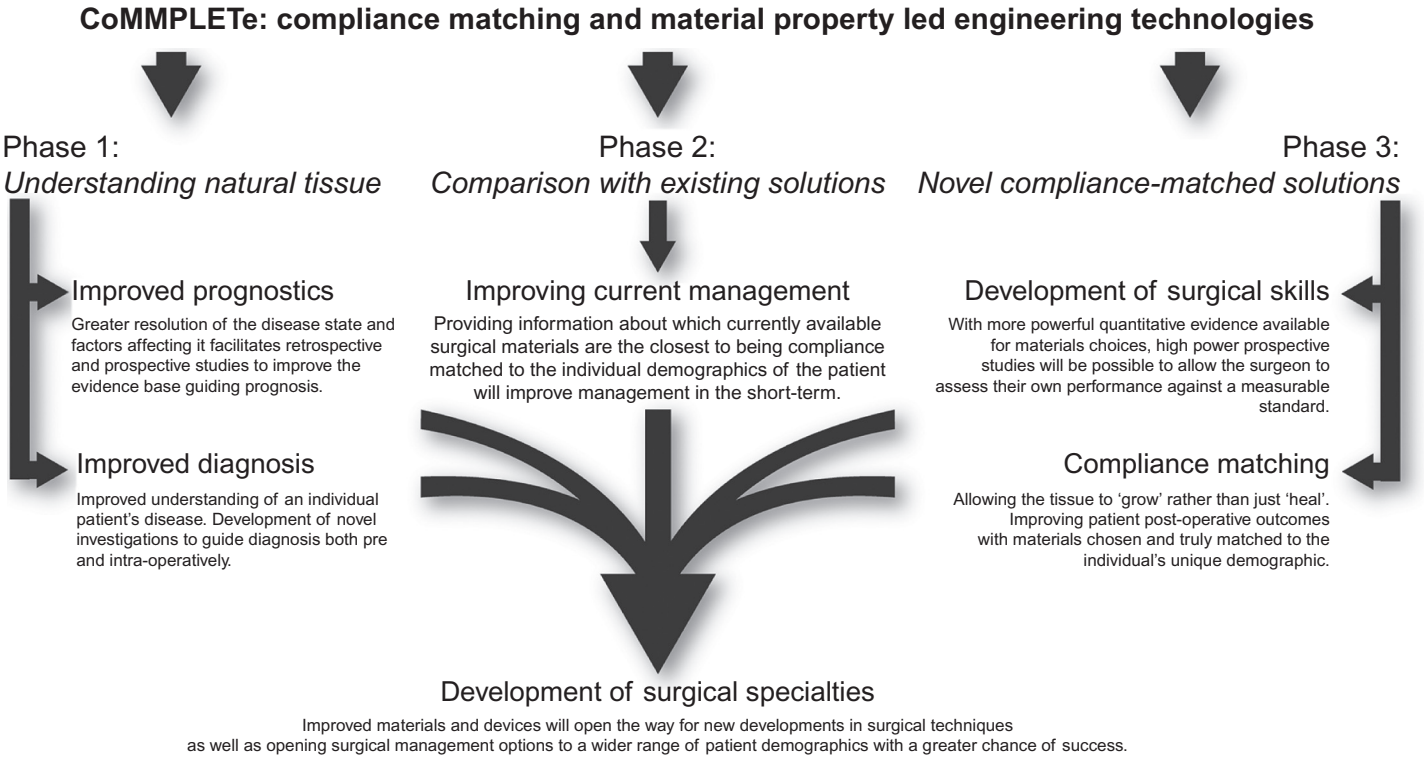

Figure 1.1 Diagrammatic schema of the CoMMPLETe approach for improved evidence-based surgical interventions and implantable device development.

factors such as age, smoking, and alcohol may have an impact on the structural properties of human tissues. As we have already discussed, understanding the true mechanical properties of the individual patient's tissues is essential for guiding repair options. As such, the first aspect of this approach involves generating large numbers of quantitative data to identify what, if any, effect these demographic factors may have on the underlying mechanical properties of tissues. This in itself will provide clinicians with a greater understanding of what risk factors may be underlying in an individual patient's condition, aiding diagnosis.

In addition, the same methodology allows a much more powerful investigation of the mechanical properties within a 'disease' state, such as a tendon tear. Identification of quantitatively distinct subclassifications within a disease state would create a more complete and clear *quantitative* classification of the spectrum of disease. In combination with the improved understanding of 'normal influences', this may identify new risk factors for specific types of injury that might affect disease course in mechanical terms. It would further increase the power of prospective and retrospective studies on prognosis and patient outcomes, controlling for more accurate risk factors. This information could then be used to guide prognostic capabilities, as well as to provide a clear evidence base for making management decisions on a patient-by-patient basis.

Furthermore, it is our vision that, in some cases, this quantifiable spectra of tissue states and disease will allow specific tools to be developed that could be used to translate the databases of information acquired *ex vivo* and apply it directly *in vivo* in the operating theatre. For example, combining mechanical testing data with the results of Fourier transform Infrared (FTIR) analysis will allow identification of specific spectra for certain tissue types, leading to the development of fibre-optic spectroscopy probes to be used in situ to infer a tissue's mechanical properties and guide management choices.

1.3.2 Phase 2: Comparison with current solutions

Using the same analytical tools developed for phase 1, it is also possible to test current management devices and methods. This enables rapid and direct comparison with the complete mechanical profile of 'normal' and 'disease' tissue states. This is a unique and important step that will allow clinicians to make informed decisions on the applicability of currently available medical devices and materials to specific patients. Using CoMMPLETe, they will be able to choose options more closely compliance matched to the underlying tissue properties with the ability to more accurately control for individual patient demographics, using a quantitative and evidence-based approach that is currently not available.

Furthermore, this quantitative data will allow the formation of a standardised database of properties that can be used to design retrospective and prospective studies, using patient data and surgical reporting, which will allow more powerful meta-analysis to provide a strong evidence base for management decisions. In addition, this approach will also help the training of junior surgeons, through development of an evidence-based set of guiding protocols for the assessment and treatment of particular musculoskeletal conditions, rather than having to learn simply through observation.

This then provides the added benefit of allowing surgeons to quantitatively assess the efficacy of their own surgical technique against a more high-powered assessment of potential postoperative outcomes.

1.3.3 Phase 3: Novel compliance-matched solutions

Whilst phase 2 is focussed on the present, phase 3 is geared toward the future. Building upon information gathered from the previous two phases, we envisage that it will be possible to specifically design materials and devices for different tissues and disease states with a level of compliance matching such that the body believes that 'there is no damage'. True compliance matching of a device to the tissue increases the chance of tissue 'growth' rather than 'healing'. This will improve personal outcomes for patients and allow novel therapies to be developed that treat the individual and the particulars of his or her condition as oppose to providing a blanket intervention for all expressions of a disease state.

In summary CoMMPLETe is a new framework that uses the same analytical tools to test the tissues (phase 1) and the current devices (phase 2) and to improve them (phase 3) in order to achieve true compliance matching and subsequent regenerative tissue growth. In the following sections we discuss the tools proposed to undertake this work, as well as some of the initial studies that have used CoMMPLETe to characterise rotator cuff pathology and the advantages of silk in device development.

1.3.4 Importance of sample quantity and quality

Key to the successful implementation of the CoMMPLETe approach is the use of techniques that generate reliable and reproducible quantitative measurements of the material properties of a tissue. As outlined in phase 1, this begins with 'normal' tissue to serve as a guide in both assessment of pathology and as design criteria in device development (phase 3). Although the definition of a 'normal' tissue in the forthcoming age of personalised medicine is somewhat of an oxymoron, the techniques discussed in this section have the potential to investigate tissue on an individual or population scale.

The introduction of basic science approaches to medicine demand that large amounts of data are acquired so as to provide high-powered statistical analysis of results and to truly clarify where differences may be the result of clinical differences. However, as with most basic science clinical studies, access to samples is often difficult and, although it is easier to obtain diseased and damaged tissue, gold standards are ideally based on the response of healthy, living tissue tested under physiological conditions. Cadaverous tissue, freezing, fixation, dehydration, and testing at room temperature, although convenient, are not truly representative of *in vivo* tissue and, as such, must be approached with caution despite often being perceived to be 'gold standards'. Even if sufficient sample numbers are accessible, a secondary consideration is that the nature of the tissue (i.e., a small tendon) or the procedure that seeks to repair it may limit the physical size of the sample. This undoubtedly leads to difficulties in the types of material tests that can be performed.

Overall, there are three general analytical approaches by which information regarding a tissue's biomechanical properties can be obtained: directly via mechanical

testing and indirectly through thermal and optical techniques. Table 1.2 provides an overview of these three approaches arranged in decreasing physical sample size and increasing technical specialisation. This provides the medical researcher with flexibility in the selection of a technique that suits the sample and hypothesis. Once selected, the technique can further inform treatment if tests are conducted using standard sample preparation procedures and set methodologies, allowing for correlation across studies and potentially across techniques, as we shall discuss later.

1.3.5 Mechanical testing

The most directly informative biomechanical tests are those that reveal a material's response to mechanical loading by subjecting a sample to specific combinations of force and deformation (standardised in terms of stress and strain, respectively). These tests can define the performance envelope of a tissue or device as they are able to apply loads akin to those encountered within the body, during manufacture and surgical implantation, and finally to cause complete failure of the material.

The commonplace test for tendons and muscle is a static tensile test wherein a sample is gripped between two fixed points and subjected to a uniaxial extension (although not discussed further, the reverse test, uniaxial compression/indentation is more suited to cartilage and bone, Adams, 2006, Donnelly, 2011). However, the difficulties of clamping fully hydrated 'squishy' samples uniformly and consistently between the grips often leads to stress concentrations at the sample–clamp interface, causing them to fail prematurely and obscure or invalidate measurements (Erhard et al., 2002). This is compounded when dealing with small (<5 mm long) samples and exemplified by the supposed 'gold standard' of tendon tensile testing displaying surprisingly wide variation depending upon the method of gripping (Vincent, 1992).

A recent solution to the difficulties of static tensile testing for tissues is dynamic shear analysis (DSA). Instead of pulling sample apart, this technique (based on rheometry) partially compresses and shears it in an oscillatory fashion between two parallel plates (Chaudhury et al., 2011c). Under DSA a sample's mechanical behaviour can be nondestructively quantified under physiological conditions. Furthermore, DSA may be applied to all biomaterials, including cartilage and bone (Holland et al., 2014; Vincent, 1990). The output of a DSA test is a sample's 'stiffness', or, more specifically, its bulk storage modulus (G') (Subbotin et al., 1996), which provides an indicator of mechanical integrity.

Determining sample modulus is also possible using quantitative ultrasound probes, which operate like DSA to directly deform a sample at a range of fixed frequencies while measuring the dampening response (Appleyard et al., 2003; Huang and Zheng, 2013; Rivaz and Rohling, 2005). Additionally, ultrasound elastography/sonoelastography is a recent and more indirect method that can be used to deduce tissue mechanical properties by investigating tissue deformation in response to loading (Drakonaki et al., 2012; Pedersen et al., 2012). Ultrasound probes have the distinct benefit over other mechanical testing techniques of being able to test *in vivo*, although the sample size is not clearly defined, and therefore, exact modulus values cannot be easily calculated (Appleyard et al., 2003; Drakonaki et al., 2012).

Table 1.2 Initial material characterisation techniques proposed within the CoMMPLETe approach

Type of test	Method	Biopsy required?	Typical sample size	Test under physiological conditions?	Speed of test (includes prep time)	Quantitative	Specialist operator?	Examples
Mechanical	Tension/ compression	Y	>5 mm	Y	30 min	Y	3	Adams (2006), Donnelly (2011)
	DSA	Y	>3 mm	Y	5–10 min	Y	2	Chaudhury et al. (2011c), Holland et al. (2014)
	Ultrasonic	N	Point test or image	Y	Minutes	Partially	2	Appleyard et al. (2003), Drakonaki et al. (2012)
	DMA	Y	Several mm	Y/N	30 min +	Y	4	Guan et al. (2013), von Fraunhofer and Sichina (1992)
Thermal	TGA	Y	~0.5 mm	N	Minutes	Y	2	Heys et al. (2008), Lim and Shamos (1974)
	DSC	Y	~0.5 mm	N	Minutes	Y	2	Chaudhury et al. (2011a), Willett et al. (2008)
Optical	Morphological (e.g., light, X-ray, MRI)	Y	>0.5 mm	N	Hours	Y/operator bias	4	Mertz (2009), Suetens (2009)
	Spectroscopic (e.g., FTIR, Raman)	N	Point test or image	Y	Seconds	Y	5	Harada and Takamatsu (2013), Krafft et al. (2009)

Abbreviations: DSA, dynamic shear analysis; DMA, dynamic mechanical analysis; TGA, thermogravimetric analysis; DSC, differential scanning calorimetry; MRI, magnetic resonance imaging; FTIR, Fourier transform infrared. Grading for specialist operator: 1 = inexperienced user, 5 = highly experienced technician.

The final dynamic test is dynamic mechanical (thermal) analysis DMTA. This technique, also called mechanical spectroscopy, is hugely informative as it is able to provide information regarding the sample modulus under a range of different combinations of stress and strain, including tension, compression, and shear (Jones et al., 2012). However, this approach, like DSA, requires biopsy samples and, if performed under tension, is subject to the same clamping issues as a tensile test. The key difference between DMTA and DSA lies in the application of a temperature ramp (typically from −150 °C to +300 °C) during sample oscillation to highlight changes in modulus, manifested as material-specific glass transitions, melts and ultimately decomposition. Recording changes in modulus as a function of temperature can then be used as a multifaceted material 'fingerprint' from which to compare and deduce sample composition to be correlated to known biomechanical properties or even used to predict biomechanical properties *ab initio* (Guan et al., 2013; Jones et al., 2012; Vollrath and Porter, 2006; von Fraunhofer and Sichina, 1992).

1.3.6 Thermal testing

Biomechanical properties can also be investigated indirectly using thermal analysis. All techniques, by the nature of exposing a tissue to a wide range of temperatures, require biopsy samples. In addition to DMTA, there are two techniques that warrant attention under the CoMMPLETe approach: thermogravimetric analysis (TGA) and differential scanning calorimetry (DSC). The main advantage of both TGA and DSC is that they require practically no sample preparation and can be performed on small, irregular-sized samples on which consistent mechanical tensile testing cannot be performed (e.g., <0.5 mg). TGA is conceptually the simplest of the thermal techniques, measuring sample mass as a function of temperature and providing information regarding sample hydration and thermal degradation (Heys et al., 2008; Lim and Shamos, 1974). DSC measures a sample's endo- or exothermic heat flow compared to a blank reference during heating or cooling, allowing quantification of subtle conformational and chemical changes in structure, stability, and integrity as a function of temperature (Miles et al., 1994, 1995). Once collected, thermal data can then be correlated to mechanical properties (Giannini et al., 2008; Willett et al., 2008).

1.3.7 Optical testing

The technique most familiar to the medical researcher will be optical studies of tissue. Although this chapter does not explain each technique in detail, for the purposes of discussion, we split the optical characterisation of tissue samples into two broad sections, morphological and spectroscopic. Morphological analysis requires the interpretation and quantification of two-dimensional or three-dimensional images (e.g., light, confocal, electron or atomic microscopy and X-ray, MRI and ultrasound; for more information see Suetens, 2009 and Mertz, 2009 and references therein). Although the majority of these techniques require both skilled sample preparation and operators for interpretation, they are generally less restrictive on sample size due to being used either *in vivo*, or, if biopsies are taken, morphological resolution ranges are submillimetre.

Spectroscopic analysis utilises a point source to probe the bulk of the tissue (e.g., IR or RAMAN) to produce a chemical fingerprint (Krafft et al., 2009), and, more recently, the advent of combinatorial techniques such as IR or RAMAN microscopy are becoming widespread in the field (Harada and Takamatsu, 2013). However, regardless of the technique used, optical techniques are indirect measurements of biomechanical properties and thus require reference to a known library from which pathological information can be deduced and cross-referenced (Kainberger et al., 1997; Klauser et al., 2013).

1.4 CoMMPLETe case study: Rotator cuff tendons

Furthering our previous discussions and as an example of an application of the CoMMPLETe approach to rotator cuff tendons, we now outline how it can be applied to tear pathology (phase 1), assessing current mechanical augmentation solutions (phase 2), and the development of novel materials and treatments for this disease (phase 3). Why is this important? Alleviating the individual and financial burden of this disease is of increasing concern as, in the US alone, it effects up to 30% of adults and costs the economy $3 billion annually as a result of impaired work (Mather et al., 2013). Although many studies have shown a significant benefit from the repair of the torn rotator cuff (Galatz et al., 2004; Gazielly et al., 1994; Mellado et al., 2005), these repairs often fail (Gazielly et al., 1994; Mellado et al., 2005) despite a high level of satisfaction following the operation regardless of repair status (a factor most likely due to the pain-relieving benefits, Mellado et al., 2005, Gazielly et al., 1994).

Why do such repairs fail? Studies in the past have looked at the mechanical causes of failure (Davidson and Rivenburgh, 2000; Gerber et al., 1994; Riley et al., 1994), such as the strength of different suturing techniques and the way in which sutures may cut through the tendon when under load (Baring et al., 2011). Increasing age has been associated with higher failure rates postoperatively (Reeves, 1968) (although this is debatable; see Fukuda et al., 1994). Yet, independent of patient age, poor tendon quality has been associated with a threefold increase in the risk of repair failure (Burkhart et al., 2014). Given that tendon quality may affect success and assuming that optimal surgical techniques are being employed, it is possible that surgical repairs may require augmentation either biologically (Kovacevic and Rodeo, 2008) or mechanically, for example with the use of patches (Chaudhury et al., 2012). However, the clinical uptake of rotator cuff repair patches is also burdened by high failure rates and concerns about effectiveness, safety, and cost (Metcalf et al., 2002). Hence, a possible explanation for the high failure rates of repairs using patches is that the material properties of rotator cuff repair patches may not be ideally compliance matched to those of human rotator cuff tendons.

1.4.1 CoMMPLETe phase 1: Understanding rotator cuff properties

Upon attempting to undertake the challenge of developing repair patches for rotator cuff augmentation, Chaudhury et al. (2011c) soon realised that the biomechanics of rotator cuff pathology was not fully understood. This was primarily due to the small

physical size of rotator cuff tendon samples causing difficulty in reliable and reproducible mechanical testing (Chaudhury et al., 2011c). Hence, they addressed these issues through a comprehensive assay of rotator cuff samples obtained intraoperatively from nearly 100 patients, the largest study to date, and applied DSA as a means to circumvent the issues surrounding clamping under tension. Their results demonstrated for the first time that the severity of a tear was correlated to a *quantitative* difference in the mechanical properties of the tissue (Figure 1.2a).

Subsequently, the group went onto further investigate the causes of reduced mechanical properties in torn rotator cuff tendon through a combination of thermal and optical studies (Chaudhury et al., 2011a,b). Through the application of DSC, they found that torn tendons had reduced thermal properties, specifically regarding the onset and peak denaturation temperature (Figure 1.2b). This suggested there was a greater proportion of denatured material in torn tendons, a finding confirmed through morphological analysis via polarised and fluorescence microscopy that indicated increased disruption of collagen structure and integrity (Figure 1.2c). Finally, a detailed spectroscopic study using FTIR revealed a host of chemical and structural features that map with rotator cuff tendon pathology. Together, these findings were

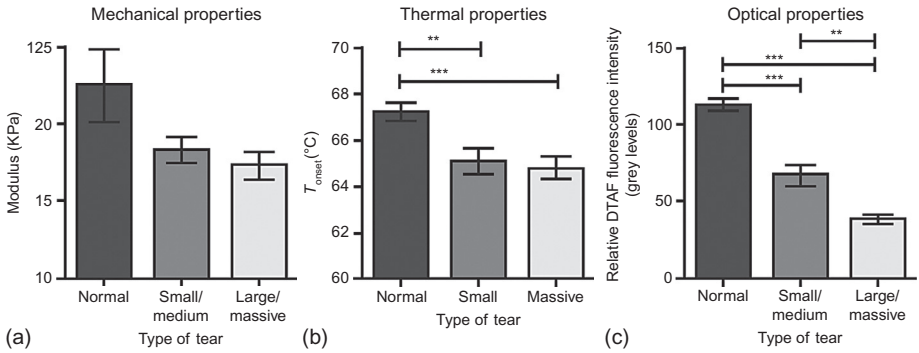

Figure 1.2 Key findings from recent studies investigating the biomechanical basis of human rotator cuff tendon pathology. Note how trends are seen across both direct (mechanical) and indirect (thermal and optical) measurements, thus providing a foundation for the CoMMPLETe approach. (a) Mechanical properties: graph comparing the mean storage moduli of normal and differently sized rotator cuff tendon tears, as obtained through DSA. Torn tendons have a lower modulus, indicating that they are less stiff. Bars represent standard error (SE). (b) Thermal properties: graph showing the T_{onset} of different tendons (T_{onset} is defined as the temperature at which the sample begins to undergo thermal denaturation). Small and massive tears were found to have a significantly lower T_{onset} compared to normal tendons ($p < 0.05$, unpaired t-test). $^{**}p < 0.01$. $^{***}p < 0.001$. Bars represent SE. (c) Optical properties: graph showing the relative collagen-DTAF fluorescence intensities of normal, small, and massive tendon tears, measured as grey scales. Massive tears had a significantly lower fluorescence intensity compared to small tears, and both tear groups were lower than normal tendons. $^{**}p < 0.01$. $^{***}p < 0.001$. Bars represent SE.
(b) and (c) Figure and caption reproduced with permission and copyright © 2011 of the Orthopaedic Research Society, taken from Chaudhury et al. (2011b) (Figures 3 and 6).

explained within the context of the literature as changes in the physiochemical environment of the tendon affecting a structural weakening of the tissue (Riley et al., 1994; Sano et al., 1997) or as a result of weaker fibrous scar tissue formation at the tear (Chen et al., 2008).

Such an approach aligned well with phase 1 of the proposed CoMMPLETe approach and provides a solid example of a bridge between biomechanical function and spectroscopic indicators, thus validating the use of classical histological techniques. Furthermore, the knowledge that torn tendons have weaker mechanical properties goes some way toward explaining the high postoperative failure rates observed.

1.4.2 CoMMPLETe phase 2: Comparison with existing patches

Building upon this newly formed understanding of the biomechanical properties of normal and torn rotator cuff tendons, Chaudhury et al. went on to characterise current mechanical augmentation solutions for rotator cuff repair (Chaudhury et al., 2012). By subjecting a range of commercially available repair patches to mechanical testing (Restore, GraftJacket, Zimmer Collagen Repair, and SportsMesh), they were able to determine which offered the most suitable compliance matching to the natural tissue. The results demonstrated that all repair grafts displayed significant variations in mechanical properties between grafts and normal tissue. Using DSA as an exemplar technique (Figure 1.3), the authors observed that all repair patches had reduced mechanical properties upon comparison to normal rotator cuff tendon. Furthermore, when interpreted within the context of their previous study, the properties of the patches were below that of those of torn tendons as well. This highlights two important points that must be considered when undertaking such comparisons under CoMMPLETe. First, the sample preparation and testing environment should remain the same. In this case samples from all DSA studies were subjected to a formalin treatment prior to testing and tested under exactly the same conditions. However, although

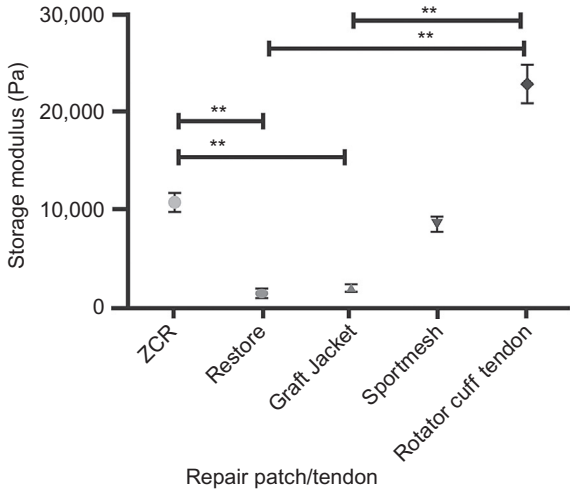

Figure 1.3 Using DSA for a comparison of the shear storage modulus (Pa) of different commercially available rotator cuff repair grafts and human rotator cuff tendons shows that GraftJacket and Restore patches have a significantly lower modulus than rotator cuff tendons. The bars represent the standard error. $^{**}p < 0.05$.
Figure and caption reproduced with permission and copyright © 2011 of the *Journal of Shoulder and Elbow Surgery Board of Trustees*, taken from Chaudhury et al. (2012).

formalin fixation was assumed to induce consistent changes to native tendon samples, such changes may not be replicated in the commercial patches and so caution must be exercised during analysis and interpretation. Second, although the compliance differences between patches was clearly evident, the basis for this variation may be a result of the intrinsic nature of the patches' material properties or extrinsic due to the engineering (i.e., weaving/architecture) of the fibres involved in the device.

1.5 Future trends and applications

1.5.1 CoMMPLETe phase 3: Developing silk-based solutions

Although studies on rotator cuff tendon have yet to arise that exemplify phase 3 of the CoMMPLETe approach, the lessons learnt so far serve as an excellent platform from which to move forward. Through a better understanding of the natural material and how it fails, it is possible to turn human constraints of rotator cuff tendon biomechanics into tomorrow's device design criteria.

One such material currently being explored with great interest for biomedical applications is silk. Since ancient times, silk has been used as a suture material and is still in widespread use today. Silk is a natural, nontoxic biopolymer produced typically by spiders and silkworms (Craig, 1997). Biochemically, its constituent protein, fibroin, demonstrates good biocompatibility, permitting various cells to adhere and proliferate (Altman et al., 2003; Hakimi et al., 2010). Biomechanically, silk is widely regarded as a useful biomaterial as it has good mechanical strength when wet, is resistant to cleavage by enzymes but still biodegradable within the body and highly permeable to both oxygen and drugs (Minoura et al., 1995). Silk is also able to perform under a wide humidity and temperature range (Hakimi et al., 2007). In fact, the biomechanical performance envelope of silk is the greatest of all biopolymers and is also highly tunable (Vollrath et al., 2013), thus lending silk to compliance modification in order to match like-with-like under phase 3 of CoMMPLETe.

The potential of silk-based biomaterials is extended further through the process of reconstitution/regeneration (Rockwood et al., 2011). This is a means by which spun fibres are solubilised by subjecting them to chaotropic agents (Holland et al., 2007), leaving the resulting protein feedstock to be reprocessed to form a variety of new materials with a vast array of properties (Omenetto and Kaplan, 2010). At the most basic level, this solution can be used to coat other materials, such as poly-(carbonate)-urethane membranes (Chiarini et al., 2003) and has been shown to facilitate improved adherence and, consequently, greater proliferation of fibroblasts in comparison to non-coated membranes (Chiarini et al., 2003). Although this reconstitution process entails some collateral damage to the silk proteins, akin to reprocessing naturally sourced collagen, given that the mechanical properties of silk are inherently superior to those of other natural biomaterials, the resulting devices often outstrip those devices fabricated from material derived from the original tissue type being repaired. As a result, more advanced structures such as films have been explored for wound dressings, support media for implantable electrodes, and controlled drug release carriers, alongside foams

and electrospun mats being tested for tissue engineering scaffolds for skin, bones, tendons, ligaments, and so on (see Altman et al., 2003; Hakimi et al., 2007; Omenetto and Kaplan, 2010, and references therein).

Although the usage of high-tech silk-based medical textiles for regenerative medicine is still just beginning (Fare et al., 2013), one area that is attracting increasing attention is the development of biocomposite devices that incorporate both fibres and reprocessed silk feedstocks in order to achieve superior mechanical properties and produce a specific architecture/morphology (i.e., porosity or surface roughness). Examples of this range from nonwoven silk-based devices optimised for neural regeneration (Huang et al., 2012) to vascular implants (Oxford Biomaterials Ltd.) and knee meniscal repair devices (Orthox Ltd.).

1.6 Conclusions

In summary, the proposed CoMMPLETe approach will aid researchers and clinicians in key aspects of musculoskeletal disease diagnostics and treatment. The quality of the information collected from biopsy and tissue samples will directly aid researchers from a large variety of disciplines. For example, bioengineering, which involves efforts to design interventions and model disease processes would greatly benefit from this improved quantitative understanding of the underlying materials both within the prosthesis and the implant site, and pharmacology could capitalise on a better understanding of the chemical environments of 'normal' and 'diseased' tissues in order to improve its understanding of drug efficacies and expand research into a wide range of pharmaceutical delivery mechanism possibilities.

Within the clinical environment, clinicians will gain a more detailed and complete understanding of the factors underlying the make-up of each individual patient's condition. This will lead to a better understanding of the likely progression of a patient's disease, and it will allow evidence-based approaches to personalise the choice of management options. In turn, it will let the clinician better inform patients and reduce the number of inappropriate treatment options undertaken. It will also help clinicians to guide the development of their own practice, through the ability to produce more accurate, quantifiable data that demonstrates what outcome rates 'should' be possible, thus contributing to the advancement of novel treatment options. Improved training of junior surgeons, through development of an evidence-based set of guiding protocols for the assessment and treatment of particular musculoskeletal conditions, will also be possible.

The approach will also have a positive benefit for public health bodies. Generating a knowledge base for musculoskeletal tissues and diseases in combination with quantitative evidence (data)-based approach to their management would provide simple, comparable data and help drive improvements in treatment outcomes across healthcare providers. If adopted, it would also reduce the number of inappropriate or unnecessary treatments being performed. Both outcomes will result in improved care, as well as increased cost-efficiency. The ability to directly compare the efficacy of new versus current treatments against clear quantifiable data further allows advancements to

be far less opaque, and it would allow funding to be more easily obtained because benefits are more easily demonstrated, when compared to the current state of the art.

It is anticipated that the proposed approach also allows for measureable benefits in a reasonably short time frame. As soon as the biomechanical properties of a tissue, musculoskeletal disease, or intervention are quantified, it can immediately improve the global understanding of a condition by informing clinicians about the disease process, its constituent properties, and associated risk factors, as well as guiding management options more effectively than presently available. Moreover, the improved insights and data should quickly lead to more informed development of novel treatments, with the development of new medical devices and materials.

Most important, however, are the benefits that the CoMMPLETe approach will bring to patients. Improving the basic science behind complex structural injuries will make it easier to better inform patients about the details underlying their own individual conditions, thus providing them with a more accurate understanding of the progression/prognosis for their disease. This should strengthen their relationships with their clinicians through better involvement with the personal management of their disease. Furthermore, novel therapies developed through the programme will allow treatments that can be tailored to a greater number of demographic factors affecting an individual. This will improve outcomes, given that only limited intervention options are presently available, and it will support the drive to deliver patient-centred care as best practice.

1.7 Sources of further information and advice

Further information can be found within the references for this article. For those interested in learning more about the wide range of thermomechanical and optical characterisation techniques discussed here, the Wikipedia pages for each technique are a truly excellent place to start before delving into textbooks and primary literature for peer-reviewed references. For those wishing to grasp more of the basic science behind silks, the first piece of literature would be a recent review by Vollrath et al. (2013), followed by Craig's comprehensive review of the evolution of arthropod silks (Craig, 1997). A good overview of the biology of the spider and the silkworm can be found in Foelix (1996) and Fedic et al. (2002). For applications of silkworm silk as a biomedical material, the review by Vepari and Kaplan (2007) is of note, as is Hakimi et al. (2007), which deals with both spider and silkworm silk.

Websites

1. Some research groups working within the field of biomedical silk applications
   - Dr. Chris Holland, Department of Materials Science and Engineering, University of Sheffield, Sheffield, UK. www.naturalmaterialsgroup.com
   - Prof. David Kaplan, Department of Biomedical Engineering, Tufts University. Medford, MA. USA. http://ase.tufts.edu/biomedical/faculty-staff/kaplan.asp

- Prof. Fritz Vollrath, Department of Zoology, University of Oxford, Oxford UK. www.oxfordsilkgroup.com
- Prof. Zhengzhong Shao, Department of Macromolecular Science, Fudan University, Shanghai, China. http://www.polymer.fudan.edu.cn/research/shaozz/English%20version/index.html
- Dr. Thomas Scheibel, Technische Universität Munich, Munich, Germany. http://www.fiberlab.de/

2. Companies producing silk-based biomaterials for regenerative medicine
- AMSilk GmbH www.amsilk.com
- Nexia Biotechnologies, Ltd. http://www.nexiabiotech.com
- Oxford Biomaterials, Ltd. www.oxfordbiomaterials.com
- Orthox, Ltd. www.orthox.co.uk
- Spiber Technologies http://www.spiber.se/
- Spiber, Inc. http://www.spiber.jp/

Acknowledgements

We thank the Engineering and Physical Sciences Research Council and the National Health Service for funding.

References

Adams, M.A., 2006. The mechanical environment of chondrocytes in articular cartilage. Biorheology 43, 537–545.

Agrawal, V., 2012. Healing rates for challenging rotator cuff tears utilizing an acellular human dermal reinforcement graft. Int. J. Shoulder Surg. 6, 36–44.

Altman, G.H., Horan, R.L., Lu, H.H., Moreau, J., Martin, I., Richmond, J.C., Kaplan, D.L., 2002. Silk matrix for tissue engineered anterior cruciate ligaments. Biomaterials 23, 4131–4141.

Altman, G.H., Diaz, F., Jakuba, C., Calabro, T., Horan, R.L., Chen, J.S., Lu, H., Richmond, J., Kaplan, D.L., 2003. Silk-based biomaterials. Biomaterials 24, 401–416.

Appleyard, R.C., Burkhardt, D., Ghosh, P., Read, R., Cake, M., Swain, M.V., Murrell, G.A.C., 2003. Topographical analysis of the structural, biochemical and dynamic biomechanical properties of cartilage in an ovine model of osteoarthritis. Osteoarthritis Cartilage 11, 65–77.

Audenaert, E., Nuffel, J., Schepens, A., Verhelst, M., Verdonk, R., 2006. Reconstruction of massive rotator cuff lesions with a synthetic interposition graft: a prospective study of 41 patients. Knee Surg. Sports Traumatol. Arthrosc. 14, 360–364.

Badhe, S.P., Lawrence, T.M., Smith, F.D., Lunn, P.G., 2008. An assessment of porcine dermal xenograft as an augmentation graft in the treatment of extensive rotator cuff tears. J. Shoulder Elbow Surg. 17, S35–S39.

Barber, F.A., Aziz-Jacobo, J., 2009. Biomechanical testing of commercially available soft-tissue augmentation materials. Arthroscopy 25, 1233–1239.

Baring, T.K., Cashman, P.P., Reilly, P., Emery, R.J., Amis, A.A., 2011. Rotator cuff repair failure in vivo: a radiostereometric measurement study. J. Shoulder Elbow Surg. 20, 1194–1199.

Bond, J., Dopirak, R., Snyder, S., 2007. Arthroscopic total rotator cuff replacement with an acellular human dermal allograft matrix. Int. J. Shoulder Surg. 1, 7–15.

Burkhart, S.S., Johnson, T.C., Wirth, M.A., Athanasiou, K.A., 1997. Cyclic loading of transosseous rotator cuff repairs: tension overload as a possible cause of failure. Arthroscopy 13, 172–176.

Burkhart, S.S., Denard, P.J., Konicek, J., Hanypsiak, B.T., 2014. Biomechanical validation of load-sharing rip-stop fixation for the repair of tissue-deficient rotator cuff tears. Am. J. Sports Med. 42, 457–462.

Burkhead Jr., W.Z., Schiffern, S.C., Krishnan, S.G., 2007. Use of Graft Jacket as an augmentation for massive rotator cuff tears. Semin. Arthroplasty 18, 11–18.

Chaudhury, S., Dicko, C., Burgess, M., Vollrath, F., Carr, A.J., 2011a. Fourier transform infrared spectroscopic analysis of normal and torn rotator-cuff tendons. J. Bone Joint Surg. Br. 93, 370–377.

Chaudhury, S., Holland, C., Porter, D., Tirlapur, U.K., Vollrath, F., Carr, A.J., 2011b. Torn human rotator cuff tendons have reduced collagen thermal properties on differential scanning calorimetry. J. Orthop. Res. 29, 1938–1943.

Chaudhury, S., Holland, C., Vollrath, F., Carr, A.J., 2011c. Comparing normal and torn rotator cuff tendons using dynamic shear analysis. J. Bone Joint Surg. Br. 93-B, 942–948.

Chaudhury, S., Holland, C., Thompson, M.S., Vollrath, F., Carr, A.J., 2012. Tensile and shear mechanical properties of rotator cuff repair patches. J. Shoulder Elbow Surg. 21, 1168–1176.

Chen, C.H., Cao, Y., Wu, Y.F., Bais, A.J., Gao, J.S., Tang, J.B., 2008. Tendon healing in vivo: gene expression and production of multiple growth factors in early tendon healing period. J. Hand Surg. Am. 33, 1834–1842.

Chiarini, A., Petrini, P., Bozzini, S., Dal Pra, I., Armato, U., 2003. Silk fibroin/poly(carbonate)-urethane as a substrate for cell growth: in vitro interactions with human cells. Biomaterials 24, 789–799.

Cho, N.S., Yi, J.W., Rhee, Y.G., 2009. Arthroscopic biceps augmentation for avoiding undue tension in repair of massive rotator cuff tears. Arthroscopy 25, 183–191.

Cole, B., Gomoll, A., Yanke, A., Pylawka, T., Lewis, P., MacGillivray, J., Williams, J., 2007. Biocompatibility of a polymer patch for rotator cuff repair. Knee Surg. Sports Traumatol. Arthrosc. 15, 632–637.

Cooper, J.A., Sahota, J.S., Gorum, W.J., Carter, J., Doty, S.B., Laurencin, C.T., 2007. Biomimetic tissue-engineered anterior cruciate ligament replacement. Proc. Natl. Acad. Sci. 104, 3049–3054.

Craig, C., 1997. Evolution of arthropod silks. Annu. Rev. Entomol. 42, 231–267.

Davidson, P.A., Rivenburgh, D.W., 2000. Rotator cuff repair tension as a determinant of functional outcome. J. Shoulder Elbow Surg. 9, 502–506.

DePaolo, C., Burton, J., 2009. Rotator Cuff Reinforcement. Synovis Orthopedic Woundcare, Inc., Irvine, USA. http://pentabiomedical.com/documenti/orthadapt/tecniche/Rotator%20Cuff%20reinforcement_CTR_Surgical%20Technique.pdf.

Derwin, K.A., Baker, A.R., Spragg, R.K., Leigh, D.R., Iannotti, J.P., 2006. Commercial extracellular matrix scaffolds for rotator cuff tendon repairbiomechanical, biochemical, and cellular properties. J. Bone Joint Surg. 88, 2665–2672.

Derwin, K.A., Codsi, M.J., Milks, R.A., Baker, A.R., McCarron, J.A., Iannotti, J.P., 2009. Rotator cuff repair augmentation in a canine model with use of a woven poly-L-lactide device. J. Bone Joint Surg. 91, 1159–1171.

Donnelly, E., 2011. Methods for assessing bone quality: a review. Clin. Orthop. Relat. Res. 469, 2128–2138.

Drakonaki, E.E., Allen, G.M., Wilson, D.J., 2012. Ultrasound elastography for musculoskeletal applications. Br. J. Radiol. 85, 1435–1445.

Dunn, M.G., Liesch, J.B., Tiku, M.L., Zawadsky, J.P., 1995. Development of fibroblast-seeded ligament analogs for ACL reconstruction. J. Biomed. Mater. Res. 29, 1363–1371.

Encalada-Diaz, I., Cole, B.J., MacGillivray, J.D., Ruiz-Suarez, M., Kercher, J.S., Friel, N.A., Valero-Gonzalez, F., 2011. Rotator cuff repair augmentation using a novel polycarbonate polyurethane patch: preliminary results at 12 months' follow-up. J. Shoulder Elbow Surg. 20, 788–794.

Erhard, L., Zobitz, M.E., Zhao, C.F., Amadio, P.C., An, K.N., 2002. Treatment of partial lacerations in flexor tendons by trimming – a biomechanical in vitro study. J. Bone Joint Surg. Am. 84A, 1006–1012.

Fare, S., Torricelli, P., Giavaresi, G., Bertoldi, S., Alessandrino, A., Villa, T., Fini, M., Tanzi, M. C., Freddi, G., 2013. In vitro study on silk fibroin textile structure for anterior cruciate ligament regeneration. Mater. Sci. Eng. C 33, 3601–3608.

Fedic, R., Zurovec, M., Sehnal, F., 2002. The silk of lepidoptera. J. Insect Biotechnol. Sericology 71, 1–15.

Foelix, R.F., 1996. Biology of Spiders, second ed. Oxford University Press, New York.

Fukuda, H., Hamada, K., Nakajima, T., Tomonaga, A., 1994. Pathology and pathogenesis of the intratendinous tearing of the rotator cuff viewed from en bloc histologic sections. Clin. Orthop. Relat. Res. 304, 60–67.

Galatz, L.M., Ball, C.M., Teefey, S.A., Middleton, W.D., Yamaguchi, K., 2004. The outcome and repair integrity of completely arthroscopically repaired large and massive rotator cuff tears. J. Bone Joint Surg. A 86, 219–224.

Gazielly, D.F., Gleyze, P., Montagnon, C., 1994. Functional and anatomical results after rotator cuff repair. Clin. Orthop. Relat. Res. 304, 43–53.

Gerber, C., Schneeberger, A.G., Beck, M., Schlegel, U., 1994. Mechanical strength of repairs of the rotator cuff. J. Bone Joint Surg. Br. 76, 371–380.

Giannini, S., Buda, R., Caprio, F., Agati, P., Bigi, A., Pasquale, V., Ruggeri, A., 2008. Effects of freezing on the biomechanical and structural properties of human posterior tibial tendons. Int. Orthop. 32, 145–151.

Guan, J., Porter, D., Vollrath, F., 2013. Thermally induced changes in dynamic mechanical properties of native silks. Biomacromolecules 14, 930–937.

Hakimi, O., Knight, D.P., Vollrath, F., Vadgama, P., 2007. Spider and mulberry silkworm silks as compatible biomaterials. Composites, Part B 38, 324–337.

Hakimi, O., Gheysens, T., Vollrath, F., Grahn, M.F., Knight, D.P., Vadgama, P., 2010. Modulation of cell growth on exposure to silkworm and spider silk fibers. J. Biomed. Mater. Res. A 92, 1366–1372.

Harada, Y., Takamatsu, T., 2013. Raman molecular imaging of cells and tissues: towards functional diagnostic imaging without labeling. Curr. Pharm. Biotechnol. 14, 133–140.

Healy, K.E., Rezania, A., Stile, R.A., 1999. Designing biomaterials to direct biological responses. Ann. N. Y. Acad. Sci. 875, 24–35.

Hennecke, K., Redeker, J., Kuhbier, J.W., Strauss, S., Allmeling, C., Kasper, C., Reimers, K., Vogt, P.M., 2013. Bundles of spider silk, braided into sutures, resist basic cyclic tests: potential use for flexor tendon repair. PLoS One 8, e61100.

Hersel, U., Dahmen, C., Kessler, H., 2003. RGD modified polymers: biomaterials for stimulated cell adhesion and beyond. Biomaterials 24, 4385–4415.

Heys, K.R., Friedrich, M.G., Truscott, R.J., 2008. Free and bound water in normal and cataractous human lenses. Invest. Ophthalmol. Vis. Sci. 49, 1991–1997.

Holland, C., Terry, A.E., Porter, D., Vollrath, F., 2007. Natural and unnatural silks. Polymer 48, 3388–3392.

Holland, C., Vollrath, F., Gill, H.S., 2014. Horses and cows might teach us about human knees. Naturwissenschaften 101, 351–354.

Horan, R.L., Toponarski, I., Boepple, H.E., Weitzel, P.P., Richmond, J.C., Altman, G.H., 2009. Design and characterization of a scaffold for anterior cruciate ligament engineering. J. Knee Surg. 22, 82–92.

Huang, Y.P., Zheng, Y.P., 2013. Development of an Arthroscopic Ultrasound Probe for Assessment of Articular Cartilage Degeneration. In: Engineering in Medicine and Biology Society (EMBC), 2013 35th Annual International Conference of the IEEE, 3–7 July 2013, pp. 144–147.

Huang, W., Begum, R., Barber, T., Ibba, V., Tee, N.C., Hussain, M., Arastoo, M., Yang, Q., Robson, L.G., Lesage, S., Gheysens, T., Skaer, N.J., Knight, D.P., Priestley, J.V., 2012. Regenerative potential of silk conduits in repair of peripheral nerve injury in adult rats. Biomaterials 33, 59–71.

Iannotti, J.P., Codsi, M.J., Kwon, Y.W., Derwin, K., Ciccone, J., Brems, J.J., 2006. Porcine small intestine submucosa augmentation of surgical repair of chronic two-tendon rotator cuff tears a randomized controlled trial. J. Bone Joint Surg. 88, 1238–1244.

Jones, D.S., Tian, Y., Abu-Diak, O., Andrews, G.P., 2012. Pharmaceutical applications of dynamic mechanical thermal analysis. Adv. Drug Deliv. Rev. 64, 440–448.

Kainberger, F., Mittermaier, F., Seidl, G., Parth, E., Weinstabl, R., 1997. Imaging of tendons – adaptation, degeneration, rupture. Eur. J. Radiol. 25, 209–222.

Klauser, A.S., Miyamoto, H., Tamegger, M., Faschingbauer, R., Moriggl, B., Klima, G., Feuchtner, G.M., Kastlunger, M., Jaschke, W.R., 2013. Achilles tendon assessed with sonoelastography: histologic agreement. Radiology 267, 837–842.

Kovacevic, D., Rodeo, S.A., 2008. Biological augmentation of rotator cuff tendon repair. Clin. Orthop. Relat. Res. 466, 622–633.

Krafft, C., Steiner, G., Beleites, C., Salzer, R., 2009. Disease recognition by infrared and Raman spectroscopy. J. Biophotonics 2, 13–28.

Langer, R., Tirrell, D.A., 2004. Designing materials for biology and medicine. Nature 428, 487–492.

LeBaron, R.G., Athanasiou, K.A., 2000. Extracellular matrix cell adhesion peptides: functional applications in orthopedic materials. Tissue Eng. 6, 85–103.

Lewis, J.S., 2009. Rotator cuff tendinopathy. Br. J. Sports Med. 43, 236–241.

Lim, J.J., Shamos, M.H., 1974. Evaluation of kinetic parameters of thermal decomposition of native collagen by thermogravimetric analysis. Biopolymers 13, 1791–1807.

Lu, H.H., Cooper Jr., J.A., Manuel, S., Freeman, J.W., Attawia, M.A., Ko, F.K., Laurencin, C.T., 2005. Anterior cruciate ligament regeneration using braided biodegradable scaffolds: in vitro optimization studies. Biomaterials 26, 4805–4816.

Mafi, P., Hindocha, S., Mafi, R., Khan, W.S., 2012. Evaluation of biological protein-based collagen scaffolds in cartilage and musculoskeletal tissue engineering – a systematic review of the literature. Curr. Stem Cell Res. Ther. 7, 302–309.

Mather, I.I.I.R.C., Koenig, L., Acevedo, D., Dall, T.M., Gallo, P., Romeo, A., Tongue, J., Williams, J.G., 2013. The societal and economic value of rotator cuff repair. J. Bone Joint Surg. 95, 1993–2000.

McCarron, J.A., Milks, R.A., Chen, X., Iannotti, J.P., Derwin, K.A., 2010. Improved time-zero biomechanical properties using poly-L-lactic acid graft augmentation in a cadaveric rotator cuff repair model. J. Shoulder Elbow Surg. 19, 688–696.

Mellado, J.M., Calmet, J., Olona, M., Esteve, C., Camins, A., Perez Del Palomar, L., Gine, J., Sauri, A., 2005. Surgically repaired massive rotator cuff tears: MRI of tendon integrity, muscle fatty degeneration, and muscle atrophy correlated with intraoperative and clinical findings. AJR Am. J. Roentgenol. 184, 1456–1463.

Mertz, J., 2009. Introduction to Optical Microscopy. Roberts and Company Publishers, Colarado, USA.

Metcalf, M.H., Savoie Iii, F.H., Kellum, B., 2002. Surgical technique for xenograft (SIS) augmentation of rotator-cuff repairs. Oper. Tech. Orthop. 12, 204–208.

Miles, C.A., Wardale, R.J., Birch, H.L., Bailey, A.J., 1994. Differential scanning calorimetric studies of superficial digital flexor tendon degeneration in the horse. Equine Vet. J. 26, 291–296.

Miles, C.A., Burjanadze, T.V., Bailey, A.J., 1995. The kinetics of the thermal denaturation of collagen in unrestrained rat tail tendon determined by differential scanning calorimetry. J. Mol. Biol. 245, 437–446.

Minoura, N., Aiba, S.I., Higuchi, M., Gotoh, Y., Tsukada, M., Imai, Y., 1995. Attachment and growth of fibroblast cells on silk fibroin. Biochem. Biophys. Res. Commun. 208, 511–516.

Moffat, K.L., Kwei, A.S., Spalazzi, J.P., Doty, S.B., Levine, W.N., Lu, H.H., 2009. Novel nanofiber-based scaffold for rotator cuff repair and augmentation. Tissue Eng. Part A 15, 115–126.

Nada, A.N., Debnath, U.K., Robinson, D.A., Jordan, C., 2010. Treatment of massive rotator-cuff tears with a polyester ligament (Dacron) augmentation: clinical outcome. J. Bone Joint Surg. Br. 92-B, 1397–1402.

Niu, X., Wang, Y., Luo, Y., Xin, J., Yonggang, L., 2005. Arg-Gly-Asp (RGD) modified biomimetic polymeric materials. J. Mater. Sci. Technol. 21, 571–576.

Omenetto, F., Kaplan, D.L., 2010. From silk cocoon to medical miracle. Sci. Am. 303, 76–77.

Pedersen, M., Fredberg, U., Langberg, H., 2012. Sonoelastography as a diagnostic tool in the assessment of musculoskeletal alterations: a systematic review. Ultraschall Med. 33, 441–446.

Reeves, B., 1968. Experiments on the tensile strength of the anterior capsular structures of the shoulder in man. J. Bone Joint Surg. Br. 50-B, 858–865.

Rhee, Y.G., Cho, N.S., Lim, C.T., Yi, J.W., Vishvanathan, T., 2008. Bridging the gap in immobile massive rotator cuff tears: augmentation using the tenotomized biceps. Am. J. Sports Med. 36, 1511–1518.

Riley, G.P., Harrall, R.L., Constant, C.R., Chard, M.D., Cawston, T.E., Hazleman, B.L., 1994. Glycosaminoglycans of human rotator cuff tendons: changes with age and in chronic rotator cuff tendinitis. Ann. Rheum. Dis. 53, 367–376.

Rivaz, H., Rohling, R., 2005. A hand-held probe for vibro-elastography. Med. Image Comput. Comput. Assist. Interv. 8, 613–620.

Rockwood, D.N., Preda, R.C., Yucel, T., Wang, X., Lovett, M.L., Kaplan, D.L., 2011. Materials fabrication from Bombyx mori silk fibroin. Nat. Protoc. 6, 1612–1631.

Sano, H., Ishii, H., Yeadon, A., Backman, D.S., Brunet, J.A., Uhthoff, H.K., 1997. Degeneration at the insertion weakens the tensile strength of the supraspinatus tendon: a comparative mechanical and histologic study of the bone-tendon complex. J. Orthop. Res. 15, 719–726.

Sato, M., Maeda, M., Kurosawa, H., Inoue, Y., Yamauchi, Y., Iwase, H., 2000. Reconstruction of rabbit Achilles tendon with three bioabsorbable materials: histological and biomechanical studies. J. Orthop. Sci. 5, 256–267.

Sclamberg, S.G., Tibone, J.E., Itamura, J.M., Kasraeian, S., 2004. Six-month magnetic resonance imaging follow-up of large and massive rotator cuff repairs reinforced with porcine small intestinal submucosa. J. Shoulder Elbow Surg. 13, 538–541.

Snyder, S.J., Bond, J.L., 2007. Technique for arthroscopic replacement of severely damaged rotator cuff using "GraftJacket" allograft. Oper. Tech. Sports Med. 15, 86–94.
Subbotin, A., Semenov, A., Hadziioannou, G., tenBrinke, G., 1996. Nonlinear rheology of confined polymer melts under oscillatory flow. Macromolecules 29, 1296–1304.
Suetens, P., 2009. Fundamentals of Medical Imaging. Cambridge University Press, New York, USA.
Thull, R., 2001. Surface functionalization of materials to initiate auto-biocompatibilization in vivo. Materialwiss. Werkstofftech. 32, 949–952.
Vepari, C., Kaplan, D.L., 2007. Silk as a biomaterial. Prog. Polym. Sci. 32, 991–1007.
Vincent, J., 1990. Structural Biomaterials, revised ed. Princeton University Press, New Jersey.
Vincent, J., 1992. Biomechanics Materials, A Practical Approach. Oxford University Press, New York.
Vollrath, F., Porter, D., 2006. Spider silk as an archetypal protein elastomer. Soft Matter 2, 377–385.
Vollrath, F., Porter, D., Holland, C., 2013. The science of silks. MRS Bull. 38, 73–80.
von Fraunhofer, J.A., Sichina, W.J., 1992. Characterization of surgical suture materials using dynamic mechanical analysis. Biomaterials 13, 715–720.
Willett, T.L., Labow, R.S., Lee, J.M., 2008. Mechanical overload decreases the thermal stability of collagen in an in vitro tensile overload tendon model. J. Orthop. Res. 26, 1605–1610.
Yao, J.Q., Blanchard, C.R., Bloor, S., 2005. Zimmer Collagen Repair Patch for Rotator Cuff Tendon Repair. Zimmer, Inc, USA. http://goo.gl/is4NJq.
Zheng, M.H., Chen, J., Kirilak, Y., Willers, C., Xu, J., Wood, D., 2005. Porcine small intestine submucosa (SIS) is not an acellular collagenous matrix and contains porcine DNA: possible implications in human implantation. J. Biomed. Mater. Res. B Appl. Biomater. 73B, 61–67.

Embroidery technology for hard-tissue scaffolds

2

A.C. Breier
Leibniz-Institut für Polymerforschung Dresden e. V., Dresden, Germany

2.1 Introduction

2.1.1 Incidence and medical relevance of critical size defects

Bone defects caused by trauma, inflammation, or tumour resection are still challenging in orthopaedic practice. Critical size defects often occur with open fractures due to extensive debridement of blast out, as well as contaminated and avital bone fragments (Hessmann et al., 1998; Mutschler and Haas, 1999). Moreover, a possible long-term consequence of open fractures is posttraumatic osteitis, resulting in a nonunion of the bone (Struijs et al., 2007). Current treatment of osteitis involves the rigorous debridement of infected and trophic-defected hard and soft tissue. This usually means a tumour-like resection into the intact part of the bone, leaving expanded segmental defects comprising the dia- and metaphyseal portions (Schnettler et al., 1997). Another major cause of critical size defects is the surgical therapy of primary and secondary bone tumours, as well as the therapy of soft-tissue sarcoma with bone infiltration. To avoid local relapse, an *en-bloc* compartment resection is required, often generating expanded bone defects (Tsuchiya et al., 2002; Winkelmann, 1999).

Ideal methods for assisting the structural and functional regeneration of these critical size defects in the clinic are lacking. Long-term recovery, repeated operations, and relapse frequently cause restrictions for the patient involving pain and limited movements. Psychic and social consequences, such as redundancy, addiction, and suicide, can follow (Klussmann, 1990).

2.1.2 Applied therapies and their limitations

If the distance between the residual bone fragments gets too large, spontaneous healing of the bone is not possible, and a critical size defect is formed. Medical intervention is needed to reconstruct the mechanical and tissue-specific functions. Filling of the voidage is required to prevent the ingrowth of connective tissue (Calori et al., 2011).

The method of distraction osteogenesis (or callus distraction) was introduced in 1969 by Ilizarov and Ledyaev. In this method, the two bone ends of the defect are clamped by an external adjustable fixation with only a small gap between them. While new bone formation occurs in the gap, developing a callus, osteogenesis is

Biomedical Textiles for Orthopaedic and Surgical Applications. http://dx.doi.org/10.1016/B978-1-78242-017-0.00002-7

induced by gradually moving the two bone segments apart. Large defect distances can be healed by this method (Suger et al., 1995), and it is used in standard clinical practice for the bridging of segmental defects, particularly after debridement of infective tissue and the resection of primary bone tumours (Cattaneo et al., 1992; Green et al., 1992; Tsuchiya et al., 2002). The new bone induced by callus distraction is adequately vascularised and approximates real bone. No established bone graft material can provide this level of performance. As a drawback, a long treatment (40–50 days/cm of the length of the defect), combined with painful distraction operations and risk of infection due to the extended use of external fixations, limits the use of this method (Garcia-Cimbrelo et al., 1992; Lai, 2002). As an alternative, bone grafting is used to fill the defect and to restore the functions of the bone.

For minor volume defects, autografts, such as shavings taken from the iliac crest of the patient, are seen as the gold standard (Calori et al., 2011; Roesgen, 1989). Bone regeneration is induced by osteoblastic activity of the transplanted cells, as well as osteoinductive growth factors deposited in the bone matrix. The limited supply of transplantable bone tissue, the need of several operations, and a painful healing process restrict the use of this method. Furthermore, failure rates up to 50% have been reported (Calori et al., 2011).

Allogenic transplants use bone tissue from a donor of the same species. Allografts have considerably less bioactivity than autografts because the immune response initiated by the transplanted antigens inhibits osteogenesis. Methods for the sterilisation of the transplants have advanced in the last years, but the risk of infection via the transfer of viral and bacterial diseases still exists (Calori et al., 2011; Rubin and Tolkhoff-Rubin, 1988; Salzman et al., 1993). The advantage of using allogenic transplants is the availability of the material. The bone can be used directly or processed into a powder, granules, cancellous or cortical chips, strips, or blocks (Calori et al., 2011). Allografts are also used to produce deminaralised bone matrix by acid extraction, containing a mixture of collagen I, noncollagenous proteins, and growth factors (Calori et al., 2011).

Scaffolding material without cellular components can be obtained from xenografts (tissue donor from a different species) or synthetic bone materials. Xenografts have successfully been used to fill segmental defects in oral and maxillofacial surgery. There is an abundant supply of animal bone material, but due to the high antigenicity of the graft and the risk of infection, these materials are denaturised to remove cellular components while maintaining the mineralised structure (Arca et al., 2011; Calori et al., 2011).

Synthetically produced inorganic bone materials include tricalcium phosphates and hydroxylapatite (HAP) ceramics derived from natural sources, such as corals, and obtained through sintering (Calori et al., 2011). Generally, these materials show high brittleness, preventing their use for mechanical stabilisation of the defect (Wipperman, 1997). Thermally processed HAP ceramics exhibit a slow resorption process, resulting in osteoimplant bonding with critical biomechanical properties. In contrast, the faster resorbing tricalcium phosphate can promote inflammatory reactions (Rueger, 1998). Calciumphosphate cements, a combination of mono- and tricalcium phosphate and calciumcarbonate, show a high compression strength and biological acceptance (Constantz et al., 1995; Wipperman, 1997), but inflammatory reactions in the surrounding soft tissue can occur (Welkerling et al., 2003).

Poly (methyl methacrylate) (PMMA) is used as a polymeric, nonresorbable bone cement, predominantly for the fixation of hip prosthesis, but also for filling segmental defects. Deficient integration into the bone, lack of long-term stability, and debris are some of the limitations. Masquelet et al. (2000) described a two-step method using PMMA cement as an interim template in diaphyseal defects. In the first surgical step, the debridement procedure, the defect is stabilised and filled with a PMMA cement spacer. Soft-tissue reconstruction takes place in a period of 6 weeks, supporting the formation of a periost-like membrane on the surface of the PMMA spacer. The second operation involves the removal of the PMMA cement while preserving the pseudosynovial membrane and filling up the defect with a resorbable bone graft. The preserved membrane has been shown to prevent bone graft resorption and to support bone healing.

2.1.3 Regeneration of critical size defects by tissue engineering

Bone tissue engineering is an expedient option for substituting lost bone segments. The artificial matrix is arranged as a three-dimensional porous structure. Autologous cells are seeded *in vitro* onto the matrix or the matrix is used to recruit cells from the surrounding tissue *in vivo*, inducing the composition of extracellular matrix. The cells get embedded in their own tissue-like matrix, and the material of the artificial structure degrades, leaving a naturally produced bone tissue in place (Rentsch et al., 2012).

To enable the formation of tissue-specific interactions of the cells, a three-dimensional artificial template (scaffold) has to be provided. A suitable material for these scaffolds ensures sufficient biocompatibility and a low inflammatory potential. For maximising the effect of the scaffold on cell proliferation and matrix accumulation, mechanical properties should mimic the biomechanics of bone (Webb et al., 2003, 2006). The structural integrity of the material will decrease during the remodelling process, as the material is degraded. It is therefore important that the degradation period is adjusted to osteoneogenesis. Mechanical properties of the artificial structure should diminish as the supporting function is transferred to the remodelled tissue (Hutmacher, 2000).

The porosity of the scaffold is an important parameter when optimising cell growth and transport of nutrients and metabolic waste. Ideally, the scaffolds have a high porosity containing a high ratio of interconnected pores. Depending on the method of production and the material used, different porosities and pore sizes have been used for bone grafts. Porosities in the range of 60–95% (Oh et al., 2007) are generally suitable, but also lower porosities of 50% have been used (Vivanco et al., 2012). For cell interactions and nutrient supply, an interconnected pore system is essential. Pore size is also a significant parameter. If the pores are too small, cell growth will be inhibited, whereas pores with a diameter that is too large do not provide the required footing for the cells, disturbing cell adhesion. Mean pore sizes in the range of 200–350 μm have been used to allow effective osteoconductive bone regeneration (Vivanco et al., 2012).

Many approaches with different combinations of scaffold materials, associated components, and cell types have been pursued (Betz et al., 2010; Blokhuis and Lindner, 2008; Kruyt et al., 2008). So far, none of the tested strategies is used routinely in clinical settings.

2.1.4 Scaffolds for bone tissue engineering

The first scaffolds used in bone tissue engineering induced pores by chemical or physical processes, such as particulate leaching, gas foaming, and phase separation (Gelinsky et al., 2008; Mikos and Temenoff, 2000). Particulate leaching uses water-soluble porogens such as salt or sugar. A solid body of a polymer/porogen composite is formed by solvent casting or melt moulding. Subsequently, the porogen is removed by leaching the composite in water. Pore size and shape are determined by the size and shape of the porogen grains, whereas the content of interconnective pores is a function of the porogen ratio (Caraballo et al., 1996).

Gas foaming has been used to avoid organic solvents in the manufacturing process. A gas, such as CO_2, is dissolved in the polymer by inducing high pressure and temperature in a solid polymer body, and then the pressure is relieved rapidly. The small pore size is a considerable limitation to this method when creating scaffold materials for tissue engineering (Mikos and Temenoff, 2000).

Sublimation effects can be used to form porous structures by adding porogens such as ammonium bicarbonate or freezing water-bearing preparations and vacuum drying the compound (Gelinsky et al., 2008; Mikos and Temenoff, 2000). Techniques based on the principles of phase separation or emulsification have also been proposed for the manufacturing of porous scaffolds. Pores are generated by using the solubility of the polymer in organic solvents. The polymer is dissolved in an organic solvent and casted to films, tubes, or blocks. It is exposed to a nonsolvent liquid, resulting in an unstable ternary system of polymer, solvent, and nonsolvent. The polymer starts precipitating from the solution, forming a porous, solidified structure (Weigel et al., 2006). Small pore sizes (<100 μm) and the inevitable use of organic solvents are disadvantages of these methods.

Pore size, pore size distribution, and the proportion of interconnected pores formed with all these methods can be controlled by changing parameters such as temperature, mixing ratio, and the applied components and additives. However, the topological distribution and shape of the pores remain random. These manufacturing procedures tend to generate scaffold bodies with core regions that are difficult to penetrate for medium or cell suspensions. Nutrient supply and cell seeding to the inner parts of the scaffold have also been reported to be insufficient (Lode et al., 2008).

To generate complex scaffolds with predefined shapes, computer-aided design (CAD) is used to model scaffolds for rapid prototyping or solid freeform fabrication. Fused deposition modelling and the similar precision extruding deposition generate three-dimensional (3D) porous structures by depositing lines of melted polymer on a motor-driven *x*-*y*-*z*-table (Weigel et al., 2006). Nonfused liquid materials, such as polymer solution (Mikos et al., 1993), or bioactive ceramic materials, such as tricalcium phosphate (Vivanco et al., 2012), can also be deposited in a similar manner. Using CAD, one can produce scaffolds with pore sizes of 200–500 μm with a 100% ratio of interconnected pores. Nozzle size determines the strut diameter and so the thickness of the pore walls. Diameters in the range of 200–500 μm can be performed, resulting in a high material fraction and thus low porosities between 50% and 75% (Vivanco et al., 2012; Weigel et al., 2006).

Other methods for fabricating structures through CAD include 3D-printing, selective laser sintering, and stereolithographic working principles. These methods are

based on the use of a precursor material that is cured chemically, thermally, or radiationally, followed by the removal of the untapped material. In 3D printing, a layer of polymer or ceramic powder is spread over a building platform. A binder solution is deposited precisely by an ink-jet print head, joining single powder particles. This process is repeated on further powder layers spread over the workpart. Living cells have also been deposited using this process (Mironov et al., 2009). The pore size and porosity of scaffolds manufactured with these techniques are mainly related to the resolution of the device used (Weigel et al., 2006).

Different types of materials have been used to build bone scaffolds. Synthetic polymers (e.g., polylactide [PLA], polyglycolide [PGA], polycaprolactone [PCL]) and their copolymers, as well as biopolymers (e.g., collagen, chitosan, or fibrin), are favoured due to their degradability. For ceramics and cements, calcium phosphate compositions such as tricalcium phosphate or HAP, as well as bioactive materials such as bioglass®, have been used (Vivanco et al., 2012; Verrier et al., 2004). The use of hybrid or composite materials with polymeric and ceramic fractions, including mineralised collagen, have also been reported (Gelinsky et al., 2008). Recently, one study tested a metallic composition of degradable magnesium foam (Lalk et al., 2013). Gas formation of the degrading alkaline earth metal *in vivo* was found to be problematic due to the formation of blowholes in the surrounding tissue.

The choice of material is complex because the materials lose their prime structural properties with the high porosities required by the scaffold. For polymeric scaffolds, the Young's moduli are in a range of 20–170 MPa (Hutmacher et al., 2001; Lin et al., 2003), while the plain polymers show values between 1200 and 3500 MPa (Wintermantel and Ha, 2009, p. 262 ff.). The Young's moduli for ceramics are between 80 and 420 GPa (Wintermantel and Ha, 2009, p. 277 ff.), but for the porous structures, the compression moduli are reduced to 1–20 GPa (Vivanco et al., 2012). The composite and hybrid materials have compression loads between those of polymeric and ceramic scaffolds. As a comparison, the Young's modulus of compact bone is quoted at between 12 and 23 GPa, depending on the direction of loading and the bone structure (Wintermantel and Ha, 2009, p. 171).

Compared to all these methods, embroidery technology will represent a further method for generating porous structures, comprising the advantages of the CAD techniques, such as defined fibre deposition, structure design, and the generation of an interconnective pore system, as shown in the following section.

2.2 Manufacturing of porous textile structures using embroidery technology

2.2.1 Principal aspects of embroidery technology

Embroidery technology is based on the same principle as a sewing machine. A sewing machine uses two threads, an upper one and a lower one, running along the top and bottom of the processed fabric (base material) in order to generate lock stitches (Figure 2.1). The stitches are made by winding the upper thread around the lower thread. Coiled on a bobbin, the upper thread is directed through a system of yarn

tension devices to an embroidery needle. Stitches are generated by pushing the needle with the upper thread through the base material (Figure 2.2a) and then lacing the upper thread around the lower thread (Figure 2.2b) via a rotary hook. After the needle retracts and returns to the starting position (Figure 2.2c), the framing system, clamping the base material, moves to a defined *xy*-position (Figure 2.2d).

Industrial embroidery machines have a horizontal block of needles (needle header) arranged in a row, enabling the processing of different yarn colours or materials in one procedure. Additionally, some types are equipped with a tape header that allows the deposition of materials not suitable for processing with the needle header, including tapes, rovings, gimps, or lacings. With a tape header, the upper thread is used for fixing the thread material on the fabric by overcasting it in a zigzag arrangement. The principle of this procedure is shown in Figure 2.3.

The movement of the framing system is controlled by a CNC unit. Special design software, named punch software and actually developed for decorative textile applications, allows manual editing of the embroidery patterns in order to create user-defined patterns with different materials and arrangements. For customary

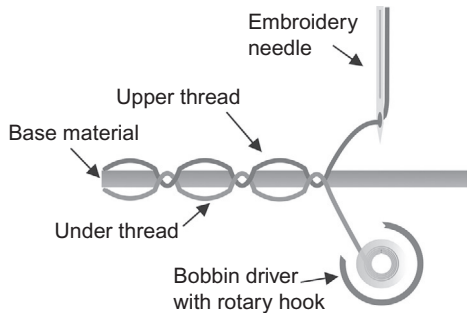

Figure 2.1 An embroidery machine relies on an overlock stitch, as does a sewing machine.

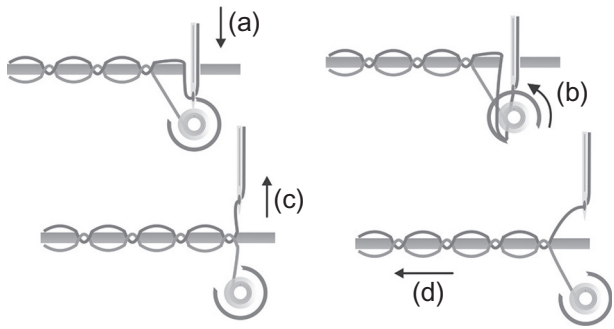

Figure 2.2 Stitches are made in four steps: (a) embroidery needle is pierced into the base material, (b) upper thread is looped around the lower thread by a rotary hook, (c) embroidery needle is retracted to the starting position, and (d) the base material, clamped into a framing system, is moved to a defined *xy*-position.

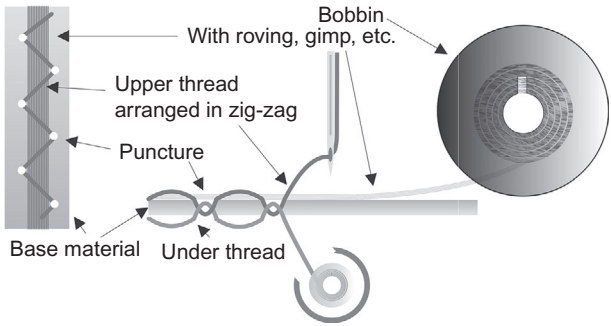

Figure 2.3 Principle of thread deposition with a tape header.

embroidery, the machines offer different types of stitches, such as running stitch, satin stitch, or chain stitch to border or to fill pattern areas. A new and more engineering-based approach for the design of stitch patterns was developed by Spickenheuer et al. (2014) that follows a more straight forward procedure. In a first step the fibre path is created by any common 2D-CAD software and subsequently the setting of stitches is optimised by a novel CAM module, named EDOpath (Spickenheuer et al., 2014).

A modern procedure for producing needle lace fabrics in the textile industry involves using a water-soluble base material. Usually, the process employs a polyvinyl alcohol (PVA) fleece or foil, which can be washed out after the embroidery process at a temperature of 50 °C. As a result, a delicately perforated fabric consisting of interlaced threads is generated.

2.2.2 Thread materials for scaffold fabrication using embroidery technology

Suitable thread materials for producing scaffolds through embroidery cannot be determined based on the thread's mechanical properties. Instead, it has to be tested empirically. High tensile strength is beneficial for a failure-free operation, but due to the thread going through a system of yarn brakes and bobbins, even bending and torsion strengths are relevant. Surface quality is also important for a frictionless passage of the thread through the yarn tension devices. Generally, all kinds of monofilament und multifilament yarns with diameters of about 50–250 µm can be processed using embroidery technology. Twisted multifilament yarns are favoured over side-by-side yarns because single filaments of the latter tend to rove out of the fibre bunch and entangle into the yarn tension devices of the upper and lower thread. This causes snarling of the thread guide and thus frequent thread breakages. Monofilament yarns should exhibit a plain surface, sleeked by a size. Due to the fineness of single filaments in a multifilament yarn, the resulting embroidered structures will show smoother and more tissue-like haptics than structures manufactured from a monofilament yarn.

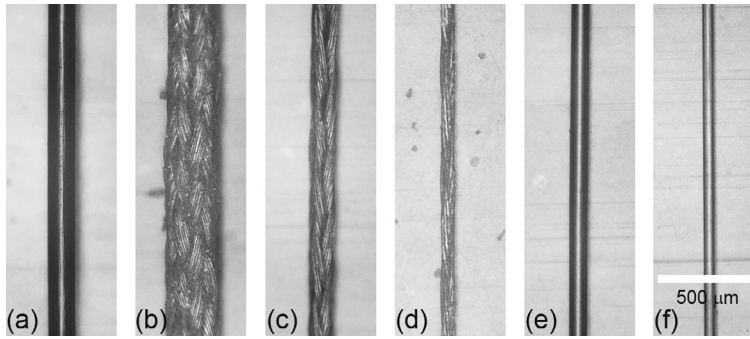

Figure 2.4 Examples of commercialised surgical thread materials: (a) polypropylene monofilament USP 4-0; (b) polyglycolic acid as a plaited multifilament USP 2-0; (c) USP 5-0 and (d) USP 7-0 and poly(lactide-*co*-caprolactone acid) monofilament suture material in (e) USP 6-0 and (f) USP 7-0.

2.2.2.1 Surgical thread materials

Commercialised surgical suture materials are available as continuous fibre threads, and, given that the materials are already accredited and tested in clinical practice, they are ideal candidates for scaffold production. The suture materials have standardised characteristics, including mechanical properties, filament diameter, and yarn count, allowing the manufacturer to maintain quality and processibility. Permanent, nondegradable thread and degradable thread with degradation times from a few weeks to some months are available.

Figure 2.4 shows examples of commercialised sutures that have been applied for the embroidery process. Figure 2.4a shows a polypropylene (PP) monofilament suture in the United States pharmacopoeia (USP) thread size 4-0, featuring a mean thread diameter of 150–199 µm. Monofilament sutures also include degradable poly(lactide-*co*-caprolactone) (PLA-CL) and polydioxanon (PDS) threads, as shown in the thread sizes USP 6-0 (95–149 µm) in Figure 2.4e and 7-0 (70–94 µm) in Figure 2.4f. In addition, multifilament yarn such as polyglycolic acid threads can be processed in USP 2-0 (300–349 µm; Figure 2.4b), 5-0 (100–149 µm; Figure 2.4c), and 7-0 (50–69 µm; Figure 2.4d).

2.2.2.2 Noncommercial fibres

In the field of biomedical textiles, many synthetic and natural biopolymers are manufactured into thread-like structures using a variety of spinning techniques. Some of these techniques, such as melt spinning, allow the gathering of a continuous fibre thread on a bobbin. Thread properties can be modified by temperature regulation and stretch forming, and contoured spinning nozzles allow the fabrication of profiled and hollow fibres (Hinüber et al., 2010). To test novel yarn materials' suitability as a biomaterial, it is important to process the yarn into a shape that is easy to handle. Embroidery technology offers a simple solution for processing the yarns into substrates for cell toxicity and biocompatibility testing. Appropriate applications for the newly developed yarns are found based on their mechanical and biological properties.

2.2.3 Embroidered scaffolds

Embroidery technology is an attractive method for the fabrication of scaffolds. A multitude of adjustable textile parameters, including stitch length, stitch assembly, stitch density, and thread size, enable a direct influence on scaffold features such as porosity, available surface area, and mechanical properties (Table 2.1)

Medical or biocompatible thread materials with diameters of 50–250 µm can be processed directly via a multineedle header. A water-soluble nonwoven fabric (e.g., PVA) is used as a base material. It is washed out after the embroidery process, so that a plane sheet consisting solely of the processed fibre is generated. To achieve a 3D formation, the plane structures can be stacked or furled. Interwoven 3D structures can be obtained by embroidering one ply on another. The mechanical properties of the scaffold can be influenced by changing the stitch mode and assembly (Figure 2.5).

An advantage of scaffolds made by embroidery technology is the high content of interconnecting pores controlled by the manufacturing process. In a manner similar to the one used in fused deposition moulding, the pores are defined by swathing the material (e.g., thread) around the interstices. The interconnecting pore system can be maintained when stacking the plane structures, as long as the plies are not squeezed. Pore size and pore size distribution can be controlled by stitch length and stacking arrangement (Figure 2.6).

Table 2.1 Textile parameters and controllable scaffold features

Textile parameters
Stitch length
Yarn orientation angle
Stitch mode (e.g., running, zigzag, random)
Thread material
Thread size
Controllable scaffold features
Porosity
Pore size
Pore size distribution
Fibre volume content/density
Available surface area
Mechanical properties (e.g., tensile strength, extensibility)

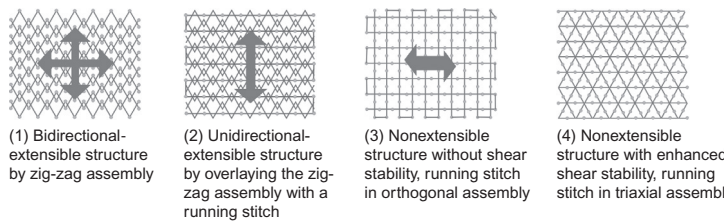

Figure 2.5 Stitch mode and assembly determine the extensibility of the structure.

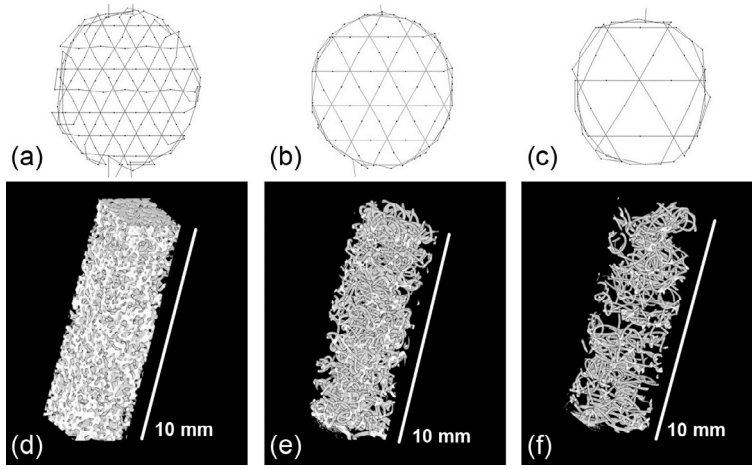

Figure 2.6 Stitch assembly (a–c) and μ-CT analysis* of the three-dimensional structure (d–f) of scaffold stacks. (a, d) Stitch length, 0.9 mm; stacking height, 20 plies; porosity = 35%. (b, e) Stitch length, 1.3 mm; stacking height, 10 plies; porosity = 80%. (c, f) Stitch length, 2.0 mm; stacking height, 10 plies; porosity = 90%. (*) μ-CT measurement by Mathias Schulze, TU Dresden, Institute of Photogrammetry and Remote Sensing.

The influence of the stitch length, stitch density, and stacking height can be demonstrated by μ-CT analysis. Figure 2.6a–c shows the embroidery design of scaffolds, assembled in a triaxial alignment with different stitch lengths. Figure 2.6d–f shows interpretations of μ-CT measurements* of stacks piled from plane structures, embroidered with a surgical P(LA-CL) monofilament suture material (USP 6-0).

The structure shown in Figure 2.6d is formed by stacking 20 plies (Figure 2.6e and f), each with 10 plies. The total height of the scaffolds is 10 mm. Shorter stitch lengths and higher ply portions lead to increased stacking density, creating a structure with decreased pore size and a lower proportion of interconnecting pores. If the stitch length is too long, as shown in Figure 2.6f, the pores become too big, and the scaffold lacks integrity and footing for the cells. The optimum ratio between stitch length and stacking density should be determined with the intended application in mind. For application in bone regeneration, the scaffold variation (Figure 2.6e) featuring a mean stitch density of 2.1 stitches/mm^2 and a ply portion of 1 slice/mm, thus shows the required pore sizes and porosity.

The porosity of the structures can be calculated by determining the material fraction and total volume of the scaffold obtained from the binary data sheet derived from the μ-CT analysis. Pore size and pore size distribution can be ascertained by a sphere model. The voids of the structure are filled with virtual spheres with diameters equivalent to the voids. The length and distribution of the diameters give information about the pore size and pore size distribution. Figure 2.7 shows images of scaffold stacks rendered from μ-CT data. Different stitch densities were applied. Figure 2.7a and c shows a stack piled from scaffolds embroidered from a USP 6-0 P(LA-CL) with

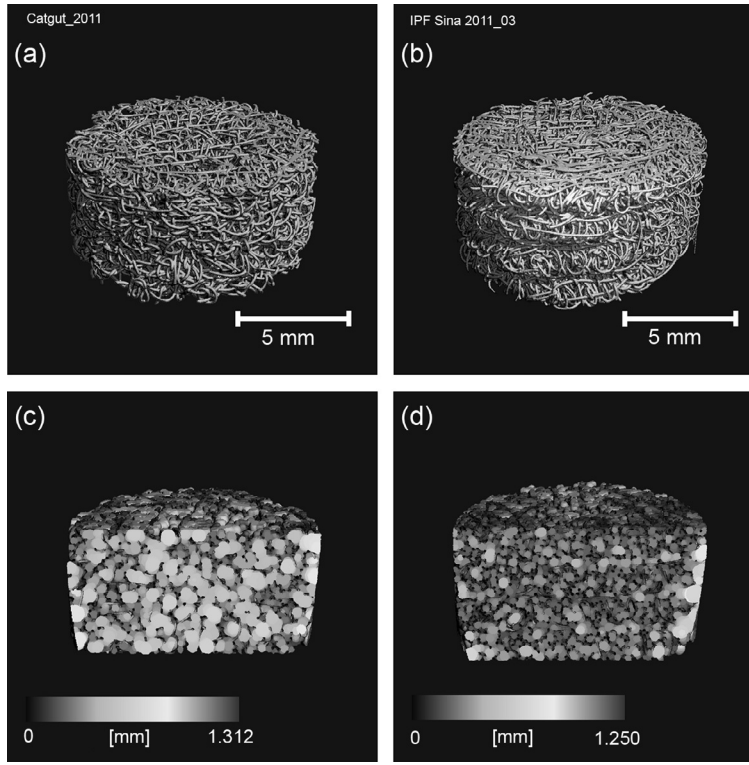

Figure 2.7 µ-CT analysis* of scaffold stacks (a, b) as a rendering of the thread structure and (c, d) filled up with spheres representing the pore sizes. Panels (a, c) represent a scaffold stack of seven plies embroidered with 1.9 stitches/mm^2 porosity 85%; (b, d) show a stack of four plies embroidered with 5.8 stitches/mm^2, porosity 76%. (*) µ-CT analysis performed by Dr. Ricardo Bernhardt, TU-Dresden, Max-Bergmann-Centre for biomaterials.

1.9 stitches/mm^2. Seven plies are necessary to attain the same height as the scaffold stack (2, 4) of four plies embroidered with a higher stitch density of 5.9 stitches/mm^2. Figure 2.7a and b shows an optical visualisation of the thread structure, and Figure 2.7c and d describes the virtual sphere model.

Figure 2.8 shows the pore size distributions of the two scaffold stacks, calculated from the sphere model. Smaller pore sizes and a denser distribution can be observed for the stack piled from scaffolds with a higher stitch density. The porosity is 76%, compared to 85% for the lower stitch density. Both scaffold stacks show porosities and pore sizes suitable for the tissue engineering of bone.

For load-bearing applications, the mechanical properties of the scaffold stacks are a decisive factor. The flat bone of the skull has been shown to have a compression strength of 73.8 MPa and an E-modulus of pressure of 2.4 GPa to forces vertically affecting the layered structure of the bone (McElhaney et al., 1970). Figure 2.9 demonstrates the mechanical behaviour of the two scaffold stacks illustrated in

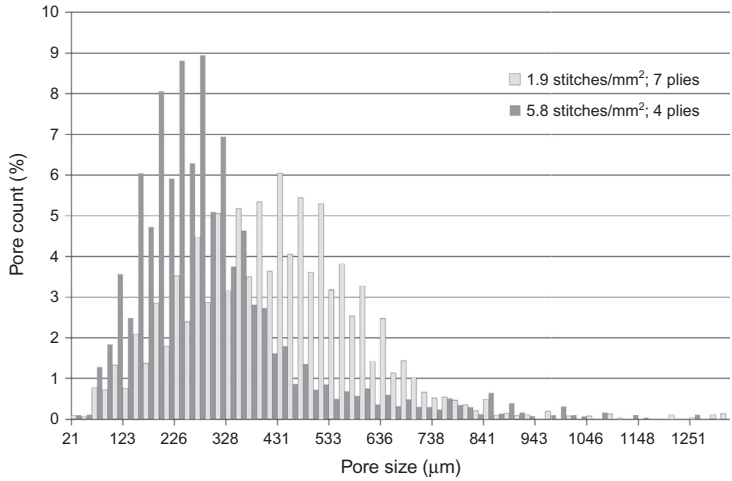

Figure 2.8 Pore size distribution of scaffold stacks embroidered with 1.9 stitches/mm^2 (light gray) and 5.8 stitches/mm^2 (dark gray).

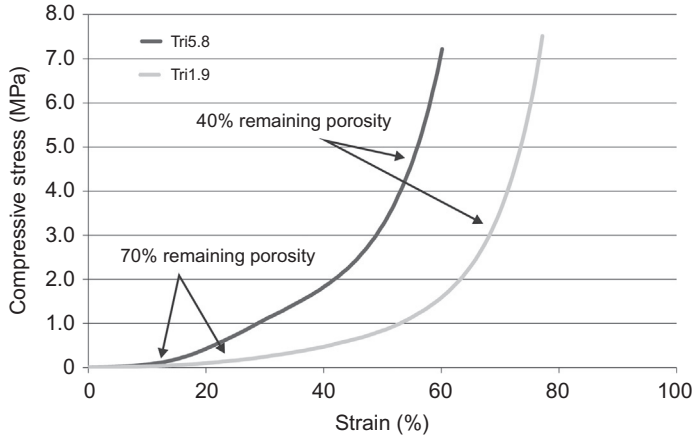

Figure 2.9 Mechanical behaviour of scaffold stacks under compression load: a stack of four plies and a stitch density of 5.8 stitches/mm^2 (Tri5.8) and a stack of seven plies and a stitch density of 1.9 stitches/mm^2 (Tri1.9).

Figure 2.7 under compression load. A deformation of up to 10% can be performed without any resistance of the material, and a period of low stiffness follows, featuring a slow ascent of the compressive strength. The onset of the material resistance occurs in the range of 70% remaining porosity calculated from the ratio of the volume fraction of the processed thread to the remaining volume of the scaffold after compression. Another flection point can be observed at a remaining porosity of about 40%. Here both structures pass into a linear ascent, showing a stiffness of

0.3–0.5 MPa. The transition of these sections turns out to be more distinct for the scaffold stack with higher stitch density (Tri5.8).

The featured embroidered structures have insufficient mechanical properties for load-bearing applications in the regeneration of bone tissue. The concept of using embroidered scaffolds for tissue engineering of load bearing bone has to be developed and adapted due to the lack of stability of the scaffolds.

2.3 Application of embroidered scaffolds for hard-tissue engineering

2.3.1 Tissue engineering strategies for hard-tissue implants based on embroidered scaffolds

To generate tissue and site-specific implants, different strategies can be pursued to meet the requirements of the implant. The location and occurrence of the defect define these requirements. The main benefit of the embroidered scaffolds is their plane quasi-2D appearance. Good permeation is probable through the plane of the textile structure, which is important for any treatment, such as surface modification or cell seeding. For *in vitro* procedures of tissue engineering, it is feasible to apply plane structures as round slices (Figure 2.10a) or wide tapes (Figure 2.10b).

Structural characteristics can be manipulated by the embroidery pattern. As already discussed, pore size can be adjusted by stitch alignment and density. Figure 2.11 shows examples of a dense alignment using a multifilament yarn (Figure 2.11a) and an open-pored structure created from a monofilament PLA-CL thread (Figure 2.11c). Structural conditions can be imitated by the embroidery pattern. Arranging the stitches in a radial manner (Figure 2.11b) results in a loose structure mimicking the natural structure of cortical and cancellous bone.

Bone is a supporting structure, and therefore, mechanical load is a critical factor for the conceptual design of a bone implant. As already shown, textile scaffolds are not suitable for this function. In case an implant is needed in a load-bearing region, such as

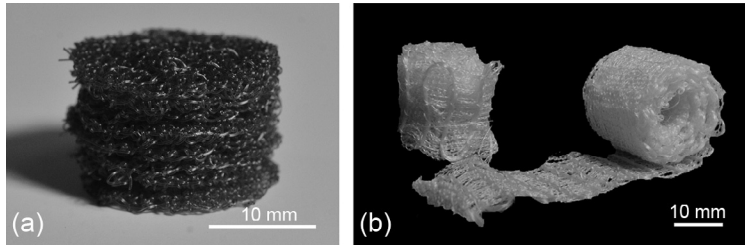

Figure 2.10 Three-dimensional scaffolds by (a) stacking round slices or (b) furling wide tapes of embroidered structures.

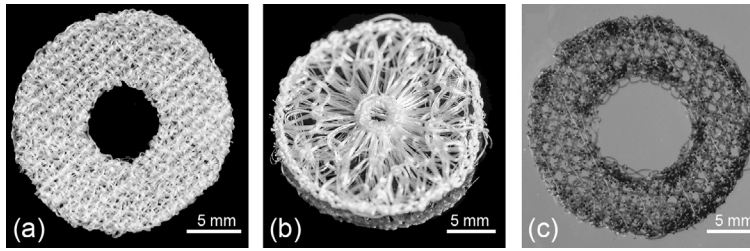

Figure 2.11 Embroidery patterns for round slices: (a) in a dense orthogonal alignment, (b) in a loose radial alignment mimicking the natural structure of cortical and cancellous bone, and (c) in an open-pored structure. Panels (a) and (b) are processed with a PHB multifilament yarn, and (c) is processed with a monofilament surgical thread made of PLA-CL.

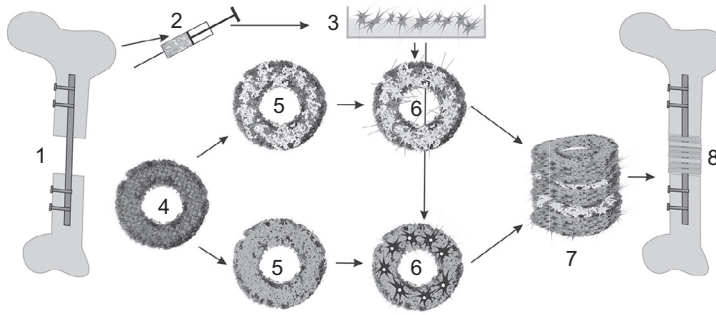

(1) Bone defect stabilised with an intramedullary rod; (2) extraction of stem cells; (3) culture of stem cells; (4) scaffold; (5) coating with components of the extracellular matrix; (6) cell seeding, e.g., osteoblasts, endothelial cells, proliferation, and differentiation; (7) tissue engineering of vascularised bone; (8) implantable bone tissue

Figure 2.12 A concept for long bone tissue engineering.

the long bones of the femur or tibia, this function can be absorbed by an intramedullary rod. The scaffolds then function as a template for guiding cells into the correct alignment. A model for the tissue engineering of long bones can be formulated as demonstrated in Figure 2.12.

First, the bone defect is stabilised with an intramedullary rod and immobilised for 3 months following the two-step method described by Masquelet and Viateau (Masquelet et al., 2000; Viateau et al., 2007). Autologous mesenchymal stem cells (MSCs), extracted from the iliac crest of the patient, are cultured *in vitro*. The embroidered scaffolds are coated with components of the extracellular matrix, and the modified scaffolds can be seeded with stem cells differentiated to osteoblasts or endothelial cells. Osteogenesis and vascularisation can be induced *in vitro*. Slices with different functions can then be piled as a stack and applied as an implant of vascularised bone tissue.

2.3.2 Coatings for improved osteoconductivity and osteoinductivity

The surface properties of the scaffold material play a decisive role in the formation of new bone tissue. Hydrophilicity and surface energy qualitatively determine the protein deposition in the first minutes after implantation (Mayer et al., 2008). Depending on the deposited proteins, specific cell types get recruited and adhere on the surface. When cells are coupled to the surface, proliferation and differentiation start, followed by protein synthesis and the production of the extracellular matrix. To control the protein deposition process, the surface can be modified. Different successfully established modification procedures are available, including plasma treatment (Curran et al., 2005; Keselowsky et al., 2004) and wet chemical modification (Rentsch et al., 2009; Wollenweber et al., 2006).

Components of the extracellular matrix can be added to the scaffold to create a suitable environment for the cells. Collagen I, a main component of bone tissue, can be used to coat the thread material by fibrillogenesis (Douglas et al., 2007). Hydrophilisation with NaOH has been found to successfully induce an increase in collagen deposition on the thread material (Rentsch et al., 2009). Adding chondroitin sulphate to the collagen solution can also lead to an immobilisation of the glycosaminoglycan in the collagen fibrils during fibrillogenesis (Douglas et al., 2007). The positive effect of the immobilised glycosaminoglycan is demonstrated by the cell reaction. An enhanced formation of focal adhesion (Douglas et al., 2007) and an increase of calcium deposition is observed for MCSs seeded on chondroitin sulphate bearing coatings (Rentsch et al., 2009).

2.3.3 Cell selection and seeding procedures

Bone tissue is interspersed with osteocytes embedded in the extracellular matrix. The cells have long cytoplasmic/dendritic processes that are connected to neighbouring cells via gap junctions. Nutrients and oxygen are provided by the bone's vasculature. Bone is constantly being rebuilt to optimise stability, depending on the loads experienced by the bone. Osteoclasts are activated to decompose bone tissue and osteoblasts form bone tissue. Osteoblasts are required for *in vitro* tissue engineering of bone-like tissue. The source and method of isolation, as well as the amplification of suitable cells, are significant.

A patient's own osteoblasts can be isolated from the periost. This requires additional surgery (Begley et al., 1993; Behrens et al., 2000) and often results in a low yield of suitable cells that do not expand well (Heath, 2000). As an alternative, autologous bone marrow can be transplanted to stimulate osteoneogenesis. (Connoly et al., 1989). Established practice involves the use of adult MSCs derived from bone marrow aspirated by iliac crest puncture. The multipotent cells are isolated with a density gradient and expanded *in vitro* (Petite et al., 2000; Quarto et al., 2001). Novel studies have suggested that adipose tissue could be used as a source of MSCs to minimise patient morbidity during cell harvesting (Pendleton et al., 2013).

The differentiation of MSCs to the osteogenic lineage can be induced *in vitro* by supplementing the culture medium with dexamethasone or ß-glycerophosphate.

The osteoblastic phenotype is identified using bone specific markers, such as alkaline phosphatase (ALP) and osteocalcin (Joyner et al., 1997), or by the synthesis and mineralisation of collagen I (Luria et al., 1987).

After a required cell count has been achieved, the cells are seeded onto the scaffold. To achieve a homogeneous cell distribution on the scaffold, the whole 3D structure must be permeable to the seeding solution. Nutrient supply in the scaffold core both *in vitro* and *in vivo* must also be sufficient to maintain viability.

Mechanical stimulation influences cell behaviour (Hess et al., 2010), so it is vital to choose the right culture system. Vunjak-Novakovic et al. showed that the culture conditions of the bioreactor critically influence the composition and histomorpholgy of engineered cartilage (Vunjak-Novakovic et al., 1999). They found that static culturing conditions, which generated only diffusive nutrient transport, led to small constructs with glycosaminoglycane accumulation only on the periphery of the scaffold. However, keeping a turbulent medium flow induced the production of fibrous capsules on the surface of the constructs. A laminar medium flow, generated by rotating vessels, achieved the best results, approximating bovine cartilage. This method was transferred to the culture of human mesenchymal stem cells and their osteogenic differentiation by Wollenweber et al. (2006) and was used for seeding textile embroidered scaffolds for bone tissue engineering by Rentsch et al. (2009).

2.3.4 Tissue engineering of hard tissue

Embroidery technology has been used to create textile scaffolds for hard-tissue implants, and their applicability has been examined in several animal studies. Rentsch et al. applied textile structures embroidered from surgical P(LA-CL) thread with a degradation rate of 180–210 days. The pore size was tailored to be 150–300 μm with a stitch density of 2.1 stitches/mm^2 and a ply portion of 1 slice/mm in order to promote bone tissue growth according to the sample shown in Figure 2.6e. The surface of the thread was hydrophilised by wet chemical modification and coated with collagen I by fibrillogenesis to enhance cell adhesion. Chondroitinsulphate, immobilised in the collagen matrix, facilitated osteogenic differentiation, as indicated by enhanced calcium deposition and mineralisation of the newly modelled bone tissue. Seeding the artificial matrix with MSCs then generated an implant with a high osteogenic potential *in vitro* (Rentsch et al., 2009).

In vivo results for the described scaffolds (implanted subcutaneously in nude rats) showed that the osteogenic potential could be maintained in the environment of the scaffolds coating. The expression of bone markers, such as osteopontin, osteonectin, collagen I, bone sialprotein, and osteocalcin, was verified by histological staining. Excellent vascularisation maintained the viability of the seeded human stem cells for over 6 weeks. However, ectopic bone formation could not be detected, neither with X-rays nor with computer tomography (Rentsch et al., 2009).

Orthotopic implantation of these scaffolds into a critical size defect induced into a nude rat femur showed good bone formation and sufficient vascularisation. These studies demonstrated the osteoinductivity of the implant model. Obviously, the porous structure provides an appropriate network for facilitating tissue ingrowth. Seeding the

scaffolds with human MSCs prior to implantation induced a higher matrix accumulation and vascularisation but an enhancement of bone formation was not observed (Rentsch et al., 2010).

These results were confirmed using a large animal defect study in sheep (Rentsch et al., 2014). A 3-cm defect in the mid-diaphyseal shaft was filled with a scaffold stack of 30 plies, coated with collagen/CS. Cells were not seeded, based on the results obtained from previous studies that showed no enhancement for bone formation. Surgery was performed according to the two-step method described by Masquelet and Viateau (Masquelet et al., 2000; Viateau et al., 2007), and the sheep that received the operation were studied for either 3 or 12 months. Quantification of new bone formation yielded a mean value of 63% for the 3-month group and 172% for the 12-month group, as compared to growth in the contralateral tibiae of the testing sheep. Biomechanical testing showed up to 63% load-to-failure compared to the nonmodified tibia. Histology revealed that the scaffold was completely intermingeled with vascularised connective tissue. Bony islets were observed around the PCL fibres at the inner part of the scaffold after 3 months, and intermediate states of bone formation were seen within the scaffold after 12 months (Rentsch et al., 2014).

2.4 Conclusion

Embroidered scaffolds have a versatile design. The material used and the scaffold characteristics, such as geometry, porosity, and pore size, can be manipulated to create a tailored scaffold to be used as an implant. At first sight, embroidery technology does not seem to be suitable for hard-tissue engineering due to the low mechanical performance of embroidery-engineered hard tissues. However, by implementing an appropriate model for transferring the mechanical load (e.g., to an intramedullary rod), the textile structures show advantages compared to other scaffolds.

Surgical P(LA-CL), chosen as an accredited thread material, was embroidered in a triaxial alignment. Piling the slices as a stack, researchers obtained appropriate porosity and pore sizes in the required range. Wet chemical modification and coating with collagen I and chondroitin sulphate were also sufficient to generate a scaffold with a suitable network of interconnecting pores. The tissue engineering model of the long bone (as suggested in Section 2.3.1) produces a highly osteoconductive and osteoinductive scaffold, superseding the *in vitro* seeding of cells.

2.5 Future trends

The human body is a composite of many kinds of hard and soft tissues, and as such, it requires appropriate replacement after tissue loss. Embroidery technology offers a wide range of approaches for tissue replacement. Embroidery scaffolds are smooth and flexible structures and would therefore be a promising application for soft-tissue engineering of skin or connective tissue. New approaches for directed fibre alignment and using the method of tailored fibre placement (TFP) (Spickenheuer et al., 2008)

allow the design of structures with adjusted mechanical properties in the direction of the force, supporting load-bearing soft tissues such as tendons and ligaments. The combination of different structures in one scaffold is also possible using embroidery technology. Different structure zones, such as bone, cartilage, or ligament, can be realised in bi- or triphasic scaffolds. Given that the embroidery process is controlled by a CAD/CAM system, it might be possible to design scaffolds tailored to the defect geometry of the patient by using a rapid prototyping procedure.

References

Arca, T., Proffitt, J., Genever, P., 2011. Generating 3D tissue constructs with mesenchymal stem cells and a cancellous bone graft for orthopeadic applications. Biomed. Mater. 6, 1–12.

Begley, C.T., Doherty, M.J., Hankey, D.P., Wilson, D.J., 1993. The culture of human osteoblasts cells on natural bone mineral. Bone 14 (4), 661–666.

Behrens, P., Wolf, E., Bruns, J., 2000. In vitro culture of human autologous osteoblast cells on natural bone mineral. Orthopaede 29 (2), 129–134.

Betz, O.B., Betz, V.M., Abdulazim, A., Penzkofer, R., Schmitt, B., Schröder, C., et al., 2010. The repair of critical-sized bone defects using expedited, autologous BMP-2 gene-activated fat implants. Tissue Eng. A 16, 1093–1101.

Blokhuis, T.J., Lindner, T., 2008. Allograft and bone morphogenetic proteins: an overview. Injury 39 (2), 33–36.

Calori, G.M., Mazza, E., Colombo, M., Ripamonti, C., 2011. The use of bone-graft substitutes in large bone defects: any specific needs? Injury 42, 56–63.

Caraballo, I., Millán, M., Rabesco, A.M., Leuenberger, H., 1996. Zero-order release periods in inert matrices. Influence of the distance to the percolation threshold. Pharm. Acta Helv. 71, 335–339.

Cattaneo, R., Catagni, M., Johnson, E.E., 1992. The treatment of infected nonunions and segmental defects of the tibia by the methods of Ilizarov. Clin. Orthop. 280, 143–152.

Connoly, J., Guse, R., Lippiello, L., Dehne, R., 1989. Development of an osteo-genic bone-marrow preparation. J. Bone Joint Surg. Am. 71 (5), 684–691.

Constantz, B.R., Ison, I.C., Fulmer, M.T., Poser, R.D., Smith, S.T., VanWagoner, M., Ross, J., Goldstein, S.A., Jupiter, J.B., Rosenthal, D.I., 1995. Skeletal repair by in situ formation of the mineral phase of bone. Science 267, 1796–1799.

Curran, J.M., Chen, R., Hunt, J.A., 2005. Controlling the phenotype and function of mesenchymal stem cells in vitro by adhesion to silane-modified clean glass surfaces. Biomaterials 26, 7057–7067.

Douglas, T., Heinemann, S., Mietrach, C., Hempel, U., Bierbaum, S., Scharnweber, D., Worch, H., 2007. Interactions of collagen types I and II with chondroitin sulfates A-C and their effect on osteoblast adhesion. Biomacromolecules 8 (4), 1085–1092.

Garcia-Cimbrelo, E., Olsen, B., Ruiz-Yague, M., Fernandez-Baillo, N., Munuera-Martinez, L., 1992. Ilisarov technique. Results and difficulties. Clin. Orthop. 283, 116–123.

Gelinsky, M., Welzel, P.B., Simon, P., Bernhardt, A., König, U., 2008. Porous three-dimensional scaffolds made of mineralized collagen: preparation and properties of a biomimetic nanocomposite material for tissue engineering of bone. Chem. Eng. J. 137, 84–96.

Green, S.A., Jackson, J.M., Wall, D.M., Marinow, H., Ishkanian, J., 1992. Management of segmental defects by the Ilizarov intercalary bone transport method. Clin. Orthop. 280, 136–143.

Heath, C.A., 2000. Cells for tissue engineering. Trends Biotechnol. 18 (1), 17–19.
Hess, R., Douglas, T., Myers, K.A., Rentsch, B., Rentsch, C., Worch, H., Shrive, N.G., Hart, D.A., Scharnweber, D., 2010. Hydrostatic pressure (HP) stimulation of human mesenchymal stem cells (hMSCs) seeded on collagen-based artificial extracellular matrices. J. Biomech. Eng. 132 (2), 021001.
Hessmann, M., Rommens, P.M., Hainson, K., 1998. Callus distraction of femur and tibia. Experiences with the mono-fixateur – indications for procedural changes. Unfallchirurg 101 (5), 370–376.
Hinüber, C., Häußler, L., Vogel, R., Brünig, H., Werner, C., 2010. Hollow poly(3-hydroxybutyrate) fibers produced by melt spinning. Macromol. Mater. Eng. 295, 585–594.
Hutmacher, D.W., 2000. Scaffolds in tissue engineering bone and cartilage. Biomaterials 21 (24), 2529–2543.
Hutmacher, D.W., Schantz, T., Zein, I., Ng, K.W., Teoh, S.H., Tan, K.C., 2001. Mechanical properties and cell cultural response of polycaprolactone scaffolds designed and fabricated via fused deposition modeling. J. Biomed. Mater. Res. 55 (2), 203–216.
Joyner, C.J., Bennet, A., Triffitt, J.T., 1997. Identification and enrichment of human osteoprogenitor cells by using differentiation stage-specific monoclonal antibodies. Bone 21 (1), 1–6.
Keselowsky, B.G., Collard, D.M., Garcıa, A.J., 2004. Surface chemistry modulates focal adhesion composition and signaling through changes in integrin binding. Biomaterials 25, 5947–5954.
Klussmann, R., 1990. Psychosocial problems from the viewpoint of psychosomatic medicine. Aktuelle Probl. Chir. Orthop. 34, 153–158.
Kruyt, M., De Bruijn, J., Rouwkema, J., Van Bliterswijk, C., Oner, C., Verbout, A., et al., 2008. Analysis of the dynamics of bone formation, effect of cell seeding density, and potential of allogeneic cells in cell-based bone tissue engineering in goats. Tissue Eng. A 2008 (14), 1081–1088.
Lai, K.A., Lin, C.J., Chen, J.H., 2002. Application of locked intramedullary nails in the treatment of complications after distraction osteogenesis. J. Bone Joint Surg. (Br.) 84 (8), 1145–1149.
Lalk, M., Reifenrath, J., Angrisani, N., Bondarenko, A., Seitz, J.M., Mueller, P.P., Meyer-Lindenberg, A., 2013. Fluoride and calcium-phosphate coated sponges of the magnesium alloy AX 30 as bone grafts: am comparative study in rabbits. J. Mater. Sci. Mater. Med. 24 (2), 417–436.
Lin, A.S.P., Barrows, T.H., Cartmell, S.H., Guldberg, R.E., 2003. Microarchitectural and mechanical characterization of oriented porous polymer scaffolds. Biomaterials 24, 481–489.
Lode, A., Bernhardt, A., Gelinsky, M., 2008. Cultivation of human bone marrow stromal cells on three-dimensional scaffolds of mineralized collagen: influence of seeding density on colonization, proliferation and osteogenic differentiation. J. Tissue Eng. Regen. Med. 2 (7), 400–407.
Luria, E.A., Owen, M.E., Freidenstein, A.J., Morris, J.F., Kuznetsow, S.A., 1987. Bone formation in organ cultures of bone marrow. Cell Tissue Res. 248 (2), 449–454.
Masquelet, A.C., Fitoussi, F., Bégué, T., Muller, G.P., 2000. Reconstruction of the long bones by the induced membrane and spongy autograft. Ann. Chir. Plast. Esthet. 45, 346–353.
Mayer, J., Blum, J., Wintermantel, E., 2008. Grundlagen des tissue engineering. In: Wintermante, I.E., Ha, S.-W. (Eds.), Medizintechnik – Life Science Engineering. Springer, Berlin.
McElhaney, J.H., Fogle, J.L., Melvin, J.W., Haynes, R.R., Roberts, V.L., Alem, N.M., 1970. Mechanical properties of cranial bone. J. Biomech. 3, 495–512.

Mikos, A., Temenoff, J.S., 2000. Formation of highly porous biodegradable scaffolds for tissue engineering. J. Biotechnol. 3 (2), 1154–1159.
Mikos, A., Thorsen, L., Czerwonka, Y.B., Langer, R., Winslow, D., Vacanti, P., 1993. Preparation and characterization of poly(L-lactic acid)foams. Polymer 35 (5), 1068–1077.
Mironov, V., Trusk, T., Kasyanov, V., Little, S., Swaja, R., Markwald, R., 2009. Biofabrication: a 21st century manufacturing paradigm. Biofabrication 1 (2), 022001.
Mutschler, W., Haas, N., 1999. Praxis der Unfallchirurgie. Georg Thieme Verlag Stuttgart, New York.
Oh, S.H., Park, I.K., Kim, J.M., Lee, J.H., 2007. In vitro and in vivo characteristics of PCL scaffolds with pore size gradient fabricated by a centrifugation method. Biomaterials 28 (9), 1664–1671.
Pendleton, C., Li, Q., Chesler, D.A., 2013. Mesenchymal stem cells derived from adipose tissue vs bone marrow: in vitro comparison of their tropism towards gliomas. PLoS One 8 (3), e58198.
Petite, H., Viateau, V., Bensaïd, W., Meunier, A., de Pollak, C., Bourguignon, M., Oudina, K., Sedel, L., Guillemin, G., 2000. Tissue-engineered bone regeneration. Nat. Biotechnol. 18 (9), 959–963.
Quarto, R., Mastrogiacomo, M., Cancedda, R., Kutepov, S.M., Mukhachev, V., Lavroukov, A., Kon, E., Marcacci, M., 2001. Repair of large bone defects with the use of autologous bone marrow stromal cells. N. Engl. J. Med. 344 (5), 385–386.
Rentsch, B., Hofmann, A., Breier, A., Rentsch, C., Moeckel, R., Scharnweber, D., 2009. Embroidered and surface modified polycaprolactone-co-lactide scaffolds as bioartificial bone substitute – in vitro characterization. Ann. Biomed. Eng. 37 (10), 2118–2128.
Rentsch, C., Rentsch, B., Breier, A., Hofmann, A., Manthey, S., Scharnweber, D., Biewener, A., Zwipp, H., 2010. Evaluation of the osteogenic potential and vascularization of 3D poly(3) hydroxybutyrate scaffolds subcutaneously implanted in nude rats. J. Biomed. Mater. Res. A 92 (1), 185–195.
Rentsch, B., Bernhardt, R., Scharnweber, D., Schneiders, W., Rammelt, S., Rentsch, C., 2012. Embroidered and surface coated polycaprolactone-co-lactide scaffolds. A potential graft for bone tissue engineering. Biomatter 2 (3), 1–7.
Rentsch, C., Schneiders, W., Hess, R., Rentsch, B., Bernhardt, R., Spekl, K., Schneider, K., Scharnweber, D., Biewener, A., Rammelt, S., 2014. Healing properties of surface-coated polycaprolactone-co-lactide scaffolds: a pilot study in sheep. J. Biomater. Appl. 28 (5), 654–666.
Roesgen, M., 1989. Verfahrensweisen der freien autologen Spongiosaplastik. Akt. Chir. 24, 83–95.
Rubin, R.H., Tolkhoff-Rubin, N.E., 1988. The problems of human immunodeficiency virus (HIV) infections and transplantations. Transplant 1, 36–42.
Rueger, J.M., 1998. Knochenersatzmittel. Heutiger Stand und Ausblick. Orhtopaede 27, 72–79.
Salzman, N.P., Psallidopoulus, M., Prewett, A.B., O'Leary, R., 1993. Detection of HIV in bone allografts prepared from AIDS autopsy tissue. Clin. Orthop. 292, 384–390.
Schnettler, R., Lieser, H., Klemm, K., 1997. Chirurgische Behandlung der posttraumatischen chronischen Osteomyelitis. Akt. Chir 32, 18–22.
Spickenheuer, A., Schulz, M., Gliesche, K., Heinrich, G., 2008. Using tailored fibre placement technology for stress adapted design of composite structures. Plast. Rubber Compos. Macromol. Eng. 37, 227–232.
Spickenheuer, A., et al., 2014. EDOpath—a novel process software for tailored fibre placement. Aachen-Dresden international textile conference, Dresden, November 27–28, 2014.

Struijs, P.A.A., Poolman, R.W., Bhandari, M., 2007. Infected nonunion of the long bones. J. Orthop. Trauma 21 (7), 507–511.

Suger, G., Fleischmann, W., Hartwig, E., Kinzl, L., 1995. Der offene Segmenttransport. Eine therapeutische Alternative bei poststraumatischen und osteitischen Weichteil- und Knochendefekten. Unfallchirurg 98, 381–385.

Tsuchiya, H., Abde-Wanis, M.E., Sakurakichi, K., Yamashiro, T., Tomita, K., 2002. Osteosarcoma around the knee. Intraepiphyseal excision and biological reconstruction with distraction osteogenesis. J. Bone Joint Surg. (Br.) 84-b, 1162–1166.

Verrier, S., Blaker, J.J., Maquet, V., Hench, L.L., Boccaccini, A.R., 2004. PDLLA/Bioglass (R) composites for soft-tissue and hard-tissue engineering: an in vitro cell biology assessment. Biomaterials 25 (15), 3013–3021.

Viateau, V., Guillemin, G., Bousson, V., et al., 2007. Long-bone critical-size defects treated with tissue-engineered grafts: a study on sheep. J. Orthop. Res. 25, 741–749.

Vivanco, J., Aiyangar, A., Araneda, A., Ploeg, H.L., 2012. Mechanical characterization of injection-molded macro porous bioceramic bone scaffolds. J. Mech. Behav. Biomed. Mater. 9, 137–152.

Vunjak-Novakovic, G., Martin, I., Obradovic, B., Treppo, S., Grodzinsky, A.J., Langer, R., Freed, L.E., 1999. Bioreactor cultivation conditions modulate the composition and mechanical properties of tissue-engineered cartilage. J. Orthop. Res. 17, 130.

Webb, K., Li, W., Hitchcock, R.W., et al., 2003. Comparison of human fibroblast ECM-related gene expression on elastic three-dimensional substrates relative to two-dimensional films of the same material. Biomaterials 24, 4681–4690.

Webb, K., Hitchcock, R.W., Smeal, R.M., Wenhua, L., Gray, S.D., Tresco, P.A., 2006. Cyclic strain increases fibroblast proliferation, matrix accumulation, and elastic modulus of fibroblast-seeded polyurethane constructs. J. Biomech. 39, 1136–1144.

Weigel, T., Schinkel, G., Lendlein, A., 2006. Design and preparation of polymeric scaffolds for tissue engineering. Expert Rev. Med. Devices 3 (6), 835–851.

Welkerling, H., Raith, J., Kastner, N., Marshall, C., Windhager, R., 2003. Painful soft-tissue reaction to injectable Norian SRS calcium phosphate cement after curettage of enchondromas. J. Bone Joint Surg. (Br.) 85 (2), 238–239.

Winkelmann, W., 1999. Extremitätenerhalt bei malignen Knochentumoren. Dtsch. Arztebl. 96 (19), 1270–1274.

Wintermantel, E., Ha, S.W., 2009. Medizintechnik-Life Science Engineering. Springer-Verlag, Berlin Heidelberg, http://dx.doi.org/10.1007/978-3-540-93936-8.

Wipperman, B.W., 1997. Hydroxlylapatitkeramik als Knochenersatzstoff. Experimentelle Untersuchungen am Segmentdefekt der Schaftibia. Hefte Unfallchirurg 260, 1–108.

Wollenweber, M., Domaschke, H., Hanke, T., Boxberger, S., Schmack, G., Gliesche, K., Scharnweber, D., Worch, H., 2006. Mimicked bioartificial matrix containing chondroitin sulphate on a textile scaffold of poly(3-hydroxybutyrate) alters the differentiation of adult human mesenchymal stem cells. Tissue Eng. 12, 345–359.

Nonwoven scaffolds for bone regeneration

3

E.R. Durham, G. Tronci, X. Yang, D.J. Wood, S.J. Russell
University of Leeds, Leeds, UK

3.1 The structure of bone and the mechanisms for self-repair

Bone is one of the most commonly transplanted tissues, with 2.2 million bone grafts performed annually worldwide (Tronci et al., 2013a). Surgeons face a diverse spectrum of clinical challenges in bone reconstruction, and this diversity reflects the variety of anatomic sites, defect sizes, mechanical stresses, and available soft tissue cover. Autologous bone grafting remains the gold standard for the reconstruction of skeletal defects (McMahon et al., 2013), although drawbacks, including limited supply, bone graft loss/resorption, and donor site morbidity, impose a pressing demand for advanced biomaterial solutions. For these reasons, the World Health Organization (WHO) has confirmed the current decade as the 'Bone and Joint Decade'.

To develop successful bone scaffolds, clinicians must adopt a multidisciplinary approach in order to understand and stimulate the natural bone regeneration process. In addition to an understanding of cell biology and genetics, this approach requires knowledge of bone structure and its hierarchical organisation, from the macro (centimetre) to the nano (extracellular matrix, ECM) scales (Figure 3.1). At the macroscopic structural level, bone consists of a dense shell of cortical bone that supports and protects. The interior porous cancellous bone optimises weight transfer and minimises friction at the articulating joints (McMahon et al., 2013). Cortical bone is composed of repeating osteon units, whereas the cancellous bone is made of an interconnecting framework of trabeculae with bone marrow-filled free spaces. These trabeculae and osteon units are composed of collagen fibres. In the osteons, 20–30 concentric layers of fibres, called lamellae, are arranged at $\pm 45^{\circ}$ surrounding the central canal, and they contain blood vessels and nerves.

Moving from the macroscopic to the molecular level, bone is a composite material, consisting of cells embedded in the ECM. The ECM plays a key role in the localisation and presentation of biomolecular signals, which are vital for neo-tissue morphogenesis. Proteoglycans, glycosaminoglycans, and mineralised collagen are integrated in a supramolecular hydrogel. Collagen fibrils are arranged with a 67-nm periodicity and 40 nm gaps where hydroxyapatite crystals are situated. The mineral phase is thought to dominate the stiffness of bone, which increases more than linearly with mineral content. The toughness of the material is thought to mainly arise from its hierarchical organisation, whereby the lowest hierarchical level contributes to the outstanding

Biomedical Textiles for Orthopaedic and Surgical Applications. http://dx.doi.org/10.1016/B978-1-78242-017-0.00003-9

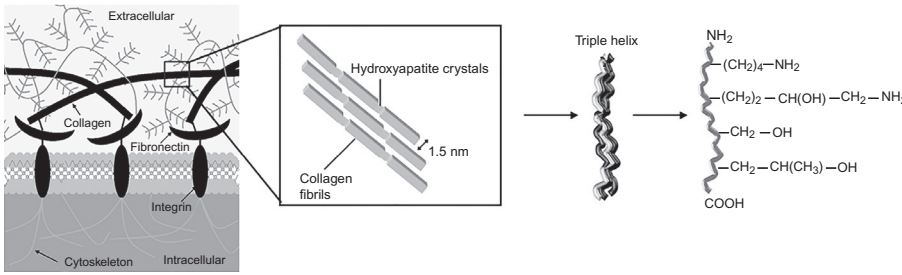

Figure 3.1 Hierarchical organisation of bone over different length scales. Bone tissue structure, function, and shape are regulated by the extracellular matrix (ECM), a supramolecular hydrogel network, in which cells are immersed. The ECM is mainly composed of collagen fibrils mineralised with hydroxylapatite crystals. Fibrils result from the assembly of collagen triple helices, which are based on left-handed polyproline chains at the molecular level.

bone fracture resistance (Dunlop and Fratzl, 2010). This unique hierarchical organisation enables bone to exhibit mechanical properties far superior to those of its single components. Thus, the repair and reconstruction of bone defects require innovative strategies that can closely mimic the complex tissue hierarchical organisation.

For bone regeneration, bone healing processes must also be given careful consideration. Bone has the capacity to repair itself, and this self-repair can be harnessed to repair small bone defects, heal nonunions, and lengthen short bones. Fracture healing is a complex regenerative process initiated in response to injury, in which bone can heal by primary or secondary mechanisms (Alman et al., 2011). In primary healing, new bone is laid down without any intermediate. This type of healing is rare in a complete bone fracture, except when the fracture is rigidly fixed through certain types of surgery. In the more common secondary mechanism of healing, immature and disorganised bone (i.e., callus) forms between the fragments. During the fracture repair process, cells progress through stages of differentiation reminiscent of those that cells progress through during normal foetal bone development. In the normal development of long bone, undifferentiated mesenchymal cells initially form a template for the bone, which then differentiates into chondrocytes. After this phase, blood vessels enter the cartilaginous template, and osteoblasts, which differentiate from perivascular and other cells surrounding the bone, form bone. The reparative process is impaired in large, critical-sized bone defects (i.e., gaps beyond 2.5 times the bone radius) (Schroeder and Mosheiff, 2011), and osteoblastic differentiation is inhibited, with undifferentiated mesenchymal tissue remaining at the fracture site. Such defects can be caused by blunt or penetrating trauma, surgical treatment of tumours or necrosis caused by radiation, or various chemical substances. These defects represent a considerable surgical challenge, are associated with high socioeconomic costs, and highly influence patients' quality of life, both private and professional (Woodruff et al., 2012). Despite huge progress being made toward the design of bone implants, the integration of all tissue properties and functions in a single biomaterial system remains a major research challenge. Researchers still need to develop reliable tools enabling

them to systematically and temporally control the material structure and organisation, properties and functions, so that next-generation scaffolds can successfully ensure full clinical relevance. Fibrous assemblies in the form of nonwoven scaffolds have been repeatedly investigated over the last 20 years in relation to tissue regeneration. As the requirements of clinicians become more and more tissue specific, and synthetic biofunctional biomaterials are developed, nonwoven scaffold engineers must be able to respond with the capability to produce truly biomimetic architectures.

3.2 Fibre manufacture from biomaterials

Biomaterials for bone regeneration should be biocompatible, biodegradable substances that support cell attachment, spread, proliferate (osteoconductive), and control cell differentiation into osteogenic lineages (Dawson et al., 2011; El-Gendy et al., 2013; Yang et al., 2003b). For a biomaterial to be suitable for manufacture into a nonwoven scaffold, it must be suitable for conversion into fibres, and the method of extrusion should not adversely affect biocompatibility or the properties of the material. A variety of natural and synthetic biomaterials can be converted into fibres, with different extrusion methods being applied depending on the composition of the biomaterial. These include, wet and dry solution spinning, melt spinning, and gel spinning. Materials extracted from a natural source, such as collagen, are attractive biomaterials, but the retention of the native structure after solubilisation and the precipitation of the regenerated product after spinning remain challenging. Synthetic biomaterials, notably those exhibiting thermoplastic behaviour, are often more straightforward to extrude due to their excellent mechanical properties, but such materials can lack suitable surface chemistry for cell attachment, and they might produce undesirable degradation products *in vivo*. One issue can be the inflammatory response of the surrounding tissues while the polymer hydrolytically degrades (Agrawal and Ray, 2001; Cai et al., 2007). Hybrid materials containing both synthetic and natural materials, such as regenerated collagen or blends of two or more polymers, provide one means for balancing the required mechanical and chemical properties. Additionally, the incorporation of materials such as hydroxyapatite tricalcium phosphate (Day et al., 2005; Mastrogiacomo et al., 2006) during spinning also enables the properties of the bulk product to be substantially modified according to specific clinical requirements. Both the biomaterial composition and the method of fibre extrusion affect the bulk properties of the resulting nonwoven scaffold architecture. One scaffold parameter that has received considerable attention is the production of fibres of submicron diameter. Nanofibrous scaffolds have long been championed by the tissue engineering community with early work on electrospun polylactide nanofibre-based tissue engineering scaffolds indicating that human mesenchymal stem cells tended to proliferate more on nanofibre scaffolds than on microdiameter fibrous scaffolds (Shanmugasundaram et al., 2004). Since then, many reports have shown that nanofibrous scaffolds support cell growth for tissue regeneration (Chung et al., 2011; Huang et al., 2011; Kumbar et al., 2008). However, conflicting evidence also suggests that nanofibres are only preferential to microfibres when using synthetic biomaterials

(Rnjak-Kovacina and Weiss, 2011). One of the challenges in designing three-dimensional scaffolds containing submicron fibres that pack closely together is facilitating adequate cell penetration into the full thickness of the fibrous assembly. The selection of an appropriate biomaterial from which to manufacture a nonwoven scaffold is, of course, a major consideration, and in bone regeneration, the evaluation of materials has included regenerated collagen, gelatine (Venugopal et al., 2008), poly(lactic acid) (Kim et al., 2006), poly(lactic-*co*-glycolic acid) (Liao et al., 2008), silk fibroin (Kim et al., 2005), chitosan (Shin et al., 2005), and polycaprolactone (Porter et al., 2009). For brevity, further discussion in this chapter is restricted to collagen and polycaprolactone nonwoven production.

3.2.1 Collagen

Collagen has been widely applied for the design of tissue-like matrices for repair (Hong et al., 2010) because of its natural occurrence in bone tissue. The collagen molecule is based on three left-handed polyproline chains, each of which contains the repeating unit Gly-*X*-*Y*, with *X* and *Y* being predominantly proline (Pro) and hydroxyproline (Hyp), respectively. The three chains are staggered from one another by one amino acid residue and are twisted together to form a right-handed triple helix (300 nm in length, 1.5 nm in diameter). *In vivo*, triple helices can aggregate to form collagen fibrils, fibres, and fascicles, which are stabilised via intermolecular enzymatic crosslinking (Buehler, 2008; Grant et al., 2009). However, collagen properties are challenging to control in physiological conditions due to the fact that collagen's unique hierarchical organisation and chemical composition *in vivo* can only be partially reproduced *in vitro*. As a result, regenerated collagen materials display noncontrollable swelling and weak mechanical properties in physiological conditions. The limited solubility in organic solvents, high swelling in aqueous solution, and noncontrollable batch-to-batch variation in chemical properties represent significant challenges to the use of collagen for the design of defined, water-stable nonwovens. To improve its stability, collagen has been widely crosslinked with *N*-(3-dimethylaminopropyl)-*N*′-ethylcarbodiimide hydrochloride (EDC) (Olde Damink et al., 1996), glutaraldehyde (GTA) (Olde Damink et al., 1995b), and hexamethylene diisocyanate (HDI) (Olde Damink et al., 1995a). In the first case, zero-length covalent net-points are formed so that no harmful and potentially cytotoxic molecules are introduced (Haugh et al., 2011). Due to the minimal net-point length, however, crosslinking of adjacent collagen molecules is unlikely because the terminal amino functions are too far apart to be bridged, resulting in nonvaried mechanical properties. In contrast to EDC, GTA and HDI involve the covalent incorporation of oligomeric segments between distant collagen molecules. The reaction of collagen with aldehydes or isocyanates in aqueous solution has been reported to result in a cascade of noncontrollable side reactions and the formation of highly reactive and potentially toxic functional groups coupled to the polymer backbone (Zhang et al., 2011). To avoid such undesirable side reactions, collagen has been crosslinked with diimidoesters, such as dimethyl suberimidate, 3,3′-dithiobispropionimidate, and acyl azide, resulting in stable

materials in physiological conditions, although the extensibility of the material was reduced (Charulatha and Rajaram, 2003). Dehydrothermal treatment or riboflavin-mediated photocrosslinking has also been applied as physical, benign crosslinking methods, although partial loss of native collagen structure and nonhomogeneous crosslinking was observed in these cases (Weadock et al., 1995). Rather than direct covalent crosslinking, alternative approaches have recently focused on the formation of injectable ECM-mimicking gels via synthetic collagen blends (Hartwell et al., 2011), as well as the design of cell-populated matrices via derivatisation with cinnamate (Dong et al., 2005) or acrylate (Brinkman et al., 2003) moieties. In these methods, although the resulting mechanical properties may be enhanced, synthetic components, such as polymers or comonomers, are required to promote the formation of water-stable matrices, and the alteration of the protein backbone and biofunctionality may result.

Reliable synthetic methods must therefore be applied in order to improve thermomechanical behaviour, without affecting biofunctionality (de Moraes et al., 2012), specifically biocompatibility and bioactivity. To address these challenges, collagen fibres can be chemically functionalised (Tronci et al., 2013c), so that a covalent network is established at the molecular level (Tronci et al., 2013b); in this way, temporal stability of both fibres and mesh architecture may be ensured in physiological conditions.

Collagen fibrillogenesis can be induced *in vitro* by exposing monomeric collagen solutions to physiological conditions, resulting in viscoelastic gels at the macroscopic level (Lai et al., 2011). The design of collagen mimetic peptides has also been proposed as an alternative strategy for recapitulating the multiscale organisation of natural collagen (O'Leary et al., 2011). However, despite the formation of hierarchical triple helix assemblies, the resultant thermal and mechanical stability is still not adequate for biomaterial applications, so that chemical functionalisation of side- or end-groups is crucial.

The functionalisation of collagen requires careful consideration, because the hierarchical organisation of collagen imposes constraints in terms of protein solubility, the occurrence of functional groups available for chemical functionalisation, and material biofunctionality. As improved synthetic methods are developed, functionalised collagen with preserved protein conformation and full biocompatibility will become available, enabling the manufacture of better performing biomimetic, nonwoven architectures.

There have been two distinct approaches to collagen fibre formation. The tissue engineering community has mainly focused on electrospinning, whereas industries producing artificial hair and textile fibres have exploited conventional wet-spinning approaches.

Electrospinning of collagen involves the extrusion of a positively charged polymer solution with the resulting fibres being collected as a nonwoven web on a grounded or negatively charged collector. The majority of studies involving the production of collagen fibres without a second carrier polymer involve the use of 1,1,1,3,3,3-hexafluoro-2-propanol (HFIP) as the solvent. The popularity of HFIP is based on the dual role it plays in collagen solubilisation – two trifluoromethyl groups serve to break hydrophobic

interactions, and the mildly acidic secondary alcohol hydroxyl assists in breaking the hydrogen bonds (Dong et al., 2009). However, cytotoxicity and the destructive effect on the structure of functionalised collagen have inspired a search for more benign solvents. Both collagen and gelatine have been successfully electrospun in a mixture of phosphate buffer saline/ethanol to produce fibres with average diameters ranging from 0.21 to 0.54 μm, depending upon the salt concentration (Zha et al., 2012). Note that vacuum drying is still normally required to remove the solvent after spinning.

The traditional wet spinning of collagen fibres has two major advantages. First, fibres can be produced with larger diameters, if required, and the fibre orientation and architecture of the nonwoven scaffold can be manipulated independent of the spinning process. Second, the stretching and drying of the extruded filaments are easier to control. In its simplest form, wet spinning involves dissolving the polymer in an appropriate solvent and then extruding the polymer solution via a spinneret into a coagulation bath containing a nonsolvent. Collagen has been solubilised in acidic environments and wet-spun into coagulation baths containing different ethanol/acetone mixtures, resulting in fibres with diameters ranging from 89 to 140 μm and tenacities of between 8.5 and 8.3 cN/tex (Meyer et al., 2010). Such fibre dimensions are larger than those typically targeted in the manufacture of tissue engineering scaffolds, but smaller diameters may be obtained through the appropriate control of manufacturing conditions. Owing to the excellent control of fibre dimensions and the high delivery speeds that are possible during production, wet spinning is an attractive route for the production of functionalised collagen fibres. Melt or thermoplastic spinning of collagen to produce fibres has also been reported, but the high temperatures required cause denaturing and are likely to disrupt functionalisation, so resulting materials are unlikely to be appropriate for tissue engineering applications (Meyer et al., 2010).

The structural and mechanical properties of chemically functionalised collagen fibres are of paramount importance in terms of the biocompatibility and mechanical performance for bone tissue engineering. Two major challenges in the production of collagen using synthetic methods are the ability to control material stability in physiological conditions and the preservation of the native protein conformation. Preservation of the triple helix structure is crucial for ensuring enzymatic implant degradability. Here, intact triple helices are required to promote effective degradation of fibrillar collagen (Gaudet and Shreiber, 2012). If the tertiary structure is significantly altered, then collagenase degradation rates could also be affected, in turn influencing material biodegradability, as well as the extent to which cells remodel the scaffold. Attenuated total reflectance and Fourier transform infrared spectroscopy (ATR-FTIR) is a useful analytical technique for elucidating the protein molecular conformation in collagen scaffolds manufactured using a synthetic route. Collagen displays distinct amide bands via FTIR, which characterise its triple helix structure. These are (i) amide A and B bands at 3300 and 3087 cm^{-1}, respectively, which are mainly associated with the stretching vibrations of N–H groups; (ii) amide I and II bands, at 1650 and 1550 cm^{-1}, resulting from the stretching vibrations of peptide C═O groups as well as from N–H bending and C–N stretching vibrations,

respectively; (iii) an amide III band centered at 1240 cm^{-1}, assigned to the C–N stretching and N–H bending vibrations from amide linkages, as well as wagging vibrations of CH_2 groups in the glycine backbone and proline side chains. Each of the previously mentioned amide bands should be exhibited in the FTIR spectra of functionalised collagen, whereby no detectable band shift will be displayed compared to the spectrum of native type I collagen (Figure 3.1). Other than qualitative findings on unchanged band positions, the FTIR absorption ratio of amide III to the 1450 cm^{-1} band (A_{III}/A_{1450}) is usually determined in order to quantify the degree of triple helix preservation. In such a case, an amide ratio close to unity is associated with the preserved integrity of the triple helices (He et al., 2011) following functionalisation of native collagen (Tronci et al., 2013b).

Other valuable analytical techniques for elucidating protein backbone conformation are circular dichroism (CD) and sodium dodecyl sulphate-polyacrylamide gel electrophoresis. CD is based on the fact that single collagen polyproline chains are stabilised into a triple helix structure via hydrogen bonds oriented perpendicularly to the triple helix axis, resulting in an optically active protein (Djabourov, 1988). This molecular feature is exploited by CD spectroscopy to investigate any alteration in protein conformation following either chemical functionalisation or fibre formation. Resulting collagen-based materials are dissolved in dilute acidic conditions and excited with plane-polarised light. Plane-polarised light can be viewed as being made up of two circularly polarised components of equal magnitude, one rotating counterclockwise (left-handed, L) and the other clockwise (right-handed, R). CD refers to the differential absorption of these two components. If, after passage through the sample being examined, the L and R components are not absorbed or are absorbed to equal extents, the recombination of L and R would regenerate radiation polarised in the original plane. However, if L and R are absorbed to different extents, the resulting radiation would be said to possess elliptical polarisation, resulting in a CD signal (Kelly et al., 2005). One of the most significant advances that has been made in relation to scaffold performance and which will aid future work on the development of functionalised collagen scaffolds is the ability to monitor scaffolds *in vivo* (Cunha-Reis et al., 2013).

3.2.2 Poly(ε-caprolactone)

Poly(ε-caprolactone) (PCL) is a biocompatible and bioresorbable semicrystalline aliphatic polyester that has been extensively reported in connection with medical applications including bone repair and regeneration. PCL has a degradation time between 2 and 4 years; however, the degradation time can be greatly altered by blending it with another polymer such as collagen. Owing to its biodegradability and exceptional mechanical properties, PCL fibre has been studied extensively in relation to bone engineering (Porter et al., 2009). Its popularity also results from its relatively low cost, ease of processing, and compatibility with both melt spinning, wet spinning, and electrospinning. The major disadvantage of PCL as a biomaterial is its lack of

biofunctionality, although this can be compensated for, to some extent, by blending it with other biofunctional materials.

The solvent electrospinning of PCL is well documented, with a large number of studies reporting PCL fibre spinning using the chloroform:methanol solvent system. By adjusting the ratio of chloroform to methanol, applied voltage, and tip to collector distance, electrospun webs with an average fibre diameter ranging from 2.3 to 10.8 μm can be obtained (Pham et al., 2006). Submicron PCL fibres can also be successfully spun using a solvent mixture of chloroform: *N*,*N*-dimethylformamide (Pham et al., 2006), and there is potential to produce webs in which both PCL nanofibres and microfibres are present, using the same equipment, although producing fibre diameters that are considerably larger than 10 μm remains a limiting factor. Melt electrospinning uses a similar set-up, but, because the polymer is extruded in a molten state, a heating element is required. In this process, the upper limit of the average fibre diameter that can be produced increases between 6 and 30 μm (Detta et al., 2010). The high temperatures that are required during melt extrusion processes means that collagen and other biofunctional materials cannot be easily incorporated in the manufacture of fibres without the risk of degradation, however. Although melt spinning using operating temperatures of 85–90 °C is not appropriate for the production of PCL/collagen blends, biofunctional materials can be incorporated post-spinning in the form of coatings on the fibre surfaces. Traditional melt spinning (as opposed to melt electrospinning) enables the production of large quantities of fibre (Charuchinda et al., 2003) and the ability to produce either continuous filament or staple fibre. This provides greater versatility in the available nonwoven production routes and therefore the types of scaffold architecture and physical properties that can be manufactured.

Wet-spun PCL fibres can be extruded from polymer solution containing acetone and then spun directly into a methanol coagulation bath. As-spun PCL fibres have been reported with a diameter of 150 μm, reduced to 67 μm by cold drawing using an extension of 500% (Williamson et al., 2006). A major benefit of wet spinning, as opposed to the melt-spinning route, is the potential to produce mixed polymer fibres that incorporate the mechanical properties of PCL with the biofunctionality of a material such as collagen. However, appropriate cosolvents are required to facilitate this. The majority of studies have reported the use of HFIP as a solvent system for electrospinning blends of collagen and PCL. This is less than ideal because of the cytotoxic nature of any residual HFIP present in the as-spun fibres. Some alternative approaches have been developed, including those reported by Chakrapani et al. (2012) who used acetic acid as a solvent system for PCL and collagen mixtures.

To improve the osteoconductivity and mechanical properties of scaffolds for bone engineering and to create a pH buffer against the acidic degradation of synthetic polymer matrices, researchers have investigated the incorporation of HA particles (Puppi et al., 2011). Ji et al. (2012) reported that nano-HA platelets significantly improved the mechanical properties, including the strength, strain, and toughness of electrospun collagen fibres. Puppi et al. (2011) wet-spun PCL fibres containing HA using acetone as a solvent and ethanol as a nonsolvent, and they produced fibres with diameters in the range of 100–250 μm.

3.3 Design and assembly of scaffold architectures

In scaffold-guided tissue regeneration, three-dimensional scaffolds serve as temporary tissue substitutes that promote tissue regeneration at the defect site (Langer and Vacanti, 1993). Scaffold design has to take into account the macroscopic properties of the material (e.g., degradability, porosity, and mechanical properties), processability, and the interaction with cells. Suitable porosity and pore interconnectivity are necessary to promote cell migration and differentiation, including within the interior of the scaffold; diffusion of oxygen and nutrient to cells (Botchwey et al., 2003); and removal of waste products from the scaffold. The same structure must also have mechanical properties that enable sharing of the physiological load, if functional neo-tissue is to develop.

In a clinical setting, a nonwoven scaffold can be used alone or in combination with other materials, growth factors, and/or cells. If the scaffold is to be used alone, it must be designed to act as a supporting structure that recruits stem/stromal cells from surrounding tissues (Shi et al., 2013; Zhang et al., 2008). In other instances, the scaffold can be designed and used as a carrier vehicle for bioactive growth factors in order to enhance osteoinduction, chondroinduction, and angiogenesis that are crucial for bone and osteochondral-tissue engineering (Green et al., 2004; Yang et al., 2004). Nonwoven scaffolds can also be used in combination with stem/stromal cells that can be directly delivered into the bone defect area to provide both osteogenesis and support elements for bone tissue engineering (Udehiya et al., 2013; Yang et al., 2001). Scaffolds may be bioactive and contain autogenic and/or allogenic stem/stromal cells that can be directly delivered into the bone defect area to provide osteogenesis, osteoinductive, and osteoconductive elements for bone tissue engineering (Yang et al., 2003a,b, 2004). It is therefore important that the required function of the nonwoven scaffold and the selection of materials are carefully considered during the design and development process.

Generally, nonwoven fabrics are highly porous, low-density fibrous assemblies of typically less than 0.40 g/cm^3. The internal pore structure is highly interconnected, and there is a relatively wide pore size distribution that can be manipulated during nonwoven fabric manufacturing. The majority of fibres in nonwoven structures are arranged in a planar, x–y orientation, with only a limited number of processes, notably air-laid, vertically lapped, carded webs, with needling and hydroentangling capable of producing a degree of fibre orientation through-thickness. The fibre orientation distribution, which can be manipulated during production of the nonwoven scaffold, strongly influences the isotropy of fabric properties including directional mechanical properties and fluid transport.

Different nonwoven architectures can be produced in the form of a scaffold depending upon the selection of manufacturing route. Nonwoven manufacture typically involves at least two sequential steps: web formation and bonding. Both dry-laid (e.g., carded, carded and lapped, air-laid) and wet-laid web formation processes utilise staple fibres that are cut to a predetermined length prior to nonwoven fabric manufacture. In contrast, spun-melt (e.g., spun-bond, melt-blown) and other direct filament deposition techniques, such as electrospun and force-spun web formation techniques,

rely on the direct collection of continuous filaments in the form of a web. Depending on the polymer composition of the fibres in the web, one or more bonding techniques may be applied: mechanical (needling, hydroentangling, stitch-bonding), thermal bonding, or chemical bonding. Mechanical bonding relies on increasing fibre entanglement and frictional resistance within the web to increase resistance to slippage, and therefore, fibre length, fibre diameter, breaking elongation, flexural rigidity, fibre mobility, and fibre–fibre friction are influential parameters.

In dry-laid web formation, the carding of fibres to produce a web involves their progressive disentanglement as they are carried on rollers clothed in wire teeth, which involves fibre–metal and fibre–fibre friction. The low melting point of some biomaterials such as PCL (e.g., 60 °C) can therefore give rise to unwanted fusing of fibres during the carding as a result of frictional heating. Another challenge is the potential for excessive fibre breakage in biomaterial fibres that have low breaking extensions of less than 5%. Short-cut (<15 mm length) biomaterial fibres can also be air-laid to form webs, minimising the potential for fibre breakage during web formation, but mechanical bonding normally results in relatively weak scaffolds. An advantage of wet-laid processes is the high weight uniformity that can be achieved in the web; however, the process requires suspension of short cut fibres in a liquid medium, which can be unsuitable for biomaterials that have poor aqueous stability.

Thermal bonding of synthetic thermoplastic biomaterials such as PCL is also feasible. Practically, fibres with a concentric core-sheath bicomponent structure are preferred in order to minimise thermal shrinkage during heating and to maximise fabric strength while preserving the required internal fabric structure. Owing to biocompatibility issues, chemical bonding, in which an adhesive is applied to the web to prevent fibre slippage, is not normally considered appropriate for tissue scaffold manufacture, unless the binder is, in itself, a biomaterial suitable for invasive use.

The production of nonwoven scaffolds with reproducible architectural features is challenging and remains an important issue with respect to quality control. In mechanically bonded tissue scaffolds, methods of controlling certain features of the internal architecture, such as pore structure, have been attempted by utilising templates (Durham et al., 2012). An example of a highly porous nonwoven architecture made by thermally bonding a carded web of bicomponent poly(lactic acid) (PLA) fibres around a removable spacer template to tune the internal pore structure is shown in Figure 3.2. Such modifications to existing nonwoven processes highlight the potential for manipulating scaffold structures in a reproducible manner during their production.

In relation to biomimetic scaffolds, a major advantage of nonwovens is their highly interconnected pore structure and the scope that is available to control pore size distribution during manufacturing. The production of scaffolds with appropriate pore sizes is fundamental for their functionality. The minimum pore size for bone engineering is approximately 100 μm, due to cell size, migration requirements, and nutrient transport (Hutmacher et al., 2007). Mean pore sizes in electrospun webs are normally substantially lower than 100 μm, which means initial cell penetration into a thick, three-dimensional scaffold can be impeded. Increasing the fibre diameter is one approach to making larger pores, but this is not always practicable, depending on the biomaterial and spinning conditions. Other methods for increasing pore size

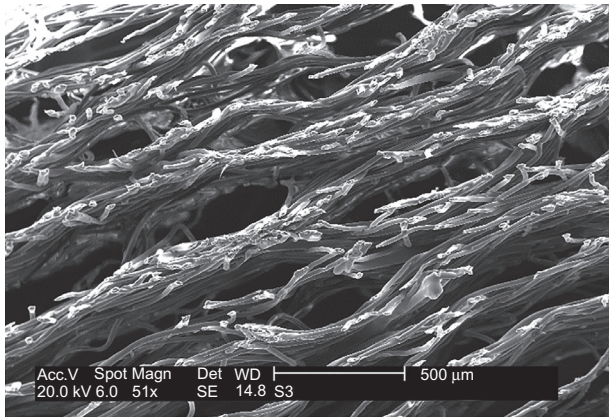

Figure 3.2 Cross section of a nonwoven scaffold produced by carding and through-air thermal bonding (100% core-sheath PLA staple fibre). The cavities correspond to regions where solid metallic spacer elements inserted prior to thermal bonding have been removed.

involve combining electrospun polymers with sacrificial material, such as a porogen, that can be subsequently removed (Nam et al., 2007; Phipps et al., 2011). Force-spinning, which relies on using centrifugal forces instead of electrical charge to stretch the polymer jet (McEachin and Lozano, 2012), is an interesting candidate for scaffold production because the submicron diameter fibres that are deposited on the collector are less densely packed than they are in electrospinning.

Given that physiological tissue, including bone, is heterogeneous in structure, the ability to manufacture templated features in electrospun webs that biomimic the native structure is of interest to tissue engineers. Templating techniques have included use of an electronic circuit chip as a collector, which enabled the production of features on the order of several hundred microns (Wu et al., 2010). The majority of other approaches have used patterns in the range of millimetres. Producing well-defined features at the micron level may be hampered by electrical charge jumping across small nonconductive areas, however. Vaquette and Cooper-White (2011) investigated 'round' collectors with a 1-mm diameter disc in the centre of the hole, a 'star' collector, and a 'ladder' collector that produced a variety of different scaffold architectures. In the manufacture of PCL scaffolds, a solvent system of chloroform/dimethylformamide or cholorform/methanol has been a route of choice, due to the conductivity of the solution, although the templating of other synthetic polymers such as poly(D,L-lactide-*co*-glycolide) has also been reported (Zhou et al., 2010).

A disadvantage of many templating techniques is that the structures remain relatively two-dimensional and do not truly biomimic the three-dimensional nature of physiological tissue such as bone. Various methods to produce multilayered structures have been explored, including stacking templated electrospun webs and fusing them using a hot pressing process (Dou et al., 2011). Collagen glue has also been used as an adhesive between stacked layers of scaffold (McCullen et al., 2010). Although such scaffolds are three-dimensional in terms of macroscopic thickness, the fibres remain orientated in the x–y directions and the pore structure reflects this. When multiple layers of web are stacked directly on top of each other, a reduction in the overall pore size can result, which is undesirable.

Three-dimensional collectors can be used to collect electrospun fibres in architectures similar to that of a cotton ball. Blakeney et al. (2011) reported the application of a spherical foam dish with stainless steel probes radiating from its centre. This collector was used to deposit PCL fibres and produced a low-density, three-dimensional structure. Fibre diameters of ~500 nm and pore sizes between 2 and 5 μm were obtained. Despite the original design of this collector, the pore size remained far below the suggested minimum pore size required for bone engineering of 100 μm.

Direct-write electrospinning is also emerging as a means for introducing biomimetic features. The original direct-write technology allowed structures to be built directly, without the use of masks enabling the rapid prototyping of complex architectures (Chrisey, 2000). Combining the technology with electrospinning facilitates the production of complex fibrous architectures by additive manufacture. Both solution and melt electrospinning have been demonstrated to be compatible with direct writing. To enable direct writing, the electrospinning process is modified so that the fibres can be collected while the fibre deposition path is still straight. At the point of fibre contact with the collector, the majority of the solvent should either have been removed or the melt solidified, so that the fibres retain their incoming morphology. To enable the direct writing in this way, a fast moving lateral collector platform is required. Polymer melts can be drawn over a larger distance while remaining on a straight trajectory, as compared to their solution-spun counterparts. This allows the tip-to-collector distance to be greater, resulting in a longer time period for the molten polymer to solidify. In order to be able to write with a continuous line, the translational speed of the collector must match the jet speed at impact (up to 1 m/min in some instances). Consideration must also be given to the turning speed/dwell time during the writing of complex patterns and incorporated into the original programmed design. These patterned webs can be repeatedly manufactured on top of each other to produce 3D structures with up to 1 cm thickness (Brown et al., 2012). To date, PCL has been frequently used because of its wide range of processing temperatures, allowing the production of fibres with a range of diameters between 19 and 28 μm (Brown et al., 2012). The resulting architectures are often geometric in design and made of multiple layers of large diameter fibres.

Solution-based electrospun direct writing requires a similar set-up, but because of the time required for the solvent to be flashed off, a larger tip-to-collector distance is required. The set-up used by Lee et al. (2012) comprised a dielectric thin plate that was capable of lateral movement independent of the sharp-pin ground electrode. Nanofibres were collected as dense depositions in a defined area (the pin electrode), and writing was accomplished by movement of the collector surface. To add stability and three-dimensionality, multiple layers of nanofibres must be written on top of each other. Various patterns, such as lines, points, lattices, and grids, can be produced. Polymer selection is limited to those that can be spun successfully in volatile solvents such as chloroform, ensuring that the majority of the solvent is evaporated prior to the fibre depositing upon the collector. Although greater control of fibre deposition is achieved, the architectures are still relatively 2D in construction.

Electrospinning into a liquid coagulating bath is a combination of electrospinning and conventional wet spinning. Wet electrospinning has received considerable

attention due to its potential for decreasing fibre packing density and increasing the pore size in scaffolds. By using a solvent with a relatively low surface tension, fibres do not float on the surface and can disperse in the solvent, allowing architectures with a more pronounced three-dimensional structure to be formed (Yokoyama et al., 2009). Further increases in pore size can be obtained by incorporating porogens such as sodium chloride into the spinning bath (Gang et al., 2012). Synthetic polymers such as poly(glycolic acid) have been spun in solutions of 1,1,1,3,3,3-hexafluoro-2-propanol and collected in a bath of tertiary-butyl alcohol. The resulting architectures contained fibres with diameters ranging from 200 to 1400 nm. PCL has been spun into ethanol, which prevented the electrospun fibres from packing densely on top of each other (Yang et al., 2012). To prevent the architecture from collapsing when the solvent is removed, freeze-drying is required after spinning.

The versatility of electrospinning as a technique for bone scaffold production is considerable, particularly when it is combined with techniques that enable better control of the fibrous architecture. Unfortunately, although a great variety of structural features can be introduced, the results cannot be described as truly biomimetic. Alternative nonwoven technologies are likely to be required to overcome some of the inherent limitations of electrospinning, and there is substantial scope given the range of processes that are already commercially available. The challenge remains to engineer improved electrospun 3D architectures with both pore sizes and mechanical properties that are properly matched to clinical needs.

3.4 Considerations for surgical implantation of nonwoven scaffolds

To meet the specific clinical requirement, the researcher must consider many factors when designing and fabricating nonwoven scaffolds. The general requirements of biomaterials and scaffold architectures have already been discussed; however, these may need to be tailored, depending on the requirements of the specific bone defect. Common surgical situations that would be suitable for reconstruction using a nonwoven scaffold are listed in Table 3.1. Depending on the defect type, nonwoven scaffolds can be applied to the defect site in different ways. For a fracture model, the nonwoven scaffold may be used as a membrane/bandage to cover the fracture and/or bone defect area, whereas, for large defect sites, the nonwoven scaffold may be used as filler/gauze, as shown in Figure 3.3. It is important to identify the intended use of nonwoven scaffolds and to incorporate appropriate features during the scaffold development phase. The final scaffold structure must be user-friendly and should be sterile and supplied in a range of different sizes. It must also be ready to use and easy to handle by the surgeon.

Consideration must also be given to the method of fixing the scaffold in the defect site. Not all nonwoven scaffolds require additional fixation because they can be pushed into place to fill the defect area. Push-fit nonwovens scaffolds must have sufficient recovery post-implantation to be able to mould to the contours of the defect

Table 3.1 Common surgical situations suitable for reconstruction using a nonwoven scaffolds

Bone defect type	Examples of surgical situations	Reference
Fracture nonunion: small bone defect after surgical procedure	Removal of benign tumour: unicameral bone cysts, periapical cyst, or tumour resection.	Khira and Badawy (2013), Di Stefano et al. (2012), and Gentile et al. (2013)
Segmental bone defect	Due to trauma or surgery	Liu et al. (2013a), Gruber et al. (2013), Horner et al. (2010), and Udehiya et al. (2013)
Flat bone	Calvaria defect	Liu et al. (2013b), Pelegrine et al. (2013), and Cooper et al. (2010)

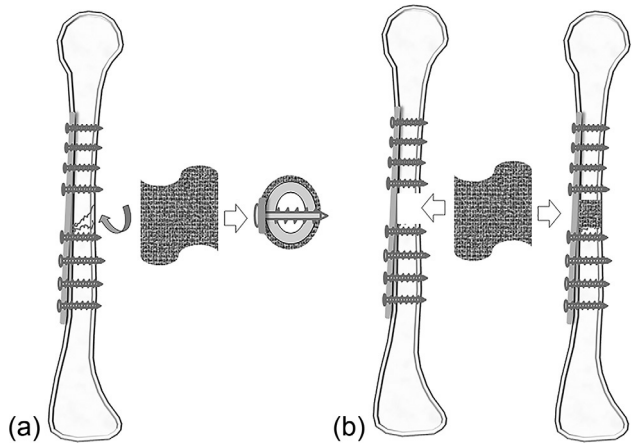

Figure 3.3 Possible use of nonwoven scaffolds for fracture repair/bone tissue regeneration (in combination with/without cells and/or growth factors). (a) Fracture model: the nonwoven scaffold may be used as membrane/bandage to cover the fracture and/or bone defect area; (b) bone defect model: the nonwoven scaffold may be used as filler/gauze to fill the bone defect area.

site, thereby remaining *in situ*. Biological glue or surgical adhesives may be helpful for keeping the scaffold in place (Kukleta et al., 2012). In a flat bone defect such as the calvaria defect, nonwoven scaffolds have the advantage of being able to be cut to the shape of the defect (Figure 3.4a). A well-fitting scaffold may not need any fixation, however, fixing may be needed if the bone defect is large. In such as case, a temporary protective layer/tissue flap may be required to cover the defect area before new bone is formed. Similarly, for nonunion fractures, the nonwoven scaffold may be kept in place by the surrounding tissues or with biological glue or surgical adhesives. In the case of spinal fusion, the nonwoven scaffold may be used as filler/gauze and/or strips to fill the defect area (Figure 3.4b), kept in place by the surrounding tissues.

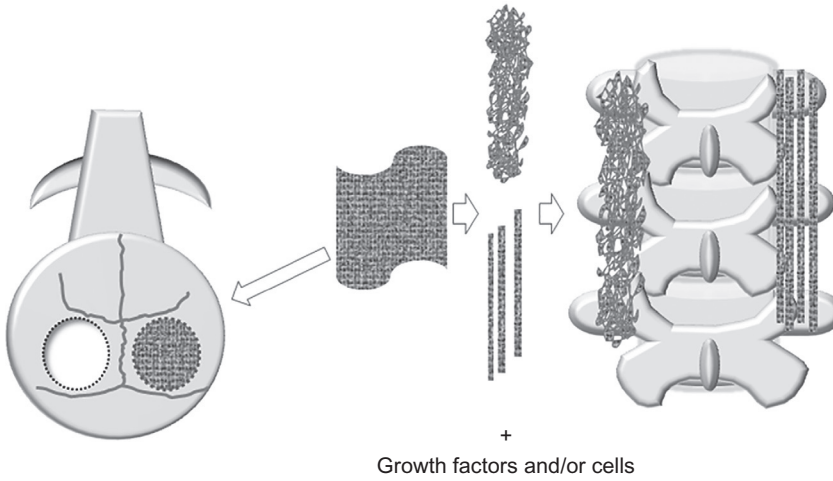

Figure 3.4 Possible application of nonwoven scaffolds in nonweight-bearing areas (in combination with/without cells and/or growth factors). (a) Calvarial defect model: the nonwoven scaffold may be used as membrane/gauze to fill the bone defect area; (b) spinal fusion model: the nonwoven scaffold may be used as filler/gauze/strips to fill areas that are required for spinal fusion.

3.5 Future trends

For nonwoven scaffolds to meet clinical requirements for bone repair and regeneration, they must be able to successfully biomimic aspects of the native tissue, and they must be sufficiently robust for surgical use. Furthermore, they need to be environmentally stable, reproducible in structure, and economically produced from appropriate biomaterials. Meeting these requirements using existing manufacturing techniques, such as electrospinning, is challenging, but the technology is rapidly evolving, and other multistage nonwoven manufacturing methods have yet to be fully explored as alternative production routes for bone scaffolds. Developments in biomaterial science are still required in order to provide fibre-forming materials that are compatible with large scale manufacture while satisfying all performance requirements. Biomaterials such as those based upon functionalised collagen have significant potential for the engineering of nonwoven scaffolds that address both biological and mechanical property requirements. The role of clinicians in guiding tissue scaffold design will continue to be fundamental to the development of functional scaffolds that meet individual patient needs. Better matching of scaffold properties to individual needs is essential if clinical outcomes are to improve, and this can increase the demand for the customisation of nonwoven scaffolds during manufacture and at the bedside. These developments have the potential to make a major impact on current scaffold manufacturing procedures, as well as the development of the regulatory framework.

Acknowledgements

The authors are supported by the Leeds Centre of Excellence in Medical Engineering funded by the Wellcome Trust and EPSRC, WT088908/z/09/z.

References

Agrawal, C.M., Ray, R.B., 2001. Biodegradable polymeric scaffolds for musculoskeletal tissue engineering. J. Biomed. Mater. Res. 55, 141–150.

Alman, B.A., Kelley, S.P., Nam, D., 2011. Heal thyself: using endogenous regeneration to repair bone. Tissue Eng. B Rev. 17, 431–436.

Blakeney, B.A., Tambralli, A., Anderson, J.M., Andukuri, A., Lim, D.-J., Dean, D.R., Jun, H.-W., 2011. Cell infiltration and growth in a low density, uncompressed three-dimensional electrospun nanofibrous scaffold. Biomaterials 32, 1583–1590.

Botchwey, E.A., Dupree, M.A., Pollack, S.R., Levine, E.M., Laurencin, C.T., 2003. Tissue engineered bone: measurement of nutrient transport in three-dimensional matrices. J. Biomed. Mater. Res. Part A 67A, 357–367.

Brinkman, W.T., Nagapudi, K., Thomas, B.S., Chaikof, E.L., 2003. Photo-cross-linking of type i collagen gels in the presence of smooth muscle cells: mechanical properties, cell viability, and function. Biomacromolecules 4, 890–895.

Brown, T., Slotosch, A., Thibaudeau, L., Taubenberger, A., Loessner, D., Vaquette, C., Dalton, P., Hutmacher, D., 2012. Design and fabrication of tubular scaffolds via direct writing in a melt electrospinning mode. Biointerphases 7, 1–16.

Buehler, M.J., 2008. Nanomechanics of collagen fibrils under varying cross-link densities: atomistic and continuum studies. J. Mech. Behav. Biomed. Mater. 1, 59–67.

Cai, K., Yao, K., Yang, Z., Li, X., 2007. Surface modification of three-dimensional poly(D, L-lactic acid) scaffolds with baicalin: a histological study. Acta Biomater. 3, 597–605.

Chakrapani, V.Y., Gnanamani, A., Giridev, V.R., Madhusoothanan, M., Sekaran, G., 2012. Electrospinning of type I collagen and PCL nanofibers using acetic acid. J. Appl. Polym. Sci. 125, 3221–3227.

Charuchinda, A., Molloy, R., Siripitayananon, J., Molloy, N., Sriyai, M., 2003. Factors influencing the small-scale melt spinning of poly(ε-caprolactone) monofilament fibres. Polym. Int. 52, 1175–1181.

Charulatha, V., Rajaram, A., 2003. Influence of different crosslinking treatments on the physical properties of collagen membranes. Biomaterials 24, 759–767.

Chrisey, D.B., 2000. The power of direct writing. Science 289, 879–881.

Chung, S., Gamcsik, M.P., King, M.W., 2011. Novel scaffold design with multi-grooved PLA fibers. Biomed. Mater. 6, 045001.

Cooper, G.M., Mooney, M.P., Gosain, A.K., Campbell, P.G., Losee, J.E., Huard, J., 2010. Testing the critical size in calvarial bone defects: revisiting the concept of a critical-size defect. Plast. Reconstr. Surg. 125, 1685–1692.

Cunha-Reis, C., El Haj, A.J., Yang, X., Yang, Y., 2013. Fluorescent labeling of chitosan for use in non-invasive monitoring of degradation in tissue engineering. J. Tissue Eng. Regen. Med. 7, 39–50.

Dawson, J.I., Kanczler, J.M., Yang, X.B., Attard, G.S., Oreffo, R.O., 2011. Clay gels for the delivery of regenerative microenvironments. Adv. Mater. 23, 3304–3308.

Day, R.M., Maquet, V., Boccaccini, A.R., Jérôme, R., Forbes, A., 2005. In vitro and in vivo analysis of macroporous biodegradable poly(D, L-lactide-co-glycolide) scaffolds containing bioactive glass. J. Biomed. Mater. Res. Part A 75A, 778–787.

de Moraes, M.A., Paternotte, E., Mantovani, D., Beppu, M.M., 2012. Mechanical and biological performances of new scaffolds made of collagen hydrogels and fibroin microfibers for vascular tissue engineering. Macromol. Biosci. 12, 1253–1264.

Detta, N., Brown, T.D., Edin, F.K., Albrecht, K., Chiellini, F., Chiellini, E., Dalton, P.D., Hutmacher, D.W., 2010. Melt electrospinning of polycaprolactone and its blends with poly(ethylene glycol). Polym. Int. 59, 1558–1562.

Di Stefano, D.A., Andreasi Bassi, M., Cinci, L., Pieri, L., Ammirabile, G., 2012. Treatment of a bone defect consequent to the removal of a periapical cyst with equine bone and equine membranes: clinical and histological outcome. Minerva Stomatol. 61, 477–490.

Djabourov, M., 1988. Architecture of gelatin gels. Contemp. Phys. 29, 273–297.

Dong, C.-M., Wu, X., Caves, J., Rele, S.S., Thomas, B.S., Chaikof, E.L., 2005. Photomediated crosslinking of C6-cinnamate derivatized type I collagen. Biomaterials 26, 4041–4049.

Dong, B., Arnoult, O., Smith, M.E., Wnek, G.E., 2009. Electrospinning of collagen nanofiber scaffolds from benign solvents. Macromol. Rapid Commun. 30, 539–542.

Dou, Y., Lin, K., Chang, J., 2011. Polymer nanocomposites with controllable distribution and arrangement of inorganic nanocomponents. Nanoscale 3, 1508–1511.

Dunlop, J.W.C., Fratzl, P., 2010. Biological composites. Annu. Rev. Mater. Res. 40, 1–24.

Durham, E.R., Ingham, E., Russell, S.J., 2012. Technique for internal channelling of hydroentangled nonwoven scaffoldsto enhance cell penetration. J. Biomater. Appl. 28 (2), 241–249.

El-Gendy, R., Yang, X.B., Newby, P.J., Boccaccini, A.R., Kirkham, J., 2013. Osteogenic differentiation of human dental pulp stromal cells on 45S5 Bioglass(R) based scaffolds in vitro and in vivo. Tissue Eng. Part A 19, 707–715.

Gang, E., Ki, C., Kim, J., Lee, J., Cha, B., Lee, K., Park, Y., 2012. Highly porous three-dimensional poly(lactide-co-glycolide) (PLGA) microfibrous scaffold prepared by electrospinning method: a comparison study with other PLGA type scaffolds on its biological evaluation. Fibers Polym. 13, 685–691.

Gaudet, I., Shreiber, D., 2012. Characterization of methacrylated type-i collagen as a dynamic, photoactive hydrogel. Biointerphases C7–25 (7), 1–9.

Gentile, J.V., Weinert, C.R., Schlechter, J.A., 2013. Treatment of unicameral bone cysts in pediatric patients with an injectable regenerative graft: a preliminary report. J. Pediatr. Orthop. 33, 254–261.

Grant, C.A., Brockwell, D.J., Radford, S.E., Thomson, N.H., 2009. Tuning the elastic modulus of hydrated collagen fibrils. Biophys. J. 97, 2985–2992.

Green, D., Walsh, D., Yang, X.B., Mann, S., Oreffo, R.O.C., 2004. Stimulation of human bone marrow stromal cells using growth factor encapsulated calcium carbonate porous microspheres. J. Mater. Chem. 14, 2206–2212.

Gruber, H.E., Gettys, F.K., Montijo, H.E., Starman, J.S., Bayoumi, E., Nelson, K.J., Hoelscher, G.L., Ramp, W.K., Zinchenko, N., Ingram, J.A., Bosse, M.J., Kellam, J.F., 2013. Genomewide molecular and biologic characterization of biomembrane formation adjacent to a methacrylate spacer in the rat femoral segmental defect model. J. Orthop. Trauma. 27, 290–297.

Hartwell, R., Leung, V., Chavez-Munoz, C., Nabai, L., Yang, H., Ko, F., Ghahary, A., 2011. A novel hydrogel-collagen composite improves functionality of an injectable extracellular matrix. Acta Biomater. 7, 3060–3069.

Haugh, M.G., Murphy, C.M., McKiernan, R.C., Altenbuchner, C., O'Brien, F.J., 2011. Crosslinking and mechanical properties significantly influence cell attachment, proliferation,

and migration within collagen glycosaminoglycan scaffolds. Tissue Eng. A 17, 1201–1208.
He, L., Mu, C., Shi, J., Zhang, Q., Shi, B., Lin, W., 2011. Modification of collagen with a natural cross-linker, procyanidin. Int. J. Biol. Macromol. 48, 354–359.
Hong, S.-J., Yu, H.-S., Noh, K.-T., Oh, S.-A., Kim, H.-W., 2010. Novel scaffolds of collagen with bioactive nanofiller for the osteogenic stimulation of bone marrow stromal cells. J. Biomater. Appl. 24, 733–750.
Horner, E.A., Kirkham, J., Wood, D., Curran, S., Smith, M., Thomson, B., Yang, X.B., 2010. Long bone defect models for tissue engineering applications: criteria for choice. Tissue Eng. Part B Rev. 16, 263–271.
Huang, S., Chien, T., Hung, K., 2011. Selective deposition of electrospun alginate-based nanofibers onto cell-repelling hydrogel surfaces for cell-based microarrays. Curr. Nanosci. 7, 267.
Hutmacher, D.W., Schantz, J.T., Lam, C.X.F., Tan, K.C., Lim, T.C., 2007. State of the art and future directions of scaffold-based bone engineering from a biomaterials perspective. J. Tissue Eng. Regen. Med. 1, 245–260.
Ji, J., Bar-On, B., Wagner, H.D., 2012. Mechanics of electrospun collagen and hydroxyapatite/collagen nanofibers. J. Mech. Behav. Biomed. Mater. 13, 185–193.
Kelly, S.M., Jess, T.J., Price, N.C., 2005. How to study proteins by circular dichroism. Biochim. Biophys. Acta Proteins Proteomics 1751, 119–139.
Khira, Y.M., Badawy, H.A., 2013. Pedicled vascularized fibular graft with Ilizarov external fixator for reconstructing a large bone defect of the tibia after tumor resection. J. Orthop. Traumatol. 14 (2), 91–100.
Kim, K.-H., Jeong, L., Park, H.-N., Shin, S.-Y., Park, W.-H., Lee, S.-C., Kim, T.-I., Park, Y.-J., Seol, Y.-J., Lee, Y.-M., Ku, Y., Rhyu, I.-C., Han, S.-B., Chung, C.-P., 2005. Biological efficacy of silk fibroin nanofiber membranes for guided bone regeneration. J. Biotechnol. 120, 327–339.
Kim, H.-W., Lee, H.-H., Knowles, J.C., 2006. Electrospinning biomedical nanocomposite fibers of hydroxyapatite/poly(lactic acid) for bone regeneration. J. Biomed. Mater. Res, A 79A, 643–649.
Kukleta, J.F., Freytag, C., Weber, M., 2012. Efficiency and safety of mesh fixation in laparoscopic inguinal hernia repair using n-butyl cyanoacrylate: long-term biocompatibility in over 1,300 mesh fixations. Hernia 16, 153–162.
Kumbar, S.G., Nukavarapu, S.P., James, R., Nair, L.S., Laurencin, C.T., 2008. Electrospun poly (lactic acid-co-glycolic acid) scaffolds for skin tissue engineering. Biomaterials 29, 4100–4107.
Lai, E.S., Anderson, C.M., Fuller, G.G., 2011. Designing a tubular matrix of oriented collagen fibrils for tissue engineering. Acta Biomater. 7, 2448–2456.
Langer, R., Vacanti, J., 1993. Tissue engineering. Science 260, 920–926.
Lee, J., Lee, S.Y., Jang, J., Jeong, Y.H., Cho, D.-W., 2012. Fabrication of patterned nanofibrous mats using direct-write electrospinning. Langmuir 28, 7267–7275.
Liao, S., Murugan, R., Chan, C.K., Ramakrishna, S., 2008. Processing nanoengineered scaffolds through electrospinning and mineralization suitable for biomimetic bone tissue engineering. J. Mech. Behav. Biomed. Mater. 1, 252–260.
Liu, K., Li, D., Huang, X., Lv, K., Ongodia, D., Zhu, L., Zhou, L., Li, Z., 2013a. A murine femoral segmental defect model for bone tissue engineering using a novel rigid internal fixation system. J. Surg. Res. 183 (2), 493–502.
Liu, X., Rahaman, M.N., Liu, Y., Bal, B.S., Bonewald, L.F., 2013b. Enhanced bone regeneration in rat calvarial defects implanted with surface-modified and BMP-loaded bioactive glass (13–93) scaffolds. Acta Biomater. 9 (7), 7506–7517.

Mastrogiacomo, M., Scaglione, S., Martinetti, R., Dolcini, L., Beltrame, F., Cancedda, R., Quarto, R., 2006. Role of scaffold internal structure on in vivo bone formation in macroporous calcium phosphate bioceramics. Biomaterials 27, 3230–3237.

McCullen, S., Miller, P., Gittard, S., Pourdeyhimi, B., Gorga, R., Narayan, R., Loboa, E., 2010. In situ collagen polymerization of layered cell-seeded electrospun scaffolds for bone tissue engineering applications. Tissue Eng. Part C Methods 16 (5), 1095–1105.

McEachin, Z., Lozano, K., 2012. Production and characterization of polycaprolactone nanofibers via forcespinning (TM) technology. J. Appl. Polym. Sci. 126, 473–479.

McMahon, R.E., Wang, L., Skoracki, R., Mathur, A.B., 2013. Development of nanomaterials for bone repair and regeneration. J. Biomed. Mater. Res. B Appl. Biomater. 101B, 387–397.

Meyer, M., Baltzer, H., Schwikal, K., 2010. Collagen fibres by thermoplastic and wet spinning. Mater. Sci. Eng. C 30, 1266–1271.

Nam, J., Huang, Y., Agarwal, S., Lannutti, J., 2007. Improved cellular infiltration in electrospun fiber via engineered porosity. Tissue Eng. 13, 2249–2257.

Olde Damink, L.H.H., Dijkstra, P.J., Luyn, M.J.A., Wachem, P.B., Nieuwenhuis, P., Feijen, J., 1995a. Crosslinking of dermal sheep collagen using hexamethylene diisocyanate. J. Mater. Sci. Mater. Med. 6, 429–434.

Olde Damink, L.H.H., Dijkstra, P.J., Luyn, M.J.A., Wachem, P.B., Nieuwenhuis, P., Feijen, J., 1995b. Glutaraldehyde as a crosslinking agent for collagen-based biomaterials. J. Mater. Sci. Mater. Med. 6, 460–472.

Olde Damink, L.H.H., Dijkstra, P.J., van Luyn, M.J.A., van Wachem, P.B., Nieuwenhuis, P., Feijen, J., 1996. Cross-linking of dermal sheep collagen using a water-soluble carbodiimide. Biomaterials 17, 765–773.

O'Leary, L.E.R., Fallas, J.A., Bakota, E.L., Kang, M.K., Hartgerink, J.D., 2011. Multihierarchical self-assembly of a collagen mimetic peptide from triple helix to nanofibre and hydrogel. Nat. Chem. 3, 821–828.

Pelegrine, A.A., Aloise, A.C., Zimmermann, A., Oliveira, R.D., Ferreira, L.M., 2013. Repair of critical-size bone defects using bone marrow stromal cells: a histomorphometric study in rabbit calvaria. Part I: Use of fresh bone marrow or bone marrow mononuclear fraction. Clin. Oral Implants Res.

Pham, Q.P., Sharma, U., Mikos, A.G., 2006. Electrospun poly(epsilon-caprolactone) microfiber and multilayer nanofiber/microfiber scaffolds: characterization of scaffolds and measurement of cellular infiltration. Biomacromolecules 7, 2796–2805.

Phipps, M.C., Clem, W.C., Grunda, J.M., Clines, G.A., Bellis, S.L., 2011. Increasing the pore sizes of bone-mimetic electrospun scaffolds comprised of polycaprolactone, collagen I and hydroxyapatite to enhance cell infiltration. Biomaterials 33, 524–534.

Porter, J.R., Henson, A., Popat, K.C., 2009. Biodegradable poly(epsilon-caprolactone) nanowires for bone tissue engineering applications. Biomaterials 30, 780–788.

Puppi, D., Piras, A.M., Chiellini, F., Chiellini, E., Martins, A., Leonor, I.B., Neves, N., Reis, R., 2011. Optimized electro- and wet-spinning techniques for the production of polymeric fibrous scaffolds loaded with bisphosphonate and hydroxyapatite. J. Tissue Eng. Regen. Med. 5, 253–263.

Rnjak-Kovacina, J., Weiss, A.S., 2011. Increasing the pore size of electrospun scaffolds. Tissue Eng. B Rev. 17, 365–372.

Schroeder, J.E., Mosheiff, R., 2011. Tissue engineering approaches for bone repair: concepts and evidence. Injury 42, 609–613.

Shanmugasundaram, S., Griswold, K.A., Prestigiacomo, C.J., Arinzeh, T., Jaffe, M., 2004. Applications of electrospinning: tissue engineering scaffolds and drug delivery system. In: Bioengineering Conference: Proceedings of the IEEE 30th Annual Northeast. IEEE.

Shi, X., Chen, S., Zhao, Y., Lai, C., Wu, H., 2013. Enhanced osteogenesis by a biomimic pseudo-periosteum-involved tissue engineering strategy. Adv. Healthcare Mater. 2 (9), 1229–1235.

Shin, S.-Y., Park, H.-N., Kim, K.-H., Lee, M.-H., Choi, Y.S., Park, Y.-J., Lee, Y.-M., Ku, Y., Rhyu, I.-C., Han, S.-B., Lee, S.-J., Chung, C.-P., 2005. Biological evaluation of chitosan nanofiber membrane for guided bone regeneration. J. Periodontol. 76, 1778–1784.

Tronci, G., Doyle, A.J., Russell, S.J., Wood, D.J., 2013a. Structure-property-function relationships in triple-helical collagen hydrogels. Mater. Res. Soc. Symp. Proc. 1498, 145–150.

Tronci, G., Doyle, A.J., Russell, S.J., Wood, D.J., 2013b. Triple-helical collagen hydrogels via covalent aromatic functionalisation with 1,3-Phenylenediacetic acid. J. Mater. Chem. B 1, 5478–5488.

Tronci, G., Russell, S.J., Wood, D.J., 2013c. Photo-active collagen systems with controlled triple helix architecture. J. Mater. Chem. B 1, 3705–3715.

Udehiya, R.K., Amarpal, Aithal, H.P., Kinjavdekar, P., Pawde, A.M., Singh, R., Taru Sharma, G., 2013. Comparison of autogenic and allogenic bone marrow derived mesenchymal stem cells for repair of segmental bone defects in rabbits. Res. Vet. Sci. 94, 743–752.

Vaquette, C., Cooper-White, J.J., 2011. Increasing electrospun scaffold pore size with tailored collectors for improved cell penetration. Acta Biomater. 7, 2544–2557.

Venugopal, J.R., Low, S., Choon, A.T., Kumar, A.B., Ramakrishna, S., 2008. Nanobioengineered electrospun composite nanofibers and osteoblasts for bone regeneration. Artif. Organs 32, 388–397.

Weadock, K.S., Miller, E.J., Bellincampi, L.D., Zawadsky, J.P., Dunn, M.G., 1995. Physical crosslinking of collagen fibers: comparison of ultraviolet irradiation and dehydrothermal treatment. J. Biomed. Mater. Res. 29, 1373–1379.

Williamson, M.R., Adams, E.F., Coombes, A.G.A., 2006. Gravity spun polycaprolactone fibres for soft tissue engineering: interaction with fibroblasts and myoblasts in cell culture. Biomaterials 27, 1019–1026.

Woodruff, M.A., Lange, C., Reichert, J., Berner, A., Chen, F., Fratzl, P., Schantz, J.-T., Hutmacher, D.W., 2012. Bone tissue engineering: from bench to bedside. Mater. Today 15, 430–435.

Wu, Y., Dong, Z., Wilson, S., Clark, R.L., 2010. Template-assisted assembly of electrospun fibers. Polymer 51, 3244–3248.

Yang, X.B., Roach, H.I., Clarke, N.M., Howdle, S.M., Quirk, R., Shakesheff, K.M., Oreffo, R.O., 2001. Human osteoprogenitor growth and differentiation on synthetic biodegradable structures after surface modification. Bone 29, 523–531.

Yang, X., Tare, R.S., Partridge, K.A., Roach, H.I., Clarke, N.M., Howdle, S.M., Shakesheff, K.M., Oreffo, R.O., 2003a. Induction of human osteoprogenitor chemotaxis, proliferation, differentiation, and bone formation by osteoblast stimulating factor-1/pleiotrophin: osteoconductive biomimetic scaffolds for tissue engineering. J. Bone Miner. Res. 18, 47–57.

Yang, X.B., Green, D.W., Roach, H.I., Clarke, N.M., Anderson, H.C., Howdle, S.M., Shakesheff, K.M., Oreffo, R.O., 2003b. Novel osteoinductive biomimetic scaffolds stimulate human osteoprogenitor activity–implications for skeletal repair. Connect. Tissue Res. 44 (Suppl. 1), 312–317.

Yang, X.B., Whitaker, M.J., Sebald, W., Clarke, N., Howdle, S.M., Shakesheff, K.M., Oreffo, R.O., 2004. Human osteoprogenitor bone formation using encapsulated bone morphogenetic protein 2 in porous polymer scaffolds. Tissue Eng. 10, 1037–1045.

Yang, W., Yang, F., Wang, Y., Both, S.K., Jansen, J.A., 2012. In vivo bone generation via the endochondral pathway on three-dimensional electrospun fibers. Acta Biomater. 9 (1), 4505–4512.

Yokoyama, Y., Hattori, S., Yoshikawa, C., Yasuda, Y., Koyama, H., Takato, T., Kobayashi, H., 2009. Novel wet electrospinning system for fabrication of spongiform nanofiber 3-dimensional fabric. Mater. Lett. 63, 754–756.

Zha, Z., Teng, W., Markle, V., Dai, Z., Wu, X., 2012. Fabrication of gelatin nanofibrous scaffolds using ethanol/phosphate buffer saline as a benign solvent. Biopolymers 97, 1026–1036.

Zhang, X., Awad, H.A., O'Keefe, R.J., Guldberg, R.E., Schwarz, E.M., 2008. A perspective: engineering periosteum for structural bone graft healing. Clin. Orthop. Relat. Res. 466, 1777–1787.

Zhang, M., Wu, K., Li, G., 2011. Interactions of collagen molecules in the presence of N-hydroxysuccinimide activated adipic acid (NHS-AA) as a crosslinking agent. Int. J. Biol. Macromol. 49, 847–854.

Zhou, X., Cai, Q., Yan, N., Deng, X., Yang, X., 2010. In vitro hydrolytic and enzymatic degradation of nestlike-patterned electrospun poly(D, L-lactide-co-glycolide) scaffolds. J. Biomed. Mater. Res. A 95A, 755–765.

Bioabsorbable fabrics for musculoskeletal scaffolds

4

Minna Kellomäki[1,2], *Kaisa Laine*[1,2], *Ville Ellä*[1,2], *Tuija Annala*[3]
[1]BioMediTech, Tampere, Finland; [2]Tampere University of Technology, Tampere, Finland; [3]Scaffdex Oy, Tampere, Finland

4.1 Introduction

The need to repair musculoskeletal tissues is increasing worldwide due to the ageing of the population and the increasing number of sports injuries. Bioabsorbable implants are already used in regenerative medicine, but tissue engineering (TE) approaches using porous bioabsorbable scaffolds, either with preseeded cells or without, are also emerging. The term scaffold refers to a highly porous, bioabsorbable implant with interconnected, suitably sized pores.

There are different approaches to applying TE, depending on whether cells are seeded into the scaffolds *in vitro* (Langer and Vacanti, 1993) or they penetrate into the scaffolds *in vivo* (Honkanen et al., 2003). A scaffold or a tissue-engineered implant can be implanted *in situ* (Honkanen et al., 2003), or it can be implanted in another anatomical location in order to grow and mature before being transferred to its final site (Mesimäki et al., 2009).

Fibrous, nonwoven scaffolds have been studied since the early days of TE, but textiles with more organized structures, weaves, knits, and braids were developed more recently. These types of textiles can be suitable for bone, cartilage, ligament, and tendon tissues because of their suitable mechanical properties. They can form highly oriented scaffolds and support the oriented ingrowth of cells. Also, TE methods are efficient and cost-effective compared to many other methods applied in experimental TE. Textiles provide the greatest benefits for healing tissue when these special features are utilized. If textile scaffolds are used to support healing tissue, then long-term support is most likely needed, and slowly degrading fibres are chosen for the scaffolds.

4.2 Bioabsorbable materials, fibre spinning and properties, and yarn preparation

Textile scaffolds are manufactured from fibres or yarns, and thus, the chosen bioabsorbable materials must be capable of being spun into fibres. Both synthetic and natural polymer groups contain raw materials that have thermal or solubility properties

Biomedical Textiles for Orthopaedic and Surgical Applications. http://dx.doi.org/10.1016/B978-1-78242-017-0.00004-0

suitable for withstanding spinning parameters. Among the synthetic polymers, the poly-α-hydroxy acids (e.g., polylactides (PLAs) such as homopolymers or copolymers, and polyglycolide (PGA)) have been most widely used, and polyhydroxyalkanoates (PHAs) have also been spun into fibres. Of the polymers of natural origin, silk, hyaluronic acid derivatives, and chitosan have been electrospun into nanofibrous structures, and to promote the regeneration of functional tissue, two or more materials can be combined (Nair and Laurencin, 2007; Moutos and Guilak, 2008). For example, some bioactive glasses (BaGs), which are resorbable in the body, have been melt-spun into fibres. BaGs need to have specific chemistry to create melting and viscosity profiles suitable for spinning, however (Brink, 1997). So, they have not been frequently used alone, but rather together with polymer fibres or matrices coated to withstand the stresses of textile manufacturing. We refer to different materials in more detail later in this chapter.

Researchers have used three different spinning methods to manufacture micro- or macroscale fibres from different polymers. If the polymer is a thermoplast and has a large enough temperature window for extrusion, melt spinning can be used. The polymer is melted and extruded into either mono- or multifilaments (Kellomäki and Törmälä, 2003). From a regulatory perspective, this method produces easier end-products because it does not require potentially harmful solvents. Fibres can be produced from the polymer solution either by dry spinning or by wet spinning (Han, 2007). In the first method, fibres are drawn from the polymer solution and solvent is evaporated in the drawing process, and in the latter one, fibres are drawn from the solution into a coagulation bath, followed by an optional bath for washing away the chemical residues. All of these methods have been used to spin bioabsorbable polymer fibres.

Typically, as-spun fibres do not have high enough strength for processing textiles, but they require orientation through a stretching phase. This phase is completed at a temperature above the glass transition temperature (and below the melting temperature area if the raw material is semicrystalline) so that polymer chains can be aligned and drawn in the desired direction, thus creating stronger fibres. The strength, Young's modulus, and strain of the filaments can be increased remarkably by this technique, benefiting the processability of the fibres into yarns and textiles (Kellomäki and Törmälä, 2003). In order to be formed into yarns, the filaments are twisted, and the looser the twist, the softer and airier the yarn. It is also possible to make multicomponent yarns from different types of filaments. From a processing point of view, yarns are easier to handle than separate filaments because, in yarns, the filaments remain closer to each other, and the influence of static electricity is reduced. Also, the mechanical properties of fibres can be improved by twisting several fibres into yarns (Freeman et al., 2007). Common finishing methods for further changing the properties of the fibres and yarns include air-jet texturing and twisting stabilized by heat (Hearle et al., 2001). Both of these methods make fibres fluffier, increasing the surface area of the textile, but these methods have not been widely used for TE scaffolds.

Manufacturers can easily use yarn properties to alter the mechanical and physical properties of the fibres, as well as the thickness and stiffness of the fabrics and textile scaffolds. Porosity, water permeability, and degradation rates can be controlled by

yarn diameter and shape, number of filaments in the bundle, and twisting. Mono- and multifilament yarns from continuous or stable fibres are used for this purpose. Multifilament yarns with a loose twist can have a high void content compared to dense monofilament yarn. Polymer composition, purity, and crystallinity, as well as physical properties, such as geometrical shape and size, also affect the mechanical properties of scaffolds and strongly influence the scaffold's degradation rate and its other biological properties. Fibre and yarn diameters further determine the thickness, stiffness, and porosity of the product, and all of these properties can be affected by the parameters of the fibre manufacturing method, including extrusion speed, twist, and fibre cross-section profiles. Processing biodegradable fibres is challenging due to the fact that biodegradable yarns are sensitive, and the usage of avivage substrates is limited (Ekevall et al., 2004; Freeman et al., 2007; Heniford, 2011).

4.3 Processing technologies for fabrics

The manufacturing of fabrics enables the rapid production of porous three-dimensional (3D) structures in a reproducible manner, so that the predetermined porous structures can be generated in large quantities. Three traditional textile manufacturing methods – weaving, knitting, and braiding – are also used to fabricate different implantable textiles from yarns. Inherently, most of the methods for manufacturing fabrics involve continuous processes. The manufacturing of discrete, separate units is challenging, especially when the units must be produced in a commercially acceptable way (i.e., using semiautomatic or automatic machines).

4.3.1 Weaving

Weaving is a method for producing fabrics through the continuous interlacing of perpendicular yarn sets: weft and warp yarns. The structure of the woven fabric can be varied by altering the interlacing pattern of yarns, the number of yarn sets, and yarn layers, or by filler yarns. At least one additional yarn set is required in 3D weaving.

Traditionally, weaving is based on lifting several fibres at constant intervals (warps) and threading a perpendicular interlacing yarn (weft) in to form a filling insertion. Yarns are lifted in repeating sequences, leading to a repeating weave pattern along the length of the fabric. More complex structures are able to manufacture fabrics using Jacquard weaving, which separately controls the movement of each warp yarn so that a variety of weaving patterns can be manufactured within the same fabric. 2D and 3D multilayer fabrics can be woven using similar weaving machines, but 3D weaving requires an additional warp set (Heniford and Koslosky, 2010).

Weaving methods enable the production of 2D structures and 3D multilayer structures with varying densities. In this process, the thickness of the fabric is related to yarn diameters and number of yarn layers. Also, tubular structures and branched tubes can be fabricated when the weft yarn is continuously wrapped around the structure. Seamless near-net shape structures can be fabricated when altering the interlacing depth of the yarn. Currently, woven fabrics as thin as 40–50 μm can be fabricated,

but the thickness can reach up to several centimetres (Heniford, 2011; Heniford and Koslosky, 2010). Seamless near-net shape structures can be fabricated by altering the interlacing depth of yarns to separate structural sections that can be shaped and remodelled after the weaving process (Miravete, 1999; Long, 2005).

4.3.2 Knitting

Knitting is a method for producing fabrics from interlocking yarn loops that can be in series in the weft or warp directions. Needles form interlooping stitches by catching the yarn on the needles and drawing the yarn loop through previous loops. In *weft knitting*, yarn loops are formed in the transverse direction by creating adjacent loops one after the other. The transverse stitching pattern is formed when knots are in a series of weft yarn. The whole fabric can be prepared from one strand of yarn, and the formed structure is flexible and distortable due to the yarn loops, with the thread enabling movement in the structure. The weft knit unravels easily, however, which makes it unsuitable for applications in which the end-user wants to cut it from a preform (e.g., a surgeon wanting to reshape the fabric with scissors in an operation theatre).

Warp knitting forms longitudinal stitching patterns in which adjacent yarn loops are interlocked with each other, and in this method, a row of loops can be formed at once. Each needle requires its own thread, and the system must be equipped with as many yarns as there are columns within the width of the fabric. Warp knitting enables the fabrication of more stable and less formable structures (Wang et al., 2011). The structure of the warp knits can better withstand holes and scissoring, making it more suitable for surgical use.

Depending on the design, the position, and the number of needles and needle beds, the structure of the knitted fabric can vary. Flat and tubular structures, as well as layered or two-faced structures with altering densities, can be manufactured. The interlocking of adjacent loops also enables the formation of webs and holes in the structure. Both warp and weft knitting utilize continuous yarns.

4.3.3 Braiding

Braiding is a method for fabricating flat and tubular structures by twisting adjacent, continuous vertical yarns around each other. The strands of yarn are ordered diagonally in the structure, and the simplest braid, plait, is a flat structure that is fabricated from three yarns. A variety of braided structures can be made by changing the number of the yarns and the floating lengths in twisting. In addition, tubular braids can be produced over the mandrels to fix the internal diameter and to create near-net shape braids (Heniford, 2011). Stuffed, tubular braids can be made by braiding over yarns or bundled yarns.

4.3.4 Other methods

Other fibre and textile methods applied in regenerative medicine and TE are nonwoven technologies, electrospinning, and rotational spinning. Of these, nonwoven structures were introduced for experimental TE in the 1990s, and they have been used most frequently, possibly due to their long commercial availability under the trade name

Ethisorb™ (http://www.depuy.com/healthcare-professionals/products/). Ethisorb™ is a composite of a fleece of undyed Polyglactin 910 (Vicryl) and undyed poly-P-dioxanon (PDS), with both Vicryl and PDS also being used as suture materials. Absorption is complete approximately 90 days after implantation (i.e., it degrades relatively rapidly). In this chapter we do not concentrate on nonwovens, however.

Typically, nonwovens are produced using staple fibres, and the structure formed is more random than one made with the previously described methods. A web can be made by wet-laid, air-laid, spun-laid, carding, or melt blowing methods. Most of the webs have relatively loose structures, and therefore, they need to be strengthened. This is typically done by bonding the web and is possible using thermal, chemical, or mechanical means or by needle punching.

The demand to mimic nature on the nanoscale has led to efforts to create an optimal scaffold to culture and house the cells through electrospinning. Several excellent reviews offer further information on this technique (e.g., Huang et al., 2003; Pham et al., 2006; Liu et al., 2013), but work done with nanoscale applications are not referred in more detail here.

Rotational spinning, either by melting the polymer (Huttunen and Kellomäki, 2011) or through the use of solution (Badrossamay et al., 2010), has emerged in recent years to produce submicron or nanoscale webs, thereby providing an alternative to electrospinning. Though interesting methods, rotational spinning techniques have not yet been used for scaffold and cell culture studies to any significant degree, and therefore, we do not discuss them in more detail to this chapter.

4.4 Fabric structures and their characteristics

Textile types each have unique properties that depend on the binding of the yarns in the structure. Different fabrics are used to achieve different physical and mechanical properties, such as thickness, strength, and flexibility. Textile properties are highly dependent on the yarn geometry and the shifting capacity of the yarn in the structure, as well as the number and area of the yarns' interlacing points in the structure. In general, knitted fabrics are the most flexible, and woven structures are the most stable, with the braided ones in between (Hutmacher, 2000; Long, 2005; Miravete, 1999). Overall flexibility can be useful in application such as skin substitutes, and braids have been utilized in tendon replacements because of their suitable uniaxial behaviour. For bone, stronger scaffolds are needed, however. Examples of textile types made from different PLA (P(L/D)LA 96/4) fibres and the scaffold types made from those textiles are given in Figure 4.1.

An optimal scaffold has a high surface area-to-volume ratio, a high degree of porosity, and pores that are highly interconnected, all of which are demands that textiles can meet. In general, textiles are lightweight, but they can be made dense when requested. A compaction feature is typical for many textile structures in order to make them mouldable and to ease implantation. Textile structures can be roughly divided into hollow and dense structures. Layered constructs enable the induction of different properties, such as density, roughness, and degradation rate, in each side of the structure by varying materials and fabric design (Freed et al., 2009). The advantage of textile structures is their

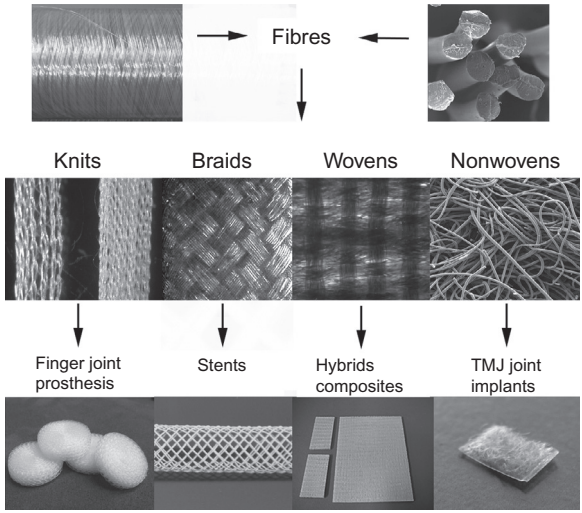

Figure 4.1 Upper row: Reel of (P(L/D)LA 96/4) multifilament after melt spinning and orientation (left) and an SEM image of the same multifilaments (right). Middle row: Textile structures made of (P(L/D)LA 96/4). Lower row: Scaffolds made of the textiles. The 3D hybrid/composite plates are made of PLA +BaG yarns.

delamination-free character, and for that reason, they withstand shear stresses. Textiles can also be used as preforms and processed further for specific applications.

Desired textile properties vary depending on the intended body site. Musculoskeletal scaffolds should flex and transform shape together with the surrounding muscles and tendons, and at the same time, they must promote new tissue growth. Friction forces between yarns hold the structure together, enabling an even distribution and balance of external mechanical stresses. Another advantage of textile structures is that yarns are in ordered places, which enables the clinician to control the scaffold's degree of porosity, pore sizes, and shape. The definite structure also allows improved control of the structural degradation of scaffolds. In addition, ordered textile structures provide for interconnected pores and the control of the porosity that are important for fluid transportation into and through the 3D structure. Fluid transfer is essential for the operation of the nutrition system, gas-exchange, and the elimination of by-products. By altering different densities, layer thicknesses, and surface topologies, fabricated structures with suitable characteristics and control of tissue ingrowth into the structure can be tailored. Generally, high porosity and high surface area are shown to promote tissue growth inside the structure. The desired surface topology and pore sizes vary depending on seeded cells. Also, cell attachment and subsequent growth in the textile scaffold can be affected by the initial properties of the yarn and different textile structures (Hutmacher, 2000; Ekevall et al., 2004; Heniford and Koslosky, 2010).

4.4.1 Characteristics of woven structures

Woven structures usually have highly ordered yarn geometry, and they are dimensionally stable and dense structures. Woven structures have the highest strength values, and they have the highest variation potential among textile structures. Currently, flat, tubular and near-net shape structures can be manufactured with varying widths from 1 mm to

several metres and thicknesses from 40 to 50 μm to several centimetres. Tubes with diameters as small as 0.5 mm have been reported. The high volume fraction of the yarns resulting from the high packing density is a major advantage of woven fabrics; the high packaging density of the yarns results in the highest compression strength compared to other textile structures. Woven structures also support high tensile loads and have low elongations (Epstein et al., 1992; Lee, 1993; Heniford, 2011).

The characteristics of woven fabrics are based on the length of float stitches and the density of the interlacing points. The most-used weaving patterns are plain weave, twill, panama, and satin, which can be created in 2D fabrics and on the surface of 3D structures. Plain weave is the densest, but twill has better resistance to abrasion, and satin is the softest.

In weaves, fibres are commonly aligned in 2D and woven structures have poor resistance in the through-the-plane direction. 3D woven fabrics can be developed to improve tensile strength in the through-the-plane direction, as well as compression and shear strengths. The damage resistance of the structure can be improved by improving thickness and direction, but, at the same time, strength values in the plane direction weaken. Strains in the plane direction cannot spread in the structure, and weight-carrying capacity is decreased (Epstein et al., 1992; Lee, 1993; Miravete, 1999; Long, 2005; Tamayol et al., 2012).

3D woven structures consisting of one binding warp yarn set and several weft yarn sets can be divided into orthogonal, through-the-thickness angle interlock, and angle interlock patterns, depending on the depths of the warp yarn meandering through the structure. In addition, multiple-layer weaving enables the fabrication of hollow spacer structures in which two separate woven surfaces are bound together with binding yarns. The interspace structure can be formed from binding yarns or woven cell walls. The density of the interlacing yarn points and the length of the binding yarns between two surfaces affect the perpendicular compactness. Hollow and spacious structures have lightweight and high energy-absorbing ability relative to their volume (Epstein et al., 1992; Miravete, 1999).

3D weaves are durable and ideal for applications that require long-term wear, because they are flexible enough to move with body's natural motions, without delaminating. Different densities through the thickness can be introduced to the structure to enhance controlled permeability and to create special reinforcement zones. Surface topography can also be varied via the weaving pattern and altering the number of yarn layers within the fabric (Epstein et al., 1992; Heniford and Koslosky, 2010; Heniford, 2011; Tamayol et al., 2012).

4.4.2 Characteristics of knitted structures

Knitted structures are composed of interlocking yarn loops with an anisotropic structure. The properties of knitted fabrics differ from those of woven structures because the yarns are not orientated into any direction, and the yarn direction changes continuously. Yarn loops can move across each other in the structure, and knitted fabrics are elastic and easy to shape. Lines of tying knots of weft-and-warp-knitted fabrics are perpendicular to each other. Warp-knitted yarns meander more from the knitting

direction than weft-knitted yarns do, resulting lower yarn mobility and thus increased stability in warp-knitted structures.

High yielding prior to tearing is a characteristic of knitted structures because the yarns in the structure can slide due to strain forces. Knitted structures also have high bursting strength, and they usually have lower yarn densities than woven structures. This leads to the higher porosity as well as to lower thickness and compression strength. Generally, knits are highly conformable, and they are able to form smooth and even contact over nonuniform anatomical structures. In addition, knitted structures function as cavity-filling bulk because they can be compressed and inserted easily into small cavities (Heniford, 2011).

Both flat and tubular structures are possible using knitted fabrics. The fabrication of holes in a knitted structure is also possible, which increases the permeability of the knitted fabric. High surface area and open pore structure yield high ingrowth potential, and the properties of knitted spacer structures are determined by the characteristics of surface knits and yarn properties in the interspace. Surface knits increase the elasticity and permeability of the structure (Epstein et al., 1992; Miravete, 1999; Horrocks and Anand, 2000; Hutmacher, 2000; Heniford, 2011).

4.4.3 Characteristics of braided structures

Braided structures are composed of three or more yarns intertwining over each other. In braids, the yarns have an axial orientation, and they form a diagonally overlapping pattern. In general, braided structures have the highest axial strength compared to other textile structures, and they are suitable for applications requiring high in-plane mechanical strength. Braids can transfer large loads and provide extension due to their structure. The characteristics of braided structures can vary by altering how the constituent yarns interrelate with each other and whether the braids are tubular or flat. Porosity and mechanical properties can be adjusted spatially by varying factors such as the number of yarns, the yarn angle relative to the vertical direction, and the number of interlacing points per width. By using unidirectional core yarns, the longitudinal strength of a braid is increased, and the strain is modified considerably. The porosity degree of braided structures usually falls between those of knitted and woven structures (Wulfhorst et al., 2006; Freeman et al., 2007; Heniford, 2011; Tamayol et al., 2012).

4.4.4 Characterization and modelling of fabrics for tissue engineering purposes

Fabric characteristics can be studied by mechanical testing, but this is a slow and an expensive method. Graphical modelling and mathematical modelling employing different mathematical formulas can be used to evaluate the characteristics of different structures and to predict their behaviour, however. Straight fibres and yarns have the best ability to carry loads, and for that reason, modelling is used to evaluate the degrees of curvature in the yarns. When yarn diameters, cross sections, and their

geometry in the structure are known, the designer can determine density, volume fractions of yarns, and their contact surfaces (Lee, 1993; Long, 2005).

In TE there is a demand for small-scale scaffolds that have accurate structures, high porosity, and high pore interconnectivity. Microcomputed tomography (μ-CT) now offers a good tool for this characterization. Imaging, followed by the reconstruction of the 3D image and analysis of the scaffold structure, is providing information that was not previously easy to obtain. For example, Figure 4.2 shows a joint scaffold: Figure 4.2a shows the original photograph of a joint scaffold (which is discussed later in this chapter), and Figure 4.2b shows its reconstructed image from which the porosity can be characterized.

Due to the demand for TE scaffolds, as well as the high costs of the *in vitro* and *in vivo* stages of the research and development work, designing and modelling tools could highly benefit the field. There are numerous computer software packages available for designing and modelling textiles, depending on the type of the manufacturing process used. Computer-aided design (CAD) is also used by the textile industry to improve work and documentation. CAD programs aid the engineering of textile assemblies in order to define structures, predict mechanical properties, and carry out common calculations. The programs input weave and knit patterns along with the yarn properties. On the other hand, computer-aided manufacturing (CAM) is dedicated to the manufacturing of advanced textile structures based on the use of conventional weaving technology. It has been used to manufacture 2D and 3D textile

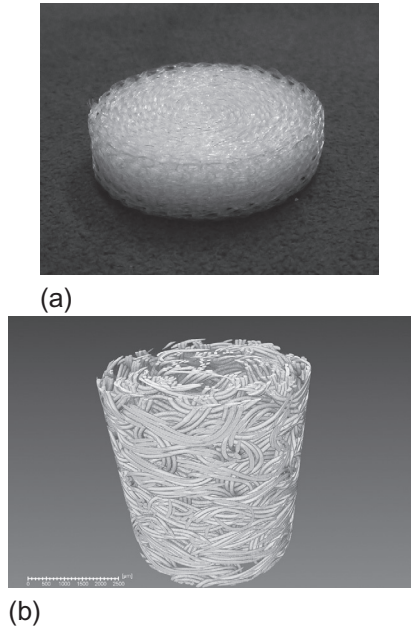

Figure 4.2 (a) A photographic illustration of P(L/D)LA 96/4 joint scaffolds. (b) A micro-CT image of an internal part of a joint scaffold.

structures with both solid and hollow architectures. Thus the CAD/CAM software for textiles is designed to streamline design and manufacturing, as well as the business side of the industry, because cost-saving is a key target of the industry.

The structural modelling of fabrics by considering their uniaxial and biaxial deformation began in the 1970s (Kawabata et al., 1973a,b) when finite deformation theories were calculated using plain-weave fabrics. Improved and more accurate models have since been proposed for plain-weave fabrics (Xiao et al., 2011). Modern techniques, such as 3D simulations, are commonly used to verify the results.

Industry will benefit from these simulations because the characteristics of the large-scale fabric systems can be studied, giving rise to real-time simulations of chosen fabric systems in order to understand the structure–property relationship. The factors influencing the structural properties of the scaffold can be divided into yarn composition or structure-related factors (e.g., filament number, fibre type, fibre strength, twist) and fabric-related factors (e.g., yarn density, fill direction, weave, crimp). Hence, the large number of factors, combined with the physical properties (e.g., nonlinear viscoelasticity, frictional effects) and fabric performance requirements (e.g., bulk, surface, transfer), creates a complex modelling task (Dastoor et al., 1994). Although there has been a lot of research in this field, no widely accepted model currently explains and expresses all aspects of a fabric's mechanical properties. Therefore, the simulation has been split into different modelling tasks at the macroscopic, mesoscopic, and microscopic scales (Vidal-Sasse and Boisse, 2012). For periodic materials in the mesoscopic scale, the modelling focuses on the smallest elementary pattern that can be distinguished. Therefore, the scale is close to the dimension of the yarn, from one to several millimetres, whereas the macroscopic scale is larger, representing the whole fabric. The microscopic scale, on the other hand, is centred on individual fibres, thus taking into account all the surrounding fibres in a yarn. On the molecular level, the fibre has certain properties due to its elemental structure, from atomic level to the level of polymeric organization, that actually forms the fibrils and finally the fibre. This low-level modelling is usually disregarded because the fibre has certain property values (e.g., elasticity, modulus) that are known and can thus be taken into account in the higher-level modelling. An approach that starts with the micro-scale fibres and then expands into the yarns and then the rows represents the basics of fabric modelling. The popular models usually represent the macroscopic scale of the fabric, because it is thought to provide reasonably correct and reliable results for most applications used with periodic fabrics. This ease of modelling comes from finite element modelling based on the smallest unit cell appropriate. The things frequently modelled are the different mechanical features of the fabric and permeability or filtration properties.

Several types of CAD software can be used to design models that suit the scaffold design in regard to TE purposes. One software package that estimates the suitability of a TE fabric construct is ProCad WarpKnit3D (Di et al., 2012; He et al., 2012). The CAD software already available in the market can be used to design the fabric in a way that accounts for the tissue engineered construct restrictions. The predominant restrictions are the fabric's mechanical properties, pore size, and pore size distribution. The modelling of fabrics has not widely been used in TE, however. But, as our

knowledge of the interactions and attractive or distractive forces between cells and yarns/3D fabric constructions increases, the modelling of the living environment can be adapted to fabric manufacturing, with all its complexity. Therefore, the CAD and CAM are still waiting to be applied to the field of TE.

4.5 Bone tissue engineering using fabrics

Bone is a hard tissue that mainly consists of ceramic, calcium phosphate (CaP), and collagen. It has to bear loads that may eventually be high, especially in long bones, and it is well vascularized, with an internal neural network. To mimic bone and fulfil the demands of a hard-tissue implant, a reinforced composite biomaterial including CaP may be an optimal solution. Bone has three main cell types: osteocytes, osteoblasts, and osteoclasts. Of these, osteoblasts are most commonly studied using scaffolds for TE bone treatments, but the other two types of cells have their own important roles in the development and remodelling of the bone toward mature tissue.

Textile reinforcements provide an appropriate alternative for bone TE due to their high structural load capacity. Bone scaffolds with pore sizes of 300–500 μm have been shown to enhance diffusion rates and to promote cell growth (Hutmacher, 2000). As tight and stiff structures, woven structures have also attracted interest given their potential for the internal stabilization of long bone fractures, annular repair, and the stabilization of the spine (Koslosky, 2010). Also, woven structures with reinforced holes for screws and other fastening components may become more common when bone plates must be attached to the bone (Heniford and Koslosky, 2010). With suitable material selection, woven structures can thus enable the introduction of bone-like strength-to-weight properties in TE implants (Koslosky, 2010).

Textile structures can also stimulate cell growth and differentiation by introducing a morphology that directs the differentiation. Multilayer woven scaffolds with multiple densities and materials have the potential to encourage stem cells to generate the correct type and amount of repairable tissue. This is especially interesting when repairing full-thickness cartilage injuries (osteochondral defects) that extend to bone (Koslosky, 2010). Bone-to-bone interfaces integrate better and faster than bone-to-cartilage interfaces (Freed et al., 2009).

Woven structures can be used on the surface of the rotator cuff to strengthen the torn tissue as well. They are used to ease the fixation of bone and tendons, and they can be placed on the connection site of the bone and tendon, with sutures fixed to the textile material. For example, partially resorbable polyurethane urea and PLA are used to reinforce a rotator cuff (Koh et al., 2002; Derwin et al., 2009, http://www.artimplant.com).

Although poly-α-hydroxy acids have been the most-used polymer group in bone TE and in textiles, textile scaffolds built from poly(3-hydroxybutyrate) fibres combined with bovine collagen I, chondroitin sulphate, and bone marrow-derived cells have been studied. The scaffolds with the cells showed the highest mineralization and good cell differentiation to osteoblasts in *in vitro* studies (Wollenweber et al., 2006). Silk has also increased in popularity for bone TE (for a good review, see Wang et al., 2006), but not all applied methods are using fibrous or textile scaffolds.

Our group has been active in developing different structures, both plain textiles and composites, specifically for musculoskeletal TE scaffolds. Starting around mid-1990s, we have worked on melt-spinning PLAs, with P(L/D)LA 96/4 being the most-spun raw material, preparing knits, weaves, braids, and nonwovens from single fibre types or several combined (e.g., Kellomäki and Törmälä, 2003, Paakinaho et al., 2009; Ellä et al., 2011). The resultant textiles have been used in many types of composites.

P(L/D)LA 96/4 knits were some of the first to be used in 2D-membrane scaffolds; they were combined with flexible, occlusive films in an experimental rabbit's alveolar defect to apply a guided bone regeneration approach that used a film to protect the healing bone from connective tissue invasion. The results showed that bone healed better with both these implant types, as compared to the control, a noncovered autologous bone-filled defect (Kellomäki et al., 2000; Puumanen et al., 2001). Using the same principle, more plate-like, two-layered membranes were prepared using the same knit and P(L/LD)LA 70/30 plates (Kellomäki et al., 2001).

The knits have also been applied to form round 3D-cylinder scaffolds, of which the basic form is the joint scaffold (Ellä et al., 2011), and researchers have employed differently modified composite scaffolds from the materials for lumbar fusion studies (Palmgren et al., 2003), in addition to testing them in calvarial bone with growth factors (Gómez et al., 2006) and with adipose stem cells and electrical stimulation for osteochondral defect repairs (Ahtiainen et al., 2012).

We have also approached composite manufacturing by preparing multifilaments of P(L/D)LA 96/4, P(L/LD)LA 70/30, poly(L-lactide-*co*-glycolide) (PLGA) 80/20, and melt-spun BaGs (Pirhonen and Ellä, 2008), by preparing multicomponent yarns from different fibre combinations, and further making textiles and 3D composites out of the textiles. The motive for the use of bioceramic and BaG components in the composite has been twofold: to use it as reinforcement and to provide osteoconductivity to the composite. Braids (e.g., Huttunen et al., 2006, 2008), weaves (e.g. Alm et al., 2010), and knits (unpublished) have been constructed and studied *in vitro* and *in vivo*. As mentioned, textiles can be further processed into 3D-plates (e.g., Bleach et al., 2001; Nazhat et al., 2001), and in Figure 4.1, the compressed plates of PLA–BaG knits are shown as an example.

The results from these experiments show the versatility of the textiles; very different approaches have been used to obtain a variety of properties from the filaments, yarns, textiles, and composites. Given that a variety of possibilities exists, the best one for each application can be selected according to requests.

4.6 Cartilage tissue engineering using fabrics

Articular cartilage is avascular and aneural tissue. The nearly frictionless, load-bearing tissue withstands repetitive loadings up to 10 times the individual's body weight. In normal conditions, little or no wear occurs in the cartilage tissue. The native tissue has an anisotropic, nonlinear, inhomogenous, and viscoelastic nature. The cartilage tissue can also be described as fluid-saturated multiphasic material in which a fibrous collagen network is saturated with water and dissolved ions. Additionally,

negatively charged proteoglycans are attached to the structure. The articular cartilage has distinct zonal structures and tissue composition dependent on depth. Collagen fibres are aligned parallel to the tissue surface in the superficial zone of the adult articular cartilage, while, in a deeper zone, collagen fibres are aligned perpendicular to the surface. Also, a distinct subpopulation of chondrocytes exists according to the depth (Moutos and Guilak, 2008; Freed et al., 2009).

From a TE point of view, an effective long-term treatment for cartilage wear does not exist, although promising studies have been reported. The nonlinear properties of cartilage, such as strain-dependent moduli and permeability, can be achieved using the properties of the extracellular matrix (ECM) or scaffold, and extended *in vitro* cultivations are not needed to achieve them. Anisotropic properties are provided by composite structures with combinations of dissimilar materials. Layered structures and fibre reinforcements have also been studied. Typically, the reinforcing structure is nonwoven, knitted, or 3D-woven. Cell growth-supporting matrices of agarose, alginate, collagen, and fibrin have been reported to enhance delivery, proliferation, and differentiation of embedded cells, and they can be in the form of hydrogel, foam, or sponge (Chen et al., 2003; Moutos and Guilak, 2008; Freed et al., 2009).

3D woven structures and knitted meshes have been studied for the TE of articular cartilage as well. For example, through-the-thickness angle interlock structures have been fabricated from PGA (Moutos and Guilak, 2008) and poly-ε-caprolactone (PCL) (Moutos and Guilak, 2008; Freed et al., 2009; Moutos and Guilak, 2010; Moutos et al., 2010). 3D woven PGA fabric is immersed in chondrogenesis-supporting hydrogel, fibrin, or agarose. The composite formed by the PGA woven fabric and the fibrin gel has been shown to recreate the physical and structural properties of native cartilage (Moutos and Guilak, 2008; Freed et al., 2009), and the tensile modulus of the structure reportedly exceeds the modulus of articular tissue when compression and shear strengths are similar to those experienced by native tissue. The anisotropic and viscoelastic nature of the articular cartilage tissue are also reached by the composite (Moutos and Guilak, 2008).

A similar 3D woven structure has been fabricated from PCL yarns with a diameter of 150 μm. These yarns have higher twist numbers and larger diameters than PGA yarns, resulting in a more tightly woven structure. The PCL scaffold also has a higher compressive Young's modulus, but it is not as strong or stiff as a PGA scaffold (Moutos and Guilak, 2008). In the Moutos and Guilak study (2008), human adult stem cells were cultivated *in vitro* in the 3D woven PCL scaffold immersed in fibrin-gel. The woven structure had five warp layers and six weft layers that were interlocked with a third set of yarns. Yarn diameters were 156 μm, and the thickness of the structure was 1.4 mm. As a result, rectangular interconnected pores (pore: 330 μm × 20 μm × 100 μm) with a void fraction of 60% were formed. The scaffold enabled the re-creation of the functional and mechanical properties of articular cartilage, and it enhanced the formation of collagen-rich ECM. The initial properties were also sustained over a period of extended cultivation, during which seeded stem cells regenerated new tissue (Moutos and Guilak, 2010).

Other studies have shown that a 3D woven scaffold can support the generation of functional cartilaginous tissue when using Matrigel and adult mesenchymal stem cells

(Freed et al., 2009), ASCs (Moutos et al., 2010), or hMSCs with the induction of proinflammatory interleukin-1 (IL-1) (Ousema et al., 2012). Although the presence of IL inhibits chondrogenesis and the maturation of MSCs, the mechanical properties of native cartilage were reached (Ousema et al., 2012). The effect of the woven structure's tightness and the cultivation conditions have also been studied with hMSCs, and it was shown that the scaffold does not affect the amount of DNA, collagen, or GAG. In this study, a tightly woven structure with bioreactor cultivation reached an aggregate moduli similar to that of normal articular cartilage when lower values were reached with static cultivation. A loosely woven scaffold and static cultivation reached the lowest values (Valonen et al., 2010).

Knitted structures have also been studied for the TE of cartilage. Knitted, round (6 mm in diameter, 1 mm thickness) P(L/D)LA 96/4 scaffolds were prepared and implanted both alone and seeded with autologous chondrocytes into porcines. The results showed that the knit's structure was too coarse and hard for cartilage repair in immature animals (Pulliainen et al., 2007). Similar scaffolds were seeded with chondrocytes, and a comparison of static and bioreactor cultures showed that the latter produced better quality tissue *in vitro* (Tiitu et al., 2008).

Composite structures in thicknesses of 200 μm to 8 mm have been manufactured by combining PLGA knitted mesh and collagen hydrogel to provide scaffold materials for partial-thickness and full-thickness cartilage repair. The thinnest structure was achieved when knitted PLGA was immersed in collagen sponge. The thickness was then increased by layering collagen sponge sheets on one or both sides of the knitted structure (Chen et al., 2003; Dai et al., 2009).

Bovine chondrocytes were cultured in the composite web and transplanted into nude mice. Results showed a spatially even distribution of cells, natural chondrocyte morphology, and abundant cartilaginous ECM deposition. Thicker structures where collagen sponge was placed on one or two sides of the knitted fabric have shown a higher expression of type II collagen and production of GAGs. The mechanical strength of the structures reached half of the Young's modulus values for articular tissue and over 60% of their stiffness (Dai et al., 2009).

Based to the previously published results, it seems likely that the optimal scaffold for articular cartilage may be a composite or hybrid of more than one material, and the scaffold should be soft, but durable in compressive conditions. For these reasons, fibre reinforcement may be beneficial. It also seems likely that the *in vitro* cell culture should be carried out in dynamic conditions. The optimal use of scaffolds for chondral defects or as deeper osteochondral applications and which cells should be used remain unknown.

4.7 Ligament and tendon tissue engineering using fabrics

Ligaments are highly ordered fibrillar structures composed of proteins, proteoglygans, water, and cells. Dense tissue has poor healing potential due to its limited vascularization. The most commonly injured ligament is the anterior cruciate ligament (ACL) in the knee (Freeman et al., 2007; Lu et al., 2005). Strong materials with certain

flexibility and deformability are required for tendon and ligament scaffolds. Polyesters such as PLLA, PGA, and PLGA have been shown to have potential as materials with suitable mechanical properties for TE in tendons and ligaments (Lu et al., 2005), and they can be used also to repair the tendons through suturing (Viinikainen et al., 2007). Less studied materials and approaches for ACL scaffolds and reconstruction include parallel fibres of poly(DTE carbonate) (Bourke et al., 2004), arranged silk strands (Altman et al., 2002), and bundled collagen fibres (Caruso and Dunn, 2005). In addition, polysaccharides, such as alginate and agarose, and proteins, such as collagen derivatives, are used as cell growth stimuli matrices. For these, braids, knits, and woven structures have been studied as reinforcement materials in composites (Lu et al., 2005; Karamuk et al., 2004; Liu et al., 2008; Ouyang et al., 2003; Wang et al., 2011; Chen et al., 2008).

Braided structures have been the most commonly studied structures for ligament applications, and they have been reported to have suitable mechanical properties compared to native ligaments. Braids can transfer high loads and provide extension, because of their structure (Laurencin and Freeman, 2005). Researchers have investigated the desired mechanical properties, porosity, and pore diameters for braided ligament scaffolds using PLAGA 10:90 braids. This study showed that the optimal pore size for ligament tissue ingrowth is between 175 and 233 μm and that the stress–strain behaviour of the braided structures is similar to the behaviour of native ligament tissue. By altering a braiding geometry, it was also possible to affect the porosity, surface area, and tensile strength of the scaffold (Cooper et al., 2005).

The mechanical properties of scaffolds can further be optimized by yarn twisting and material selection (Freeman et al., 2007). For example, PGA, PLLA, and PLGA 82:18 braids have been compared. PGA braids showed the highest tensile strengths but also the fastest degradation rates, which then led to scaffold failure in *in vitro* studies. PLLA showed better long-term mechanical properties (Lu et al., 2005). The improvement of mechanical properties has also been studied in relation to yarn twisting and multilayer braiding (Freeman et al., 2007; Laurent et al., 2012). Twisting PLLA fibres into bundles and bundles into yarns before braiding has been shown to result in a significant increase in ultimate tensile strength and an increase in ultimate strain and toe region of the braided scaffold. Twisting before braiding has also been shown to improve similarities between the strain–stress behaviour of scaffolds and that of native tissue (Freeman et al., 2007).

Cellular response can be influenced by modifying polymer surfaces or by immersing textile reinforcements in hydrogel sponge, and many studies are focused on developing composite scaffolds. For example, a four-axis 3D PLLA braid in collagen sponge was shown to have mechanical properties comparable to those of native tissue, but the cell adhesion and proliferation of ACL cells were improved through the introduction of collagen sponge in *in vitro* studies. The results were compared to those for a plain PLLA braid (Ide et al., 2001).

Knitted and woven structures are studied less often for tendon and ligament TE purposes. Nonetheless, knitted structures reportedly have higher connective porosity than braided structures do, improving tissue ingrowth. A plain knitted silk structure in collagen sponge was also shown to be a potential alternative for tendon and ligament

reconstruction (Chen et al., 2008; Wang et al., 2011). In addition, weft-knitted PLGA 10:90 (Ouyang et al., 2003) might be used with cell sheets (Ouyang et al., 2005), and a braided silk core coated with a knitted silk structure has produced promising results in large animal studies (Fan et al., 2009).

Woven ribbons and tethers could have potential for tendon and ligament TE, but they are studied much less often than braided structures. Woven structures have high strength and stiffness in one direction and controllable variability in compliance and compression in other directions (Heniford and Koslosky, 2010). Although woven structures could have suitable mechanical properties, cellular ingrowth may be lacking (Karamuk et al., 2004).

4.8 Tissue-engineered joints

Previously, joints have been treated using biostable total joint prosthesis or implants. A new method for reconstructing the small joints in the hands and feet was invented in the 1990s. This method followed the principle of guided tissue regeneration (GTR) or *in situ* TE in which a porous scaffold is implanted between the bones and the cells are grown inside the scaffold, with the tissue maturating *in situ*.

In 1994, in Finland, research inspired by the Vainio method (Vainio, 1989) led to the development of melt-spinning poly-L,D-lactide 96/4 into 4-filament yarns, followed by the design and manufacturing of scaffolds from these fibres, and then *in vitro* (Ellä et al., 2011), preclinical (Länsman et al., 2006; Waris et al., 2008a,b), and clinical experiments (e.g. Honkanen et al., 2003; Honkanen et al., 2009) to confirm the functionality of the scaffolds (see Figure 4.2 for the image). The scaffolds have been shown to induce fibroblast ingrowth that later maturates to dense connective tissue. This acts as a natural cushion between the bone ends and thus helps the mobility of the joint. It does not, however, repair the cartilage tissue at the ends of the bones. These scaffolds were originally intended for rheumatoid arthritis patients, but they were clinically studied for osteoarthritis patients, too, and they have received a CE-mark for both indications and for the treatment of small joints in the hands and feet (http://www.scaffdex.com).

Around the same time in Sweden, another scaffold type utilizing the same principle was originated for the thumb carpometacarpal (CMC) joint, using polyurethane urea copolymer, which is a very slowly, or only partially, degradable polymer. This method has also been commercialized under the trade name Artelon, and list of publications about the studies behind this product can be found at http://www.artimplant.com. Unfortunately, in 2013, the company Artimplant declared bankruptcy, and the future of this implant type is currently uncertain.

Experiments treating damage to the temporomandibular joint have also explored the use of a composite disc of P(L/DL)LA 70/30 foil and P(L/D)LA 96/4 nonwoven structures seeded with adipose stem cells. This combination was considered to have potential based on *in vitro* studies, and the discs were implanted in rabbits after discectomy. The results from the preclinical stage were promising, but the design of the scaffold needs to be modified (Mäenpää et al., 2010; Ahtiainen et al., 2013).

4.9 Fabrics commercially available for temporary tissue repair

Some biodegradable textile structures are commercially available for temporary soft tissue and organ reinforcement. The most common applications address hernia, fascia, or periosteal repair, but they are also intended to support wounds, organs, ligaments, and tendons (Table 4.1). The applied biodegradable polymers include PLA copolymers, polyglactin 910, esterified hyaluronan, PHAs, and polyurethane urea.

The applied textile processing methods include weft and warp knitting, weaving, and braiding. One nonwoven is included in this table because of its unique three-layer structure, as is one composite with fleece and foil. Some of the commercial products reportedly target porous 3D structures, and their promoters claim that they support the ingrowth of cells and tissues and the preservation of sufficient cell nutrition, thus utilizing a more-GTR approach. However, the published scientific evidence for these claims is minor, and none of these structures is promoted for combination treatment with the specific cells and for TE purposes.

From a regulatory perspective, the commercialization of plain scaffolds instead of scaffolds with cells is much simpler, however, because combinational products consisting of scaffolds and living cells are treated as an Advance Medicinal Therapy Product in the EU (http://ec.europa.eu/health/human-use/advanced-therapies/). Therefore, it is understandable that companies try to commercialize a medical device. such as a plain scaffold, if possible.

4.10 Future trends

In the future TE research will likely involve the development of composite scaffolds and more complex scaffold structures. Also, novel biomaterials and material combinations, either as composites or hybrid structures, will be favoured because, using single-component options, it has been challenging to find optimal solutions. Composite scaffolds with textile reinforcement and cell growth stimuli hydrogel sponge are widely studied, and the field's next challenge is to construct textile materials so that they can better serve as biologic substrates. Current material candidates for these substrates include collagen fibres. Stronger and thinner biomaterials and smaller constructions are under investigation as well. The challenges for the future are the miniaturized sizes of the structures and the scaffolds. This extremely small size scale, together with the thin fibres, poses a serious obstacle in terms of developing the machinery needed for production, and this may lead to a completely new process for designing and building the equipment for manufacturing textiles and scaffolds for TE purposes.

From the biological perspective, the selection of purpose-specific cells and other components, such as growth factors, is a key task for the future, and the need for off-the-shelf products will drive functional and safety studies of autologous cells. Adding growth factors then increases the complexity of the product, leading to uncertainty regarding their necessity and safety in clinical use.

Table 4.1 Commercial biodegradable textile structures for musculoskeletal indications

Product	Company	Structure	Material	Indication	Reference
Vicryl®	Ethicon (J&J)	Warp knit and weaved	Polyglactin 910	Temporary support of wounds and organs	http://www.ethicon.com/emea/fi
Ethisorb™ DuraPatch	DePuy	Composite of fleece and foil	Vicryl (polyglactin 910) + PDS (poly-P-dioxanon) fleece and PDS foil	Bridging defects of dura mater	http://www.depuy.com/healthcare-professionals/products/
Hyalonect	Anika Therapeutics	Weft knit	Esterified hyaluronan (HYAFF11)	Periosteum substitute for orthopaedic traumas and reconstruction, no load bearing	http://www.anikatherapeutics.com
TephaFLEX®	Tepha Medical Devices	Warp knit	Polyhydroxyalkanoates (PHA, P4HB)	Reinforcement of soft tissue	http://www.tepha.com
BioFiber® Surgical Mesh	Tepha Medical Devices	Warp knit	Polyhydroxyalkanoates (PHA, P4HB)	Rotator cuff and other tendon injuries	http://www.tornier.com
Kensey-Nash	Epi-Guide	3 layer nonwoven	70:30 poly (L-lactide-*co*, DL-lactide) copolymer	Periodontal restorative surgeries and assists in the regeneration of bone and periodontal support tissues	http://www.kenseynash.com
Artelon tissue reinforcement (Sportmesh)	Artimplant	Woven	Polyurethane urea (partially resorbable)	Reinforcement of rotator cuff, Achilles tendon, and spring ligaments	http://www.artimplant.com
Artelon Spacer	Artimplant	Woven	Polyurethane urea (partially resorbable)	STT and CMCI joints in hand	http://www.artimplant.com
RegJoint™	Scaffdex	Weft knit	Poly-96L/4D-lactide copolymer	Small joints in hand (MCP, PIP, DIP, CMCI) and foot (MTPs)	http://www.scaffdex.com
STR GRAFT (expected to be on market by 2014)	Soft Tissue Regeneration, Inc.	Braided	Poly-L-lactide homopolymer	Soft tissue augmentation and rotator cuff repair	http://www.news-medical.net/news/20130103/FDA-clears-Soft-Tissue-Regeneratione28099s-STR-GRAFT.aspx

Some currently available commercial products claim to involve porous 3D-structures that support the ingrowth of cells and tissues, as well as the preservation of sufficient cell nutrition. But the published scientific evidence behind these claims is minor, and none of these structures is promoted for treatment in combination with specific cells or for TE purposes. The research into biodegradable textile structures is now expanding to focus on applications for repairing tendons and ligaments, however.

The modelling of fabrics and scaffolds has not been widely used in TE, and the field has not yet embraced the optimization of the production methods using available software, such as the Taguchi method. As our knowledge of the interactions and attractive and distractive forces between cells, yarns, and 3D fabric constructions increases, the modelling of living environments can be adapted to the fabric manufacturing process, with all its complexity. The complexity of a real TE product and all its components leads to stringent regulatory demands regarding the safety and functionality of this type of product. As a result, the commercialization of new TE products appears to have been delayed, and this remains a big challenge for the industry.

References

Ahtiainen, K., Mauno, J., Ellä, V., Hagström, J., Lindqvist, C., Miettinen, S., Ylikomi, T., Kellomäki, M., Seppänen, R., 2013. Autologous adipose stem cells and polylactide discs in the replacement of the rabbit temporomandibular joint disc. J. R. Soc. Interface 10 (85), 20130287. http://dx.doi.org/10.1098/rsif.2013.0287.

Ahtiainen, K., Sippola, L., Nurminen, M., Mannerström, B., Haimi, S., Suuronen, R., Hyttinen, J., Ylikomi, T., Kellomäki, M., Miettinen, S., 2012. Effects of chitosan and bioactive glass modifications of knitted and rolled polylactide-based 96/4L/D scaffolds on chondrogenic differentiation of adipose stem cells. J. Tissue Eng. Regen. Med. http://dx.doi.org/10.1002/term1614.

Anika Therapeutics. Available from: http://www.anikatherapeutics.com (accessed May 2013).

Alm, J., Frantzén, J.P.A., Moritz, N., Lankinen, P., Tukiainen, M., Kellomäki, M., Aro, H.T., 2010. In vivo testing of a biodegradable woven fabric made of bioactive glass fibers and $PLGA_{80}$ – a pilot study in the rabbit. J. Biomed. Mater. Res. B Appl. Biomater. 93, 573–580.

Altman, G.H., Horan, R.L., Lu, H.H., Moreau, J., Martin, I., Richmond, J.C., Kaplan, D.L., 2002. Silk matrix for tissue engineered anterior cruciate ligaments. Biomaterials 23, 4131–4141.

Artimplant. Available from: http://www.artimplant.com (accessed May 2013).

Badrossamay, M.R., McIlwee, H.A., Goss, J.A., Parker, K.K., 2010. Nanofiber assembly by rotary jet-spinning. Nano Lett. 10 (6), 2257–2261. http://dx.doi.org/10.1021/nl101355x.

Bleach, N.C., Tanner, K.E., Kellomäki, M., Törmälä, P., 2001. Effect of filler type on the mechanical properties of self-reinforced polylactide-calcium phosphate composites. J. Mater. Sci. Mater. Med. 12, 911–915.

Bourke, S.L., Kohn, J., Dunn, M.G., 2004. Preliminary development of a novel resorbable synthetic polymer fiber scaffold for anterior cruciate ligament reconstruction. Tissue Eng. 10 (1–2), 43–52.

Brink, M., 1997. (Doctoral thesis). Bioactive Glasses with a Large Working Range. Åbo Akademi University, Finland, p. 44.

Caruso, A.B., Dunn, M.G., 2005. Changes in mechanical properties and cellularity during long-term culture of collagen fiber ACL reconstruction scaffolds. J. Biomed. Mater. Res. A 73A, 388–397.

Chen, G., Sato, T., Ushida, T., Hirochika, R., Shirasaki, Y., Ochiai, N., Tateishi, T., 2003. The use of a novel PLGA fiber/collagen composite web as a scaffold for engineering of articular cartilage tissue with adjustable thickness. J. Biomed. Mater. Res. 67, 1170–1180.

Chen, X., Qi, Y.Y., Wang, L.L., Yin, Z., Yin, G.L., Zou, X.H., Ouyang, H.W., 2008. Ligament regeneration using a knitted silk scaffold combined with collagen matrix. Biomaterials 29, 3683–3692.

Cooper, J.A., Lu, H.H., Ko, F.K., Freeman, J.W., Laurencin, C.T., 2005. Fiber-based tissue-engineered scaffold for ligament replacement: design considerations and in vitro evaluation. Biomaterials 26, 1523–1532.

Crawford, M., 2012. New approaches, better products: innovation in product research and development comes in number of different forms and disciplines. Orthop. Des. Technol. 6.

Dai, W., Kawazoe, N., Lin, X., Dong, J., Chen, G., 2009. The influence of structural design of PLGA/collagen hybrid scaffolds in cartilage tissue engineering. Biomaterials 31, 2141–2152.

Dastoor, P.H., Hersh, S.P., Batra, S.K., Rasdorf, W.J., 1994. Computer-assisted structural design of industrial woven fabrics. Part I: need, scope, background, and system architecture. J. Text. Inst. 85 (2), 89–109.

DePuy. Available from: http://www.depuy.com/healthcare-professionals/products/ (accessed October 2013).

Derwin, K.A., Codsi, M.J., Milks, R.A., Baker, A.R., McCarron, J.A., Iannotti, J.P., 2009. Rotator cuff repair augmentation in a canine model with use of a woven poly-L-lactide device. J. Bone Joint Surg. Am. 91 (5), 1159–1171. http://dx.doi.org/10.2106/JBJS.H.00775.

Di, J., Samuelson, L.L., Bernaki, S.H., Gerber, D.A., King, M.W., 2012. Growth of pancreatic islets on collagen coated textile scaffolds. In: 9th World Biomaterials Congress, Chengdu, China.

Ekevall, E., Gplding, C., Mather, R.R., 2004. Design of textile scaffolds for tissue engineering: the use of biodegradable yarns. Int. J. Cloth. Sci. Technol. 16, 184–193.

Ellä, V., Annala, T., Länsman, S., Nurminen, M., Kellomäki, M., 2011. Knitted polylactide 96/4L/D structures and scaffolds for tissue engineering. Shelf life, in vitro and in vivo studies. Biomatter 1 (1), 1–12.

Epstein, M., Suokas, E., Nurmi, S., Karttunen, M., 1992. Komposiitit ja tekstiililujite. VTT, Espoo.

Ethicon. Available from: http://www.ethicon.com/emea/fi (accessed May 2013).

EU. Available from: http://ec.europa.eu/health/human-use/advanced-therapies/ (accessed October 2013).

Fan, H., Liu, H., Toh, S.L., Goh, J.C.H., 2009. Anterior cruciate ligament regeneration using mesenchymal stem cells and silk scaffold in large animal model. Biomaterials 30, 4967–4977.

Freed, L.E., Engelmayr Jr., G.C., Borenstein, J.T., Moutos, F.T., Guilak, F., 2009. Advanced material strategies for tissue engineering scaffolds. Adv. Mater. 21, 3410–3418.

Freeman, J.W., Woods, M.D., Laurencin, C.T., 2007. Tissue engineering of the anterior cruciate ligament using a braid-twist scaffold design. J. Biomech. 40, 2029–2036.

Gómez, G., Korkiakoski, S., González, M.-M., Länsman, S., Ellä, V., Salo, T., Kellomäki, M., Asahammakhi, N., Arnaud, E., 2006. Effect of FGF and polylactide scaffolds on calvarial bone healing with growth factor on biodegradable polymer scaffolds. J. Craniofac. Surg. 17 (5), 935–942.

Han, C.D., 2007. Rheology and Processing of Polymeric Materials. Oxford University Press, New York.

He, T., Sippel, K.K., Inman, A.O., El-Shafei, A., Monteiro-Rivière, N.A., King, M.W., 2012. Novel 3D scaffold designs for tissue engineering applications using textile technologies. In: 9th World Biomaterials Congress, Chengdu, China.

Hearle, J.W.S., Hollick, L., Wilson, D.K., 2001. Yarn Texturing Technology. Woodhead Publishing Limited, Cambridge.

Heniford, R., 2011. Textile forming technology leads material future. Med. Device Diagn. Ind. 33.

Heniford, R.C., Koslosky, J.M., 2010. Weaving innovation into device design. Orthotec. 1.

Honkanen, P.B., Kellomäki, M., Konttinen, Y.T., Mäkelä, S., Lehto, M.U.K., 2009. A midterm follow-up study of bioreconstructive polylactide scaffold implants in metacarpophalangeal joint arthroplasty in rheumatoid arthritis patients. J. Hand Surg. 2, 179–185.

Honkanen, P.B., Kellomäki, M., Lehtimäki, M.Y., Mäkelä, S., Törmälä, P., Lehto, M.U.K., 2003. Bioreconstructive joint scaffold implant arthroplasty in metacarpophalangeal joints: short-term results of a new treatment concept in rheumatoid arthritis patients. Tissue Eng. 9 (5), 957–965.

Horrocks, A.R., Anand, S.C., 2000. Handbook of Technical Textiles. Woodhead Publishing Limited and CRC Press, Boca Raton, Florida and UK.

Huang, Z.-M., Zhang, Y.-Z., Kotaki, M., Ramakrishna, S., 2003. A review of polymer nanofibers by electrospinning and their applications in nanocomposites. Compos. Sci. Technol. 63 (15), 2223–2253.

Hutmacher, D.W., 2000. Scaffolds in tissue engineering bone and cartilage. Biomaterials 21, 2529–2543.

Huttunen, M., Ashammakhi, N., Törmälä, P., Kellomäki, M., 2006. Fibre reinforced bioresorbable composites for spinal surgery. Acta Biomater. 2, 575–587.

Huttunen, M., Kellomäki, M., 2011. A simple and high production rate manufacturing method of submicron polymer fibers. J. Tissue Eng. Regen. Med. 5 (8), e239–e243. http://dx.doi.org/10.1002/term.421.

Huttunen, M., Törmälä, P., Godinho, P., Kellomäki, M., 2008. Fiber-reinforced bioactive and bioabsorbable hybrid composites. Biomed. Mater. 3, 034106. http://dx.doi.org/10.1088/1748-6041/3/3/034106.

Ide, A., Sakane, M., Chen, G., Shimojo, H., Ushida, T., Tateishi, T., Wadano, Y., Miyanaga, Y., 2001. Collagen hybridization with poly(L-lactic acid) braid promotes ligament cell migration. Mater. Sci. Eng. 17, 95–99.

Karamuk, E., Mayer, J., Raeber, G., 2004. Tissue engineered composite of a woven fabric scaffold with tendon cells, response on mechanical simulation in vitro. Compos. Sci. Technol. 64, 885–891.

Kawabata, S., Niwa, M., Kawai, H., 1973a. The finite deformation theory of plain weave fabrics. Part I: the biaxial deformation theory. J. Text. Inst. 64, 21–46.

Kawabata, S., Niwa, M., Kawai, H., 1973b. The finite deformation theory of plain weave fabrics. Part II: the uniaxial deformation theory. J. Text. Inst. 64, 47–61.

Kellomäki, M., Paasimaa, S., Törmälä, P., 2001. Pliable polylactide plates for guided bone regeneration: manufacturing and in vitro. Proc. Inst. Mech. Eng. H 214 (6), 615–629.

Kellomäki, M., Puumanen, K., Waris, T., Törmälä, P., 2000. In vivo degradation of composite membrane of P(ε-CL/L-LA) 50/50 film and P(L/D)LA 96/4 mesh. In: Stallforth, H., Revell, P.A. (Eds.), Materials for Medical Engineering. Wiley-VCH, Weinheim, pp. 79–85.

Kellomäki, M., Törmälä, P., 2003. Processing of resorbable poly-alpha-hydroxy acids for use as tissue-engineering scaffolds. In: Hollander, A.P., et al., (Eds.), Methods in Molecular

Biology, Biopolymer Methods in Tissue Engineering, vol. 238. Humana Press, Totowa, NJ, pp. 1–10.

Kensey Nash. Available from: http://www.kenseynash.com (accessed May 2013).

Koh, J.L., Szomor, Z., Murrell, G.A.C., 2002. Supplementation of rotator cuff repair with a bioresorbable scaffold. Am. J. Sports Med. 30, 410–413.

Koslosky, J., 2010. The fabric of healing. Orthop. Des. Technol. 6, 56–59.

Langer, R., Vacanti, J.P., 1993. Tissue engineering. Science 260 (5110), 920–926. http://dx.doi.org/10.1126/science.8493529.

Laurencin, C.T., Freeman, J.W., 2005. Ligament tissue engineering: an evolutionary materials science approach. Biomaterials 26, 7530–7536.

Laurent, C.P., Durville, D., Mainard, D., Ganghoffer, J.-F., Rahouadj, R., 2012. A multilayer braided scaffold for anterior cruciate ligament: mechanical modeling at the fiber scale. J. Mech. Behav. Biomech. Mater. 12, 184–196.

Lee, S.M., 1993. Handbook of Composite Reinforcements. Wiley-VCH, Palo Alto.

Liu, H., Ding, X., Zhou, G., Li, P., Wei, X., Fan, Y., 2013. Electrospinning of nanofibers for tissue engineering applications. J. Nanomater. 2013, 11. Article ID 495708, http://dx.doi.org/10.1155/2013/495708.

Liu, Y., Ramanath, H.S., Wang, D.-A., 2008. Tendon tissue engineering using scaffold enhancing strategies. Trends Biotechnol. 26, 201–209.

Long, A.C., 2005. Design and Manufacture of Textile Composites. Woodhead Publishing Limited, UK.

Lu, H.H., Cooper Jr., J.A., Manuel, S., Freeman, J.W., Attawia, M.A., Ko, F.K., Laurencin, C.T., 2005. Anterior cruciate ligament regeneration using braided biodegradable scaffolds: in vitro optimization studies. Biomaterials 26, 4805–4816.

Länsman, S., Pääkkö, P., Ryhänen, J., Kellomäki, M., Waris, E., Törmälä, P., Waris, T., Ashammakhi, N., 2006. Poly-L/D-lactide (PLDLA) 96/4 fibrous implants: histological evaluation in the subcutis of experimental design. J. Craniofac. Surg. 17 (6), 1121–1128.

Mesimäki, K., Lindroos, B., Törnwall, J., Mauno, J., Lindqvist, C.J., Kontio, R., Miettinen, S., Suuronen, R., 2009. Novel maxillary reconstruction with ectopic bone formation by GMP adipose stem cells. Int. J. Oral Maxillofac. Surg. 38 (3), 201–209. http://dx.doi.org/10.1016/j.ijom.2009.01.001.

Miravete, A., 1999. 3-D Textile Reinforcements in Composite Materials. Woodhead Publishing Limited and CRC press, Boca Raton, Florida and UK.

Moutos, F.T., Guilak, F., 2008. Composite scaffolds for cartilage tissue engineering. Biorheology 45, 501–512.

Moutos, F.T., Estes, B.T., Guilak, F., 2010. Multifunctional hybrid three-dimensionally woven scaffolds for cartilage, tissue engineering. Macromol. Biosci. 10, 1355–1364.

Moutos, F.T., Guilak, F., 2010. Functional properties of cell-seeded three-dimensionally woven poly(ε-caprolactone) scaffolds for cartilage tissue engineering. Tissue Eng. A 16, 1291–1301.

Mäenpää, K., Ellä, V., Mauno, J., Kellomäki, M., Suuronen, R., Ylikomi, T., Miettinen, S., 2010. Use of adipose stem cells and polylactide discs for tissue engineering of the temporomandibular joint disc. J. R. Soc. Interface 7 (42), 177–188. http://dx.doi.org/10.1098/rsif.2009.0117.

Nair, L.S., Laurencin, C.T., 2007. Biodegradable polymers as biomaterials. Prog. Polym. Sci. 32 (8–9), 762–798.

Nazhat, S.N., Kellomäki, M., Törmälä, P., Tanner, K.E., Bonfield, W., 2001. Dynamic mechanical characterization of biodegradable composites of hydroxyapatite and polylactides. J. Biomed. Mater. Res. B Appl. Biomater. 58, 335–343.

News Medical. Available from: http://www.news-medical.net/news/20130103/FDA-clears-Soft-Tissue-Regeneratione28099s-STR-GRAFT.aspx (accessed November 2013).

Ouyang, H.W., Goh, J.C., Thambyah, A., Teoh, S.H., Lee, E.H., 2003. Knitted poly-lactide-co-glycolide scaffold loaded with bone marrow stromal cells in repair and regeneration of rabbit Achilles tendon. Tissue Eng. 9, 431–439.

Ouyang, H.W., Toh, S.L., Goh, J., Tay, T.E., Moe, K., 2005. Assembly of bone marrow stromal cell sheets with knitted poly (L-lactide) scaffold for engineering ligament analogs. J. Biomed. Mater. Res. B Appl. Biomater. 75, 264–271.

Ousema, P.H., Moutos, F.T., Estes, B.T., Caplan, A.I., Lennon, D.P., Guilak, F., Weinberg, J.B., 2012. The inhibition by interleukin 1 of MSC chondrogenesis and the development of biomechanical properties in biomimetic 3D woven PCL scaffolds. Biomaterials 33, 8967–8974.

Paakinaho, K., Ellä, V., Syrjälä, S., Kellomäki, M., 2009. Melt spinning of poly(L/D)lactide 96/4: effects of molecular weight and melt processing on hydrolytic degradation. Polym. Degrad. Stab. 94 (3), 438–442.

Palmgren, T., Ylinen, P., Tulamo, R., Kellomäki, M., Törmälä, P., Rokkanen, P., 2003. Lumbar intervertebral disc replacement using bioabsorbable self-reinforced poly-L-lactide full-threaded screws, or cylindrical implants of polylactide polymers, bioactive glass and polyactive. Vet. Comp. Orthop. Traumatol. 16, 138–144.

Pham, Q.P., Sharma, U., Mikos, A.G., 2006. Electrospinning of polymeric nanofibers for tissue engineering applications: a review. Tissue Eng. 12 (5), 1197–1211.

Pirhonen, E., Ellä, V., 2008. Melt spinning. In: Wnek, G.E., Bowlin, G.L. (Eds.), second ed. Encyclopedia of Biomaterials and Biomedical Engineering, vol. 3. Informa Health Care, New York, NY, pp. 1816–1823.

Proxy Biomedical. Available from: http://proxybiomedical.com (accessed May 2013).

Pulliainen, O., Vasara, A.I., Hyttinen, M.M., Tiitu, V., Valonen, P., Kellomäki, M., Jurvelin, J.S., Peterson, L., Lindahl, A., Kiviranta, I., Lammi, M.J., 2007. Poly-L/D-lactic acid scaffold in the repair of porcine knee cartilage lesions. Tissue Eng. 13 (6), 1347–1355.

Puumanen, K., Kellomäki, M., Ristilä, V., Böhling, T., Pihlajamäki, H., Törmälä, P., Waris, T., 2001. Repair of maxillary alveolar cleft defects with two different bioabsorbable implants: an experimental study in growing rabbits. Eur. J. Plast. Surg. 24, 66–73.

Scaffdex. Available from: http://www.scaffdex.com (accessed May 2013).

Tamayol, A., Akbari, M., Annabi, N., Paul, A., Khademhosseini, A., Juncker, D., 2012. Fiber-based tissue engineering: progress, challenges, and opportunities. Biotechnol. Adv. 31, 669–687.

Tepha. Available from: http://www.tepha.com (accessed May 2013).

Tiitu, V., Pulkkinen, H.J., Valonen, P., Pulliainen, O., Kellomäki, M., Lammi, M.J., Kiviranta, I., 2008. Bioreactor improves the growth and viability of chondrocytes in the knitted poly-L,D-lactide scaffolds. Biorheology 45 (3–4), 539–546.

Tornier. Available from: http://www.tornier.com (accessed May 2013).

Vainio, K., 1989. Vainio arthroplasty of the metacarpophalangeal joints in rheumatoid arthritis. J. Hand Surg. Am. 14 (2 Pt 2), 367–368.

Valonen, P.K., Moutos, F.T., Kusanagi, A., Moretti, M.G., Diekman, B.O., Welter, J.F., Caplan, A.I., Guilak, F., Freed, L.E., 2010. In vitro generation of mechanically functional cartilage grafts based on adult human stem cells and 3D-woven poly(ε-caprolactone) scaffolds. Biomaterials 31, 2193–2200.

Vidal-Sasse, E., Boisse, P., 2012. Modelling the structures and properties of woven fabrics. In: Chen, X. (Ed.), Modelling and Predicting Textile Behaviour. Woodhead Publishing Limited, Cambrigde, UK, pp. 144–179.

Viinikainen, A., Göransson, H., Huovinen, K., Kellomäki, M., Törmälä, P., Rokkanen, P., 2007. The strength of the 6-strand modified Kessler repair performed with triple-stranded of triple-stranded bound suture in a porcine extensor tendon model: an ex vivo study. J. Hand Surg. 32A, 510–517.

Wang, X., Han, C., Hu, X., Sun, H., You, C., Gao, C., Haiyang, Y., 2011. Applications of knitted mesh fabrication techniques to scaffolds for tissue engineering and regenerative medicine. J. Mech. Behav. Biomech. Mater. 4, 922–932.

Wang, Y., Kim, H.J., Vunjak-Novakovic, G., Kaplan, D.K., 2006. Stem cell-based tissue engineering with silk biomaterials. Biomaterials 27 (36), 6064–6082.

Waris, E., Ashammakhi, N., Lehtimäki, M., Tulamo, R.-T., Kellomäki, M., Törmälä, P., Konttinen, Y.T., 2008a. The use of biodegradable scaffold as an alternative to silicone implant arthroplasty for small joint reconstruction: an experimental study in minipigs. Biomaterials 29 (6), 683–691.

Waris, E., Ashammakhi, N., Lehtimäki, M., Tulamo, R.-T., Törmälä, P., Kellomäki, M., Konttinen, Y.T., 2008b. Long-term bone tissue reaction to polyethylene oxide/polybutylene terephthalate copolymer (polyactive) in metacarpophalangeal joint reconstruction. Biomaterials 29 (16), 2509–2515.

Wollenweber, M., Domaschke, H., Hanke, T., Boxberger, S., Schmack, G., Gliesche, K., Scharnweber, D., Worch, H., 2006. Mimicked bioartificial matrix containing chondroitin sulphate on a textile scaffold of poly(3-hydroxybutyrate) alters the differentiation of adult human mesenchymal stem cells. Tissue Eng. 12, 345–359.

Wulfhorst, B., Gries, T., Weit, D., 2006. Textile Technology. Hanser Publishers, Munich.

Xiao, M., Geng, Z., Liao, K., 2011. An improved model of rigid bodies for plain-weave fabrics based on the dynamics of multibody systems. Text. Res. J. 81 (13), 1381–1394.

Nanofibers for ligament and tendon tissue regeneration

5

Victor Leung, Heejae Yang, Frank Ko
University of British Columbia, Vancouver, BC, Canada

5.1 Introduction

Tendons and ligaments are bundles of soft tissues that connect muscle to bone and bone to bone, respectively. As a result, they play a major role in our musculoskeletal mobility by transmitting forces and providing joint stability. These soft tissues can be damaged by extrinsic influences, such as trauma, atrophy, and overuse, and intrinsic factors, such as diseases and muscle imbalance. Accordingly, considerable effort has been directed toward studying injuries to these soft tissues. Unfortunately, the unique mechanical properties of ligaments and tendons create significant challenges for restoring mobility in patients suffering from tissue damage. Despite the intricate healing processes that human bodies have developed, the native healing of ligaments and tendons has not been satisfactory, mainly due to the mismatch between the mechanical properties of the native tendon or ligament and the scar tissue. In some cases, harsh tissue surroundings further complicate the difficult healing process, as in the case of anterior cruciate ligament (ACL) injuries in which the presence of synovial fluid prevents blood clotting and therefore normal healing response (Vunjak-Novakovic et al., 2004). Given this insufficient healing, the demand for medical intervention is great, and those seeking it range from workers and professional athletes hoping to return to their activities in a timely manner to others requiring effective healing to reduce pain. For example, in the United States, approximately 200,000 cases of ACL injuries are reported annually (Hewett et al., 2007), and 232,000 cases of Achilles tendon sports injuries were reported in the year 2002 alone (Abousleiman et al., 2008). Also, according to research by Abousleiman et al. (2005), the U.S. Bureau of Labor Statistics documented approximately 45,000 injuries from tendinosis in the year 1999. Given this strong demand, strategies for improving and expediting tendon and ligament healing will not only help many patients, but they will also reduce the cost associated with treatment, long-term care, and loss of productivity.

Early efforts to mitigate inadequate healing most often involved primary repair surgeries in which damaged tissues were reaffixed, but the outcome was poor because the weaker scar tissue limited patient motion while posing risks for further damage (Rodrigues et al., 2012). Artificial prostheses have also been tested as either replacements or supports for reconstruction. Although early results for many artificial prostheses showed promise, follow-up studies showed overwhelmingly poor long-term results, especially for ligament prostheses, due to various complications related to

Biomedical Textiles for Orthopaedic and Surgical Applications. http://dx.doi.org/10.1016/B978-1-78242-017-0.00005-2

the synthetic materials used (Dauner and Planck, 1996; Grøntvedt et al., 1996; Rodrigues et al., 2012; Silver et al., 1991; Wening et al., 1996). In addition, synthetic prostheses could not mimic the unique collagenous structure in native tendon and ligament tissues, leading to mismatch in structural behavior under loading. As a result, grafting remained the gold standard for tendon and ligament repair, with autograft preferred over allograft due to risks of rejection and disease transmission. Autografting requires the extraction of healthy tendons or ligaments, which themselves have limited healing capability. So, donor-site morbidity is of more critical concern when autografting tendon or ligament as opposed to other tissues such as skin. To address such a complicated series of needs related to tendon and ligament healing, many researchers have focused their attention on the tissue engineering approach, aiming to fully restore the structural and biological functions of the soft tissues (Cooper et al., 2005; Deng et al., 2009; Rodrigues et al., 2012; Vunjak-Novakovic et al., 2004).

As a niche area in tissue engineering, scaffolds composed of electrospun nanofibers have recently gained much momentum in research. Nanofibers are those with diameters below 100 nm and an aspect ratio above 1:1000 (Ko, 2004), but the term is often used loosely to describe fibers with diameters under approximately 1000 nm. Nanofibers have attracted interest due to the comparatively large surface area they provide for cell activities, as well as their structural similarities to the native tissue's extracellular matrix (ECM) (Leung et al., 2011). In addition, through studies on nanofibrous scaffolds over the past decade, many have found that these scaffolds are not only feasible for supporting cell attachment and tissue regeneration, but they are also desirable platforms for releasing therapeutic elements such as drugs and growth factors. These outcomes eventually led to studies on healing-process moderation and cell differentiation control using nanofibrous scaffolds, with early results showing their superiority over other forms of scaffold, including gel and microfibers (Leung et al., 2011). The electrospinning technique used for fabricating nanofibers was also found to be highly versatile, supporting the use of a wide variety of biocompatible materials while offering a high degree of customization of mechanical properties, thus enabling scaffolds to be tailored for specific tissues.

This chapter introduces readers to nanofibers as a new frontier in tendon and ligament regeneration, and it discusses the current state of the technology and future directions for research. The following sections begin with an introduction to current approaches to restoring patient mobility and the associated challenges, which have led to studies on nanofibers as a potential solution. We then introduce methods for fabricating nanofibers and controlling their properties, before discussing the application of nanofibers in tendon and ligament regeneration. Through this summary on current nanofiber technology, we hope to identify unmet needs, while encouraging further investigations that can bring nanofiber technology closer to market readiness for ligament and tendon applications.

5.2 Current treatment and challenges

The need for improved intervention methods such as nanofiber-based products stems from the insufficient self-healing of ligament and tendon tissues and the inability of current technology to adequately address market needs. It is therefore necessary to first understand the native healing process, current techniques for intervention, and

the challenges presented by these approaches, in order to gain a clearer perspective on the potential effect of nanofiber technology applications.

5.2.1 Native healing processes in tendon and ligament tissues

The native healing processes in tendon and ligament tissues are analogous to those present in other soft tissues (Martin, 1997; Rodrigues et al., 2012; Woo et al., 1999), although the precise type of fibroblastic cells involved are different. Both begin with the inflammation stage, which involves blood clotting at the breach and secretion of inflammatory factors for recruiting cells to phagocytize bacteria and debris, while releasing growth factors. The inflammatory phase lasts up to 5 days, and the proliferation stage begins when fibroblasts arrive at the site, often overlapping with the later stage of inflammation (Rodrigues et al., 2012; Woo et al., 1999). In the proliferation stage, which lasts up to several weeks after the breach, fibroblasts synthesize collagen and ECM components to form the granulation tissue, replacing the clot to provide strength for the tendon and ligament tissues. Vascularization of the granulation tissue also takes place at this stage. The subsequent remodeling stage, which can last many months to more than 1 year, is marked by decreased cellular activities and the equalization of ECM generation and degradation (Rodrigues et al., 2012; Woo et al., 1999). The granulation tissue becomes more fibrous and oriented, before being converted into a stronger scar tissue that remains at the site.

The healing of the tendon or ligament depends greatly on the successful formation of a blood clot and the subsequent migration of cells that induce inflammation and collagen secretion. Blood clot formation is difficult for tissues in harsher environments, such as the ACL, which is surrounded by synovial fluid (Vunjak-Novakovic et al., 2004), and therefore, ACL healing propensity is considered low. Several diseases, such as tendonitis, can also prevent healing mechanisms from activating (Liu et al., 2008), requiring external aids such as surgical intervention for restoring function.

For tendons and ligaments that do heal, the major challenge for native healing largely stems from scar tissue formation. Although granulation and scar tissues are necessary for revascularization and the connection of damaged tissues, their mechanical behaviors are different from those of the original tissue, in terms of strength, flexibility, and viscoelasticity (Rodrigues et al., 2012). This the lack of strength can cause patients to risk reinjuring, and the difference in flexibility and viscoelasticity can greatly limit their joint and muscle functions, thereby affecting mobility. Moreover, in some tendon injuries, the scar tissue may cause adhesion between the tendon proper and its protective sheath, disabling any sliding inside the sheath and therefore any motion associated with that tendon (Woo et al., 1999). In other injuries, adhesion may also be formed with surrounding tissues, which also affects motion.

5.2.2 Current treatments for damaged tendon and ligament tissues

Clinicians did not give much attention to medical interventions for treating injured tendon and ligament tissues until the turn of the twentieth century. The first treatments of an injured ACL were reported by Mayo Robson in 1895 and Battle in 1898, and

these treatments involved surgical affixation using materials such as silk and catgut (Robson, 1903; Wening et al., 1996). Such primary repair surgeries showed early promise. For example, Mayo Robson's initial patient, who suffered from a fall, claimed to have perfect knee function after 6 years (Robson, 1903). However, more recent studies showed deteriorating long-term results with high incidences of unstable joints. Odensten et al. (1984) reported 23 out of 35 primary repair surgery patients required early follow-up after 2 years, and Grøntvedt et al. (1996) reported that nearly half of the 50 patients in their study experienced unstable joints 2–5 years post-surgery. The main reason for the failure of the primary repair of soft tissues such as ligament and tendon, as mentioned previously, is the inability of the scar tissue to mechanically behave like the tissue it replaces. This is especially true for tissues with complicated structures, such as the flexor tendon in the area between the distal crease in the palm and the middle crease of the finger, known as zone 2 flexor tendon, which has a high tendency to adhere to the protective sheath after reparative procedures. In fact, the difficulty in restoring mobility in patients with zone 2 flexor tendon injuries has led Bunnell to describe the zone as "no man's land" (Newmeyer and Manske, 2004).

Shortly following the work by Mayo Robson on primary repair, Hey Groves performed the first ACL reconstruction via grafting in 1917, transplanting an iliotibial band for that purpose (Groves, 1919). Despite early criticisms of their effectiveness, research on ligament grafts continued, leading to the pioneering works of Campbell in the 1930s (Campbell, 1936), and then Jones (1963) and Brückner (1966) in the 1960s, followed by MacIntosh in early 1970s (Galway et al., 1972). Many of their efforts focused on grafts consisting of patellar tendon with attached bone, which remains one of the common graft choices for ACL repair (Fu et al., 1999, 2000). In addition to having sufficient tensile properties, the patellar tendon-bone grafts can facilitate proper graft fixation at the bone ends. Hamstring tendons, such as the quadruple semitendinosus, are also commonly used as grafts due to their adequate tensile properties, small incision sites, and thicker tendinous portions (Fu et al., 1999, 2000). Unlike grafts with bony attachments, hamstring tendon grafts involve fixation that relies on tendon healing inside osseous tunnels, which may become a concern in some surgeries involving harsh healing conditions (Fu et al., 1999, 2000). In the clinical study by Grøntvedt et al. (1996), none of the 48 patients with patellar tendon-bone autografts required reoperation, and the mobility as well as joint functions for these patients were superior to those treated with primary repair surgeries. The superior mechanical properties of tendon grafts and the clinically established methods for fixation enabled autografts to remain the preferred method for injured ligament treatment. However, as with any autografts, the removal of healthy tissues creates concern regarding scarring at the donor site, especially when the tissue source is tendon that has lower self-healing ability. Moreover, autografts at the damage site may undergo necrosis in the early stages postoperation until vascular structures are re-established.

Seeing the need to address donor site morbidity, many have examined synthetic ligament and tendon prostheses. One of the first documented uses of synthetic ligament prosthesis is the work by Lange (1903) using braided silk, although the procedure was not successful, possibly due to the difficulty of fixation, as implied by his

later modifications to the fixation techniques. In addition to silk, several synthetic materials emerged as potential ligament prosthesis, such as Polyflex, Dacron, and Gore-Tex, which were investigated from the 1970s to the 1980s. Polyflex, which is composed of polyethylene, was the first prosthesis tested for American Food and Drug Administration (FDA) approval for this application, and it failed quickly in the late 1970s due to high alternating stresses causing fatigue failure (Wening et al., 1996). The high alternating stresses also prompted future synthetic prosthesis design to adopt a fiber-based approach. Dacron and Gore-Tex were also tested for ligament replacement or autograft augmentation in the 1980s, but they were ultimately unsuccessful. Gore-Tex prostheses suffered from fatigue failure as a result of low tissue ingrowth, and Dacron failed to improve joint stability due to stress shielding, which led to disorganized tissue ingrowth (Silver et al., 1991; Wening et al., 1996). Polypropylene was tested as a ligament-augmentation device for autografts, but it was plagued by the same stress-shielding issue as Dacron prostheses, leading to a high tendency for complications. In addition, carbon fiber-based composites were tested for ligament replacement, with high initial tissue ingrowth, but foreign-body responses and shedding of carbon particulates ultimate led to the discontinuation of studies on carbon-based prostheses (Wening et al., 1996). Tendon prostheses, on the other hand, enjoyed a slightly higher level of success, with one famous example being the Hunter tendon prostheses as part of a two-stage flexor tendon reconstruction process for potentially restoring hand function and addressing the issue of the "no man's land" (Hunter, 1965; Hunter and Salisbury, 1971). The technique involved Dacron rods coated by silicone, the so-called Hunter rods, which were implanted into the hand in the first stage of the process, with fixation achieved at the distal phalanx while the proximal end remained free. Following implantation, mesothelium pseudosheaths were formed around the Hunter rods. In the second stage, after approximately 3 months, the Hunter rods were replaced with tendon grafts, which would gradually restore hand function in patients. Patients using earlier Hunter prostheses were not able to regain active use of their digit until after the completion of the second stage surgery, which prompted investigation into the second generation of tendon prostheses in order to enable active use by supporting fixation via bone ingrowth into sintered titanium plugs at both ends of the rod (Hunter et al., 1988). Figure 5.1 shows the two generations of tendon prostheses, with the top ones being active designs that support fixation at both ends and the bottom ones

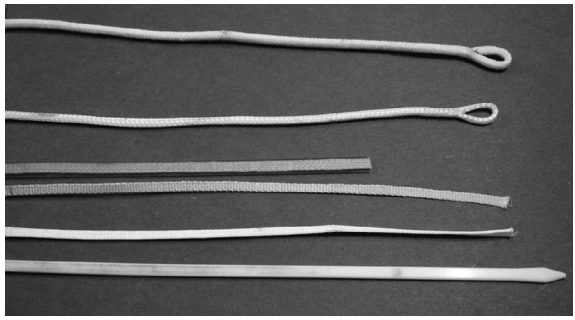

Figure 5.1 Passive and active tendon prostheses currently on the market.

being passive designs. The Hunter method, despite being costly and requiring lengthy healing period, remained a standard procedure for hand injuries. Although Hunter's original intention was to use the silicone rods as a permanent replacement, the difficulty in achieving reliable fixation at both ends of the rod left this goal unachieved, despite the transition from passive to active designs enabling caregivers to extend the period between the two stages of the reconstruction process, a period that could be indefinite for elderly patients (Hunter et al., 1988). Thus, despite the amount of research directed toward synthetic tendon and ligament prostheses, there have been limited successes in this area, with no current clinically satisfactory prostheses for ACL replacement.

5.2.3 The tissue engineering approach

Thus far, autografting remained the standard method for ligament and tendon reconstruction, with primary repair and synthetic prostheses unlikely to exhibit sufficient potential for replacing autografts. With donor site morbidity remaining a significant challenge, especially for patients with multiple injuries, many began investigating tissue engineering as a potential solution, however, leading to the technique becoming recognized by the U.S. National Science Foundation as an emerging area of national importance (Skalak et al., 1988). Instead of relying on native healing or replacement with autologous tissue or synthetic prostheses, tissue engineering attempts to cultivate the formation of functional ligament or tendon tissues with appropriate structure and properties, using a combination of materials, cells, and cell-signaling elements. In tissue engineering scaffolds, materials provide a three-dimensional platform allowing the attachment, proliferation, and differentiation of tendon and ligament fibroblastic cells. In many cases the scaffolds are also designed to gradually degrade as new tissues develop in the scaffold, eliminating the need for surgical removal. The scaffold materials can be in various forms, and researchers have demonstrated cell survival and proliferation in scaffolds composed of gel (Drury and Mooney, 2003; Hartwell et al., 2011), fibers (Ko, 1997; Ko et al., 1998), pellets (Burg et al., 2000), sponges (Li and Zhang, 2005; Yannas and Burke, 1980), and more. The optimal form depends on the specific application. For example, gel scaffolds are injectable into specific sites, but they lack integrity when subjected to loads, whereas pellets may remain intact under compression. Fibers, on the other hand, have higher tensile strength, reaching the order of 10 MPa for skin scaffolds such as BioFix and Resolut LT (Rho et al., 2006), and they can be formed into hierarchical structures such as sutures and tubes. A wide variety of materials, both natural and synthetic, have also been examined as tissue engineering matrices. Many natural materials, especially those from biological sources, have been found to display desirable biological functions, such as antimicrobial potential and cell affinity enhancement, and therefore, they have been considered for tendon and ligament scaffolds. Examples include the earlier work on collagen gel (Haddad-Weber et al., 2010) and fibers (Kemp et al., 1995), silk fibers (Ayutsede et al., 2005; Sukigara et al., 2003, 2004), and collagen–glycosaminoglycan (GAG) (Louie et al., 1998). Although these scaffolds supported fibroblast attachment and spreading, as well as new tendon or ligament generation, their loss of tensile integrity over time and insufficient stress-bearing remained challenges. Synthetic materials, on the other hand, can enable customization of physical properties such as degradation

rate, tensile strength, and stiffness. However, their relative lack of cell affinity and signaling ability must also be addressed.

In addition to the scaffold matrix, bioactive elements are often included to enhance functional properties, through the incorporation of antibiotics, anti-inflammatory drugs, and biominerals such as hydroxyapatite. To further control tissue regeneration, signaling elements such as growth factors are often used to induce desirable cell response.

5.3 Nanofiber scaffolds as a new frontier in tissue engineering

Earlier work on synthetic ligament prostheses indicated that fibrous constructs may be more suitable to withstanding the high alternative stresses experienced *in vivo*. Fibers have also been used widely as tissue scaffolds, including wound dressings such as BioFix, Resolut LT, and Kaltostat, as well as experimental ligament scaffolds composed of silk and synthetic polymers. Being highly connective, fibers can be fabricated into hierarchical textile structures, including woven and nonwoven fabric, and various braided structures, allowing fibers to be tailored for specific topical and implant applications (Ko, 1997). For example, Cooper et al. (2005) presented a braided ACL scaffold using poly(lactic-glycolic acid) (PLGA) containing ends with high angle fiber orientation for bony attachment, with an intra-articular zone at the center with low angle fiber orientation. Building on the developments related to fiber-based ligament and tendon scaffolds, many researchers began examining nanofibers as a means for further improving tissue growth. Nanofibers have a higher surface area-to-volume ratio compared to micro- or macro fibers, and they also mimic more closely the native ECM, which is composed of nanofibrous collagen. Further studies on nanofibers for tissue regeneration also indicated that they are suitable for drug and growth factor delivery, because their comparatively high surface area allows for more efficient drug loading and release (Leung and Ko, 2011). The development of drug-loaded nanofibers can therefore lead to scaffolds that can control biological activities such as fibroblastic cell attachment, proliferation, and differentiation, in order to facilitate timelier ligament or tendon restoration with biomechanically appropriate properties.

One of the earliest results on fibroblast cell interaction with nanofibers was presented by Ko et al. (1998), who demonstrated the positive effect of increased surface area on cell attachment and growth via a comparison with microfiber scaffolds. The difference in cell behavior on nanofibrous and microfibrous scaffolds was further clarified in the later work by Gandhi et al. (2007) on *Bombyx mori* silk. The work by Li et al. (2005b) also showed superior ECM generation from mesenchymal stem cells (MSCs) and chondrocytes seeded on nanofibrous scaffolds.

5.3.1 Nanofiber fabrication

There are several methods for fabricating nanofibers, such as fiber drawing with micropipette tips, template synthesis using nanoporous membrane molds, phase separation using a solvent incompatible with the fiber matrix, molecular self-assembly,

and electrospinning (Ramakrishna et al., 2005). Although each method has its respective advantages and drawbacks, electrospinning has been the preferred approach due to its simplicity, flexibility, and ability to be scaled up. Electrospinning textile fibers was patented by Formhals in 1934 (Formhals, 1934), but the fabrication of submicron fibers was not well known until the publication of several pioneering reports by the Reneker group in the 1990s (Ko et al., 1998; Li and Xia, 2004). Since then, studies of nanofiber products have exponentially increased, as investigators attempt to create applications with large surface areas, and these studies have revitalized a range of multidisciplinary research into filtration, energy, catalysis, medical devices, and more.

The principles of electrospinning were based on earlier work by Rayleigh in 1882, who was trying to overcome liquid surface tension by using an electrostatic charge (Katti et al., 2004). Yet, the first application of this finding involved spraying solution droplets rather than fiber formation, as outlined in the 1902 patent by Cooley and Morton (Hutmacher and Dalton, 2011). In fiber electrospinning, a high voltage in the range of 5–30 kV is applied to a syringe containing a polymer solution, and, as the electrostatic repulsion between the polymer molecules overcomes solution surface tension, the solution exiting the containment syringe changes from droplet shaped to cone shaped, eventually forming a fiber jet. As the fiber jet travels toward a grounded collector, electrostatic repulsion and solvent evaporation reduce the diameter of the jet, and the corresponding decrease in bending stability causes the jet to undergo significant bending, resembling a whipping motion, which further reduces the fiber jet diameter until it reaches the collector. The diameter and surface properties of the resultant nanofibers depend heavily on solution parameters such as viscosity, surface tension, and solvent choice, as well as electrospinning parameters such as voltage, solution feed rate, and spinning distance (Ramakrishna et al., 2005). The theoretical relationships between solution and electrospinning parameters and the nanofiber morphology have also been modeled and extensively discussed in the work by Fridrikh et al. (2003), Wan et al. (2010), and D'Amore et al. (2010). Experimentally, the effects of these parameters on fiber morphology were shown through the work by Katti et al. (2004), who studied PLGA electrospun nanofibers and their use in skin regeneration and drug delivery.

The nanofiber structure can also be controlled via solution and exit nozzle modifications. A schematic diagram of the electrospinning process and examples of nozzle and collector modification are shown in Figure 5.2. The simplest electrospinning setup, with a single-phase polymer electrospinning solution, can create uniform, homogeneous nanofibers. To obtain a nanofiber membrane containing multiple polymer phases, one can install multiple nozzles each containing a different polymer. Alternatively, two electrospinning nozzles can be modified into a coaxial setup in which a polymer solution is spun through the outer nozzle and a different solution is spun through the inner one, creating a nanofiber with a core-shell structure. Interestingly, in a coaxial setup, the core solution does not have to be spinnable, because the shear force experienced by the shell solution can extract the core solution out of the nozzle (Jiang et al., 2006). Core-shell nanofibers are commonly examined for drug release applications, especially for growth factor delivery that requires a protective shell. The same core-shell nanofibrous structure can also be achieved by electrospinning an emulsion rather than a homogeneous solution. In this case, the amount of the core phase must be sufficient to

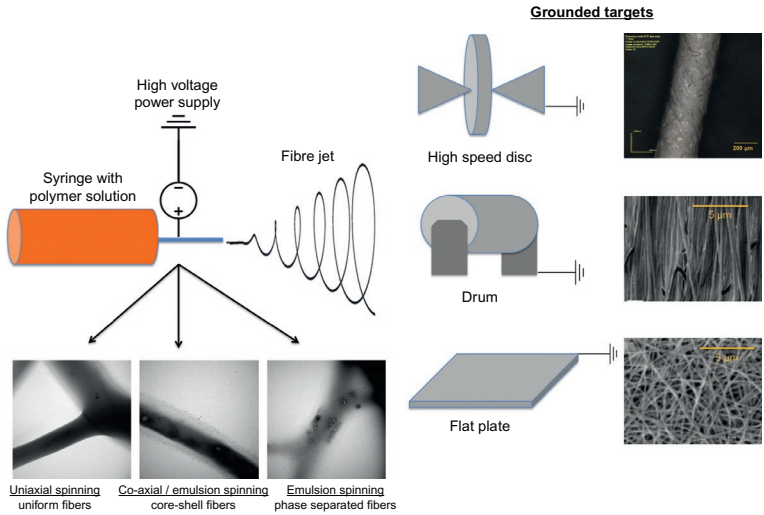

Figure 5.2 Diagram of electrospinning setup, with examples of solution, nozzle, and collector modifications.

form a stable, continuous core (Wei et al., 2011; Yarin, 2011). Alternatively, the amount of core phase or stabilizer can be changed to produce a composite nanofiber with a random distribution of the emulsified phase (Xu et al., 2005).

In addition to nozzle and solution modifications, the fiber collector can be customized to fabricate nanofibers with different geometries. The ground collector can be of different shapes as long as it remains grounded, and current studies on electrospinning have demonstrated nanofiber collection on plates, drums, wire frames (Reneker and Chun, 1996), detachable tubes (Kuraishi et al., 2009), and more. Although randomly oriented fiber membranes collected on plate collectors provide a large surface area for various applications, wire frames and drums spinning at high rotation rates have been shown to produce highly oriented nanofibers (Li et al., 2007), which are suitable for cardiac and neural tissue regeneration because they can support cells that have preferred alignment, and these nanofibers can actually be used in any application that requires strong directional properties. Fibers collected on the edges of conductive plates can be removed as a thread, which can be useful on its own or as a precursor to textile products such as sutures and woven fabric. Detachable tube collectors can serve as a mold for controlling fiber geometry, leading to tubular constructs that can be useful for cardiovascular applications, as suggested in the work by Stitzel et al. (2006) on tubular scaffold as an arterial substitute.

5.3.2 Materials

The flexibility of the electrospinning technique in controlling the size, morphology, orientation, and structure of the nanofibers is complimented by the wide variety of materials that can be electrospun. Since the pioneering work of Reneker and Chun

(1996), hundreds of different polymers have been electrospun for different applications. For polymers electrospun for tissue regeneration, however, the basic requirements are that the polymer must be biocompatible, and it cannot cause irritation or allergic responses in patients. When considering materials for ligament and tendon scaffolds, the tensile behavior of the materials must also be considered, because property mismatch is a major reason that primary repair surgeries fail to address patient needs. Polymers electrospun for tissue applications can be natural, synthetic, or combinations of both, with their advantages discussed previously in Section 5.2.3.

Nanofibers of natural polymers, either in the form of proteins or polysaccharides, have been electrospun in previous studies, and their effectiveness as tissue scaffolds has been demonstrated. Collagen was one of the first electrospun natural polymers to be examined for tissue regeneration due to its resemblance to native ECM and the presence of functional groups for cell interaction, such as the arginine-glycine-aspartic sequences that enhance cell attachment. The positive effect of collagen nanofibers on cell growth has been documented in various studies, such as the one by Li et al. (2005a) that highlighted the superiority of MSC growth on electrospun protein scaffolds over tissue culture plate controls. In addition to collagen, ECM proteins such as elastin and fibrin have been electrospun into nanofibers in the past. Silk was also actively studied due to its abundance and extensive use in tissue repair throughout history. In addition to having demonstrated positive cell adhesion and differentiation results, follow-up studies have also showed that the mechanical properties of silk nanofibers can be controlled via postelectrospinning treatments (Gandhi et al., 2009b). Polysaccharides, on the other hand, have been electrospun either individually or cospun with ECM proteins for structural and functional purposes. For example, alginate (Bhattarai and Zhang, 2007; Bhattarai et al., 2006), chitosan (Bhattarai et al., 2005), and GAG components such as hyaluronic acid (Ji et al., 2006; Li et al., 2006) have been electrospun as robust fibrous scaffolds, with possibilities for customizing mechanical properties through ionic or covalent crosslinking. Chitosan and hyaluronic acid have also been cospun with collagen as reinforcements. Interestingly, the work by Hsu et al. (2010) suggests that, when hyaluronic acid was combined with collagen, the production of matrix metalloproteinase inhibitors was reduced relative to the proteinase, which may facilitate tissue generation with reduced scarring, an important factor in determining the mechanical properties of regenerated ligament tissue or whether tendon-sheath adhesion would occur. Other GAG polysaccharides, such as chondroitin sulfate, have been added to electrospinning solutions for further enhancing cell proliferation (Zhong et al., 2007).

Although the biological properties of natural polymers continue to fuel interest in electrospinning them for tissue scaffolds, much effort has also been directed toward the use of synthetic polymer nanofibers due to their often superior and customizable mechanical properties. The ability to tailor the tensile behavior of nanofiber scaffolds is especially important for tendon and ligament applications due to their function in transmitting loads, as well as recent evidence suggesting improved organization of regenerated tendon tissues under tensile strain. Desirable tendon and ligament scaffolds constructed from synthetics are also biodegradable, with degradation rates similar to tissue formation rates. Common biodegradable polymers for electrospinning

include polyvinyl alcohol (PVA), polyurethane (PU), polycaprolactone (PCL), poly-DL-lactic and poly-L-lactic acid (PLLA or PDLLA), polyglycolic acid (PGA), and a copolymer of the two previous substances (PLGA). Given that these synthetic polymers are applied *in vivo* as tendon or ligament scaffolds, their behavior in degradation environments must also be considered. Studies have shown that the elastic modulus and tensile strength of synthetic polymer nanofibers can be reduced up to 90% in aqueous environment (Beachley and Wen, 2009), Li et al. (2010) also showed that, under a tensile load, PLGA nanofibrous scaffolds experience a faster degradation than load-free scaffolds do, as indicated by a quick drop in their tensile modulus.

5.4 Tailored nanofiber scaffolds for tendon and ligament regeneration

The challenges faced by previous generations of reconstruction approaches were largely related to their inability to impart specific mechanical or biological properties. Therefore, the flexibility of fabrication techniques and material choices becomes highly important when designing tendon and ligament scaffolds. In addition, advancements in electrospinning and post-spinning processing techniques in the last decade can also be utilized to create highly customized nanofiber scaffolds.

5.4.1 Mechanical properties

Primary repair surgeries were not able to restore mobility because the resulting scar tissues had significantly different tensile behavior than the surrounding native tissues did, whereas many synthetic prostheses caused stress-shielding that led to disorganized tissue growth. Earlier tissue scaffolds were also unable to adequately address these challenges because they could not maintain structural integrity before new tissue formation. As a result, nanofiber integrity became one of the major focuses of ligament scaffold research.

Tensile behavior, such as ultimate strength, elastic modulus, and maximum elongation, as well as the degradation behavior of these properties, largely depends on the material choice of the nanofiber matrix. Synthetic polymers, such as PCL and PLGA, are often used to fabricate nanofibers that are stronger, more extensible, and less stiff compared to those fabricated from natural polymers, especially proteins such as collagen. The tensile stress–strain relationships for several common biocompatible polymers for medical nanofibers have been discussed in Leung et al. (2011). In ligament and tendon scaffolds, however, the need for bearing loads prior to new tissue generation poses an added challenge; the nanofibers must not only remain sufficiently strong over a fixed time, but they must also mechanically behave like the tissue that they temporarily replace. Tendons and ligaments have nonlinear elastic tensile behavior (Louie et al., 1998; Silver et al., 1991), as shown in Figure 5.3. Under low deformations, deformation is contributed by the uncrimping of collagen fibrils, resulting in a toe region of the stress–strain curve with relatively low slopes. As the deformation

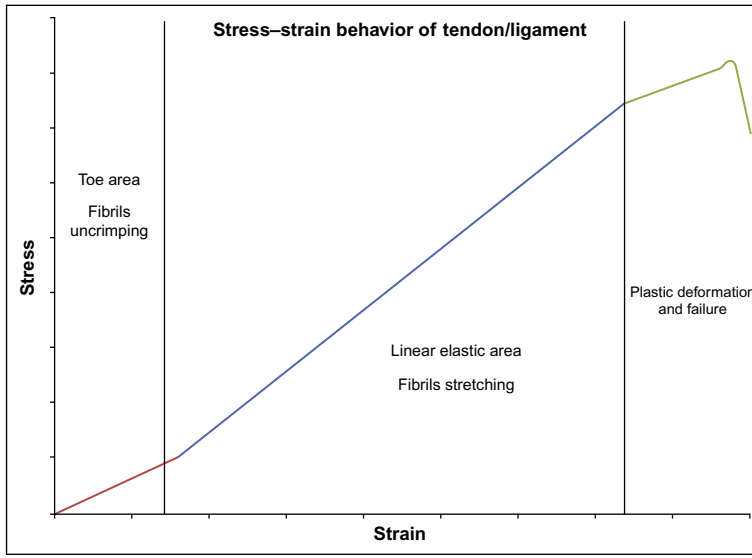

Figure 5.3 Nonlinear tensile behavior of native tendon/ligament.

increases, collagen fibrils begin to elastically and plastically deform, forming two other regimes in the stress–strain behavior up until the failure of the tissue. It is important to mimic the toe region as well as the elastic region in scaffold design, because it is unlikely that a patient will stretch his or her muscles or bones to the point of plastic deformation. There are several methods for mimicking the initial, low modulus response and the subsequent toe-elastic deformation transition, such as adjusting solution conductivity to fabricate nanofibers with coiled morphology, and coelectrospinning a nanofiber construct containing multiple polymers with different elastic moduli. Recently, Surrao et al. (2012) produced crimped PLA nanofibers with wavelengths of approximately 50 μm by soaking an electrospun membrane in a phosphate-buffered saline solution heated to above the PLA glass transition temperature. Although Surrao et al. were able to mimic the toe region of the stress–strain curve, the behavior was not sustainable upon repeated loading, indicating the need for improving consistency. In another example, Ladd et al. (2011) fabricated a scaffold containing a PLLA/collagen blend on one end and a PCL/collagen blend on the other to mimic the muscle-tendon junction. Because PLLA and PCL have different tensile strengths and stiffnesses, the composite design by Ladd et al. effectively displayed a gradient of tensile behavior from the stiffer PLLA end to the more compliant PCL end, with an intermediate region at the center containing both PLLA and PCL.

Despite showing potential in obtaining tailored nonlinear tensile behavior, these studies highlighted a major challenge in nanofiber scaffold design. The scaffold proposed by Surrao et al. (2012) was only able to achieve ultimate tensile loads in the range of 1–1.5 N, which corresponded to a strength of approximately 1 MPa, whereas the one demonstrated by Ladd et al. (2011) failed at under 1 MPa, with the failure

starting at the PCL end, which had lower tensile strength. In comparison, earlier studies indicated that human ACL has a tensile strength in the range of 13–38 MPa (Silver et al., 1991). The elastic modulus of the human ACL is in the range of 65–111 MPa (Silver et al., 1991), with the wide range likely resulting from nonlinear stress–strain behavior. Assuming that the toe region extends to 8% strain, it can be approximated that, at the upper end of the toe region, the ACL can withstand a tensile stress of around 5 MPa. It is therefore clear that nanofiber integrity must be improved for effective clinical use. Researchers have extensively explored the possible techniques for enhancing the tensile strength of nanofibers, and their discoveries have led to different strengthening methods, including fiber alignment, annealing, crystallization bath, and particle reinforcement. The simplest method for enhancing tensile strength is to align nanofibers in the direction of loading. Alternatively, nanofibers can be aligned differently in a controlled manner to produce gradient tensile behavior, such as diagonally to the direction of loading, leading to an initial low-modulus stage in which fibers realign themselves to the direction of loading, followed by elastic deformation. Heat treatment approaches such as annealing under loads have also been reported to increase the tensile strength and stiffness of nanofibers, by enhancing polymer crystallinity or encouraging physical crosslinking (Gandhi et al., 2009b; Tan and Lim, 2006). For protein-based nanofibers, polymer crystallization can also be induced through soaking in a solvent bath, as described by the work of Gandhi et al. (2009b) on silk nanofibers. By soaking silk nanofibers in methanol, Gandhi et al. showed that the crystallinity of the silk increased, leading to a threefold enhancement of tensile strength, from 6.2 to 18.5 MPa, while the same methanol treatment performed under 10% prestretching led to a further increase in tensile strength to 22.2 MPa. Moreover, by reinforcing nanofibers with nanoparticle fillers, tensile strength can be increased to an even greater degree, as shown by Gandhi et al. (2009b), who produced an additional twofold increase in tensile strength to 44.5 MPa by adding 1 wt% single-walled carbon nanotubes. Furthermore, recent studies have shown that, although pristine carbon nanotubes may pose health hazards, those functionalized with proteins or carboxyl groups have shown no adverse effects thus far (Bianco et al., 2005), indicating the potential for their use in medical products.

5.4.2 Degradation properties

Although much attention has been rightfully focusing on mimicking the nonlinear tensile behavior of tendon and ligament tissues, it is equally important to ensure that the load-bearing function of the scaffold does not deteriorate before new tissue is formed. From a material standpoint, it is difficult to design a scaffold that can maintain constant tensile behavior in an aqueous environment for a precise length of time, before undergoing degradation to avoid surgical removal. The physiological load that has to be carried by a tendon or ligament scaffold poses an additional design challenge. In order to support tendon and ligament growth and temporarily replacing their functions, the nanofiber scaffold should degrade in a predictable and controllable manner, such that there is sufficient time for fibroblasts to populate the scaffold and produce

new, vascularized tissues, while not interfering with the remodeling stage that begins later in the healing process.

The degradation properties of nanofibers are mostly determined by the material choice, with natural polymers without any modifications known to degrade rapidly, while synthetic polymers have degradation rates that depend on their hydrophobicity. Although nanofibers composed of polymers with more alcohol end groups, such as PVA, can dissolve immediately in water, other hydrophilic polymers, such as PGA, can remain intact for longer. Hydrophobic polymers, such as PLA and PCL, can remain intact for up to several months in the body, but marginally swellable polymers, such as polycaprolactone ethyl ethylene phosphate (PCLEEP), can remain in the body for years (Chew et al., 2005). One of the common methods for controlling nanofiber degradation time is to use a copolymer such as PLGA. By combining lactic acid (LA) and glycolic acid (GA) at different ratios, researchers have caused nanofibers to maintain their mechanical properties for varying lengths of time. For example, in the work by Surrao et al. (2012), the PLGA nanofibers, containing 85 wt% LA and 15 wt% GA, were able to maintain their tensile strength and modulus for 3 months.

Much like tensile behavior, further fine tuning of degradation properties is possible through postelectrospinning modifications, which are especially useful for protein-based polymers that have desired biological responses but can dissolve immediately in aqueous environments. Natural polymers are often modified via crosslinking treatments, which stabilize the polymer molecules against the aqueous environment by forming hydrogen, ionic, or covalent bonds between one another. Figure 5.4 shows the effect of ionic and covalent crosslinking on alginate and nanofiber degradation.

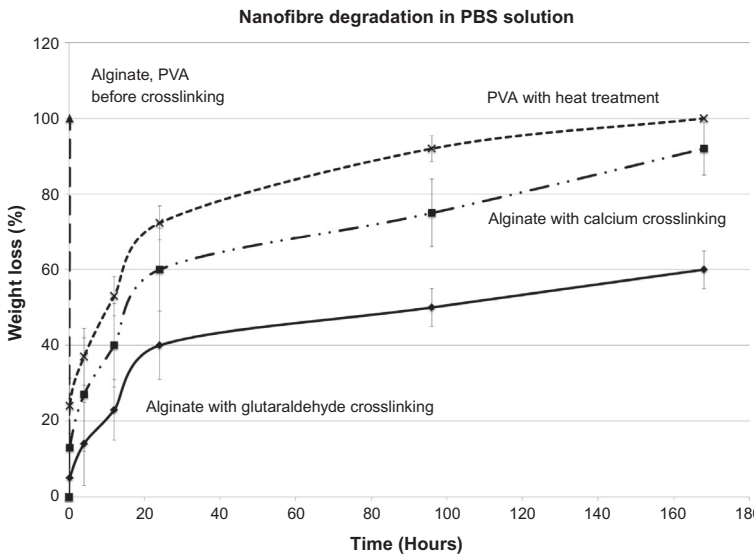

Figure 5.4 Nanofiber degradation profiles for alginate and PVA nanofibers, showing the effect of physical crosslinking via heat treatment at 140 °C, and chemical treatment in ionic and covalent crosslinking baths.

In several nanofiber studies involving collagen or collagen composites, crosslinking with glutaraldehyde was shown to promote nanofiber stability in PBS solutions, as well as *in vivo* during animal studies. Moreover, once carefully washed to remove excess glutaraldehyde, fibroblast cells seem to remain viable on glutaraldehyde crosslinked scaffolds (Lee et al., 2007). Ionic crosslinking has also been shown to enhance the integrity of sodium alginate nanofibers in water, via exchanging the monovalent sodium ions at the carboxyl ends of the guluronate group with divalent calcium ions (Bhattarai et al., 2006). However, once a scaffold is placed in the PBS solution, reverse ion-exchange with sodium causes quicker alginate nanofiber degradation, allowing alginate-based scaffolds to maintain intact only for several days. For synthetic nanofibers, glutaraldehyde can also be used to form covalent bonds, leading to permanent crosslinking. Yet, in many studies, nanofibers from synthetic polymers were modified by physical crosslinks via heat- or solvent-induced polymer chain entanglement, such as the methanol treatment for silk nanofibers outlined in the work by Gandhi et al. (2009b). In another example, PVA nanofibers can also be heated to 80–150 °C for improved integrity in water and PBS solutions, as shown in our work summarized in Figure 5.4.

Although crosslinking can and is often performed to enhance nanofiber longevity in an aqueous environment, the technique can also change nanofiber mechanical properties. In many cases, crosslinked nanofibers have a higher stiffness and lower extensity than they did before crosslinking, due to tighter interlocking between polymer molecules and the formation of fiber welds at their junctions. However, in several studies on collagen nanofibers, crosslinking with glutaraldehyde was shown to increase the maximum elongation of the nanofibers, which is likely due to the coiled structure of the collagen (Zhong et al., 2006). In this case, covalent bonds were formed between the coils from different strands of collagen fibrils without destroying the overall structure, such that under tension, collagen coils could still unwind themselves, while the covalent bonds formed between the fibrils ensured that the bundle of collagen remained intact, therefore preventing disintegration. The effect of crosslinking on coiled collagen fibrils has significant implications for ligament scaffold design. In addition to prolonging collagen nanofiber longevity *in vivo*, it may also be able to address the lack of stability in artificially crimped or coiled nanofibers such as those highlighted by Surrao et al. (2012), leading to structures that can mimic the nonlinear deformation behavior while remaining consistent after repeated loading.

5.4.3 Biological response

A robust scaffold with appropriate degradation properties forms the basis for supporting ligament or tendon growth, but it is also necessary to mediate the ECM regeneration process for restoring full tissue functions, because excessive scarring or insufficient tissue ingrowth has repeatedly caused earlier reconstruction approaches to fail. Many studies have investigated the incorporation of drugs and signaling molecules such as growth factors to facilitate cell activities and subsequent collagen deposition in different forms of scaffolds, and the recent attention on nanofibers has prompted researchers to combine their knowledge on drug and growth factor delivery

with this new material. Antibiotics are one of the most common types of drugs studied in connection with nanofiber-based soft tissue scaffolds, with common examples being Cefazolin (Katti et al., 2004), Rifampin (Zong et al., 2002), and fusidic acid (Said et al., 2011) in PLA- or PLGA-based nanofibers. Although targeting the inflammation stages early in the regeneration process, antibiotic-loaded scaffolds tend to be quick releasing. In addition to preventing prolonged inflammation and infection, antibiotic-loaded scaffolds might also prevent abdominal adhesion (Bölgen et al., 2007). In their scaffold design, Bölgen et al. (2007) showed that a layer of electrospun PCL could act as a physical barrier against postsurgical tissue adhesion, and when the layer is loaded with the antibiotic Biteral, the scaffold further reduced adhesion in an animal model, likely by reducing the bacteria that could change the balance between fiber deposition and resorption. Although designs such as the Biteral-loaded scaffold are currently limited to preventing abdominal adhesion, they nonetheless have implications for future tendon repair, because scar-induced adhesion with the protecting sheath is one of the reasons that primary tendon repair failed. In addition to antibiotics, growth factors are also useful for facilitating ligament or tendon reconstruction, as identified in previous studies involving different forms of tissue scaffolds. The effects of several growth factors, including transforming growth factor β1 (TGF-β1), platelet-derived growth factor (PDGF), epithelial growth factor (EGF), and fibroblast growth factor (FGF-2), on ACL fibroblast activities have been extensively documented in the work by Murray et al. (2003) on collagen-GAG-lyophilized scaffolds. By seeding ACL cells from human explants on the growth factor-loaded scaffolds, Murray et al. showed that TGF-β1 was able to increase cell proliferation on the scaffold, as well as the collagen production rate and smooth muscle actin expression, while PDGF and FGF-2 showed increased proliferation and collagen synthesis rates, and EGF showed no significant effect. The positive results of TGF-β1 incorporation for encouraging tissue growth were also confirmed in subsequent work on nanofiber scaffolds, which indicated significant increases in cell proliferation and ECM deposition rates (Hromadka et al., 2008). In electrospinning, growth factors and proteins can be incorporated into nanofiber matrix through direct blending, covalent binding, emulsion, and coaxial electrospinning (Ji et al., 2011). Moreover, growth factors can also be encapsulated in nanoparticles to ensure a sustainable effect. For example, Liu and Ma (2010) showed that loading FGF into dextran nanoparticles before their incorporation into a PLA electrospinning solution improved cell proliferation and tendon healing as compared to the healing produced by blending FGF directly into a PLA matrix. Despite the positive initial results, Hromadka et al. (2008) also pointed out in their review that TGF-β1 may lead to hypertrophic scarring unless eliminated early, as might be accomplished by using TGF-β inhibitors such as fibromodulin. In addition to inhibiting the overproduction of collagen, a PLGA microsphere system containing an antifibrogenic factor, stratifin, might also reduce hypertrophic scarring on skin (Rahmani-Neishaboor et al., 2012). Stratifin acts to increase the expression of matrix metalloproteinase (MMP) in fibroblast cells, which breaks down ECM and thereby eliminates excess collagen. Such scar prevention mechanisms will also be significant for mitigating a major concern in ligament/tendon reconstruction, the mechanical property differences between scar and native tissue.

Given the intricate nature of the tissue regeneration process, precise control of therapeutic release rates is important, because specific therapeutic effects may be beneficial for one stage but detrimental in the next. Among the examples mentioned earlier in this section, antibiotics may be useful at the inflammation stage, but they may interfere with fibroblast growth in the proliferation stage, whereas growth factors may help proliferation and ECM deposition but may cause scarring due to excessive collagen production. As a result, in the last decade, strategies have been formulated to control release rate of therapeutics from nanofibers in order to optimize tissue regeneration. The choice of a nanofiber matrix plays a significant role in determining the release mechanisms, depending on their degradation behavior and affinity with the therapeutics. For example, hydrophilic compounds such as proteins and growth factors tend to concentrate on the nanofibers' surfaces when electrospun with hydrophobic matrices, leading to the desorption-driven release of the compound once the nanofibers are exposed to aqueous environments (Gandhi et al., 2009a). Further modifications to the release rate in a desorption-driven release system can be accomplished by changing the surface area available on the fiber membrane, as quantified by Srikar et al. (2008), who derived a semiempirical equation, shown in Equation (5.1), relating fractional release M_t/M_{d0} (in which M_t is the mass of drugs released at time t and M_{d0} is the initial mass of drugs) to a porosity factor α, and characteristic time τ_r that depends on porosity size and the effective diffusion coefficient (Gandhi et al., 2009a). Desorption-driven release systems are usually quick and therefore may be useful in targeting the early stages of the tissue reconstruction process. In other cases, the therapeutic compounds are more compatible with the matrix in solution and are distributed within the nanofibers upon electrospinning, leading to release dominated by Fickian diffusion, with the rate dependent on fiber morphology. If the matrix degradation is much slower than the drug release, diffusion-driven release is most commonly described by the Higuchi model, as shown in Equation (5.2), in which M_∞ is the mass released at infinite time and K_H is a constant determined empirically (Siepmann and Peppas, 2011). However, when the matrix is biodegradable, as in PLGA and PVA scaffolds, polymer degradation often plays a significant role in the drug release in addition to release due to diffusion. Such mixed release mechanisms are often described by the Korsmeyer–Peppas model, shown in Equation (5.3), in which K_m is another empirical constant and n is the diffusion exponent, with a values of approximately 0.45 indicating Fickian diffusion-driven release from cylindrical geometries, values between 0.45 and 0.89 indicating combined contributions to release by diffusion and polymer erosion, and a value of 0.89 indicating zero-order release (Siepmann and Peppas, 2001). To adjust the extent of diffusion- and erosion-controlled release, the matrix choice can be adjusted, as can be accomplished by using a different GA-to-LA ratio for a PLGA matrix. In addition, with less mobile compounds involving larger particles, release can be driven solely by polymer degradation, which can be described by the Hixson–Crowell model, as shown in Equation (5.4), with M_0 representing initial amount of drug and K_{HC} being an empirical constant (Shoaib et al., 2006). Further modification to drug release behavior can also be carried out through a multilayer approach, by combining drug-loaded layers with barrier and sacrificial layers. In one example, Okuda et al. (2010) demonstrated the incorporation of two different dyes

into a four-layered nanofiber structure, in which one dye released immediately after incubation, whereas the other dye experienced a delayed release due to the barrier layer (Okuda et al., 2010).

$$\frac{M_t}{M_{d0}} = \alpha\left[1 - \exp\left(\frac{-\pi^2 t}{8\tau_r}\right)\right] \tag{5.1}$$

$$\frac{M_t}{M_\infty} = K_H t^{0.5} \tag{5.2}$$

$$\frac{M_t}{M_\infty} = K_m t^n \tag{5.3}$$

$$3M_0^{0.5} - 3M_t^{0.5} = K_{HC} t \tag{5.4}$$

One of the challenges in tendon and ligament construction is ensuring the formation of organized tissue in the scaffold, which earlier synthetic prostheses failed to do. Although drug and growth factor delivery can help enhance cell response on the scaffold, the tissue that cells deposit must ultimately be similar to native tissues, which are fiber bundles mainly composed of aligned collagen fibrils. Given that the nanofiber scaffold serves as a platform for cell adhesion and subsequent collagen deposition, its organization has significant effects on tissue alignment. Li et al. (2007) reported that, when using aligned PCL nanofibers as a scaffold, the cell deposition of meniscal fibroblasts and human mesenchymal stem cells (hMSCs) corresponded to the fiber orientation, with the actin filaments in the hMSC organized along the aligned fibers. In addition, Li et al. also reported superior directional properties for the scaffold, which may open opportunities in mimicking the mechanical properties of organized structures such as tendons and ligaments. In another study, Lee et al. (2005) reported an aligned polyurethane nanofiber scaffold and showed that ligament fibroblasts form a spindle shape orienting along the fibers. Compared to randomly aligned nanofibers, the ligament fibroblasts produced significantly more collagen. Moreover, when the scaffold was subjected to uniaxial tensile strain along the fiber direction, collagen production by the ligament fibroblast further increased. With the directional sensitivity of ligament fibroblasts demonstrated by Lee et al. on aligned nanofiber scaffolds, it is possible that the new tissue can undergo more optimal organization in the remodeling stage.

5.5 Nanofiber assembly into three-dimensional tendon or ligament scaffolds

In the previous sections, we introduce nanofiber scaffolds and discuss strategies for controlling their mechanical and biological properties, as well as their potential impact on tendon/ligament regeneration. However, thus far, the discussion has been

limited to nanofibers electrospun into a membrane, which can only serve as proof-of-concept models for various functional and therapeutic modifications. To develop nanofiber scaffolds that can be applied in ligament and tendon reconstruction, it is necessary to also examine strategies for forming nanofibers into appropriate three-dimensional (3D) constructs, because planar fiber membranes cannot be applied directly as temporary tissue replacements. In addition, given that tendon and ligaments have at least one end attached to bones, scaffold fixation must be carefully designed, and this has remained a major challenge in implant design since the early days of synthetic prostheses.

Being highly connective, nanofibers can be formed into various hierarchical structures, using common textile techniques such as those summarized in the work by Ko (1997). For example, knitted microfiber scaffolds have been commonly used for ligament scaffolds due to their high porosity for cell infiltration and tissue ingrowth. Ge et al. (2005) demonstrated PLA- and PLGA-based knitted scaffolds that remained structurally intact in *in vitro* degradation environments, with a relatively small reduction in tensile strength from 60 to 40 MPa after 20 weeks, while the maximum elongation remained the same. Despite these attractive structural properties, the lower fiber density in the constructs meant that earlier knitted scaffolds required soaking in gel before application to allow cell infiltration, which was not desirable for situations such as ACL injury, because the gel-fiber composite may separate easily in the joint. To address the gel-fiber disadvantage, Sahoo et al. (2006) fabricated a nanofiber–microfiber composite in which a PLGA microfiber knitted backbone was supported by PLGA electrospun nanofibers on all surfaces and between loops. In this design the nanofibers served the function of the gel, supporting cell infiltration, while providing a much larger surface area for cells. In a comparison with the knitted microfiber-gel system, Sahoo et al. showed that both bone marrow stromal cell proliferation and ECM expression were higher in the nanofiber–microfiber composite scaffold, highlighting a potential application of nanofibers into existing implants. Building on their earlier work, Sahoo et al. (2010) later presented a similar scaffold in which the PLGA nanofibers were loaded with FGF, which showed tenogenic effects and further simulation of MSC differentiation under mechanical loading. In addition, it is also possible to construct the backbone of knitted scaffolds using nanofibers, by collecting them as a yarn using a disc collector setup or by attenuating and orienting nanofibers collected on a drum (Ko et al., 2003).

The establishment of a 3D construct provides a basis for an effective tendon and ligament scaffold, but strategies for their fixation must also be considered because insufficient fixation will cause improper load transfer that can, in turn, lead to reconstruction failure or further injuries. Taking an approach that differed from the knitted scaffold method mentioned previously, Cooper et al. (2005) adopted a braided scaffold design, also using PLGA microfiber as the matrix. Braided scaffolds were usually considered porous and could therefore reduce cell infiltration compared to knitted scaffolds, but the scaffold presented by Cooper et al. addressed this concern by designing a loosely braided intra-articular zone between two densely braided ends known as bony attachment zones. The intra-articular zone, while maintaining a braided structure, has a porosity of approximately 59% with average pore diameters of 212 μm

(Cooper et al., 2005), which is more porous than the knitted scaffold presented by Ge et al. (2005), which displayed 44% porosity and average pore diameters in the range of 180 μm. In addition to fiber densities, fiber orientations of the intra-articular zone and bony attachment zones are different, with the bony attachment zones having higher angles of orientation and a more-crisscrossed fiber structure to promote bone integration, while the intra-articular zone has more fibers oriented along the direction of loading to enhance stress-bearing ability. With a loosely braided structure in the articular zone, the braided scaffold could also mimic the nonlinear tensile behavior observed in native tissues, with the toe region contributed by the straightening of the loose fiber structure, much like the uncoiling of collagen fibrils in the native tissue. Although the current braided scaffold design is limited to microfibers, it is possible to transfer this technique to nanofibers as well, starting with the yarn collection technique mentioned previously. In fact, researchers have recently begun investigating strategies for consistently producing nanofiber yarns (Ali et al., 2012), and they are exploring simple braided constructs using nanofiber yarns for sutures (Hu et al., 2010) and ligament scaffold applications (Barber et al., 2011). Figure 5.5 shows an example of a braided thread composed of six silk nanofiber yarns fabricated in our recent work. Using a similar technique, Barber et al. (2011) presented a braided PLA nanofiber scaffold for tendon and ligament reconstruction, which was able to support hMSC proliferation, and, when cultured with growth factors under tensile strain, hMSC differentiation into tenogenic lineage was observed.

In addition to supporting fixation by fiber alignment, surface modification can be used to enhance bone ingrowth. A possible solution is to take the sintered titanium plugs at the ends of Hunter tendon prostheses as examples, incorporating similar structures in the scaffold. This can be accomplished by co-electrospinning the scaffold matrix with titanium dioxide, which has been demonstrated in recent work

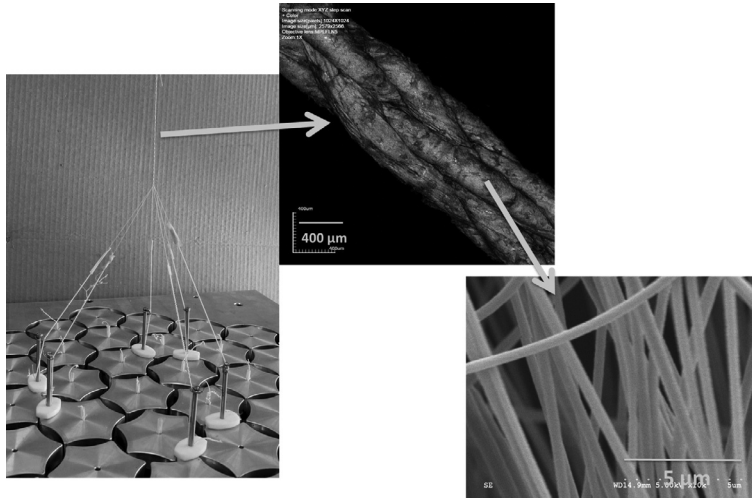

Figure 5.5 Nanofiber thread fabricated by three-dimensional braiding.

(Kim et al., 2010; Wang et al., 2012). Titanium dioxide can be purchased as a nanopowder with particle sizes below 100 nm, or it can be synthesized into nanoparticles or nanotubes using precursors such as titanium isopropoxide (Wang et al., 2012). Interestingly, titanium nanotubes have also been identified as a carrier for antimicrobial agents (Ma et al., 2012), opening additional opportunities for processing drug-loaded nanofiber ligament and tendon scaffolds. Minerals such as hydroxyapatite and dicalcium phosphate anhydrate (DCPA) have also been investigated in nanofiber scaffolds to induce osteoblast activities and bone ingrowth, due to their similarity to the apatite in human bone (Chae et al., 2013; Cui et al., 2010). Although improved bone regeneration has been demonstrated in studies that involved incorporating hydroxyapatite particles into nanofiber matrices, it has also been shown that hydroxyapatite and DCPA can be mineralized in nanofiber matrices postelectrospinning. For example, nanofiber matrices can be electrospun with sodium phosphate, with mineralization initialized upon submersing the resultant nanofiber into a calcium solution at an appropriate pH (Chae et al., 2013). The ability to mineralize bone-like crystals postelectrospinning has significant implications for tendon and ligament scaffolds. Although the crystals are more useful for bone fixation and less for soft tissue growth, it is possible to submerse only one or both ends of a nanofiber scaffold into a calcium bath, leading to hydroxyapatite mineralized in the specific areas required to create a fixation zone.

5.6 Conclusion

More effective and timelier recovery from tendon and ligament injuries could have a profound impact on socioeconomic costs, as well as the wellbeing of different members of our society, including seniors regaining the mobility required to take care of themselves, athletes reengaging in their activities, and the general public returning to the work force. Having unsuccessfully explored different methods for enabling this recovery, such as primary repair and synthetic prostheses, autografting remained the preferred technique for tissue reconstruction, even though donor site morbidity continued to plague patients and caregivers. Tissue engineering scaffolds were introduced as potential alternatives to autografts, but shortcomings still existed, because scaffolds with both sufficient bioactivity and structural properties proved difficult to fabricate. Electrospun nanofibers were therefore proposed as a new form of scaffold with the potential to address the current shortcomings, given their large surface area, resemblance to native ECM, and ability to be manufactured into 3D hierarchical structures.

Using the electrospinning technique, nanofibers can be fabricated into different morphologies, orientations, and internal structures, using a wide range of biocompatible polymers with different intrinsic mechanical and biological behavior. In addition, nanofiber properties can be further tailored through their specific organization in a construct or postelectrospinning treatments such as prestretching and crosslinking. To induce tissue production with appropriate organization, drugs and growth factors can be incorporated into nanofibers, and their release behavior can be optimized to focus on specific responses. Moreover, recent discoveries have also shed light on

potential methods for minimizing scarring in the tissue regeneration process, which remains an unsolved challenge for prostheses and primary repair strategies, both in terms of tissue adhesion and mechanical properties. Although electrospinning technology enables the creation of highly customized tissue scaffolds that can support tendon and ligament cell activities and tissue generation, advanced composite fabrication techniques are necessary to build appropriate constructs that can fully utilize the mechanical and biological functions built into the constituent nanofibers. At the construct level, it is necessary to ensure that the structure can be fixated into bones and that all constituents will remain within the structure when exposed to physiological loads. This is different from the fiber level in which the design parameters are based on biological response, degradation, and fiber mechanical properties.

In order to translate the strong potential of nanofibers into clinical use for tendon and ligament reconstruction, several additional requirements must be fulfilled. First, although there were limited demonstrations in animal models, most experiments conducted were *in vitro*. The resultant mechanical and biological behavior observed may therefore serve as a guideline for design, but they cannot be completely relied on. For example, the degradation behavior of a PLGA-based scaffold may be different *in vivo* from that observed in PBS solutions. Other important questions include whether aligned nanofibers, which are important for organized ECM production and directional mechanical properties, will remain aligned *in vivo* and under alternating loads, as well as how well 3D nanofiber constructs can maintain their geometry in locations such as a knee joint. Addressing such questions requires more focus on translational studies that may expedite readiness for clinical trials. In addition, there is a lack of more comprehensive studies that combine multiple aspects of scaffold development. For example, it would be desirable to demonstrate a 3D nanofiber braided scaffold that can be fixated to bones and facilitate antibiotic and growth factor release, with an appropriate degradation rate and ligament-like nonlinear tensile behavior. Although each aspect has been individually demonstrated in separate studies, the viability of these desirable properties combined in a single product remains an open question. Addressing such an open question will bring the technology closer to clinical readiness, but it will also call for increased collaboration between a wide range of specializations, including experts in pharmaceuticals, materials, mechanical devices, and textiles. Through such collaborations, design goals and fabrication can be collectively formulated while considering the intricate set of objectives for an effective, safe, and market-ready soft-tissue scaffold.

References

Abousleiman, R., Mcfetridge, P.S., Sikavitsas, V.I., 2005. A new paradigm in tendon tissue engineering. In: The 2005 Annual Meeting of the American Institute of Chemical Engineers.

Abousleiman, R.I., Reyes, Y., Mcfetridge, P., Sikavitsas, V., 2008. Tendon tissue engineering using cell-seeded umbilical veins cultured in a mechanical stimulator. Tissue Eng. Part A 15, 787–795.

Ali, U., Zhou, Y., Wang, X., Lin, T., 2012. Direct electrospinning of highly twisted, continuous nanofiber yarns. J. Text. Inst. 103, 80–88.

Ayutsede, J., Gandhi, M., Sukigara, S., Micklus, M., Chen, H.-E., Ko, F., 2005. Regeneration of *Bombyx mori* silk by electrospinning. Part 3: characterization of electrospun nonwoven mat. Polymer 46, 1625–1634.

Barber, J.G., Handorf, A.M., Allee, T.J., Li, W.J., 2011. Braided nanofibrous scaffold for tendon and ligament tissue engineering. Tissue Eng. Part A 19, 1265–1274.

Beachley, V., Wen, X., 2009. Fabrication of nanofiber reinforced protein structures for tissue engineering. Mater. Sci. Eng. C 29, 2448–2453.

Bhattarai, N., Zhang, M., 2007. Controlled synthesis and structural stability of alginate-based nanofibers. Nanotechnology 18, 455601.

Bhattarai, N., Edmondson, D., Veiseh, O., Matsen, F.A., Zhang, M., 2005. Electrospun chitosan-based nanofibers and their cellular compatibility. Biomaterials 26, 6176–6184.

Bhattarai, N., Li, Z., Edmondson, D., Zhang, M., 2006. Alginate-based nanofibrous scaffolds: structural, mechanical, and biological properties. Adv. Mater. 18, 1463–1467.

Bianco, A., Kostarelos, K., Prato, M., 2005. Applications of carbon nanotubes in drug delivery. Curr. Opin. Chem. Biol. 9, 674.

Bölgen, N., Vargel, İ., Korkusuz, P., Menceloğlu, Y.Z., Pişkin, E., 2007. In vivo performance of antibiotic embedded electrospun PCL membranes for prevention of abdominal adhesions. J. Biomed. Mater. Res. B Appl. Biomater. 81B, 530–543.

Brückner, H., 1966. Eine neue Methode der Kreuzbandplastik. Chirurg 37, 413–414.

Burg, K.J., Porter, S., Kellam, J.F., 2000. Biomaterial developments for bone tissue engineering. Biomaterials 21, 2347–2359.

Campbell, W.C., 1936. Repair of the ligaments of the knee: report of a new operation for the repair of the anterior cruciate ligament. Surg. Gynecol. Obstet. 62, 964–968.

Chae, T., Yang, H., Ko, F., Troczynski, T., 2013. Bio-inspired dicalcium phosphate anhydrate/poly(lactic acid) nanocomposite fibrous scaffolds for hard tissue regeneration: in situ synthesis and electrospinning. J. Biomed. Mater. Res. A 102, 514–522.

Chew, S.Y., Wen, J., Yim, E.K., Leong, K.W., 2005. Sustained release of proteins from electrospun biodegradable fibers. Biomacromolecules 6, 2017–2024.

Cooper, J.A., Lu, H.H., Ko, F.K., Freeman, J.W., Laurencin, C.T., 2005. Fiber-based tissue-engineered scaffold for ligament replacement: design considerations and in vitro evaluation. Biomaterials 26, 1523–1532.

Cui, W., Li, X., Xie, C., Zhuang, H., Zhou, S., Weng, J., 2010. Hydroxyapatite nucleation and growth mechanism on electrospun fibers functionalized with different chemical groups and their combinations. Biomaterials 31, 4620–4629.

D'Amore, A., Stella, J.A., Wagner, W.R., Sacks, M.S., 2010. Characterization of the complete fiber network topology of planar fibrous tissues and scaffolds. Biomaterials 31, 5345–5354.

Dauner, M., Planck, H., 1996. Ligament replacement polymers (replacement products). In: Salamone, J.C. (Ed.), Polymeric Materials Encyclopedia. CRC Press, Boca Raton.

Deng, D., Liu, W., Xu, F., Yang, Y., Zhou, G., Zhang, W.J., Cui, L., Cao, Y., 2009. Engineering human neo-tendon tissue in vitro with human dermal fibroblasts under static mechanical strain. Biomaterials 30, 6724–6730.

Drury, J.L., Mooney, D.J., 2003. Hydrogels for tissue engineering: scaffold design variables and applications. Biomaterials 24, 4337–4351.

Formhals, A., 1934. Process and Apparatus for Preparing Artificial Threads. U.S.A. patent application.

Fridrikh, S.V., Yu, J.H., Brenner, M.P., Rutledge, G.C., 2003. Controlling the fiber diameter during electrospinning. Phys. Rev. Lett. 90, 144502.

Fu, F.H., Bennett, C.H., Lattermann, C., Ma, C.B., 1999. Current trends in anterior cruciate ligament reconstruction. Part I: biology and biomechanics of reconstruction. Am. J. Sports Med. 27, 821–830.

Fu, F.H., Bennett, C.H., Ma, C.B., Menetrey, J., Lattermann, C., 2000. Current trends in anterior cruciate ligament reconstruction. Part II. Operative procedures and clinical correlations. Am. J. Sports Med. 28, 124–130.

Galway, R., Beaupre, A., Macintosh, D., 1972. Pivot shift: a clinical sign of symptomatic anterior cruciate insufficiency. J. Bone Joint Surg. Br. 54, 763–764.

Gandhi, M., Yang, H., Shor, L., Ko, F., 2007. Regeneration of *Bombyx mori* silk by electrospinning: a comparative study of the biocompatibility of natural and synthetic polymers for tissue engineering applications. J. Biobased Mater. Bioenergy 1, 274–281.

Gandhi, M., Srikar, R., Yarin, A.L., Megaridis, C.M., Gemainhart, R.A., 2009a. Mechanistic examination of protein release from polymer nanofibers. Mol. Pharm. 6, 641–647.

Gandhi, M., Yang, H., Shor, L., Ko, F.K., 2009b. Post-spinning modification of electrospun nanofiber nanocomposite from *Bombyx mori* silk and carbon nanotubes. Polymer 50, 1918–1924.

Ge, Z., Goh, J., Wang, L., Tan, E., Lee, E., 2005. Characterization of knitted polymeric scaffolds for potential use in ligament tissue engineering. J. Biomater. Sci. Polym. Ed. 16, 1179–1192.

Grøntvedt, T., Engebretsen, L., Benum, P., Fasting, O.V.E., Mølster, A., Strand, T., 1996. A prospective, randomized study of three operations for acute rupture of the anterior cruciate ligament. Five-year follow-up of one hundred and thirty-one patients. J. Bone Joint Surg. 78, 159–169.

Groves, E.W.H., 1919. The crucial ligaments of the knee-joint: their function, rupture, and the operative treatment of the same. Br. J. Surg. 7, 505–515.

Haddad-Weber, M., Prager, P., Kunz, M., Seefried, L., Jakob, F., Murray, M.M., Evans, C.H., Nöth, U., Steinert, A.F., 2010. BMP12 and BMP13 gene transfer induce ligamentogenic differentiation in mesenchymal progenitor and anterior cruciate ligament cells. Cytotherapy 12, 505–513.

Hartwell, R., Leung, V., Chavez-Munoz, C., Nabai, L., Yang, H., Ko, F., Ghahary, A., 2011. A novel hydrogel-collagen composite improves functionality of an injectable extracellular matrix. Acta Biomater. 7, 3060–3069.

Hewett, T.E., Shultz, S.J., Griffin, L.Y., 2007. Understanding and Preventing Noncontact ACL Injuries. Human Kinetics, Champaign, IL, 1.

Hromadka, M., Collins, J.B., Reed, C., Han, L., Kolappa, K.K., Cairns, B.A., Andrady, T., Van Aalst, J.A., 2008. Nanofiber applications for burn care. J. Burn Care Res. 29, 695–703.

Hsu, F.-Y., Hung, Y.-S., Liou, H.-M., Shen, C.-H., 2010. Electrospun hyaluronate—collagen nanofibrous matrix and the effects of varying the concentration of hyaluronate on the characteristics of foreskin fibroblast cells. Acta Biomater. 6, 2140–2147.

Hu, W., Huang, Z.M., Liu, X.Y., 2010. Development of braided drug-loaded nanofiber sutures. Nanotechnology 21, 315104.

Hunter, J., 1965. Artificial tendons: early development and application. Am. J. Surg. 109, 325–338.

Hunter, J.M., Salisbury, R.E., 1971. Flexor-tendon reconstruction in severely damaged hands a two-stage procedure using a silicone-dacron reinforced gliding prothesis prior to tendon grafting. J. Bone Joint Surg. 53, 829–858.

Hunter, J.M., Singer, D.I., Jaeger, S.H., Mackin, E.J., 1988. Active tendon implants in flexor tendon reconstruction. J. Hand Surg. 13, 849–859.

Hutmacher, D.W., Dalton, P.D., 2011. Melt electrospinning. Chem. Asian J. 6, 44–56.

Ji, Y., Ghosh, K., Shu, X.Z., Li, B., Sokolov, J.C., Prestwich, G.D., Clark, R.A., Rafailovich, M. H., 2006. Electrospun three-dimensional hyaluronic acid nanofibrous scaffolds. Biomaterials 27, 3782–3792.

Ji, W., Sun, Y., Yang, F., Van Den Beucken, J.J., Fan, M., Chen, Z., Jansen, J.A., 2011. Bioactive electrospun scaffolds delivering growth factors and genes for tissue engineering applications. Pharm. Res. 28, 1259–1272.

Jiang, H., Hu, Y., Zhao, P., Li, Y., Zhu, K., 2006. Modulation of protein release from biodegradable core-shell structured fibers prepared by coaxial electrospinning. J. Biomed. Mater. Res. B Appl. Biomater. 79, 50–57.

Jones, K.G., 1963. Reconstruction of the anterior cruciate ligament a technique using the central one-third of the patellar ligament. J. Bone Joint Surg. 45, 925–932.

Katti, D.S., Robinson, K.W., Ko, F.K., Laurencin, C.T., 2004. Bioresorbable nanofiber-based systems for wound healing and drug delivery: optimization of fabrication parameters. J. Biomed. Mater. Res. B Appl. Biomater. 70, 286–296.

Kemp, P.D., Cavallaro, J.F., Hastings, D.N., 1995. Effects of carbodiimide crosslinking and load environment on the remodeling of collagen scaffolds. Tissue Eng. 1, 71–79.

Kim, H.M., Chae, W.-P., Chang, K.-W., Chun, S., Kim, S., Jeong, Y., Kang, I.-K., 2010. Composite nanofiber mats consisting of hydroxyapatite and titania for biomedical applications. J. Biomed. Mater. Res. B Appl. Biomater. 94B, 380–387.

Ko, F., 1997. Medical Application for Textile Structures. Textile Asia, Taiwan.

Ko, F.K., 2004. Nanofiber technology: bridging the gap between nano and macro world. In: Guceri, S., Gogotsi, Y.G., Kuznetsov, V. (Eds.), Nanoengineered Nanofibrous Material. Kluwer Academic Publishers, Dordrecht, pp. 1–18.

Ko, F., Laurencin, C.T., Borden, M.D., Reneker, D.H., 1998. The dynamics of cell-fiber architecture interaction. In: Proceedings of the Annual Meeting of the Biomaterials Research Society, San Diego, CA.

Ko, F., Gogotsi, Y., Ali, A., Naguib, N., Ye, H., Yang, G.L., Li, C., Willis, P., 2003. Electrospinning of continuous carbon nanotube-filled nanofiber yarns. Adv. Mater. 15, 1161–1165.

Kuraishi, K., Iwata, H., Nakano, S., Kubota, S., Tonami, H., Toda, M., Toma, N., Matsushima, S., Hamada, K., Ogawa, S., 2009. Development of nanofiber-covered stents using electrospinning: in vitro and acute phase in vivo experiments. J. Biomed. Mater. Res. B Appl. Biomater. 88, 230–239.

Ladd, M.R., Lee, S.J., Stitzel, J.D., Atala, A., Yoo, J.J., 2011. Co-electrospun dual scaffolding system with potential for muscle—tendon junction tissue engineering. Biomaterials 32, 1549–1559.

Lange, F., 1903. Über die Sehnenplastik. Verh. Dtsch. Orthop. Ges. 2, 10–12.

Lee, C.H., Shin, H.J., Cho, I.H., Kang, Y.-M., Kim, I.A., Park, K.-D., Shin, J.-W., 2005. Nanofiber alignment and direction of mechanical strain affect the ECM production of human ACL fibroblast. Biomaterials 26, 1261–1270.

Lee, S.J., Yoo, J.J., Lim, G.J., Atala, A., Stitzel, J., 2007. In vitro evaluation of electrospun nanofiber scaffolds for vascular graft application. J. Biomed. Mater. Res. A 83, 999–1008.

Leung, V., Ko, F., 2011. Biomedical applications of nanofibers. Polym. Adv. Technol. 22, 350–365.

Leung, V., Hartwell, R., Yang, H., Ghahary, A., Ko, F., 2011. Bioactive nanofibres for wound healing applications. J. Fiber Bioeng. Inform. 4, 1–14.

Li, D., Xia, Y., 2004. Electrospinning of nanofibers: reinventing the wheel? Adv. Mater. 16, 1151–1170.

Li, Z., Zhang, M., 2005. Chitosan—alginate as scaffolding material for cartilage tissue engineering. J. Biomed. Mater. Res. A 75, 485–493.
Li, M., Mondrinos, M.J., Gandhi, M.R., Ko, F.K., Weiss, A.S., Lelkes, P.I., 2005a. Electrospun protein fibers as matrices for tissue engineering. Biomaterials 26, 5999–6008.
Li, W.-J., Tuli, R., Okafor, C., Derfoul, A., Danielson, K.G., Hall, D.J., Tuan, R.S., 2005b. A three-dimensional nanofibrous scaffold for cartilage tissue engineering using human mesenchymal stem cells. Biomaterials 26, 599–609.
Li, J., He, A., Han, C.C., Fang, D., Hsiao, B.S., Chu, B., 2006. Electrospinning of hyaluronic acid (HA) and HA/gelatin blends. Macromol. Rapid Commun. 27, 114–120.
Li, W.-J., Mauck, R.L., Cooper, J.A., Yuan, X., Tuan, R.S., 2007. Engineering controllable anisotropy in electrospun biodegradable nanofibrous scaffolds for musculoskeletal tissue engineering. J. Biomech. 40, 1686–1693.
Li, P., Feng, X., Jia, X., Fan, Y., 2010. Influences of tensile load on in vitro degradation of an electrospun poly (L-lactide-co-glycolide) scaffold. Acta Biomater. 6, 2991–2996.
Liu, X., Ma, P.X., 2010. The nanofibrous architecture of poly(L-lactic acid)-based functional copolymers. Biomaterials 31, 259–269.
Liu, H., Fan, H., Wang, Y., Toh, S.L., Goh, J.C., 2008. The interaction between a combined knitted silk scaffold and microporous silk sponge with human mesenchymal stem cells for ligament tissue engineering. Biomaterials 29, 662–674.
Louie, L., Yannas, I.V., Spector, M., 1998. Tissue engineered tendon. In: Patrick, C., Mikos, A.G., Mcintire, L. (Eds.), Frontiers in Tissue Engineering. Elsevier Science, New York.
Ma, M., Kazemzadeh-Narbat, M., Hui, Y., Lu, S., Ding, C., Chen, D.D., Hancock, R.E., Wang, R., 2012. Local delivery of antimicrobial peptides using self-organized TiO_2 nanotube arrays for peri-implant infections. J. Biomed. Mater. Res. A 100, 278–285.
Martin, P., 1997. Wound healing—aiming for perfect skin regeneration. Science 276, 75–81.
Murray, M.M., Rice, K., Wright, R.J., Spector, M., 2003. The effect of selected growth factors on human anterior cruciate ligament cell interactions with a three-dimensional collagen-GAG scaffold. J. Orthop. Res. 21, 238–244.
Newmeyer III, W.L., Manske, P.R., 2004. No man's land revisited: the primary flexor tendon repair controversy. J. Hand Surg. 29, 1–5.
Odensten, M., Lysholm, J., Gillquist, J., 1984. Suture of fresh ruptures of the anterior cruciate ligament: a 5-year follow-up. Acta Orthop. 55, 270–272.
Okuda, T., Tominaga, K., Kidoaki, S., 2010. Time-programmed dual release formulation by multilayered drug-loaded nanofiber meshes. J. Control. Release 143, 258–264.
Rahmani-Neishaboor, E., Hartwell, R., Jalili, R., Jackson, J., Brown, E., Ghahary, A., 2012. Localized controlled release of stratifin reduces implantation-induced dermal fibrosis. Acta Biomater. 8, 3660–3668.
Ramakrishna, S., Fujihara, K., Teo, W.-E., Lim, T.-C., Ma, Z., 2005. An introduction to electrospinning and nanofibers. World Scientific Publishing, Singapore.
Reneker, D.H., Chun, I., 1996. Nanometre diameter fibres of polymer, produced by electrospinning. Nanotechnology 7, 216.
Rho, K.S., Jeong, L., Lee, G., Seo, B.-M., Park, Y.J., Hong, S.-D., Roh, S., Cho, J.J., Park, W.H., Min, B.-M., 2006. Electrospinning of collagen nanofibers: effects on the behavior of normal human keratinocytes and early-stage wound healing. Biomaterials 27, 1452–1461.
Robson, A.M., 1903. VI. Ruptured crucial ligaments and their repair by operation. Ann. Surg. 37, 716.

Rodrigues, M.T., Reis, R.L., Gomes, M.E., 2012. Engineering tendon and ligament tissues: present developments towards successful clinical products. J. Tissue Eng. Regen. Med. 7, 673–686.
Sahoo, S., Ouyang, H., Goh, J.C.-H., Tay, T., Toh, S., 2006. Characterization of a novel polymeric scaffold for potential application in tendon/ligament tissue engineering. Tissue Eng. 12, 91–99.
Sahoo, S., Toh, S.L., Goh, J.C.H., 2010. A bFGF-releasing silk/PLGA-based biohybrid scaffold for ligament/tendon tissue engineering using mesenchymal progenitor cells. Biomaterials 31, 2990–2998.
Said, S.S., Aloufy, A.K., El-Halfawy, O.M., Boraei, N.A., El-Khordagui, L.K., 2011. Antimicrobial PLGA ultrafine fibers: interaction with wound bacteria. Eur. J. Pharm. Biopharm. 79, 108–118.
Shoaib, M.H., Tazeen, J., Merchant, H.A., Yousuf, R.I., 2006. Evaluation of drug release kinetics from ibuprofen matrix tablets using HPMC. Pak. J. Pharm. Sci. 19, 119–124.
Siepmann, J., Peppas, N., 2001. Modeling of drug release from delivery systems based on hydroxypropyl methylcellulose (HPMC). Adv. Drug Deliv. Rev. 48, 139–157.
Siepmann, J., Peppas, N.A., 2011. Higuchi equation: derivation, applications, use and misuse. Int. J. Pharm. 418, 6–12.
Silver, F., Tria, A., Zawadsky, J., Dunn, M., 1991. Anterior cruciate ligament replacement: a review. J. Long Term Eff. Med. Implants 1, 135.
Skalak, R., Fox, C.F., Fung, Y.C., 1988. Preface. In: Tissue Engineering.Proceedings of NSF Workshop on Tissue Engineering, Granlibakken, Lake Tahoe, California.
Srikar, R., Yarin, A.L., Megaaridis, C.M., Bazilevsky, A.V., Kelley, E., 2008. Desorption-limited mechanism of release from polymer nanofibers. Langmuir 24, 965–974.
Stitzel, J., Liu, J., Lee, S.J., Komura, M., Berry, J., Soker, S., Lim, G., Van Dyke, M., Czerw, R., Yoo, J.J., 2006. Controlled fabrication of a biological vascular substitute. Biomaterials 27, 1088–1094.
Sukigara, S., Gandhi, M., Ayutsede, J., Micklus, M., Ko, F., 2003. Regeneration of *Bombyx mori* silk by electrospinning—part 1: processing parameters and geometric properties. Polymer 44, 5721–5727.
Sukigara, S., Gandhi, M., Ayutsede, J., Micklus, M., Ko, F., 2004. Regeneration of *Bombyx mori* silk by electrospinning. Part 2. Process optimization and empirical modeling using response surface methodology. Polymer 45, 3701–3708.
Surrao, D.C., Fan, J.C.Y., Waldman, S.D., Amsden, B.G., 2012. A crimp-like microarchitecture improves tissue production in fibrous ligament scaffolds in response to mechanical stimuli. Acta Biomater. 8, 3704–3713.
Tan, E.P., Lim, C., 2006. Effects of annealing on the structural and mechanical properties of electrospun polymeric nanofibres. Nanotechnology 17, 2649.
Vunjak-Novakovic, G., Altman, G., Horan, R., Kaplan, D.L., 2004. Tissue engineering of ligaments. Annu. Rev. Biomed. Eng. 6, 131–156.
Wan, Y., Gao, W., Wang, H., Yang, R., Ko, F., 2010. Diameter prediction for electrospun nanofibers. Int. J. Nonlinear Sci. Numer. Simul. 11, 151–154.
Wang, X., Gittens, R.A., Song, R., Tannenbaum, R., Olivares-Navarrete, R., Schwartz, Z., Chen, H., Boyan, B.D., 2012. Effects of structural properties of electrospun TiO_2 nanofiber meshes on their osteogenic potential. Acta Biomater. 8, 878–885.
Wei, K., Li, Y., Lei, X., Yang, H., Teramoto, A., Yao, J., Abe, K., Ko, F.K., 2011. Emulsion electrospinning of a collagen-like protein/PLGA fibrous scaffold: empirical modeling and preliminary release assessment of encapsulated protein. Macromol. Biosci. 11, 1526–1536.

Wening, J.V., Katzer, A., Jungbluth, K.H., Schultz, S., Dauner, M., Planck, H., 1996. Ligament replacement, artificial. In: Salamone, J.C. (Ed.), Polymeric Materials Encyclopedia. CRC Press, Boca Raton.

Woo, S.L., Hildebrand, K., Watanabe, N., Fenwick, J.A., Papageorgiou, C.D., Wang, J.H., 1999. Tissue engineering of ligament and tendon healing. Clin. Orthop. Relat. Res. 367, S312–S323.

Xu, X., Yang, L., Xu, X., Wang, X., Chen, X., Liang, Q., Zeng, J., Jing, X., 2005. Ultrafine medicated fibers electrospun from W/O emulsions. J. Control. Release 108, 33–42.

Yannas, I., Burke, J.F., 1980. Design of an artificial skin. I. Basic design principles. J. Biomed. Mater. Res. 14, 65–81.

Yarin, A., 2011. Coaxial electrospinning and emulsion electrospinning of core-shell fibers. Polym. Adv. Technol. 22, 310–317.

Zhong, S., Teo, W.E., Zhu, X., Beuerman, R.W., Ramakrishna, S., Yung, L.Y.L., 2006. An aligned nanofibrous collagen scaffold by electrospinning and its effects on in vitro fibroblast culture. J. Biomed. Mater. Res. A 79, 456–463.

Zhong, S.P., Teo, W.E., Zhu, X., Beuerman, R., Ramakrishna, S., Yung, L.Y.L., 2007. Development of a novel collagen—GAG nanofibrous scaffold via electrospinning. Mater. Sci. Eng. C 27, 262–266.

Zong, X., Kim, K., Fang, D., Ran, S., Hsiao, B.S., Chu, B., 2002. Structure and process relationship of electrospun bioabsorbable nanofiber membranes. Polymer 43, 4403–4412.

Absorbable, drug-loaded, extruded fiber for implantation

6

Kevin D. Nelson
TissueGen, Inc., Dallas, TX, USA

6.1 Introduction

Tissue engineering and regenerative medicine based on three-dimensional scaffolds that have the ability to induce selected cell growth may be the next breakthrough in medicine. It's not just enough to arrest the progress of disease or to stop degradation from injury; the goal is to actually restore function. It appears that this restoration may be possible in some cases based on the data and concepts presented in this chapter.

Solution extrusion that can take place at room or body temperature can incorporate growth factors and other biologically significant molecules with a high degree of retained biological activity. These loaded fibers can be formed into scaffolds. The scaffolds can then be implanted directly into the body, or they can be seeded with cells outside the body first and later implanted. In both cases, by virtue of the biological molecules that are released from these fibers, signals can be sent to the cells, directing specific cell types to grow in one direction and another cell type to grow in a different direction. This signaling and directing of cellular growth within the scaffolding can be used to create functional, three-dimensional, physiologically significant structures that can restore function that was lost due to injury or disease.

6.1.1 Definition of drugs

In this chapter, we use the terms "drug" and "active agent" to mean any molecule, or in some cases collections of molecules, whose intent is to be physiologically active in locally altering how the body functions. The effect may be to induce the body to do something positive, such as direct specific cells to do a beneficial task, or it may be to block the body from doing something potentially harmful, such as preventing adhesions or reducing scarring. The drug or therapeutic agent may be a small pharmaceutical molecule, or it may be a much larger biologically derived molecule such as a peptide, protein, carbohydrate, oligonucleotide, RNA, or DNA. Biologically derived therapeutic agents are typically encapsulated within an emulsion or by excipient molecules that protect the active agents during extrusion, sterilization, and storage.

6.1.2 Range of release rates

Biodegradable, drug-loaded fibers release their drug over periods of time ranging from days to months. The rate at which the drugs are released depends on many factors, including the drug distribution profile within the cross section of the fiber, the

Biomedical Textiles for Orthopaedic and Surgical Applications. http://dx.doi.org/10.1016/B978-1-78242-017-0.00006-4

chemical or physical attraction between the drug and the fiber, the size of the drug, the type and degradation rate of the polymer, the porosity of the polymer, the presence and properties of excipients used in the fiber, the hydrophobic/hydrophilic balance of the drug and the polymer, and the geometry of the fiber, to name a few. These properties are discussed later in this chapter.

6.1.3 Chapter overview

In this chapter, we briefly discuss the typical polymers that are used and the different means whereby they can be extruded to create medically significant textiles. We also discuss how drugs are incorporated and released, the mathematical models used to simulate the release, and finally, some of the current and potential future uses for these structures.

Absorbable, drug-loaded fibers have significant potential in many areas of medicine. There are numerous clinical areas where absorbable fibers are currently used and many others that appear to be likely candidates. Most of these applications could theoretically benefit from the addition of some type of local drug release. This chapter introduces the reader to methods for fabricating fibers and controlling the release kinetics, and it introduces areas where drug-loaded, biodegradable fibers may provide the greatest advances over current treatment options.

6.2 Materials and fabrication techniques

There are many types of polymers that can be used to form fibers of sufficient quality for medical device implantation (Nair and Laurencin, 2005). This chapter limits itself to biodegradable polymers. This is not because permanent polymers do not play a critical role in medical textiles; indeed, by volume, they dominate the current market of implantable textile devices. However, the world of biodegradable polymers deserves more attention, and for future applications such as tissue engineering and regenerative medicine, they will likely play a dominant role. Therefore, it is critically important to introduce this family of polymer fibers. In this light then, whenever a generic term such as "polymer" is used in this chapter, it refers to a biodegradable polymer. Most of the time when considering biodegradability, it is appropriate to think about the general family of alpha-hydroxyesters such as poly(lactides), poly(*p*-dioxanone), poly (glycolic acid), their various copolymers, and blends.

6.2.1 Extrusion techniques

Thermally stable polymers that melt before they degrade are usually melt extruded. Melt extrusion is the least expensive and simplest form of fiber extrusion. Polymers that degrade prior to melting must be extruded by solution extrusion. There are many different types of solution extrusion that are explained in much more detail later in this chapter.

6.2.1.1 Melt extrusion material requirements

The melt extrusion process consists of melting the polymer pellets through a combination of applied heat and friction. This molten polymer is then forced under high pressure through a small orifice or, more typically, a "shower head" of orifices called a spinneret. The molten polymer stream flowing out of the spinneret freezes into a solid fiber at some distance from the spinneret, and it is then typically reheated and drawn numerous times as the fiber traverses the extrusion line to the final product. The material requirements for loading a drug into a fiber using melt extrusion are:

- The polymer must melt and withstand high shear stresses without unacceptable degradation of the polymer's molecular weight.
- The drug of interest must be able to withstand the melt temperature and high shear stresses associated with melt extrusion without loss of biological activity.
- The drug must be soluble or at least wettable and dispersible within the polymer melt.

Any drug–polymer combination that meets the above criteria can be used to successfully melt-extrude a drug-loaded fiber. The drawback of this technique is that there are a limited number of pharmaceutical agents and no biologically derived agents that can withstand the temperature and stress of the melt extrusion process with retained biological function. Therefore, this process has a limited scope of application.

6.2.1.2 Solution extrusion material requirements

In solution spinning, the polymer is always dissolved in a solvent, which is then pumped through a spinneret similar to a melt extrusion spinneret. In solution spinning, the fiber then proceeds down the extrusion line where it is also stretched, but not generally heated to the temperatures required for a melt-extruded fiber. Therefore, solution spinning differs from melt spinning in several important ways: (1) the polymer is dissolved (typically at room temperature) in a solvent as opposed to being melted; (2) the stretching operations may be at much lower temperatures with wet extrusion than with melt extrusion; and (3) wet extrusion has additional postprocessing requirements to remove residual solvent from the fiber before it is ready for use in medical fields. The use of solvents at the beginning and the process of removing solvents at the end make solution spinning a more complicated, generally less environmentally friendly, and typically much more costly process. However, the benefit of this technique is that it can be done at or near room temperature, and it can therefore be used to load even very sensitive biological molecules into the fibers for medical applications, assuming that the drug can be appropriately protected from solvents, the extrusion process, sterilization, and degradation during storage. This allows the incorporation of thermally sensitive drugs, such as biologically derived proteins, including growth factors, enzymes, and cytokines, as well as mitogenic or chemotactic factors. Solution-spun fibers can also be loaded with carbohydrates, oligonucleotides, and even live viruses (Beck et al., 2004; Nelson et al., 2004a,b).

The material requirements for loading a drug into a fiber using solution spinning are:

- The polymer must be soluble in a solvent at some temperature (usually room temperature).
- The drug of interest must be able to withstand the conditions of the solvent/polymer physiochemical environment, such as pH, temperature, and solvent exposure, either by itself or as a "protected" molecule. The protection can come in the form of excipients, emulsions, nanoparticle or microsphere incorporation, or some other method. The chapter further addresses this requirement in later sections.
- The solvent must be removable in a way that precipitates the polymer molecules and drug into a fiber. The way in which the solvent is removed determines the type of solution spinning:
  - If the solvent is removed by exposing the polymer/solvent/drug stream to a coagulating fluid in which the solvent is miscible, but it is a nonsolvent for the polymer (and preferably the drug), this is called "wet extrusion."
  - If the solvent is removed by evaporation as the polymer/solvent/drug falls through warm air (or appropriate inert gas), it is called "dry spinning" or sometimes "dry-jet spinning."
  - In cases where the polymer concentration is sufficiently high, a combination of wet and dry spinning may be used, during which the polymer falls initially through the air and then into a coagulating bath. This process is known as "gel spinning."
  - If the solvent is removed by evaporation, but the fiber is formed by jetting the liquid polymer through a fine needle, driven by a high electric potential between the tip of the needle and a grounded baseplate, it is called "electrospinning."
- There must be a way to remove residual solvent without damaging the drug or polymer following fiber processing, because even small amounts of organic solvents (classically used in most solution spinning techniques) can cause problems upon implantation. The US Food and Drug Administration has published tables and calculations for maximum allowable residual solvent levels in medical devices; see "Guidance for Industry: Q3C Impurities: Residual Solvents" for guidance on calculating residual solvent exposure.

Any drug–polymer combination that meets the above criteria can be solution-extruded to create a drug-loaded fiber, assuming that the fiber can be dissolved at sufficiently high concentration and it has a high enough molecular weight to be extruded.

6.2.1.3 *Wet spinning*

Wet spinning is the oldest and most complicated of the solution spinning techniques; however, with the complexity comes additional power over the morphology of the fiber and, hence, the drug elution rate, as shown below. The complication arises from the many phases and rapidly changing conditions during the course of fiber fabrication.

The first phase is the polymer solution, which is created by dissolving the polymer in a solvent or solvent system. The choice of the solvent system impacts drug protection schemes, solution viscosity, and ultimately fiber properties and drug release rates. There has been significant research into mixing good and poor solvents (with respect to dissolving the polymer) to create an "optimal" solvent system (Albrecht et al., 2001; Tan et al., 2000; Wang et al., 1996) for dissolving the polymer. The most basic concept with regard to dissolving the polymer is an understanding of how polymer and solvent

molecules interact from a thermodynamic perspective in the liquid state. In a "good" solvent, the polymer–solvent interaction is thermodynamically preferred to the polymer–polymer interaction. Therefore, the polymer chains tend to straighten out and limit their interactions with themselves or their neighbors so as to maximize solvent exposure to the polymer chain. A "theta solvent" is one for which the polymer–polymer interaction is thermodynamically equal to the polymer–solvent interaction. In this case, the polymer chains tend to adopt a random-walk configuration, not caring if they touch themselves or a neighbor or a solvent molecule. A "poor solvent" is one for which the polymer–polymer interaction is thermodynamically favored over the polymer–solvent interaction. In this case, the polymer chains tend to ball up on themselves or potentially aggregate with their neighbors, but by definition, a poor solvent creates a rather dilute solution, limiting aggregation (Flory 1941; Fried 2003).

The ultimate fiber mechanical properties depend to a large extent on the solution properties. For example, fibers created from polymer dissolved in a poor solvent tend to be weak and brittle, as there is negligible chain alignment and little interchain entanglement. Fibers spun from theta solvents typically end up with many interchain entanglements and tend to make elastic, high-strength fibers. Fibers spun from good solvents tend to have a high degree of polymer chain alignment, which tends to make rather ductile fibers (Morris, 2011; Musaev et al., 1983).

The viscosity of the polymer solution changes with respect to the "goodness" of the solvent system (of course, it primarily varies with polymer concentration and temperature). For a given concentration and temperature, in a poor solvent, the viscosity tends to be low, increases with a good solvent, and is highest with a theta solvent for which there is maximum entanglement (Tan et al., 2000). As early as 1940, it was known that the viscosity of solutions depended strongly on the shape of the polymer (Mehl et al., 1940). The viscosity of the polymer solution controls the rate at which the polymer solution can be extruded into the coagulating bath and the speed at which it can be taken up into the first draw station of the extrusion line.

The interaction between the solvent system (including any added nonsolvent) and the coagulating bath nonsolvent in the case of wet extrusion provides more power over the morphology of the fiber than other spinning methods, which is what makes it the preferred spinning method for drug-loaded fibers. Figure 6.1 illustrates the huge impact that changes in solvent systems can have on the internal morphology of a fiber made by wet-extrusion techniques. This figure shows the degree of porosity in the wall of a hollow fiber as a function of changes in the solvent system, while keeping the coagulating bath nonsolvent constant.

As is obvious, the chemistry taking place between the coagulating bath nonsolvent and the various choices of solvent systems provides the ability to have pores, channels, and/or spongy or nonporous structures. Clearly, both the mechanical strength of the fiber and the rate of drug delivery vary significantly as a function of the porosity and internal morphology of the fiber.

The choice of a coagulating bath nonsolvent system is also very important. The requirements for the nonsolvent system in the coagulating bath are that: (1) the nonsolvent system, as the name implies, must be a sufficiently powerful nonsolvent for the polymer that the polymer molecules precipitate in its presence; (2) the nonsolvent

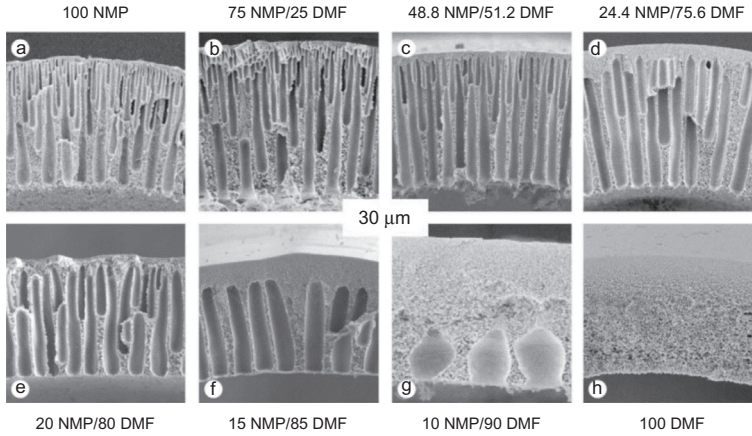

Figure 6.1 Morphological changes in hollow fiber due to changes in the polymer solvent while leaving the coagulating bath unchanged.
This is a reprint of Figure 2A from Albrecht et al. (2001).

system of the coagulating bath must be highly miscible with the solvent system used to dissolve the polymer; (3) the nonsolvent system of the coagulating bath must not damage the drug; and (4) the component(s) of the coagulating bath nonsolvent system must be removable from the fiber in such a way as to pass residual solvent analysis without damaging either the drug or the fiber.

The rate at which the nonsolvent system precipitates the polymer molecules plays a large role in fiber shape and density. There has been a significant amount of research directed toward changing the coagulation bath environment to affect fiber properties (Bahrami et al., 2003).

A simple ternary diagram may help the reader understand the chemistry taking place that causes such different morphologies within the fiber. Figure 6.2 shows a ternary diagram in which each apex of the equilateral triangle represents a different component of this triphasic solution: polymer, solvent, and nonsolvent (ignoring the drug for now). Each apex represents 100% concentration of the appropriate component; for example, the apex-labeled polymer at that point in diagram represents 100% polymer, no solvent, and no nonsolvent. Each exterior line of the triangle represents a zero concentration value of the component of the apex opposite that line. Therefore, the points in the diagram represent all possible concentrations (ranging from 0% to 100%) of these three components of the solution. As an illustration of how to use and think about this diagram, if you start with the pure polymer labeled as point "A" in the diagram, you are at the polymer apex. Then, a certain amount of solvent is added to dissolve the polymer, moving your location to point "B." This moves your point down the line opposite the nonsolvent apex (because you have not added any yet, the concentration of this component is zero, and hence, your position is determined by the percent solvent and percent polymer). Assuming that you now add nonsolvent to the solvent system or that nonsolvent diffuses in from the coagulating bath, the

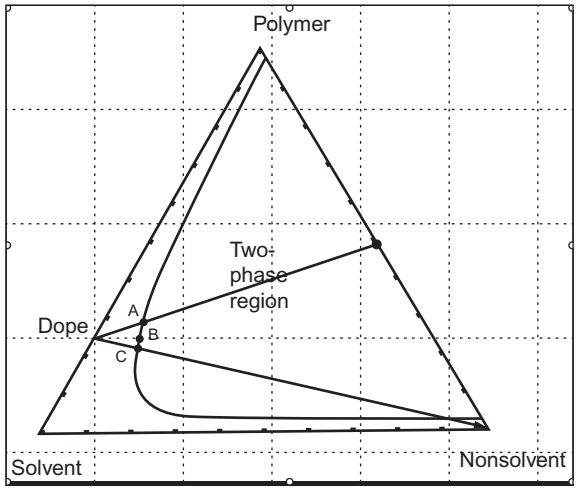

Figure 6.2 Ternary diagram showing an example of a binodal line separating the single-phase region from the two-phase region. This figure shows the pathway starting with raw polymer at point "A," which is then made into the polymer solution that is to be extruded by adding solvent, moving to point "B." During the extrusion process, nonsolvent from the coagulation bath enters the system, moving to point "C." Following extrusion, residual solvents are removed in a postprocess, taking us to point "D."

trajectory of your composition now moves out into the triangle to point "C" on the diagram, as now all three components are present. However, it is important to realize that this is not typically homogeneous across the cross section of the fiber, because solvent diffuses faster from the outside of the fiber than it does in the middle, and nonsolvent entering from the coagulation bath first encounters the outermost part of the fiber. Therefore, this ternary diagram is really only valid at any given radius of the forming fiber and will vary substantially from the outside edge to the middle. This has important ramifications on the extrusion process. For example, if the outside edge changes much faster than the inner part of the fiber, a "skin" can be formed on the surface of the fiber that has nearly no solvent and consists of precipitated polymer surrounded by a poor solvent. This skin has quite low tensile strength and can lead to fiber breaks in the bath. Another failure mode of skin formation is the flattening of the fiber down the extrusion line as the middle of the forming fiber starts to lose solvent. The significantly stiffer skin will flatten under these conditions, like a squeezed tube of toothpaste, rather than uniformly shrink. Therefore, when choosing a solvent or coagulating bath system, the kinetics of fiber formation play a key role in the choice of solvent and nonsolvent systems. The coagulation needs to be relatively slow to avoid the problems of skin formation, yet fast enough that the fiber can be removed from the coagulation bath.

As the fiber moves through the extrusion process, the solvent and nonsolvents are evaporating, and ultimately through some kind of postprocess, residual solvents are largely removed and your ternary diagram point has almost arrived back at the beginning point of pure polymer, point "D" in the diagram. If you traced the pathway that was taken through this process it would obviously be a closed loop, beginning and ending at pure polymer. The key to understanding morphological changes is in the intersection of your closed loop with the binodal line shown in Figure 6.2. This line represents phase separation within this ternary system. Outside of the binodal line, the

system exists as a single phase; within the binodal line, the system becomes biphasic. This relatively simple system can be biphasic in two ways: it can have a continuous polymer-rich phase with a dispersed phase of polymer-poor regions, or it can be a continuous polymer-poor phase with a dispersed phase of polymer-rich regions. As the fiber is being extruded and begins to harden, this polymer-rich/polymer-poor phase separation from the ternary diagram becomes set in the fiber's internal morphology. Due to this, wet-extruded fibers often show macrovoids in their cross sections where a polymer-poor phase has developed. It is clear that these voids impact not only the release rate of drugs from these fibers, but also their mechanical strength. The fiber cross sections of Figure 6.3 clearly illustrate this phenomenon. Unfortunately, there are not yet good predictive models of how to choose an appropriate solvent system and coagulating bath nonsolvents to get the desired amount of internal porosity. Our efforts to use Hildebrand coefficients to predict polymer solvent interactions leading to porosity were unfruitful.

To summarize, choosing the right solvent system for dissolving the polymer: (1) determines the means by which the drug must be protected; (2) determines the internal morphology of the fiber and, therefore, governs to a great extent the release rate from the fiber; (3) plays a significant role in determining the strength of the final product; and (4) determines to some extent the rate of the extrusion process.

6.2.1.4 *Dry/jet spinning*

In dry/jet spinning, the polymer is dissolved in a solvent as in wet spinning. However, rather than extruding into a liquid coagulating bath, the polymer solution falls into a gas or vapor. Typically, the gas or vapor is heated to help remove the solvent. It is common to use either an inert gas or the vapor of a nonsolvent to coagulate the fiber, as may be used in wet extrusion.

Clearly, solvent choice is as important in dry/jet spinning as it is in wet extrusion. However, in order for dry/jet spinning to work, the polymer solution must be highly viscous and have very good elongational tenacity, because the spinning dope must

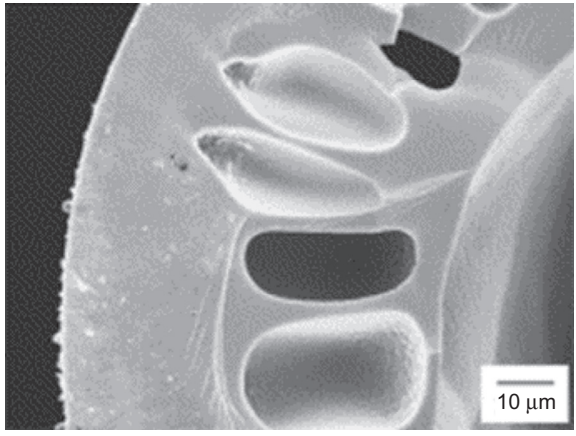

Figure 6.3 Cross section of a hollow fiber showing macrovoids.
Reprinted from Figure 5 in Xu et al. (2011).

support the entire weight of the forming fiber from the time it leaves the spinneret. Not all polymers are soluble at high enough concentrations, nor do they have sufficiently high elongational tenacity to be dry/jet extruded. For those cases where dry/jet spinning is possible, it reduces the complexity of the system compared to wet extrusion because there is no or limited invading nonsolvent.

6.2.1.5 Gel spinning

In gel spinning, the polymer is also dissolved in a solvent, as in wet spinning. However, rather than being immersed directly into a coagulation bath, the spinneret is some distance above the coagulation bath. As it free falls through the gap (usually called the "air gap") toward the coagulation bath, the polymer solution achieves a few potential advantages. In the air gap, the fiber accelerates more rapidly than it would if the spinneret was immersed. This acceleration helps to align the polymer molecules to strengthen the fiber. It can also help reduce skin formation because the removal of solvent in the air drop may be slower than in the coagulation fluid (depending on the volatility of the solvent and the choice of nonsolvent(s) in the coagulating bath). These advantages come with an increased level of complexity by adding another variable to an already complicated situation; however, for many polymer systems, an air gap helps the quality of the fiber.

6.2.1.6 Electrospinning

Electrospinning is quite different from other forms of solution spinning in that the polymer solution is brought to the tip of a needle that is maintained at a very high voltage potential with respect to a ground plate located some distance from the needle tip. This electrostatic potential is sufficient to drive the polymer solution from the tip of the needle to the ground plate. In electrospinning, there are no coagulating baths, no stretching, and, frequently, no control over exactly where the fiber at any given instant will strike the ground plate. Electrospinning typically creates a fiber mat rather than a bobbin of yarn or monofilament fibers, as are produced by the other spinning methods described previously. By keeping the grounding plate, which can be flat, cylindrical, or any other shape, in motion, the fiber moves onto the plate. In the case of a cylindrical grounding plate, a monofilament fiber can be created, and this fiber can experience stretch similar to the stretch created by the other solution spinning techniques described; however, this application is not the most common one for electrospinning. For an excellent review article on drug loading and release from electrospun fibers, see Natu et al. (2011).

Electrospinning has several advantages. There are fewer variables, and the drug can be loaded into electrospun fibers. Fiber diameter is typically much smaller than it is in other forms of extrusion. Electrospun fibers are typically measured in nanometers, whereas other extruded fibers are typically measured in microns. Generally speaking, the other extrusion processes create fibers with a very narrow size distribution, whereas electrospun fibers classically have a wide tolerance of fiber size within the fibrous mat. As the electrospun fibers collect on the mat, the pore size between fibers decreases and can become a well-controlled quality of the formed mat.

Electrospinning holds an important place in drug-loaded, tissue-engineering/regenerative medicine. Its role is usually to provide flat sheets or preformed cylinders, rather than fiber strands.

6.2.2 Types of fibers

6.2.2.1 Monofilament

The simplest format for extrusion is a single monofilament fiber. As discussed previously, the internal morphology of the fiber is a function of the extrusion process. The distribution of drugs across the cross section of the fiber is also a function of the extrusion process. In all cases of drug-loaded fiber for which the drug is mixed with the polymer prior to extrusion, the drug is assumed to be uniformly distributed throughout the polymer solution (or melt). As the polymer solution or melt leaves the spinneret or electrode tip, it is drawn (stretched) by gravity, a roller in the extrusion line, or an electric field. This stretching of the liquid creates new surface area, which must be created by "flowing" material from the inner part of the polymer stream to the surface. The dissolved drug is part of that flow, and, hence, the higher the degree of stretching the fiber during this early phase of the extrusion process, the more drug will flow from the inside portion of the polymer stream to the surface. This creates a difference in the concentration of the drug between the inside of the fiber and the surface. Therefore, prolonged drug delivery should favor fibers that experience as little drawing as possible during the liquid phase of their manufacturing process, whether melt or solution extruded. However, as the fiber begins to harden, there is less flow to the surface as the fiber is drawn, so later draw stations have much less tendency to increase the surface concentration of the drug. As will be discussed later, this "in-bath" draw (during which the wet-extruded fiber is stretched significantly while still in the coagulation bath and still largely a liquid) or a melt draw (in melt extrusion, the fiber is stretched before the "freeze line" where the fiber begins to become solid) may be one of the primary contributing causes of the so called "burst release" from drug-loaded fibers.

6.2.2.2 Core-sheath fiber format

All of the described methods of fiber extrusion can create various fiber formats, such as monofilament, hollow, and core-sheath. These formats allow interesting capabilities for drug loading and release. Crow and Nelson (2006) developed a method using a wet-extrusion technique to create a bicomponent fiber in which the inner core was a hydrogel and the outer sheath was a synthetic polymer. This method has been used to deliver proteins (nerve growth factor (NGF) (Nelson et al., 2002) and vascular endothelial growth factor (VEGF)) and live viruses (Nelson et al., 2004a,b). The release kinetics profile of drugs from these hydrogel-core fibers shows a very interesting, near zero-order release rate. The biologically active agent exists in high concentration within the hydrogel core. The synthetic polymer sheath acts as a barrier to diffusion. Figure 6.4 shows the release profile of an adenovirus from the poly(L-lactic-*co*-glycolic acid) (PLGA) sheath over a xanthan/galactomannan hydrogel core. Figure 6.5 shows the release of VEGF from a similar fiber. This same format can also be used with small molecules; for example,

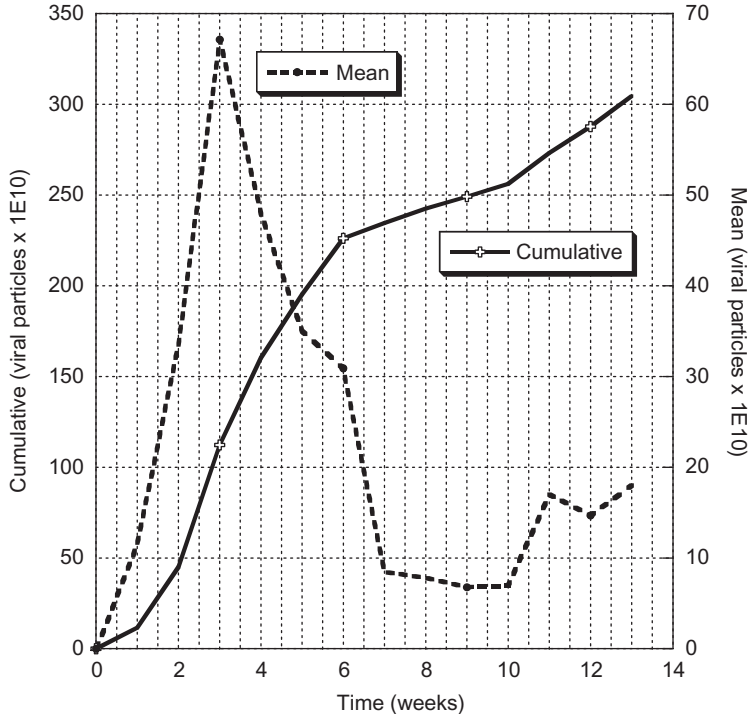

Figure 6.4 Release kinetics of a betagalactosidase adenovirus from a gel-core fiber. The figure shows the mean release at each time point, as well as the cumulative release. There is rapid nearly zero-order release for the first 3 weeks, which then rapidly decreases over the next 4 weeks.

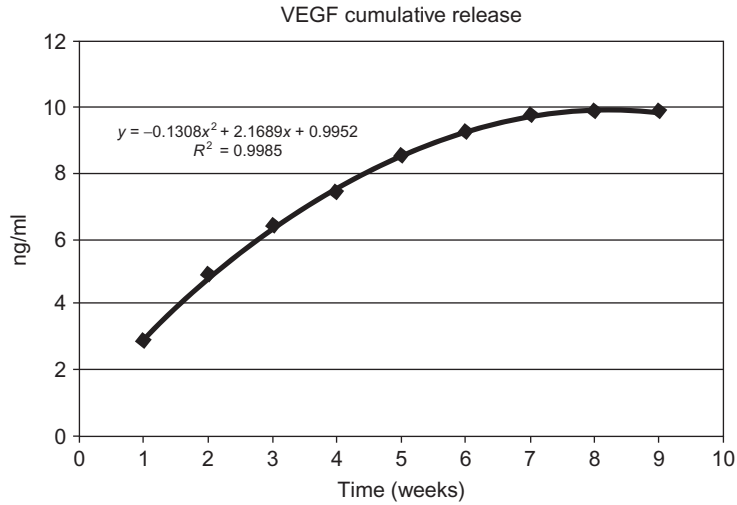

Figure 6.5 Release of VEGF from a gel-cored fiber.

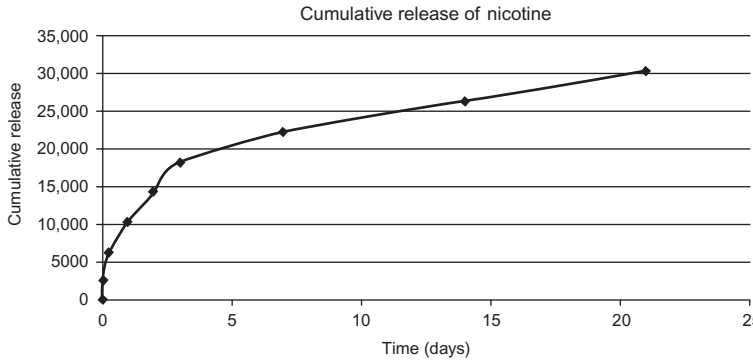

Figure 6.6 Cumulative release of nicotine from a gel-core fiber.

we have loaded and delivered nicotine from a similar hydrogel-core, with a poly(L-lactic acid) (PLLA) sheath, as shown in Figure 6.6.

Zilberman et al. (2009) reversed the core-sheath concept as originally done by Crow, in that Zilberman used a polygluconate core for strength and a 75/25 poly(D,L-lactic-*co*-glycolic acid) (PDLGA) sheath as the drug-loaded portion. In their work, Zilberman et al. (2009) chose to use an emulsion as their protection scheme, which, following extrusion, they lyophilized to create a highly porous polymer network.

Core-sheath fibers have also been made by electrospinning. These fibers show reduced burst release and prolonged delivery (Yang et al., 2008). The low burst release from electrospinning fibers may be due to the much lower stretching that typically occurs in electrospinning compared with other forms of solution spinning.

Similar to core-sheath extrusion, the drug may be coated on the fiber by dipping the fiber in a polymer solution containing a drug (King and Jones, 2006). In other cases, the drug may by physically or chemically attached to the fiber surface. As an example, the drug may be contained within cyclodextrins that are attached by various chemistries to the surface (Nierstrasz, 2007). Surface-coated or surface-attached drugs often have low total drug capacity and quite rapid release rates.

6.3 Drug loading and release

6.3.1 Protection methods for solution spinning

There are several ways in which the drug can be protected from the potentially harsh solvent system environment to which it is exposed during solution spinning. Nelson et al. (2003) developed the concept that the drug must be phase separated from the surrounding polymer matrix in order to protect the drug from the polymer. Perhaps the simplest way to achieve phase separation is to consider a water-in-oil emulsion where the hydrophilic drug (such as a protein) is dissolved in the dispersed aqueous phase, and the polymer dissolved in its appropriate solvent system is the continuous

"oil" phase. The solvent system for the polymer is chosen such that it is essentially immiscible with the aqueous phase of the emulsion. These emulsions then may be directly extruded according to any of the solution spinning methods described previously (Crow et al., 2005; Rissanen et al., 2010; Xiaoqiang et al., 2010; Yang et al., 2008). In all cited cases, the retention of biological activity is very high.

Excipients may also be used to protect the drug. The pharmaceutical industry has a rich history of using excipients to protect drugs and proteins from degradation. It is outside the scope of this chapter to give a comprehensive review of excipients, but the reader is referred to several excellent review articles (Kamerzell et al., 2011; Ohtake et al., 2011). As a brief summary, excipients are molecules that typically interact with the drug or protein molecule in way that favorably protects the protein or drug from aggregating, denaturing, and other destructive processes when exposed to harsh conditions. Excipients can be small molecules such as sugars, or they can be large molecules such as polymers or carbohydrates. As illustrated in the previously referenced review articles, there is a great deal of literature available to help one find an appropriate excipient for the protein or drug of interest. In the case of solution spinning, it is desirable to find an excipient that is soluble in the solvent system used to dissolve the polymer, yet sufficiently protective to preserve the biological activity of the protein or drug of interest. In this case, the excipient-encased drug may then be directly dissolved in the polymer solution in which the excipient molecule(s) provide(s) an effectual phase separation between the drug and the surrounding polymer matrix, thereby protecting the drug or protein.

Another method for protecting the drug includes encapsulating the drug in nanoparticles. These drug-loaded particles are then loaded into the polymer solution prior to extrusion as with other types of solution extrusion. For this method to adequately protect the drug, the nanoparticle must be stable in both the polymer and coagulating bath solvent systems. Normally, for drug-loaded nanoparticles, the entire nanoparticle is released from the fiber while still encapsulating the drug. This is one of the primary means of protection for drugs that are to be delivered inside the cell. For example, if the drug is a DNA or RNA strand, it must be protected not just during extrusion and sterilization, but also after it is endocytosed by the target cell. The lysosome microenvironment inside the cell is marked by a significant drop in pH and the presence of protease (Boyer and Tannock, 1992). The nanoparticle in this case must safely protect the drug through all of these rigorous environments, finally releasing the drug safely within the cytosol, or perhaps, it must specifically target transport and delivery to the nucleus (Veiseh et al., 2010). Much research has been done in the area of gene therapy to find the best nonviral way to escort genetic sequences into a cell (Khalil et al., 2006; Levine et al., 2013), and intracellular or nuclear delivery is the most challenging area of drug delivery.

One last means of protecting the drug to be mentioned here is microsphere loading. The drug is first loaded into a microsphere using any of various techniques. The microsphere is added to the polymer solution and extruded, embedding the microsphere into the fiber. This technique works well if the microsphere is insoluble in the polymer solution and is capable of protecting the drug from both the solvent and coagulating bath solvent/nonsolvent systems. However, there may be significant strength issues

with the fiber because the microspheres may appear to the forming fiber as defect areas, and thus, they may prevent the fiber from being drawn as normal. Because the microsphere must be insoluble in the polymer solvent system, this technique is classically employed when very different polymer types are used. For example, if an aqueous-based extrusion of something, such as a chitosan fiber, needs to deliver a drug that is not compatible with this solvent system, the involved microsphere may utilize a totally different system in its own construction (Zilberman et al., 2009).

6.3.2 Mathematical modeling of release kinetics

Mathematical modeling is an important tool for understanding the release kinetics and predicting how the fiber will perform *in vivo*. For a good review article on various mathematical models that have been proposed see Dash et al. (2010) and Siepmann and Peppas (2001). Each mathematical model has advantages and limitations depending on the assumptions made. Specifically for drug release from a fiber, the model proposed by Sagiv et al. (2003) is perhaps the most appropriate because it assumes cylindrical geometry and some amount of "burst release." This model allows for release into a finite volume and the ability to enter the concentration of the drug within the fiber as a function of the radius of the fiber.

The Sagiv model starts by fitting release kinetics data (typically gathered *in vitro*) where the drug mass released at various time points is known. The Sagiv model allows the drug release from a fiber to have an "initial burst," which is defined by release rates faster than would be predicted by pure Fickian diffusion under the assumption of uniform concentration within the fiber. It then assumes that, following the "burst release," the remainder of the release is nicely fit by Fickian diffusion from an infinitely long cylinder. The model also assumes that the fiber diameter remains constant and that the diffusion coefficient, D, remains constant over the duration of the release kinetics experiment. This last assumption is significant, and it is discussed in greater detail below. This model then requires an iterative process to determine D, the diffusion coefficient, and tL, the "lost time" due to the initial burst release.

The concept of tL must be explained in order for one to use and understand this model. If there was no such thing as initial burst release, at time zero, the mass released would be zero and all data points would lie on a smooth line following Fickian diffusion from a cylinder. In reality, however, real data usually shows an initial burst followed by an abrupt change during which the burst release is completed and the remainder of the data points follow that nice cylindrical Fickian diffusion curve. If the curve fit for the group of data points that do follow Fickian diffusion is extrapolated backwards in time to the point of zero mass released, the time at which the extrapolated diffusion curve hits zero mass release would be a negative number. To accommodate "negative time," a constant amount of time, tL, is added artificially to all data points in the model to bring the theoretical Fickian diffusion curve to an "adjusted" zero time. The tL parameter then describes the time that was "lost" by the burst release. The reason it is called "lost time" is illustrated by a simple example. Suppose that the time-adjusted theoretical curve fit hits some percent release in 3.5 days, but, as a result of the burst release, the actual data hits that same percent

release in 2 days. We can then say that there were 1.5 days of "lost" release time due to the initial burst release.

The diffusion coefficient, D, is a lumped parameter that represents the resistance to diffusion, and it is contributed to by a wide range of physiochemical properties of the fiber and the drug, as well as the interaction between the two. For example, the internal and external porosity of the fiber, the hydrophilic/hydrophobic nature of the fiber and drug, any charged or polar groups that may be present within the pores of the fiber or on the surface of the drug, and the degradation rate of the fiber all contribute to the measured value of the diffusion coefficient. The diffusion coefficient also depends on the size, shape, and solubility of the drug, and, if there are excipients present, the excipient–polymer interactions as well as the excipient–drug interactions. The size, shape, and solubility of the drug, in turn, depend on the stability of the drug at the given temperature and within its local chemical environment, which is a function of ionic strength, pH, and the presence of any small molecules that may impact the drug, its excipients, or the polymer.

The Sagiv model conceptually divides the data points into two groups: the first group of data points is the "initial burst," and the second group of data is "diffusion controlled." As the iterative process to determine D and tL continues, individual data points may move from one group to another until the best fit is determined. It is this author's opinion that the burst release properties, such as tL, will be very similar both *in vitro* and *in vivo*, with the only major assumption being that the drug's solubility is similar in both the *in vitro* release media and the biological milieu into which it is implanted. This opinion is based on my experience with *in vitro* release experiments. I have seen that a large part of the burst release is done within 5–10 min, with the majority being complete by an hour, and therefore, it should be largely independent of host response to the fiber implant, although there presently seems to be little or no data in the literature to support this supposition. The diffusion coefficient, D, on the other hand, is more variable between the *in vitro* experiment and the *in vivo* reality. It has been known for a long time that, postimplantation, protein adsorption from the host begins almost immediately (Pitt and Cooper, 1986). Based on the above discussion of the diffusion coefficient, it seems clear that protein adsorption (including on the outside surface of the fiber and the coatings of the pores and internal structures of the fiber), enzymatic attack, cell adhesion and matrix production, cell proliferation, and cellular attempts to remodel the fiber all potentially change how the drug interacts with this newly created protein–fiber interface and, thereby, alter the diffusion coefficient. Many of the physiochemical characteristics previously offered to explain the diffusion coefficient, such as pore size, hydrophilic/hydrophobic areas, and polar or charged groups, can potentially start to change within minutes of the fiber being exposed to the biological environment into which it is implanted, because proteins adsorb to both the internal and external surfaces of the fiber. The degree to which the diffusion coefficient changes is largely a function of pore size and how prone fiber's constituent polymer is to adsorb protein. In addition to these biologically mediated changes in the diffusion coefficient, there are other physical contributors. For example, as the polymer degrades, it typically becomes more porous, and some fibers become more crystalline as they degrade (Crow et al., 2005). These physical features

of the fiber also potentially change the diffusion coefficient. Interestingly, some of these physical changes in the fiber may be seen in the *in vitro* release experiments. If the release time extends into the time when the fiber begins to degrade, the data starts to deviate from the pure Fickian diffusion curve (as you will recall, the model was based on a time-invariant, constant diffusion coefficient). Therefore, deviations from pure Fickian diffusion late in the Sagiv model fit are very likely indicators that physical changes are beginning to happen within the fiber.

The following figures show unpublished data from TissueGen Inc. of a growth factor released from a fiber. Figure 6.7 shows the fractional release as a function of time in days, indicating that, over approximately 30 days, about 30% of the total loaded growth factor was released. Figure 6.8 shows the Sagiv model fit of that data, and it plots the fractional release as a function of normalized time $t = TR^2/D + t\mathrm{L}$, where T is the actual time measured in seconds, R is the radius of the fiber, D is the mathematically fit diffusion coefficient, and $t\mathrm{L}$ is the lost time constant. This model makes it clear that the first data point is clearly off the Fickian diffusion curve, but the second data point (in this case, the 3 h time point) is quite close, and by the third point (6 h), the data seems to be following Fickian diffusion very well. It is interesting that the last few data points begin to deviate from pure Fickian diffusion. For this dataset, the diffusion coefficient was calculated to be $D = 1.1 \times 10^{-13}$, and $t\mathrm{L} = 0.04$. The same data

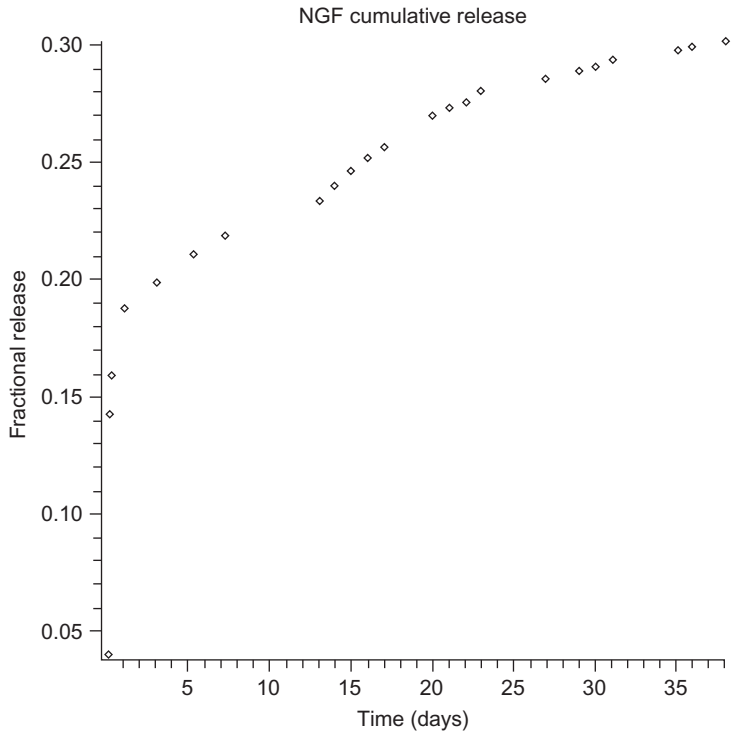

Figure 6.7 Cumulative release of NGF from a polydioxanone fiber, showing the fraction released as a function of time in days.

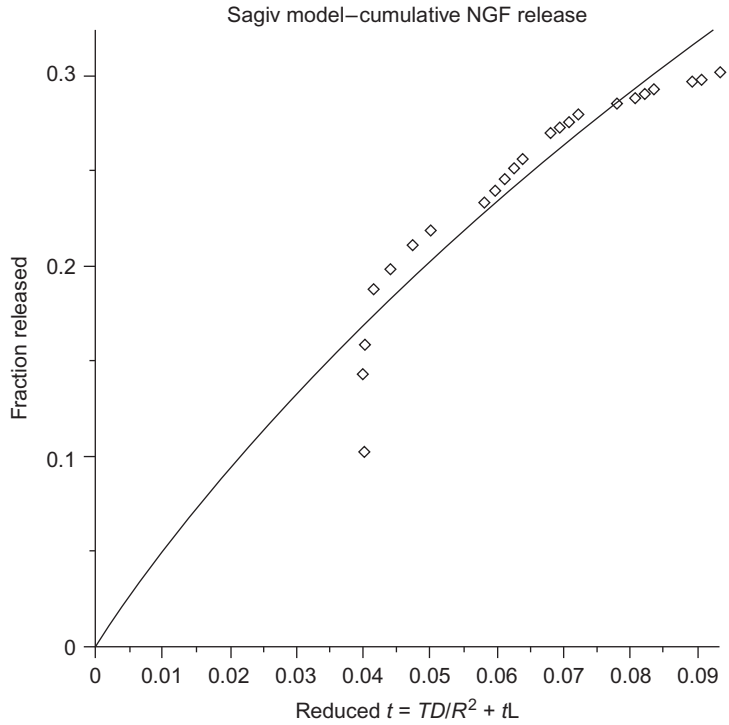

Figure 6.8 Same NGF data set mathematically fit using the Sagiv model. Note the initial points that are below the line constitute the "burst release," which in this case represents 3–6 h. The remainder of the data points follow the Fickian diffusion curve rather well until the final days when they start to fall below the line. For this data, $D = 1.1 \times 10^{-13}$ and $t\mathrm{L} = 0.04$.

was fit using the Korsmeyer–Peppas model, as shown in Figure 6.9, which is given by the simple relationship

$$\frac{M_t}{M_\infty} = Kt^n \tag{6.1}$$

where n should be within the range of 0.45–0.89 for cylindrical devices (Siepmann and Peppas, 2001); however, for this data set $n = 0.2$ and $k = 0.0152$. Although the Korsmeyer–Peppas equation fits the data quite nicely, there is little physical interpretation of the data, other than to provide rather wide ranges of values of expected values for n. However, this dataset falls far from the expected range for release from a cylinder. The Sagiv model, on the other hand, allows a very specific interpretation of the results; for example, it shows an initial burst release lasting from 3 to 6 h followed by approximately 30 days of very well characterized Fickian controlled release, with the final few points beginning to deviate from the Fickian diffusion curve. The Sagiv model is much more difficult to implement, but it does provide details such as the actual diffusion coefficient and the degree to which the data follows pure Fickian

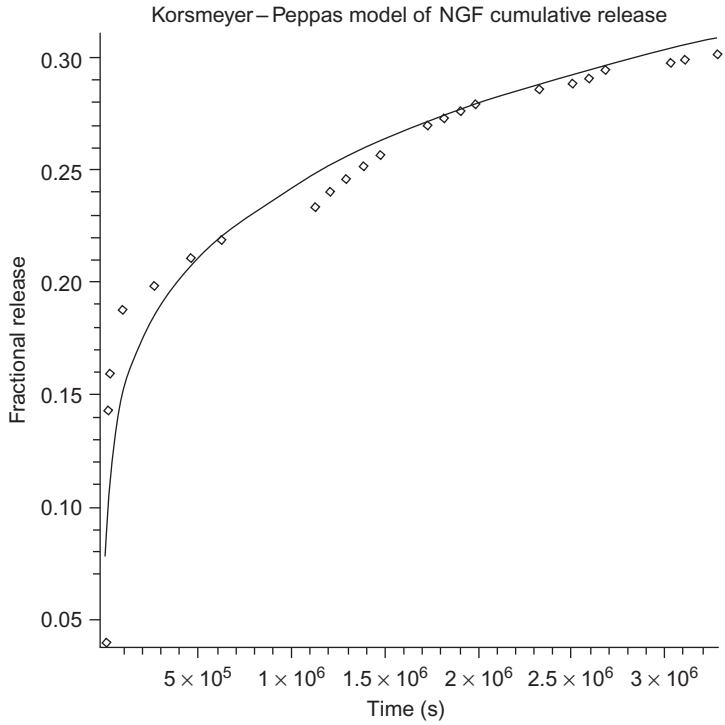

Figure 6.9 The same NGF data set using the Korsmeyer–Peppas model to fit the data showing a very nice overall fit of the data. For this dataset $n = 0.2$ and $k = 0.0152$.

diffusion, as well as an exact measure of burst release. Each of these analyses allow comparison between fibers, and they are excellent means of providing quality control.

6.4 Applications

There are several items to consider when contemplating drug delivery from a fiber:

- Size and strength requirements of the fiber.
- Type of drug to load.
- Desired release profile.
- Desired degradation rate of the fiber.
- Need to convert the fiber into a textile.

The release kinetics of drugs from biodegradable fibers is governed by several important factors:

- Concentration of drug within the fiber.
- Drug distribution across the cross section of the fiber.

- Drug size.
- Solubility of the drug in the surrounding media (usually aqueous).
- Hydrophobic or hydrophilic nature of the drug.
- Drug–polymer or excipient–polymer interactions that may retard the release of the drug from the fiber.
- Porosity of the fiber.
- Crystallinity of the polymer.
- Degradation rate of the polymer system.

Controlling the release kinetics is never precise and is a matter of finding balance amid many competing goals.

6.4.1 Drug depot

Biodegradable fibers make excellent drug depots in situations where mechanical strength is required as well as when it is not. There are numerous reasons why it is advantageous to use a drug-loaded fiber as the delivery vehicle, as opposed to other formats in clinical use today, such as microspheres or nanoparticles.

(1) Fibers remain in place once implanted in the body. For clinical applications such as tumor remediation, during which the drug needs to be delivered at a specific location within the body, a drug-loaded fiber will remain in place much better than microspheres or nanoparticles, which have been shown to migrate widely (Doane and Burda, 2013). In those cases where wide distribution is desired, nanoparticles are exceptional; however, where localization is desired, the nanoparticles must be made magnetic or modified in some other way in order to sequester them to a specific physiological location within the body, such as a tumor (Veiseh et al., 2010). If a fiber can be implanted in a specific location, say within the tumor, it will stay there, and it will release the drug there, and no modifications that may or may not raise additional issues with biocompatibility or other safety issues are needed.
(2) The release rate of a drug from a cylinder is inherently slower than the release rate from a sphere, assuming equal radius. Most of the time, the desire is for prolonged release. Implantable drug delivery is often used to ensure that the drug is delivered at the right location (and usually only at the right location), to flatten out the peak and valley concentration profile that is typical of oral doses of medicine, and to remove any possible issues with patient compliance. Therefore, slow, sustained release is almost always preferred. Infinitely long cylinders (most practical fibers) provide the best means of meeting these goals.
(3) In the rare case of adverse reaction to the drug, a fiber can be easily removed, whereas it is impossible to remove thousands of microspheres or trillions of nanoparticles. Therefore, drug delivery from a fiber is also inherently safer than drug delivery from other formats.

These points all apply whether the fiber is supplying mechanical support or acting as a drug depot.

6.4.2 Medical devices

6.4.2.1 Suture

Sutures are the most commonly implanted biomaterial, accounting for the vast majority of clinically used biodegradable fiber. Sutures come in many different sizes and morphologies: braided, monofilament, natural, synthetic, and so on. Sutures are designed to fit a specific need based on intended anatomical location. Sutures have been in use for more than a millennia; however, the ability to load drugs into the suture gives this ancient technology a new twist. Simple drugs such as antibiotics can be easily loaded into sutures, and they have been for several decades (Cattabriga et al., 1996). The introduction of growth factors and other biologically derived drugs allow the suture to actually participate in the wound-healing process.

Initially, the field of biomaterials sought "inert" materials that would simply be bystanders with regard to the biological reactions taking place around them following implantation into the body. Over the past couple of decades, that elusive goal of finding an inert material has given way to seeking a material that will take an "active" part in the wound-healing process. The activity can be to inhibit unwanted activity such as platelet adhesion and/or to promote positive activity such as cell attachment and proliferation. Until now, this has been done largely with surface coatings and by attaching signaling molecules to the surfaces, such as the peptide sequence of L-arginine, glycine, and L-aspartic acid (Arg-Gly-Asp or RGD), which has been shown to promote cell adhesion (Dawson et al., 2011). With the advent of fibers that can release mitogenic or chemotactic factors, however, this platform can now release soluble factors into the biological environment to impact cells that are diffusion distances away, not just those already in contact with the surface. Also, by releasing growth factors and other types of signaling molecules, rather than simply creating a surface that enhances cell attachment, we can now "talk" to the cells in the environment, giving them "messages" that alter their behavior in desirable ways. Sutures loaded with growth factors that are slowly released may play a role in directing or leading the body's biological response in very specific ways. For example, sutures used in a dermal wound may have the potential to upregulate elastin production over collagen production in the fibroblasts that enter the wound space, giving way to less scar tissue and, thus, resulting in a more pliable, natural tissue. In another example, sutures that release neurotrophic factors may be able to entice axonal elongation when used to repair severed peripheral nerves. As more signaling molecules are discovered, the range of possibilities increases. For example, if it were known which factors upregulate the formation of tight junctions, it might be possible to create anastomotic junctions that are far superior to what is possible today.

6.4.3 Tissue engineering

A significant percentage of the human body's tissues and organs are fibrous in nature. Because of this, it is reasonable that, with appropriate weaving, knitting, braiding, or some other form of fabrication, it may be possible to mimic the fibrous nature of the body with synthetic fibers. This three-dimensional construct of synthetic fiber might

then serve as a basis for scaffolding for the body to execute reconstruction or regeneration following injury or disease.

Organs and soft tissues can be roughly divided into two groups, hollow and solid. Hollow organs are generally cylindrical, such as blood vessels, digestive tracts and ducts, and urinary track tubes. In these cases, the general construction of the hollow organs is similar. There is always some type of epithelial cell lining on the inner surface of the tube, usually a smooth muscle layer, and an outer layer that consists of capillaries to feed the tissue or organ, as well as macrophages and other cell types to support the organ or tissue.

Solid tissues, such as muscle tissue, nerve tissue, tendons, ligaments, and meniscus, have less within-group commonality. For example, muscle and nerve tissue are highly cellular and well vascularized, but tendons, ligaments, and meniscus are nearly acellular and have little or no active blood supply in adults.

It follows then that tissue engineering approaches may vary widely between hollow and solid tissue and organs.

6.4.3.1 *Scaffolding*

The construction of a large building initially requires scaffolding; however, the need for the scaffolding decreases as the building materials are put into place. Similarly, in the body, as appropriate cells begin to populate the synthetic fiber-based scaffold, the need for the scaffold diminishes, and it must be replaced by natural tissue. Therefore, the synthetic fibers should be biodegradable. Back to the building analogy, the functionality of the building depends on the right building materials being in the right place: shingles on the roof and glass in the windows. Anatomically, the same idea holds true; specific cells must be at specific three-dimensional locations within the tissue or organ or things may not function properly. The point of scaffolding is to direct the right cell type to the right anatomical location and to ensure that there is sufficient access to nutrients for the cell to survive once in place. Drug-eluting fibers that have the ability to release growth factors may be capable of forming scaffolding that can direct cell growth and migration for regenerative medicine applications.

6.4.3.2 Ex vivo *tissue growth*

There are two basic approaches to scaffolding for tissue engineering and regenerative medicine. The first, called *ex vivo* tissue growth, is to create the scaffolding, to seed it with cells outside of the body (typically from the patient for whom the scaffolding is intended), and then to allow the cells to populate the scaffolding. It is then possible to implant the newly grown tissue into the host. This approach has several important advantages. For example, it allows control over the type of cells to which the scaffolding is exposed. The cells grow and divide in a controlled environment. However, there are several disadvantages to this approach. For one, it is very difficult to provide oxygen and nutrients to thick sections of tissue growing in an external, artificial environment. Therefore, at this time, only thin tissues can be considered using this approach. Another disadvantage of growing the tissue in culture is that fewer types of cells are generally used

than would be found in normal, healthy tissue within the body. For example, it is hard to duplicate mast cells and macrophages that randomly populate actual tissue. Finally, in the controlled environment, the full range of cytokines and growth factors normally found in the body are not present in the tissue culture dish. Although this decreased population of signaling molecules makes the tissue culture a much less complicated system, perhaps there are reasons why a more complicated system is needed.

6.4.3.3 In vivo *tissue growth*

The second approach is to directly implant the scaffold into the patient and allow nature to populate the scaffold as it will. This approach has several disadvantages. The scaffolding becomes flooded with blood, which is a very complicated tissue, and deposits a layer of protein, bringing cells into the scaffold in a completely uncontrolled way. During any wound-healing process, there is a virtual "cytokine storm" for the first few days as the body is trying to re-establish homeostasis. So, directly implanted scaffolds start from a position of chaos and disorder in a very aggressive biological environment. Unintended cell types fill the scaffold, and the initial host response to wall off the new material is exactly contrary to the desired enticing of functional cells of the organ or tissue into the right position within the scaffold. To achieve homeostasis, the functional cells are typically shut down as the "first responders" (e.g., neutrophils, macrophages, and finally fibroblasts) have a well-orchestrated routine of creating scar tissue and knitting together tissue as best they can. How can a scaffold in this kind of environment induce sufficient cell migration to establish functional tissue? If there are chemotactic molecules and growth factors being released from the fibers of the scaffold, these signaling molecules can reach the appropriate receptors, and they can entice the parenchymal cells to begin to enter the scaffold in the wound bed. In the peripheral nervous system, it has been shown that even with no growth factors, the simply presence of a physical scaffold of fibers can induce axonal regeneration across 10–18 mm gaps (Cai et al., 2004; Ngo et al., 2003). Some success has also been achieved in the central nervous system (Tang et al., 2004).

6.4.3.4 *Hollow-organ tissue engineering*

Because of the thin-walled nature of hollow organs, they have the potential to be created via *ex vivo* tissue growth. For example, in recent years, we have seen this process used to construct the very successful tissue-engineered artificial bladder (Atala et al., 2006). One challenge with constructing scaffolding for hollow organs is the ability to selectively entice appropriate cell types into their thin and confluent layers. We have shown in Figure 6.10 the ability of the cell culture to directionally entice axonal elongation toward strands of fiber that are loaded with NGF. Cells generally follow concentration gradients. The Nelson et al. (2003) patent describes the ability to load drugs with a concentration gradient along the length of a fiber. It is also possible to construct three-dimensional concentration gradients. These gradients may entice specific cells to grow along or through specific pathways as they follow the appropriate concentration gradient. It has yet to be shown that cells *in vivo* will exhibit this same behavior.

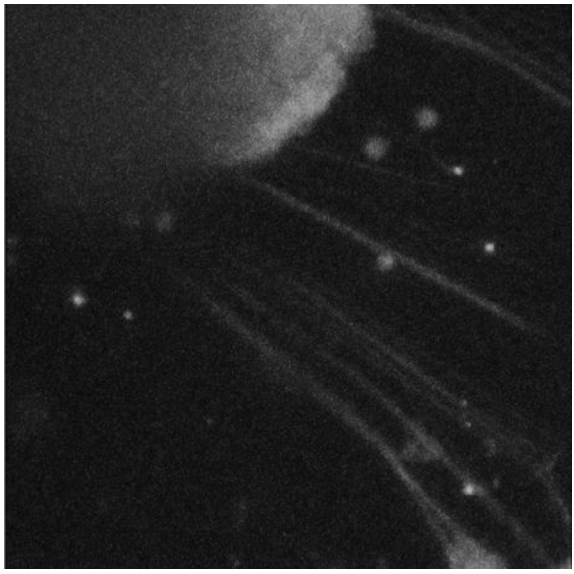

Figure 6.10 Dorsal root ganglion cells expressing neurites that are all traveling in the same direction toward a fiber releasing NGF (not visible in the picture).

Getting the right cell to the right place within the fiber scaffold is only the first half of the problem; the cells must be able to create their own matrix on which to grow, and they must interact appropriately with one another, including forming junctions. Ultimately, the only test that counts is whether or not the cells begin to function normally after their arrival at the "right spot" within the scaffold.

6.5 Chapter summary

Tissue engineering and regenerative medicine based on three-dimensional scaffolds that have the ability to induce selected cell growth may be the next breakthrough in medicine. It's not just enough to arrest the progress of disease or to stop degradation from injury; the goal is to actually restore function. It appears that this restoration may be possible in some cases based on the data and concepts presented in this chapter.

Solution extrusion that can take place at room or body temperature can incorporate growth factors and other biologically significant molecules with a high degree of retained biological activity. These loaded fibers can be formed into scaffolds. The scaffolds can then be implanted directly into the body, or they can be seeded with cells outside the body first and later implanted. In both cases, by virtue of the biological molecules that are released from these fibers, signals can be sent to the cells, directing specific cell types to grow in one direction and other cell type to grow in a different direction. This signaling and directing of cellular growth within the scaffolding can be used to create functional, three-dimensional, physiologically significant structures that can restore function that was lost due to injury or disease.

References

Albrecht, W., et al., 2001. Formation of hollow fiber membranes from poly(ether imide) at wet phase inversion using binary mixtures of solvents for the preparation of the dope. J. Membr. Sci. 192 (1–2), 217–230.

Atala, A., Bauer, S.B., Soker, S., Yoo, J.J., Retik, A.B., 2006. Tissue-engineered autologous bladders for patients needing cystoplasty. Lancet 367 (9518), 1241–1246.

Bahrami, S.H., Bajaj, P., Sen, K., 2003. Effect of coagulation conditions on properties of poly (acrylonitrile-carboxylic acid) fibers. J. Appl. Polym. Sci. 89 (7), 1825–1837.

Beck, A.W., et al., 2004. Ultrasound-Guided Placement of Bioresorbable Fibers into Pancreatic Adenocarcinoma Tumors Achieves Prolonged Adenoviral Gene Transfer. American Chemical Society, Newport News, VA.

Boyer, M.J., Tannock, I.F., 1992. Lysosomes, lysosomal enzymes, and cancer. Adv. Cancer Res. 60, 269–291.

Cai, J., et al., 2004. Synergistic improvements in cell and axonal migration across sciatic nerve lesion gaps using bioresorbable filaments and heregulin-B1. J. Biomed. Mater. Res. A 69 (2), 247–258.

Cattabriga, M., et al., 1996. Tetracycline fiber used alone or with scaling and root planing in peridontal maintenance patients: clinical results. Quintessence Int. 27, 395–400.

Crow, B.B., Nelson, K.D., 2006. Drug releasing biodegradable fiber implant of various materials and structural compositions used for the delivery of therapeutics. United States of America, Patent No. 7,033,603.

Crow, B.B., et al., 2005. Evaluation of in vitro drug release, pH change, and molecular weight degradation of poly(L-lactic acid) and poly(D, L-lactide-co-glycolide) fibers. Tissue Eng. 11 (7–8), 1077–1084.

Dash, S., Murthy, P.N., Nath, L., Chowdhury, P., 2010. Kinetic modeling on drug release from controlled drug delivery systems. Acta Pol. Pharm. Drug Res. 67 (3), 217–223.

Dawson, J., et al., 2011. Collagen scaffolds with or without the addition of RGD peptides support cardiomyogenesis after aggregation of mouse embryonic stem cells. In Vitro Cell. Dev. Biol. Anim. 47 (9), 653–664.

Doane, T., Burda, C., 2013. Nanoparticle mediated non-covalent drug-delivery. Adv. Drug Deliv. Rev. 65, 607–621.

Flory, P.J., 1941. Physical chemistry of polymers thermodynamics of solutions of high polymers. J. Chem. Phys. 9 (8), 660.

Fried, J.R., 2003. Conformations, solutions and molecular weight, Polymer Science and Technology, second ed. Prentice Hall PTR, Englewood Cliffs, NJ, pp. 87–147.

Kamerzell, T.J., et al., 2011. Protein—excipient interactions: mechanisms and biophysical characterization applied to protein formulation development. Adv. Drug Deliv. Rev. 63, 1118–1159.

Khalil, I.A., Kogure, K., Akita, H., Harashima, H., 2006. Uptake pathways and subsequent intracellular trafficking in nonviral gene delivery. Pharmacol. Rev. 58 (1), 32–45.

King, M.W., Jones, A.D., 2006. In: Anand, S.C., Kennedy, J.F., Rajendran, S. (Eds.), Medical Textiles and Biomaterials for Healthcare. first ed. Woodhead Publishing Limited, Boca Raton, FL, pp. 425–431.

Levine, R.M., Scott, C.M., Kokkoli, E., 2013. Peptide functionalized nanoparticles for nonviral gene delivery. Soft Matter 9, 985–1004.

Mehl, J.W., Oncley, J.L., Simha, R., 1940. Viscosity and the shape of protein molecules. Science 92, 132–133.

Morris, E.A., 2011. Bench-Scale, Multifilament Spinning Conditions Effect on the Structure and Properties of Polyacrylonitrile Precursor Fiber, first ed. University of Kentucky, Lexington, KY.

Musaev, K.N., Yunusov, M.Y., Tyagai, E.D., Nigmatov, K., 1983. Effect of the nature of the solvent on the structure and certain properties of acetate fibers. Fibre Chem. 15 (5), 354–357.
Nair, L.S., Laurencin, C.T., 2005. Polymers as biomaterials for tissue engineering and controlled drug delivery. Adv. Biochem. Eng. Biotechnol. 102, 47–90.
Natu, M.V., de Sousa, H.C., Gil, M.H., 2011. Electrospun drug-eluting fibers for biomedical applications. In: Zilberman, M. (Ed.), Active Implants and Scaffolds for Tissue Regeneration. Springer-Verlag, Berlin, Heidelberg, pp. 57–85.
Nelson, K.D., et al., 2002. Innovative Fiber Format for the Delivery of Proteins. International Controlled Release Society, Seoul, South Korea.
Nelson, K.D., et al., 2003. Drug releasing biodegradable fiber implant. United States of America, Patent No. 6,596,296.
Nelson, K.D., et al., 2004a. Drug delivery Fibers for Potential Solid Tumor Treatment. In: IEEE MetroCon, Arlington, TX.
Nelson, K.D., Ganter, J., Flemming, J., 2004b. New Bi-component Fibers Capable of Releasing Viruses with Retained Biological Activity. International Controlled Release Society, Honolulu, HI.
Ngo, T.-T.B., et al., 2003. Poly(L-lactide) microfilaments enhance peripheral nerve regeneration across extended nerve lesions. J. Neurosci. Res. 72, 227–238.
Nierstrasz, V.A., 2007. Textile-based drug release systems. In: Van Langenhove, L. (Ed.), Smart Textiles for Medicine and Healthcare. Woodhead Publishing Limited, Cambridge, England, pp. 50–73.
Ohtake, S., Kita, Y., Arakawa, T., 2011. Interactions of formulation excipients with proteins in solution and in the dried state. Adv. Drug Deliv. Rev. 63, 1053–1073.
Pitt, W.G., Cooper, S.L., 1986. FTIR-MR studies of the effect of shear rate upon albumin adsorption onto polyurethaneurea. Biomaterials 7, 340–347.
Rissanen, M., et al., 2010. Effect of protein-loading on properties of wet-spun poly(L, D-lactide) multifilament fibers. J. Appl. Polym. Sci. 116 (4), 2174–2180.
Sagiv, A., Parker, N., Parkhi, V., Nelson, K.D., 2003. Initial burst measures of release kinetics from fiber matrices. Ann. Biomed. Eng. 31, 1132–1140.
Siepmann, J., Peppas, N.A., 2001. Modeling of drug release from delivery systems based on hydroxypropyl methylcellulose (HPMC). Adv. Drug Deliv. Rev. 48, 139–157.
Tan, J., Noh, S.-H., Chowdhurry, G., Matsuura, T., 2000. Influence of surface tensions of solvent/nonsolvent mixtures in membrane casting solutions in the performance of poly(2,6-dimethyl-1,4-phenylene) oxide membranes. J. Membr. Sci. 174, 225–230.
Tang, X.-Q., et al., 2004. Functional repair after dorsal root rhizotomy using nerve conduits and neurotrophic molecules. Eur. J. Neurosci. 20, 1211–1218.
Veiseh, O., Gunn, J.W., Zhang, M., 2010. Design and fabrication of magnetic nanoparticles for targeted drug delivery and imaging. Adv. Drug Deliv. Rev. 62, 284–304.
Wang, D., Li, K., Teo, W.K., 1996. Polyethersulfone hollow fiber gas separation membranes prepared from NMP/alcohol solvent systems. J. Membr. Sci. 115, 85–108.
Xiaoqiang, L., et al., 2010. Encapsulation of proteins in poly(L-lactide-co-caprolactone) fibers by emulsion electrospinning. Colloids Surf. B: Biointerfaces 75, 418–424.
Xu, L., Rungta, M., Koros, W.J., 2011. Matrimidderived carbon molecular sieve hollow fiber membranes for ethylene/ethane separation. J. Membr. Sci. 380, 1–2.
Yang, Y., et al., 2008. Release pattern and structural integrity of lysozyme encapsulated in core-sheath structured poly(DL-lactide) ultrafine fibers prepared by emulsion electrospinning. Eur. J. Pharm. Biopharm. 69, 106–116.
Zilberman, M., Golerkansky, E., Elsner, J.J., Berdicevsky, I., 2009. Gentamicin-eluting bioresorbable composite fibers for wound healing applications. J. Biomed. Mater. Res. A 89, 654–666.

Anterior cruciate ligament prostheses using biotextiles☆

7

M. Laflamme, J. Lamontagne, R. Guidoin
Laval University, Québec, Québec, Canada

7.1 Introduction

The knee is an austere environment: in a normal individual, 2–4 million flexions/extensions are accomplished per year. The types of stress encountered during these cycles include tension, abrasion, bending, torsion and compression (Olson et al., 1988). The intra-articular portion of the knee is relatively avascular, which makes it difficult for cells and structures to survive. Probably the most complex of these structures and the most commonly injured ligament is the anterior cruciate ligament (ACL). It was initially referred to as a *crucial* ligament because of the cruciate or crossed arrangement of the anterior and posterior ligaments within the joint (Bolton and Bruchman, 1985). Over the years different trends in ACL surgery have emerged: primary repair, augmentation devices, allografts, prosthetic devices, autografts and now tissue engineering, not to mention the transition from knee arthrotomy to well-developed arthroscopic techniques. All these approaches are reviewed in this chapter, with a strong emphasis on the different types of synthetic implants and why, after early enthusiasm regarding preliminary results, the high failure rates made surgeons abandon them.

7.2 Anatomy and structure of the anterior cruciate ligament

The ACL is much more complex than a simple band of dense connective tissue measuring 32 mm by 7–12 mm between the femur and the tibia (Duthon et al., 2006). It originally appears as a mesenchymal condensation in the blastoma at 6.5 weeks of gestation, well before joint cavitation (Figure 7.1) (Ellison and Berg, 1985). By the 20th week, the two different bundles of the ligament can be distinguished (Petersen and Zantop, 2006). Some authors think that the presence of cruciate ligaments at this early stage of development plays a role in the resulting shape of the femoral condyles and tibial plateau (Lohmander et al., 2004).

☆ Note: This chapter is a reproduction of Chapter 20 'Anterior cruciate ligament prostheses using biotextiles' by M. Laflamme, J. Lamontagne and R. Guidoin, originally published in *Biotextiles as medical implants*, ed. Martin W. King, Bhupender S. Gupta and Robert Guidoin, Woodhead Publishing Limited, 2013, ISBN: 978-1-84569-439-5.

Biomedical Textiles for Orthopaedic and Surgical Applications. http://dx.doi.org/10.1016/B978-1-78242-017-0.00007-6

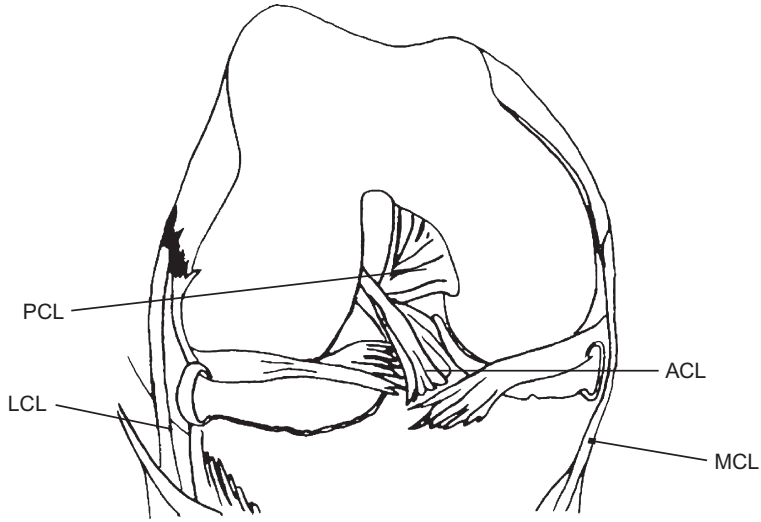

Figure 7.1 The anatomy of the ACL in relation to the knee joint architecture. Proximally, it is attached to the posterior aspect of the medial surface of the lateral femoral condyle, passing in front of the PCL and attaching distally on the tibial plateau.

The ACL is intra-articular and completely surrounded by synovium from the posterior capsule, thus making it extrasynovial. Proximally, it is attached in the shape of a semicircle, with the anterior border straight and the posterior border convex, to the posterior aspect of the medial surface of the lateral femoral condyle. Distally, the ACL is attached to a fossa anterior and laterally to the anterior tibial spine. It passes beneath the transverse meniscal ligament and it often blends with fibres from the anterior and posterior horns of the lateral meniscus (Figure 7.2). The fibres of the ACL are narrowest in mid-substance and, as they go anteriorly, medially and distally, they twist themselves on

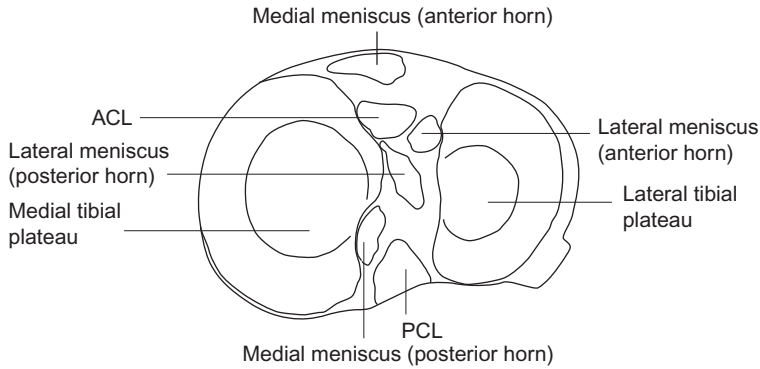

Figure 7.2 Insertion sites on the tibial plateau. Distally, the ACL is attached to a fossa anterior and lateral to the anterior spine. It passes beneath the transverse meniscal ligament and it often blends with fibres from the anterior and posterior horns of the lateral meniscus.

each other about 5 mm from the proximal insertion (Schutte et al., 1987). This section is where the ligament starts to fan out, and it explains why the distal attachment is much broader than the proximal one. This lateral spiral of approximately 90° is explained by the orientation of the bony attachments (Petersen and Zantop, 2006).

Girgis divided the ACL ligament into two main bundles: anteromedial (AM) and posterolateral (PL) (Girgis et al., 1975). Others have defined more than two bundles, but Girgis's concept is the most popular. The bundles are named after their insertion on the tibia. The AM bundle is more vertical and originates at the anterior and proximal aspect of the femoral attachment, while the PL part originates at the posterodistal aspect of the same attachment (Figure 7.3) (Amis and Dawkins, 1991). The latter is composed of more fascicles (Duthon et al., 2006). These two bundles are not isometric; as the knee moves, there is always a bundle that is under tension. When the knee is extended, the PL is tight and the AM is lax and, when the joint is flexed, tension is reversed. The AM bundle is the primary restraint against anterior tibial translation, and the PL bundle tends to stabilize the knee near full extension, particularly against rotatory loads (Petersen and Zantop, 2006).

The microarchitecture of the ACL is also complex and allows the ligament to withstand different stresses and strains. It is composed of multiple fascicles surrounded by the paratenon. Each fascicle is composed of 3–20 subfasciculi that are enclosed by the epitenon. The subfasciculi themselves are made of subunits, again surrounded by connective tissue called the endotenon. The subunits are made of collagen fibrils of two types, small and large, that form wavy fibres arrayed in various directions, either spiral or along the axis of the ligament. The larger inhomogeneous fibrils resist high-tensile stresses and the small homogeneous ones maintain the three-dimensional organization of the ligament (Strocchi et al., 1992).

Type I collagen comprises approximately 90% of the total collagen found within the ligament (Dodds and Arnoczky, 1994). Type I collagen fibrils are oriented parallel to the longitudinal axis of the ligament (Petersen and Tillmann, 1999) and are responsible for its tensile strength (Amiel et al., 1989). Type III collagen (the remaining 10% of the total collagen) is in the loose connective tissue dividing collagen bundles and is implicated in the ligamentization process. Together, they account for 75% of the dry

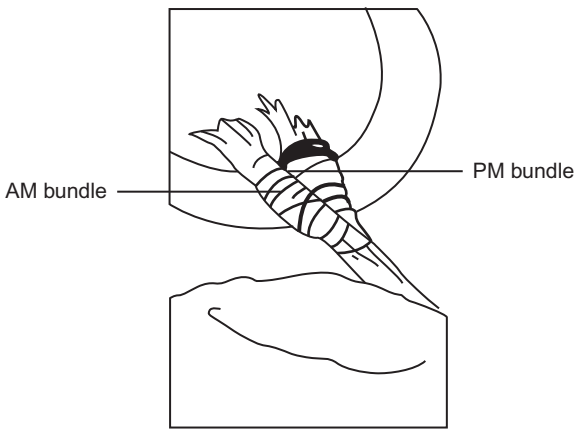

Figure 7.3 The ACL divided into anteromedial and posterolateral bundles, named after their insertion on the tibia. The former is more vertical and originates at the anterior and proximal aspect of the femoral attachment, while the posterolateral part originates at the posterodistal aspect of the same attachment.

weight of the ligament. Small amounts of type II collagen can be found in two distinct areas of the ACL. First, there is a zone located 5–10 mm proximal to the tibial attachment in the anterior part of the ligament (Petersen and Tillmann, 1999; Amiel et al., 1989) that faces the anterior rim of the intercondylar fossa where the ligament impinges during knee extension. In this area, dense fibrous tissue surrounds the ligament and collagen bundles are larger and cross each other at sharp angles. This zone of the ACL consists of fibrocartilage made of type II collagen, which is mineralized and resembles bone (Amiel et al., 1989). This phenomenon is explained by Pauwel's theory of causal histogenesis (Petersen and Tillmann, 1999; Amiel et al., 1989), which states that the tissue develops and adapts as a secondary response to intermittent compressive and shearing forces as the ligament passes around the notch (Duthon et al., 2006) and impinges on the anterior rim. There is also a transitional zone of fibrocartilage made of collagen type II where the ligament attaches to bone. This allows a gradual change in stiffness and prevents stress concentration in those areas. Type IV and VI collagen are also present minimally (Woo et al., 1988).

Between fibrils, there are elongated fibroblasts and an extracellular matrix (ECM) mainly made of water (60–80% of the wet weight), proteoglycans and glycosaminoglycans interacting with the collagen. Among the collagen fibrils also lies abundant elastic tissue made of elastin and oxylatan fibres, which help the knee to withstand modest multidirectional stresses and absorb recurrent maximal stresses, respectively (Strocchi et al., 1992). Duthon et al. divided the ligament into three microscopic zones: the proximal part, which is less solid and more cellular; the middle part, consisting of spindle-shaped fibroblasts and a high density of collagen fibres; and the distal zone, which is the most solid and is made of chondroblasts and fibroblasts (Duthon et al., 2006).

The major blood supply of the ACL comes from the middle genicular artery, which pierces the posterior capsule and gives off branches to the ligament in the intercondylar notch (Figure 7.4). Other branches arise from the medial and lateral inferior genicular arteries. Two main networks nourish the ligament: the periligamentous vessels and the endoligamentous vessels (Dodds and Arnoczky, 1994). The former comes

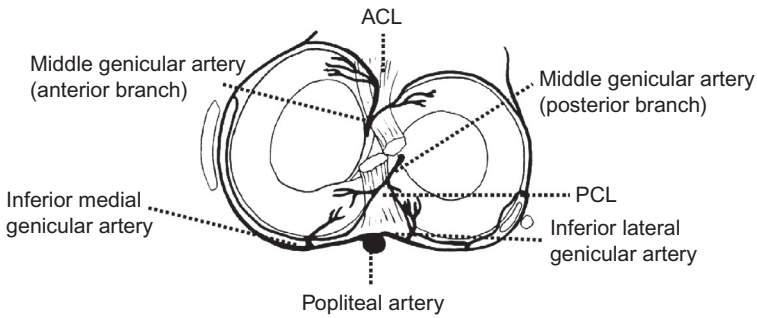

Figure 7.4 Vascularization of the cruciate ligaments is mainly from the middle genicular artery and partially by the medial and lateral inferior genicular arteries. The middle genicular artery pierces the posterior capsule and gives off branches in the intercondylar notch.

from the synovial membrane, which completely envelopes the ligament, and from the richly vascularized fat pad (inferior genicular artery). This is consistent with the concept of leaving as much fat pad as possible during knee surgeries. These small vessels then give rise to branches that penetrate the ligament transversely and anastomose with the endoligamentous network, mainly oriented in a longitudinal direction (Petersen and Tillmann, 1999). There are no intraligamentous vessels crossing the bony attachment sites of the ligament to the femur and tibia. The distribution of blood vessels within the ligament is not homogeneous, with the distal part being less vascularized. The zone where the anterior part of the ligament is covered with fibrocartilage secondary to compressive forces from the intercondylar notch is also considered avascular. According to Petersen et al., this limited blood supply and the occurrence of fibrocartilage are factors in the poor healing potential of the cruciate ligament (Petersen and Tillmann, 1999).

The ACL is primarily innervated by posterior articular branches of the tibial nerve (Amiel et al., 1989). Most of the fibres are coupled with vessels and thus have vasomotor functions while others run independently. They account for 1% of the volume of the ligament. Sensory-ending fibres have been described in the ACL. The Ruffini, the Vater–Pacini and the Golgi-like tension receptors are mechanoreceptors with a proprioceptive function (Woo et al., 1988). These receptors are responsible for the ACL reflex, where stimulation of the nerve fibres by a deformation of the ligament affects the motor activity of the muscles around the knee (Duthon et al., 2006). When the ACL is ruptured, with the loss of joint position sense comes the loss of feedback from those receptors leading to weakness of the quadriceps femoris (Konishi et al., 2002). Finally, the fourth type, the free-nerve endings, act primarily as nociceptors. Some surgeons leave the stumps of the torn ACL, on the grounds that some mechanoreceptors and proprioceptive functions may remain.

7.3 Biomechanics of the ACL

The ACL resists anterior tibial translation and rotational loads. With a ruptured ACL, the anterior translation of the tibia relative to the femur can be four times greater than in normal knees (Beynnon et al., 2002). It also restrains internal rotation significantly and plays a minor role in controlling the external rotation and varus-valgus angulation (Duthon et al., 2006). Moreover, the ACL prevents mediolateral translation of the tibia (Oni, 1998). In an ACL-deficient knee, this poor translation can lead to tears in the medial meniscus and hypertrophy of the tibial spine and notch, and it increases contact loading of the medial compartment of the knee (Bryant and Cooke, 1988).

When an ACL is ruptured, the axis of rotation shifts more medially and the tibial rotation causes a coupled anterior tibial translation, magnifying the movements of the tibial plateau (Mannel et al., 2004; Amis et al., 2005). The primary insult is damage to the lateral compartment, mainly the posterior aspect, and injury to the medial compartment occurs secondarily. The lateral compartment is most frequently injured mainly because it can sublux more easily.

In the absence of the ACL, muscles around the knee produce compensatory mechanisms, resulting in a net posterior force and flexor and external rotation moment on the tibia in an attempt to maintain normal kinematics (Shiavi et al., 1991). In patients with an ACL-deficient knee, Williams et al. also showed that voluntary muscle control that was diminished in the preoperative evaluation, mostly the quadriceps and lateral head of the gastrocnemius, improved significantly following surgery (Williams et al., 2005).

7.4 Clinical problems associated with the ACL

ACL rupture is relatively common, with an incidence of approximately 0.3 per 1000 per annum in North America (Allum, 2001; Good et al., 1993). This results in substantial costs to health care systems and has promoted widespread performance of ACL reconstruction as a day case in North America (Allum, 2001). The main diagnostic tools are history and clinical examination. Usually, patients present with a history of a twisting or cutting force applied to the lower limb with the knee in variable degrees of flexion, or there may be a history of a direct blow, particularly to the lateral aspect of the leg. A field sport injury is more often a valgus mechanism, while a skin injury implicates more rotational forces (Oni, 1998). A flexion internal-rotation injury appears to be the mechanism that best explains the pattern of bone injuries observed in acute ACL disruption. As the body comes to a sudden halt, anterior translation of the internally rotated tibia of the flexed knee occurs, and as the femur translates posteriorly, it externally rotates and its lateral edge catches the rim of the tibia. A complete rupture of the two bundles will lead to increased anterior tibial translation and internal rotation, resulting in instability and giving way.

During clinical examination, three tests are routinely performed. The anterior drawer test is performed with the patient supine, the hip flexed at 45° and the knee flexed at 90° (Figure 7.5). The foot is then stabilized and the tibia is drawn forward

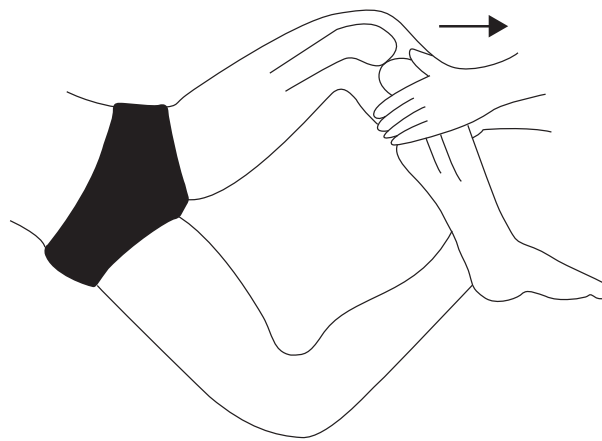

Figure 7.5 The anterior drawer test. It is performed with the patient supine, the hip flexed at 45° and the knee flexed at 90°. The foot is stabilized and the tibia is drawn forward on the femur. In an ACL-deficient knee, there is a posteroanterior translation of the tibia in relation to the femur. This translation is even greater when the knee is flexed to 30° (Lachman test).

on the femur. The patient is still in the supine position for the Lachman test, but the knee is flexed to 30°. One hand is placed over the proximal tibia, displacing it anteriorly, while the other hand stabilizes the femur. In an ACL-deficient knee, the anteroposterior translation at 30° (Lachman test) is much greater than at 90° (anterior drawer test), as demonstrated by Good et al. in a cadaveric model, confirming the advantages of the Lachman over the anterior drawer test (Good et al., 1993). The pivot shift test consists of applying a combined internal rotation and valgus to the tibia in the flexion/extension range and, if positive, demonstrates rotational instability. It is an exaggeration of the normal movement of the lateral tibial plateau due to absence of ACL restraint (Oni, 1998).

Zantop et al. studied the rupture pattern of ACL-injured knees and noted that 56% of the patients had a complete rupture of the two bundles at the same location, the proximal portion being the most frequent (Zantop et al., 2007). For 12%, the PL bundle was still intact, but all the patients had ruptured their AM bundle. According to these authors, when the PL bundle is intact, it should be carefully dissected and preserved to provide landmarks for tunnel placement and to enhance proprioceptive properties and vascularity of the graft in the postoperative period.

The frequency of associated injuries varies depending on the mechanism of injury: medial meniscal tear (25–31%), lateral meniscal tear (2–41%), medial collateral ligament injury (15–50%) and lateral collateral ligament injury (4–8%). Moore observed more tears in the lateral meniscus in acute rupture, the medial meniscus being more associated with chronic pathologies (Moore, 2002). Cartilage tears may also be observed in 23% of acute rupture. The definition and diagnosis of partial ACL tear is not clear. Biomechanically, opinions vary whether a partial tear represents failure in the absence of gross macroscopic disruption due to microscopic rupture of collagen fibrils, or whether the process begins with microfailure and progresses to involve major fibre bundles and finally the entire ligament (Duri and Aichroth, 1995). Clinically, the patient with a partial tear may have pain that will last several days/weeks compared with the complete rupture where the pain is at the moment of the injury followed by symptoms of giving way. Thereafter, the patient with a partial tear may experience locking or pseudolocking symptoms. The diagnosis is arthroscopic because the physical examination is often inconclusive and magnetic resonance imaging (MRI) is unreliable for partial ACL tear. The partial disruption can occur anywhere along the ligament, the superoanterior attachment being the most frequent, followed by the posterolateral band and intrasubstance tears. Given that part of the function is lost, conservative treatment should focus on aggressive rehabilitation to regain a functional and stable knee before more invasive measures are undertaken.

Indications for ACL reconstruction include symptomatic instability with activities of daily living and/or athletic activities, functional impairment in patients unwilling to alter their lifestyle and failure of nonoperative management (Pattee and Friedman, 1992). Relative contraindications include the presence of degenerative joint disease, failure of the patient to comply with a pre- and postoperative rehabilitation programme, a sedentary lifestyle and relatively mild instability.

Multiple studies have evaluated risk factors for ACL injury, hoping to target individuals for appropriate preventive interventions. Shoe type and artificial playing surfaces certainly play a role (Gordon and Steiner, 2004). Female athletes clearly have predisposing factors: their rate of ACL injury is two to four times higher than men's in soccer and basketball. Many factors have been identified to account for this. Anatomically, females have a smaller ACL than men after correction for body weight and a narrower intercondylar notch. There are also gender-specific neuromuscular differences (Petersen and Zantop, 2006), such as a reduced protective role of dynamic knee stabilizers and a diminished ability to resist anterior shear with muscle cocontractions. Even the different stages of the menstrual cycle may increase the risk. Finally, the use of a brace to prevent an ACL injury is very controversial.

7.5 Diagnosis and treatment of ACL ruptures

Plain radiographs provide many indications suggestive of acute ACL rupture: avulsion fracture of the lateral tibial plateau, or Segond fracture, which is in fact an injury to the lateral joint capsule; avulsion of the Gerdy's tubercle; and a lateral notch lesion, which is a compression fracture of the lateral femoral condyle of more than 2 mm seen on lateral radiograph. A tibial rim lesion on the posterolateral lip of the lateral tibial plateau can also be found alone or associated with the lateral notch lesion and is termed a kissing contusion. Joint effusions can also be detected on simple radiographs (Figure 7.6).

MRI has become the radiological modality of choice for the diagnosis of ACL ruptures (Figure 7.7). It offers direct, noninvasive visualization of the ACL and other soft-tissue structures. The reported sensitivity of MRI for acute ACL tears is around 90% (Munshi et al., 2000). Specificity is as high as 95–100% (Moore, 2002). Some authors warn surgeons that MRI inevitably leads to some false positive cases ending in overenthusiastic surgeries (Tsai et al., 2004). Thus, the decision to perform

Figure 7.6 Second fracture on plain radiograph.

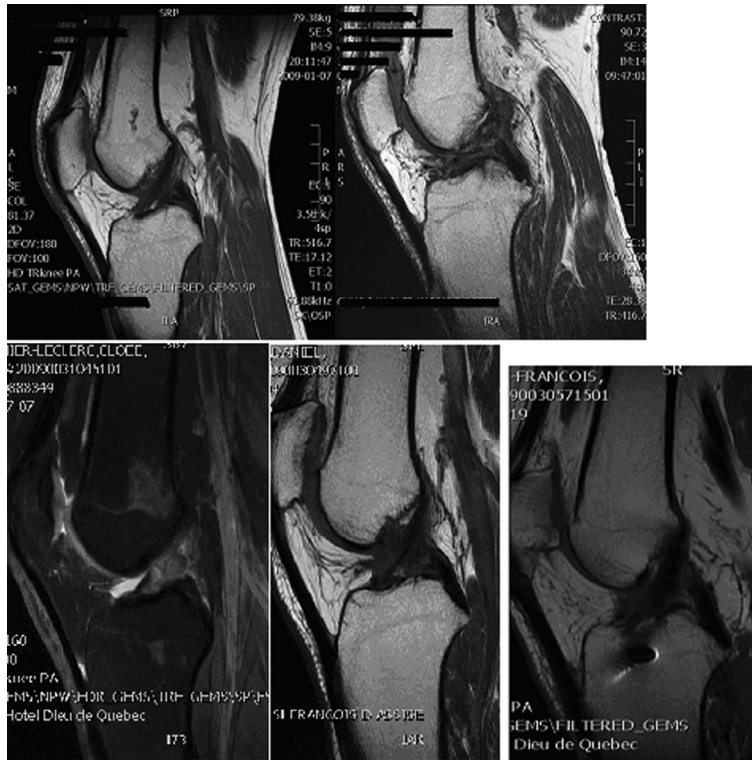

Figure 7.7 T1-weighted MRI of a normal ACL (right) and a ruptured ACL (left). It manifests as the focal interruption of the ligament. At the bottom, the T2-weighted image shows hyperintense edema and fluid replacing the ACL, as is typical of ruptures. The fourth MRI image shows an ACL reconstruction, and the last one is a partial rupture of the ACL.

surgery should be based on clinical findings; imaging should support these findings and help to plan surgery if necessary. MRI is not as accurate in differentiating complete tears from partial tears, nor is it as sensitive in detecting chronic tears (Moore, 2002). Bone contusions are often observed with an ACL rupture on MRI, depending on the severity of the trauma (Oni, 1998). They are most often found in the lateral femoral condyle and in the posterior aspect of the tibial plateau. If failure of the reconstructed ACL is suspected, the diagnosis of rerupture may be difficult with MRI, and clinical findings may be more helpful. Invasive double-contrast arthrography is now reserved for patients with contraindications to MRI and those in whom the diagnosis remains unclear.

In the 1980s and 1990s, management of a ruptured ACL greatly improved, but in the 2000s, much controversy over the proper treatment of this injury remains. The primary goals of ACL reconstruction are to restore knee function, stability and

normal kinematics, to enable return to preinjury level of activity and to prevent the development of early degenerative joint disease (Zelle et al., 2005a). The success rates of the surgery vary between 73% and 95% and return to preinjury activity level varies between 37% and 75%; however, surgeons are unable to fully restore normal kinematics via the actual reconstructive techniques (Ekdahl et al., 2008). Graft failure can be caused by another traumatic event or by nontraumatic factors such as technical errors, fixation failure and failure of biological graft incorporation into the bone tunnels.

At the present time, there is no evidence that reconstruction of the ACL reduces the incidence or progression of degenerative changes, but stabilization should reduce the incidence of meniscal pathology (Allum, 2001) and have a protective effect on the cartilage structure of the knee. The prevalence of late osteoarthritis after ACL surgery has been reported to range from 4% to 50% (Drogset et al., 2006). This cartilage degeneration after ACL chronic injury could be caused by a kinematic gait change that shifts ambulatory loading applied to cartilage. This shift may cause regions of cartilage to become newly loaded, to be subject to altered levels of compression and tension or to become unloaded. Due to the low level of adaptation potential of cartilage, this could lead to cartilage degeneration and osteoarthritis (Chaudhari et al., 2008). The most important factor for developing posttraumatic osteoarthritis after an ACL injury is probably the status of the menisci (Meunier et al., 2007; Patel et al., 2000). Thus, early stabilization of the knee following the injury can reduce the risk of secondary meniscus tear and is advantageous for long-term outcomes.

Initially, primary repair was tried, but in a study by Meunier et al., this was comparable with nonsurgical management in terms of subjective outcomes and osteoarthritis development (Meunier et al., 2007). Moreover, Drogset et al. showed a 10 times higher revision rate with this technique compared to bone–patellar tendon–bone autograft after 16 years (Drogset et al., 2006). Therefore, this procedure is no longer used. There has been interest in thermal shrinkage of capsuloligamentous tissues as treatment for partial ACL tears and elongated ACL grafts, but results are contradictory and this modality is not yet clearly validated among orthopaedic surgeons (Amis and Dawkins, 1991). Thus, the gold standard surgery is reconstruction of the ACL.

7.6 Autograft for ACL reconstruction

In 1917, Groves reported the use of a proximally based strip of iliotibial band that was passed through drill holes in the lateral femoral condyle and proximal tibia to substitute for the torn ACL (Pattee and Friedman, 1992). Thereafter, multiple modifications to his technique developed. Cho was the first to describe a distally based semitendinous tendon transfer in 1975. The graft was passed through drill holes in the tibia and femur and sutured to the iliotibial band. Again, many surgeons modified the procedure. The patellar tendon has also been used in many different ways, starting in the late 1930s with Campbell. Some used the medial border, and others employed the

central portion, with or without leaving a pedicle distally. In 1972, Walsh even reported the use of meniscal tissue in the reconstruction of the ACL.

There are three main steps in ACL reconstructive surgery, with each one being crucial to the success of the procedure. These are graft selection, graft position and graft fixation. First, the choice of graft is a very controversial issue among orthopaedic surgeons. Evidence in favour of one procedure over the other is lacking in the literature. The surgeon's preference is a significant factor; this might be influenced by commercial companies, by their desire to vary their techniques, and by whether or not they have residents assisting or performing the procedure. Strength is not a concern; both the bone–patellar tendon–bone and hamstring autografts have greater ultimate strength to failure and stiffness than the native ACL (Forster and Forster, 2005). There might be a trend toward loss of extension in the bone–patellar tendon–bone group, while hamstring graft patients have been more likely to lose more than 5° of flexion (Kartus et al., 2001; Goldblatt et al., 2005).

The popularity of the bone–patellar tendon–bone graft is related to the initial quality of fixation, high initial strength and stiffness, potential for bone-to-bone healing, better stability over time, improved rate of return to sport, and overall increased activity level. Some reports draw attention to more pitfalls and serious complications using the patellar tendon procedure (Forssblad et al., 2006). The principal drawback concerns donor-site morbidity (Figure 7.8). There is a risk of patellar fracture, potential increase in patellofemoral joint pain and kneeling pain, retained patellar tendon weakness or rupture, patellar tendonitis and flexion contracture by shortening of the patellar tendon. Anterior knee pain mainly depends on a too slow rehabilitation protocol and lack of extension, as shown by Kartus (Kartus et al., 2001).

Recent improvements in fixation techniques and perhaps reduced donor-site morbidity, particularly anterior knee pain, disturbed anterior knee sensibility and kneeling discomfort, have encouraged surgeons to increase the use of the hamstring graft (Goldblatt et al., 2005). Moreover, rapid recovery from surgery and greater ability to participate in accelerated rehabilitation further support this procedure. Complications following

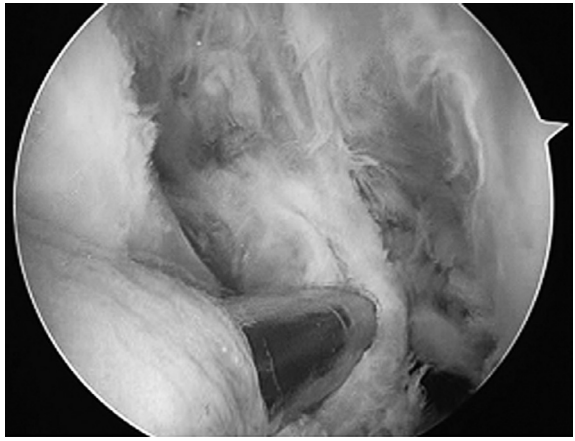

Figure 7.8 Debridement of the ruptured ACL stump before the reconstruction procedure.

hamstring graft harvest include saphenous vein injury and haematomas and the possibility of prematurely avulsed tendon during harvesting. Other disadvantages of this procedure include slower healing of the graft attachment site and potential hamstring muscle weakness (Sajovic et al., 2006). However, Williams et al. did not find any difference in muscle control of semitendinous and gracilis muscle between neuromuscular testing preoperatively and 6 months after ACL reconstruction using hamstring tendons (Williams et al., 2005). They concluded that graft harvest does not alter the innervations of the muscles. Under MRI, the semitendinous and gracilis tendons were in the process of regeneration or had regenerated in most subjects. One technical difficulty when using this graft is that the strands must be equally tensioned. If not, a four-strand graft is equivalent in strength to a two-strand graft, which is much weaker (Goldblatt et al., 2005).

Multiple studies have tried to answer the question as to the preferred autograft on ACL reconstruction. In a cohort study with a 7-year follow-up, Roe et al. showed a greater prevalence of osteoarthritis in the group with bone–patellar tendon–bone autograft reconstruction compared to the hamstring group, but there was no difference in laxity and subjective outcomes (Roe et al., 2005). In a prospective randomized comparison between the hamstring and patellar autografts, Sajovic et al. showed that both had good subjective outcomes and objective stability but the patellar tendon group had a higher prevalence of osteoarthritis at 5 years (Sajovic et al., 2006). In another randomized clinical trial comparing the two grafts, Aglieti et al. concluded that both grafts were equivalent (Aglietti et al., 2004). In a meta-analysis, Goldblatt et al. showed that the incidence of instability is not significantly different between bone–patellar tendon–bone and three- or four-strand hamstring autograft. However, there was an increased incidence of patients experiencing intermediate-range laxity in the group with a hamstring autograft, although it was not totally unstable (Goldblatt et al., 2005). Forster's systematic review also showed no difference in Lachman testing or the chance of returning to the same level of sport and clinical knee scores. Overall, when it comes to clinical outcomes, there is no consensus over graft choice, and no choice is ideal for all patients. The decision should be based on each patient's functional demands and surgeon preferences and opinions. Forssblad et al. noted a dramatic shift from patellar tendon to hamstring tendon in ACL reconstructions performed in Sweden in recent years (Forssblad et al., 2006). They evaluated the cost of those surgeries and concluded that the cost of the hamstring procedure was €329 more than the patellar tendon procedure. They did not, however, include costs for potential revision procedures and rehabilitation.

Other autograft options include the quadriceps tendon and the contralateral patellar tendon. DeAngelis had successful results with the use of a central quadriceps tendon free graft after 5 years, with very low donor-site morbidity (DeAngelis et al., 2008). Others described a double-bundle technique using a quadriceps tendon graft with a patellar bone block in one single tibial tunnel (Sonnery-Cottet and Chambat, 2006). Shelbourne et al. use the contralateral patellar tendon as graft (Shelbourne et al., 2007), justifying this with the fact that rehabilitation is contradictory when using the ipsilateral patellar tendon. They state that the donor site needs to be stimulated immediately after surgery to grow in size and in strength, which is best done with aggressive quadriceps muscle strengthening, which in turn causes swelling and

decreases range of motion. This is not encouraging for the ACL graft, where a full range of motion is needed. In a previous study by the same author, the group with contralateral autograft had a return to full competitive sport 1.4 months sooner than patients with ipsilateral graft (Jari and Shelbourne, 2002). The authors think this procedure could be helpful for patients with a small patellar tendon, poor quadriceps strength in the involved leg or trouble regaining full range of motion and reducing swelling before the surgery.

The traditional single-bundle reconstruction is designed to replicate the anatomy of the AM bundle (Figure 7.9). The debate regarding the reconstruction of the two different bundles comes principally from the fact that the PL bundle is an important structure for stabilizing the knee, especially in full extension, as explained previously. Yagi et al. clearly demonstrated a biomechanical advantage of the two-bundle construct, especially during rotatory loads (Yagi et al., 2002). Since Cho et al. found that diameter of collagen fibrils in the double-bundle group was larger than in the single-bundle group, there has been speculation that the former might have a greater tensile strength, but this has yet to be confirmed (Cho et al., 2004). This technique would thus reproduce the anatomy more closely, as stated by Petersen and Zantop (2006).

Jarvela in a prospective randomized trial comparing single- versus double-bundle reconstructive surgery of the ACL, showed that rotational stability was significantly better in the latter group at an average follow-up of 14 months (Jarvela, 2007). However, the anterior stability was similar and the knee scores were equal. To explain why four patients in the single-bundle group experienced failure against none in the double-bundle group, they stated that the better rotational stability in the double-bundle group could protect against the occurrence of subsequent knee traumas. They concluded that this might become the procedure of choice for patients in high-demand pivoting sports.

Those against this quite recent procedure might argue that this is a demanding surgery. Because there are more tunnels, more grafts and more fixations, more opportunities exist for technical difficulties or failures than in the traditional single-bundle

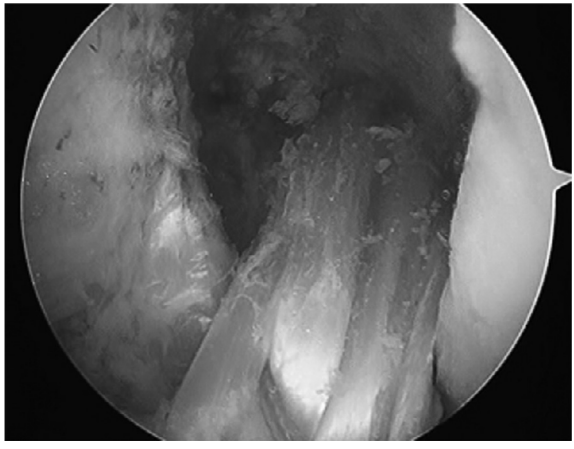

Figure 7.9 Single-bundle hamstring autograft ACL reconstruction.

technique (Jarvela, 2007). As an alternative to the double-bundle four-tunnels procedure, Frank et al. described a technique with hamstring tendon, during which only one tunnel is drilled in the lateral femoral condyle to minimize the theoretical risk of devascularizing the condyle and two tibial tunnels (Figure 7.10) (Frank et al., 2007).

The graft position also includes drilling of tunnels and tensioning (Figure 7.11). The placement of tunnels is one, if not the main, cause of failed ACL reconstructive surgery. In the literature, it is suggested that more physiological loading of the graft is achieved when graft placement is closer to the anatomical location. The femoral tunnel placement is critical because small variations have a large impact on laxity and motion (Figure 7.11) (Ekdahl et al., 2008). The femoral tunnel is essential to maintaining tension in the ligament. It is located at 1 o'clock or 11 o'clock in the frontal plane, depending on whether it is a left or a right knee operation. A graft placed too

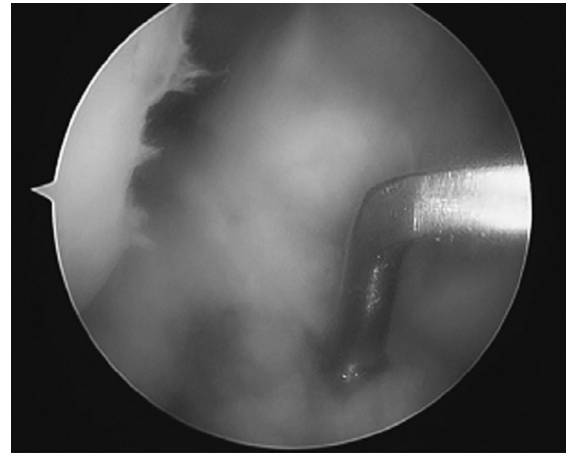

Figure 7.10 Positioning of the guide for tibial tunnel placement.

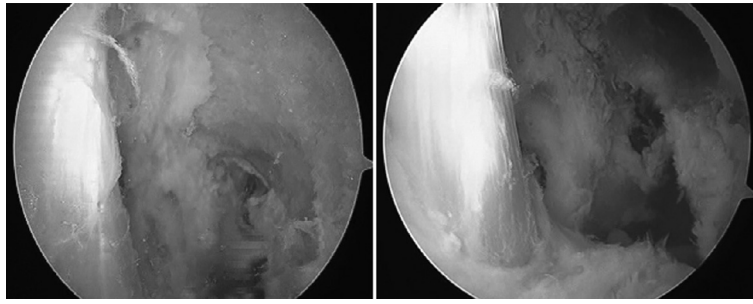

Figure 7.11 Drilling of the femoral tunnel after the completion of the notchplasty. After drilling, note the position of the femoral tunnel in relation to the PCL and the intercondylar fossa.

centrally (12 o'clock) may be unable to resist rotatory loads due to the lack of a moment of arm. The anteroposterior and proximodistal positioning of the tunnel greatly affect fibre length, as shown by Grood et al. (Hefzy and Grood, 1986). Too anterior tunnel placement elongates the graft and results in instability, and because the graft stretches as the knee flexes, a flexion deficit may occur. The position of the tibial tunnel is also critical (Figure 7.12). If too anterior, the graft will impinge on the anterior rim of the intercondylar fossa. Impingement is defined as interference with the frictionless motion of graft in and about the exit points of graft from the bony tunnels, sidewall and roof of the intercondylar notch (Moore, 2002). It is caused by abnormal tunnel placement and/or horizontal graft position. It is greatest at the terminal 10–15° of extension and causes decreased range of motion, mainly lack of extension, pain and instability if the impingement has caused the graft to stretch or fail. To prevent this, many surgeons prefer to place the tunnel in the posterior part of the tibial insertion. Notchplasty to avoid impingement should be minimal because excessive removal of the bone of the lateral wall, especially in the posterior aspect, lateralizes the femoral insertion site and could increase the external rotation of the tibia (Figure 7.13). Some of this rotatory moment is exerted when the graft is tightened (Figures 7.14 and 7.15) (Zantop et al., 2007).

The ideal position for tensioning the graft is probably in 30° of flexion. In this position, stability is re-established even at low tension levels, but there is a danger of reducing the normal range of motion and putting the tibia in posterior subluxation if tension is increased. Excessively high tension may also reduce the biomechanical properties of the graft. Insufficient tensioning of the graft can lead to stress shielding by the other structures of the knee, however, resulting in a graft with a small cross-sectional area secondary to a lack of stimulation. The optimal tension to apply when fixing the implant is still unknown (Grood et al., 1992).

The rehabilitation programme is an important part of ACL reconstructive surgery and has mostly taken a standard form since Shelbourne's publication (Shelbourne and Nitz, 1990). The graft should be protected by closed chain exercises in the early post-operative period without any period of immobilization or restricted weight bearing.

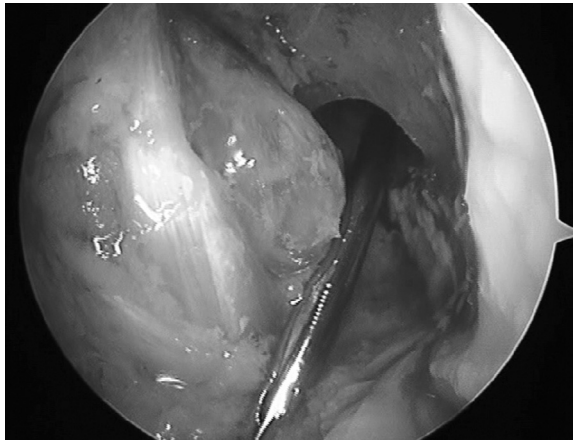

Figure 7.12 A guidewire is inserted from the tibial tunnel into the femoral tunnel to eventually pull the graft into position. This is the orientation of the future graft.

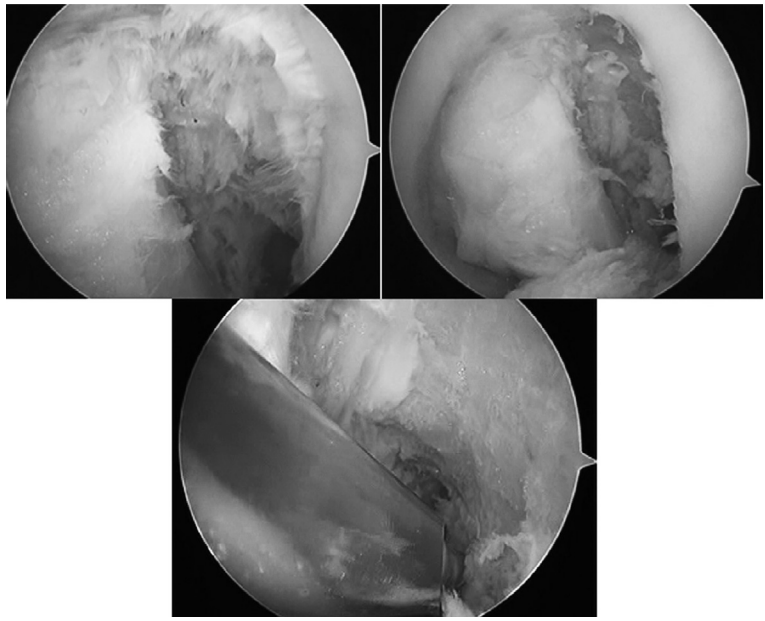

Figure 7.13 Notchplasty during ACL reconstruction. The first image is before the notchplasty. The second shows that a part of the procedure has been performed, and finally, the notchplasty is completed.

Figure 7.14 The graft is pulled in the tunnels.

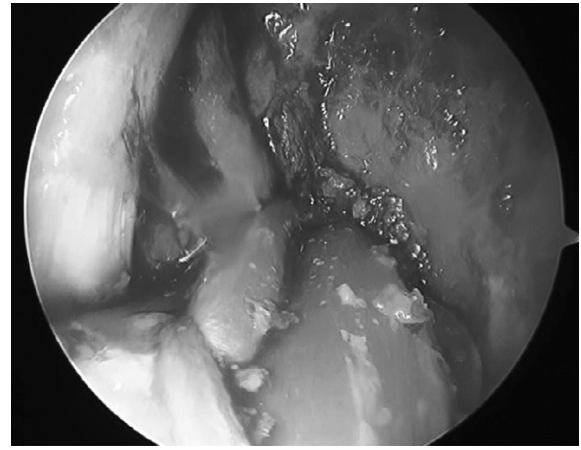

The use of the continuous passive motion machine has now been almost completely abandoned. Marumo et al. suggest a low-aggression rehabilitation programme to allow the graft to undergo the process of ligamentization. Training in proprioception has been shown to be a very important aspect of the rehabilitation process (Marumo et al., 2005). The third aspect, graft fixation, is discussed in Section 7.8.

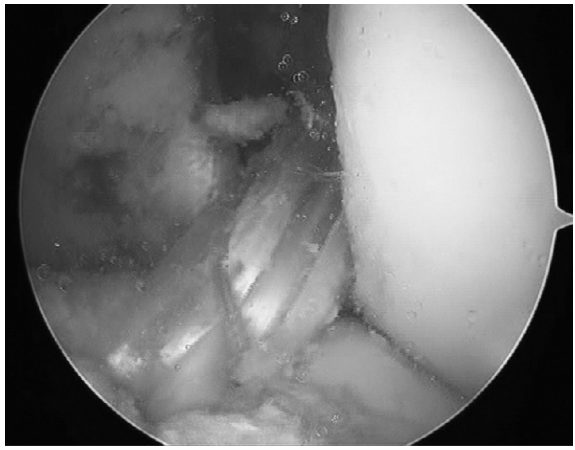

Figure 7.15 After adequate positioning of the leg and tensioning of the graft, it is fixed in place and here is the final position of the graft at the end of the surgery.

7.7 Allograft for ACL reconstruction

The use of allograft for ACL reconstruction for both primary and revision surgeries began in the 1980s and has gained popularity over the past 10–15 years (Kuhn and Ross, 2007). The Achilles tendon, bone–patellar tendon–bone, anterior and posterior tibialis, peroneus, fascialata and hamstrings are the main soft tissues used as allografts. Flexor hallucis longus and toe extensors have also been used. The use of an allograft initially reduces hospital costs via shorter operation, anaesthesia and recovery room times, with improved immediate postoperative pain and function, even though the graft itself can be costly (Prodromos et al., 2007).

The maximal tensile strength of an allograft is less than that of autograft but stronger than the native ACL. Long-term stability may be less than that of an autograft (Prodromos et al., 2007). There are some contradictory studies regarding whether an allograft can be incorporated as fast as an autograft. According to Lee, revascularization and recollagenation are slower than they are in autografts. His case report showed a freeze-dried Achilles tendon incorporated into the bone through Sharpey's fibres attachment. By 1 year, all four usual zones were present and maximal stability was reached by 18 months (Lee et al., 2004).

Multiple studies have tried to compare the clinical results of allograft and autograft. Krych et al. conducted a meta-analysis comparing outcomes between bone–patellar tendon–bone autografts and allografts (Krych et al., 2008). There was a clear advantage on the autograft side regarding the rupture rate and hop test parameters. However, when the sterilizing process was excluded, results were similar. Borchers et al. even showed with univariate logistic regression models that allograft use is a risk factor for ACL graft failure, and this risk is even higher with a higher level of activity (Borchers et al., 2009). Another study did not show any difference in perioperative morbidity between autogenous and allogenous bone–patellar tendon–bone grafts (Saddemi et al., 1993). Moreover, Rihn et al. found similar subjective and objective clinical

outcomes between bone–patellar tendon–bone allografts and autografts (Rihn et al., 2006). According to Prodromos et al., allografts had lower normal stability rates than autografts, either with bone–patellar tendon–bone or with hamstring/soft-tissue grafts (Prodromos et al., 2007). Graft failure was two to three times higher, even when the deleterious effects of radiation were excluded. They list possible causes of increased laxity in allografts: immunological response, lack of cryopreservation, increased donor age, increased graft shelf time, subclinical infection, radiation sterilization and ice crystal damage produced by the freezing process.

Reports of allograft infections include those involving the transmission of *Clostridium* species, group A streptococcus, hepatitis C virus and HIV. Gamma irradiation has bactericidal and virucidal properties but alters biomechanical properties, mainly the ultimate failure load and stiffness, of a soft-tissue allograft in a dose-dependent manner (Rihn et al., 2006; Salehpour et al., 1995). Doses as low as 2.5 Mrad have been shown to reduce these properties. Sun et al. had a failure rate of 34.4% at an average 31 months follow-up in ACL-reconstructed knees with 2.5 Mrad gamma-irradiated bone–patellar tendon–bone allograft, compared with 6.1% for autograft and 8.8% for nonirradiated allograft. They also showed that only 31.3% of the irradiated-allograft group had a side-to-side difference of less than 3 mm according to the KT-2000 compared with 87.8% and 85.3% in the autograft and nonirradiated allograft group, respectively (Sun et al., 2009). Thus, radiation doses should be kept between 1.5 and 2.5 Mrad, but even if this dose is effective in reducing bacterial contamination, it is not effective against viral agents (Ekdahl et al., 2008). In fact, more than 2.5 Mrad is required to inactivate HIV (Rihn et al., 2006). The risk of HIV transmission from an allograft has been estimated to be approximately 1 in 1.6 million (Mroz et al., 2008). The other method of sterilization, ethylene oxide, had unacceptably high rates of chronic synovitis and dissolution of the graft. More recently, a novel electron beam sterilization procedure was studied and could become an alternative to gamma irradiation because of its minimal effect on mechanical properties (Fideler et al., 1995).

The potential advantages of a bone–patellar tendon–bone allograft are a lessened chance of harvest-related patellofemoral symptoms, availability of larger grafts, and superior cosmetic results (Indelicato and Talley, 1995). A bone–patellar tendon–bone allograft is particularly useful in revision surgery when tunnels are widened. Another indication is the need for multiligamentous reconstructions (Kuhn and Ross, 2007). Potential drawbacks include potential immune reactions, disease transmission, and altered mechanical properties caused by sterilization and delayed graft incorporation (Krych et al., 2008), which implies a less aggressive rehabilitation protocol. In fact, patients usually feel good clinically very early and must be very careful not to compromise the ligamentization process. An allograft might not be a good option in skeletally immature patients, patients with prior knee infection and immunocompromised patients.

7.8 Graft healing in ACL reconstructive surgery

The type of graft, possible graft motion and fixation methods have been shown to directly affect the time-course and quality of graft-tunnel healing. Those known to have a slower healing process are the soft-tissue autograft and allograft (Indelicato and

Talley, 1995). The effects of tensioning, graft-tunnel diameter disparity, and graft length within the bone tunnel are other aspects that remain unclear (Ekdahl et al., 2008).

As early as 4 days after implantation, an inflammatory response takes place at the bone–tendon interface (Kousa et al., 2003). After 6 weeks, the graft is completely covered by a vascular synovial envelope, and at 20 weeks, the intrinsic vasculature of the graft is completed. This suggests that the phenomenon of ligamentization, as described by Amiel, occurs in the successfully reconstructed ACL within a year after surgery (Amiel et al., 1986). Ligamentization is initiated by the necrosis of fibroblasts secondary to ischemia in the ligament removed from the donor site. Cell necrosis induces local inflammation, followed by repopulation by infiltrating fibroblasts, which orient themselves along the collagen fibre 'scaffold' and secrete collagen and other matrix proteins. With the inflammatory process and fibroblast repopulation, new blood vessels appear within the ligament. These sequential processes ultimately result in the gradual remodelling of the collagen fibres characteristic of an ACL (Stone et al., 2007). This process can be simplified as the transition of the biochemical and histological parameters of the graft from tendinous to ligamentous appearance, even though the two tissues are biochemically distinct in the new intra-articular environment specific to the ACL. This corresponds to the work of Marumo et al. who examined tissue samples of patients following ACL autograft reconstruction and concluded that the biochemical characteristics of the graft resembled those of the native ACL (Marumo et al., 2005). Unfortunately, during the healing process, the graft gradually weakens and its structural properties decrease; as yet, no study has shown that it eventually returns to its original strength (Ekdahl et al., 2008). Thus, a normal ligament never forms after reconstruction.

According to several animal models, there is a slower incorporation graft rate into the bone tunnel with soft-tissue grafts, as compared to bone plug grafts such as bone–patellar tendon–bone (Figure 7.16). Complete incorporation of the bone plugs can be seen as early as 6 weeks. The insertion site consists of four zones: tendon, fibrocartilage, mineralized fibrocartilage and bone, whose pattern is similar that found at the original direct insertion site of an ACL (Ekdahl et al., 2008). Bone plugs of bone–patellar tendon–bone graft become anchored to bone walls by appositional bone formation, and grafted bone becomes necrotic as new bone forms. By 16–20 weeks, complete bony incorporation of the graft into the tunnels is present. With soft-tissue grafts, fixation occurs predominantly with fibrous tissue, with collagen fibres interspersed along the load axis (Zelle et al., 2005b). By 26 weeks, the continuity of the collagen fibres between the graft and tunnel is almost completely mature, and there

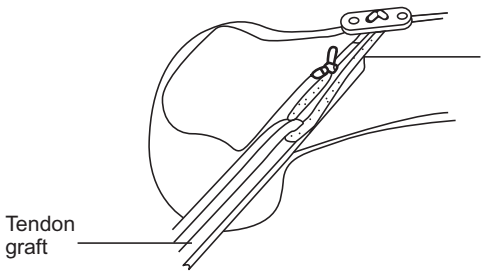

Figure 7.16 Relationship of the graft and its fixation device within the femoral tunnel; the relatively small area of the bone–tendon interface is worth noting.

is significant remodelling of the trabecular bone surrounding the tendon. This process is consistent with the morphology of Sharpey's fibre development. There is concern as to whether the tendon–bone interface is strong enough to support an aggressive early postoperative rehabilitation programme. The length of the graft in the intra-osseous tunnel did not affect graft properties in animal models, and a discrepancy of 2 mm or less in the diameter of the tunnel to the graft does not appear to affect healing (Yamazaki et al., 2006; Yamazaki et al., 2002).

Graft fixation is crucial and is the weakest link in the initial 6–12-week period, during which healing of the graft to the bone occurs (West and Harner, 2005). Many types of device exist and there is still controversy in the literature as to which is preferable for biological incorporation. Fixation outside the tunnel, known as suspensory methods, and aperture methods, which use an interference screw or cramp close to the origin and insertion of the implant, have been described. When an interference screw is used, a direct chondral insertion site appears, and when the graft is fixed with a cramp, a fibrous insertion pattern is present. The former is thus stiffer, albeit vulnerable, during the early phase of healing (Petersen and Laprell, 2000). There is concern regarding tunnel expansion with suspensory fixation, but the radiological appearance does not yet have an impact on clinical results. These tunnel expansions are most likely caused by micromotion and synovial fluid extravasation in the tunnels (Jansson et al., 1999). An early aggressive rehabilitation programme can certainly play a role in graft motion within tunnels and may delay graft healing, which is in fact inversely proportional to graft-tunnel motion (Rodeo et al., 1999).

Finally, for improved graft healing, gene therapy to achieve a continuous release of growth factors, mesenchymal stem cells and periosteum as a biological scaffold is currently under investigation. In fact, numerous studies have demonstrated the ability of periosteum to induce new chondroid and bone formation (Zelle et al., 2005b). Some studies have even shown good results with autologous hamstring tendon grafts wrapped in periosteum with minimal bone tunnel widening and good knee stability (Adachi et al., 2004; Javernick et al., 2006).

In brief, the most common causes for failure of ACL reconstructive surgery are errors in diagnosis and surgical technique, such as graft impingement, improper tunnel placement, improper graft tensioning, inadequate fixation of the graft and missed concomitant pathology at the time of surgery. A traumatic event can also occur and, in such cases, revision ACL surgery is often indicated. The key to success is to clearly identify the reason for failure, because outcomes are not as good as in primary reconstruction, ranging between 50% and 80% (Gordon and Steiner, 2004).

7.9 The use of synthetic materials and prostheses in ACL reconstructive surgery

For many clinicians and scientists, tissue engineering was to become the solution for the problems encountered with ACL reconstruction. This multidisciplinary field incorporates knowledge from mechanical physics, biomaterials, biology and chemistry to try

to replicate many types of different tissues. The main goal is simple: to create a specific tissue for a specific function, with properties that reflect as closely as possible those of the injured original. In the field of orthopaedic surgery and mainly in ACL reconstruction, the idea of trying to develop a synthetic ligament came naturally. Some surgeons wanted an alternative to overcome the problems encountered with the options available at this time. Although autografting has good outcomes, it is accompanied by complications related to donor sites, and allografts have problems with immunogenic response, infection and the risk of disease transmission.

Synthetic materials were developed in the early 1970s. The first trial was with prosthesis, which means that these grafts were meant to function as permanent ones, completely replacing the native ACL (Table 7.1). The second type of implant is the augmentation device. It is designed to reinforce the autogenous tissue, not to replace it. It gives initial strength to the graft during its more vulnerable period. The last type of device is the scaffold. It serves as a frame so that cell in-growth can develop and eventually replace completely the synthetic material that will progressively be reabsorbed. Each of the three designs is discussed in detail.

The pioneers of ACL prosthetic replacement devices are Corner in 1914, who used a silver wire (Corner, 1914), and Alwyn-Smith, who experimented with silk sutures as replacements (Alwyn-Smith, 1918). Since then, many different models of prosthesis have been proposed and developed, beginning in the 1970s with the Polyflex® (Richards Medical Co, Memphis, TN) and Proplast® (Vitek, Inc, Houston, TX). The tremendous number of new designs demonstrates that there was no consensus on many of the underlying concepts. For a ligament to be biofunctional and to withstand the high mechanical demands of a knee joint, it needs to enjoy both good biocompatibility and good bioendurance. Scientists could not agree on the best type of textile structure: twisted, braided, woven, knitted, or a combination of those. The best type of material is also debated: polyester, high-performance polyethylene, carbon,

Table 7.1 General characteristics of ACL prosthesis devices

Commercial name	Manufacturer	Class	Type of fibres
Stryker®	Stryker, Michigan, USA	Woven/ knitted	PET
ABC Surgicraft®	Surgicraft, Redditch, UK	Braided	PET/PET-C
Gore-Tex®	WL Gore and Associates, Arizona, USA	Braided	PTFE
Leeds-Keio®	Neoligament Ltd, UK	Woven	PET
LARS®	Surgical Instruments and Devices, Arc-sur-Tille, France	Loose/ knitted	PET
Kennedy-LAD®	3 M, Minnesota, USA	Braided	Polypropylene

PET: polyethylene terephthalate; C: carbon; PTFE: polytetrafluoroethylene.

polytetrafluoroethylene (PTFE) or polypropylene. Carbon fibre was abandoned early because of convincing studies of its ineffectiveness and the production and migration of carbon wear particles in the joint space creating a 'black knee'. Three commercialized ligaments are presented to illustrate this problem.

7.9.1 The Stryker® ligament (Stryker, Kalamazoo, MI)

The Stryker® is a multilayer polyethylene terephthalate (PET)-polyester (Dacron®) ligament (Figure 7.17). Ten longitudinal yarns and one multifilament transversal yarn are woven together in a simple frame. An external envelope of tubular-knitted velour with a porous external side to help tissue incorporation and a central radio-opaque polypropylene monofilament for mechanical support were added. This ligament was designed to be used with the 'over-the-top' technique. There are currently two main techniques for implanting the new ligament: the over-the-top technique, during which the ligament is passed in the tibial tunnel and behind the femoral condyle, and the 'double-tunnel' technique, during which the graft goes through a bone tunnel in the tibia and in the femur.

Anderson et al. published a prospective study in which 57 patients had ACL reconstruction with a Dacron® ligament and were followed for an average of 34 months (Andersen et al., 1992). Overall, 71% of the patients were satisfied, but they recorded 10 ruptures in a range from 3 to 21 months. One patient had a chronic synovitis and one developed a deep infection (Andersen et al., 1992). Other studies showed similar results, with only 55% good-to-excellent results at 5 years (Gillquist and Odensten, 1993), 20% failure at 2 years and 37.5% at 5 years (Wilk and Richmond, 1993). The distribution of this implant stopped in 1994 in the United States due to a lack of demand and the frequency of adverse device-related events.

Twenty-three explanted ligaments were extensively studied and authors concluded that the prosthesis was encapsulated by thick granulomatous and collagenous tissue (Guidoin, 1994). The collagen infiltration was almost limited to the external shell and between the envelope and the core. Often the external shell was no longer even present. A moderate foreign body inflammatory reaction was observed, with macrophages and foreign body giant cells (Poddevin et al., 1995a).

The structure was frayed over much of its length, and small flattened wear zones were seen around the condyle area, but the main zones of breakage were at the exit

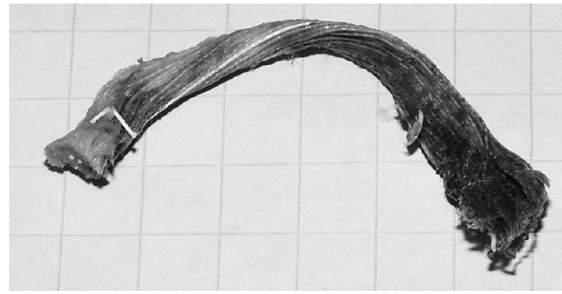

Figure 7.17 The Stryker® ligament is made of multilayers of polyethylene terephthalate (PET) and polyester (Dacron®).

from the tibial tunnel and at the entry to the intra-articular zone of the femoral condyle. They were examined under scanning electron microscopy (SEM). The external knitted shell showed compression and crushing injury near the femoral condyle, while the inner braided part showed more abrasion damage. There were also signs of axial fibres splitting in the internal zone. This difference in wear could be due to the difference in textile structure. For all these reasons, this device is no longer a good option.

7.9.2 The ABC Surgicraft® ligament (Surgicraft, Redditch, UK)

The ABC Surgicraft® ligament is made from untwisted yarns of a mixture of carbon and PET fibres that are multiply braided. The two extremities are reinforced by an external winding of polyester. The central part is intentionally loose and contains 24 parallel and independent braids. Each braid is made of three multifilament yarns of polyester and a fourth yarn of carbon in the middle to give rise to a composite structure. In some models, the fourth yarn is also made of polyester. Both surgical techniques can be used with this implant. Initial studies made by the group that designed the implant showed promising results (Tarachand, 1990; O'Brien et al., 1991), but Mody et al., with an average follow-up of 34 months, experienced four failures requiring early revision (12%) and noted a progressive loss of stability, with only 41% good results (Figure 7.18) (Mody et al., 1993).

To explain this poor performance, authors examined more closely many explanted prostheses. They were all PET/PET implants used with the two-bone tunnels technique. They found an important encapsulation of the prosthesis, and in half of the studied devices, collagen was seen in the core between yarns and individual fibres. There was a moderate inflammatory reaction similar to the Stryker® ligament. Under SEM, compressed and flattened fibres near the eyelet, which served as an attachment system, were visualized. Abrasion damage between the bone–yarn and yarn–yarn

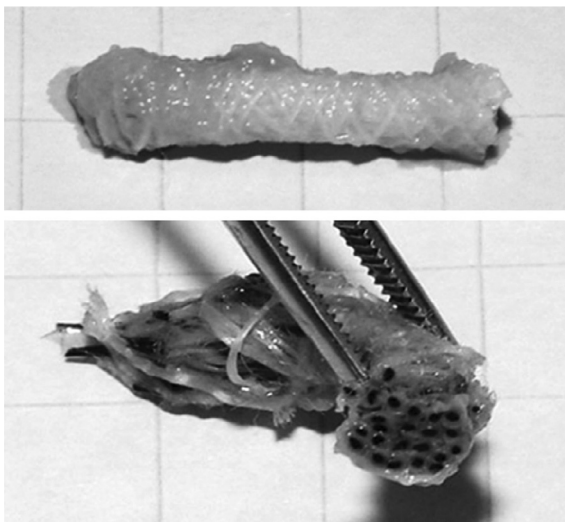

Figure 7.18 The ABC® Surgicraft ligament is made of yarns of a mixture of carbon and PET fibres that are multiply braided. The central part is intentionally loose and contains 24 parallel and independent braids. Each braid is made of three multifilament yarns of polyester and a fourth yarn of carbon in the middle to give rise to a composite structure.

contacts were confirmed by fibres peeling and splitting on the surface of the implants. The main break zone was located near the exit of the tibial tunnel and showed abundant axial splitting and bushy ends. These bad results made this implant unsuitable for clinical use.

7.9.3 The Gore-Tex® ligament (W.L. Gore & Associates, Flagstaff, AZ)

The Gore-Tex® ligament is made of continuous multifilament yarns of tightly braided microporous PTFE (Figure 7.19). Its ultimate strength is more than twice the human ACL tensile strength and it is also very stiff. For these reasons, it initially seemed promising. Between 1982 and 1990, 18,000 Gore-Tex implants were used worldwide with the over-the-top technique (Friedman, 1991; McCarthy et al., 1993). Effusion and sterile synovitis were frequent, as was rupture, which happened more often on the femoral side (Steadmann et al., 1995; Indelicato et al., 1989; Gries and Steadman, 1996). Infection was reported in 2–3% of cases. Loosening of initially well-tensioned grafts was observed quite often and explained by osteolysis enlarging osseous tunnels, which is thought to be due to a localized inflammatory reaction created by microbreakage and, secondarily, particle debris (Rubenstein et al., 1998). Moreover, Guidoin et al. noted poor healing of the ligament, probably secondary to the polymer itself (Guidoin et al., 2000). Although it presented good initial stability, deterioration over time led to the abandonment of this device. It was taken off the market by its manufacturer in June 1993, shortly after Sledge presented bad results (44% failure rate at 5 years) (Sledge et al., 1992).

7.9.4 The Leeds-Keio® ligament (Neoligament Ltd, UK)

Over 50,000 Leeds-Keio® (LK) grafts were implanted worldwide, mainly in the 1980s and early 1990s (Murray and Macnicol, 2004). The LK ligament is made of woven PET. It was thought at first that this device promoted natural in-growth of collagen fibres, and it was classified as a scaffold (Fujikawa et al., 1984). Later, some studies

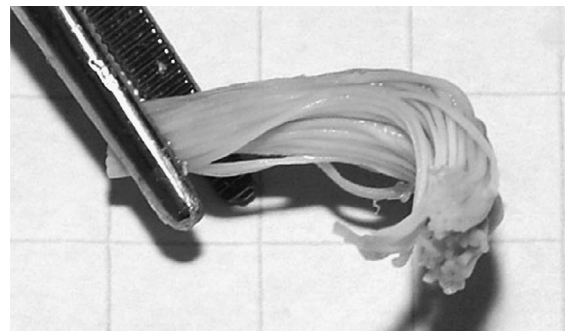

Figure 7.19 The Gore-Tex® ligament is made of continuous multifilament yarns of tightly braided microporous polytetrafluoroethylene (PTFE).

suggested that it acted more as a pure prosthesis. It contains short tubular sections at each end that incorporate a bone plug used for fixation (Seedhom, 1988).

Clinical studies on the LK are contradictory. Jones et al. reviewed 50 patients who had ACL reconstruction with the LK ligament with a mean follow-up of almost 12 years (Jones et al., 2007). The majority of them also had an extra-articular ligament placed so that it ran parallel to the intra-articular component on the lateral aspect of the knee. Patient satisfaction and level of activity were notably high (90%) and only 12% were confirmed to have ruptured their grafts, leading to the conclusion of good long-term functional stability. Ghalayini et al. conducted a prospective randomized controlled trial comparing the bone–patellar tendon–bone autograft and the LK graft and showed clinical equivalence at 5 years between the two groups (26 and 24 patients) for the Lysholm score and the one-hop test but not for the Tegner activity score (Ghalayini et al., 2010).

In Rading's study, 3 of the 24 patients were reoperated on because of a rupture of the graft and another 6 developed important subjective instability during the first 2 years following surgery (Rading and Peterson, 1995). The mean difference in anterior tibial translation measured was 3.7 mm compared to their normal contralateral knee. All these elements determined the ineffectiveness of this synthetic ligament. In the same way, Murray et al. reviewed 18 patients with a mean follow-up of 13.3 years and noted that 56% of them had increased laxity and 28% were known to have ruptured their grafts (Murray and Macnicol, 2004). By way of comparison, Scavenius et al. reported a 50.7% rate of laxity after 7 years of conservative therapy in ACL-deficient knees. This implant is no longer seen as a viable option for ACL reconstruction (Scavenius et al., 1999).

7.9.5 Ligament advanced reinforcement system (Surgical Instruments and Devices, Arc-sur-Tille, France)

The Ligament Advanced Reinforcement System (LARS®) device is made of PET with an intraosseous segment composed of longitudinal fibres bound together by a transverse knitted structure, while the intra-articular segment is composed of parallel longitudinal fibres twisted at 90°. The special feature of this implant is that this latter portion is made of fibres that are oriented clockwise or counterclockwise, depending on whether it is a right or left knee; this mimics the natural ligament structure and reduces shearing forces. According to Dericks, this configuration is more resistant to torsional fatigue and to wear and tear (Dericks, 1995). The porosity of the material also allows tissue in-growth.

Although Talbot et al. did not show convincing results using the LARS® for ligament reconstruction following knee dislocation (Talbot et al., 2004), other studies are encouraging (Lavoie et al., 2000a; Nau et al., 2002). In the one conducted by Lavoie et al., only 1 patient out of 47 had fixation failure secondary to an early return to sports and none presented symptoms of synovitis. Even if no obvious rupture of the implant was documented, patients did not return to their preinjury level of activity and anteroposterior laxity was still present after surgery. Nau et al. conducted

a prospective randomized trial comparing the LARS® ligament to the gold standard bone–patellar tendon–bone autograft with the same postoperative rehabilitation and a follow-up of 2 years. Interestingly, there was no case of reactive synovitis (Nau et al., 2002). The failure rate was identical, with one patient in each group requiring revision for that reason. Although laxity was greater in the LARS® group throughout the follow-up period, clinical scores were better in this group early in the study but were similar after 2 years. In fact, the LARS® group returned to sports earlier, which could be explained by the period of ligamentization required in the autograft before patients could return to full recreational activities. Purchase conducted a study with a longer follow-up period (14.1 years) with an implant made of similar material to the LARS® (Purchase et al., 2007). It showed encouraging results, without any effusion observed and, at 9.5 years, only one graft failure out of nine patients. Huang et al. also showed encouraging results in 81 cases of various knee ligament reconstructions at an average of 29 months follow-up (Huanag et al., 2010). A systematic review in 2010 concluded complication rates were comparable to those of traditional surgical techniques and patient satisfaction scores were high, but it was equivocal with regard to graft stability and long-term functional outcomes of the LARS® (Huanag et al., 2010; Lavoie et al., 2000b). Hamido augmented the short- and small-sized autograft hamstring graft with the LARS® and had good results at 5 years (Hamido et al., 2011). These interesting results, combined with the low level of complications of this implant, might be the best actual option in the field of prosthetic ligament devices, although more has to be done to evaluate long-term outcomes and failure rates and to document tolerance of the knee to the LARS® ligament (Figure 7.20).

7.10 Complications with synthetic ligaments

Savares et al. followed over 160 synthetic ligaments implanted between 1983 and 1990 for 80 months (Savarese et al., 1993). They concluded that this could not be considered a good option because most surgeons are apprehensive about the extremely high number of tears. Why are ruptures so frequent and the half-life of these prostheses so inferior to those of natural ligament? Many factors have to be taken into consideration, including patient age and activity level, and surgical technique. For example, poor tunnel positioning or inadequate notchplasty can lead to unequal stress distribution within the graft and abrasion on bony edges (Gries and Steadman, 1996).

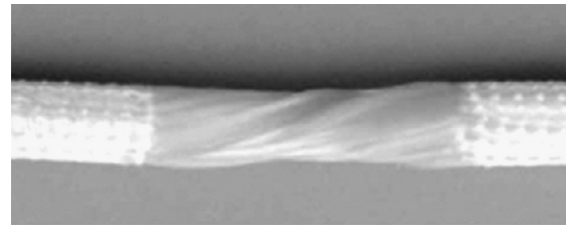

Figure 7.20 Left LARS® ligament.

Synthetic ACL prostheses were originally promoted because some thought they could enable faster rehabilitation than the autologous graft could. It is now well known that autografts are weak at implantation and go through a period of morphological changes in the first 12 weeks that make them more vulnerable, in contrast to the synthetic ligament that is initially strong. Esposito invalidated this theory in a prospective comparative study between the ABC Surgicraft® and the patellar tendon autograft. After 6 months of rehabilitation, no functional differences between the two groups could be identified (Esposito et al., 1997).

The physiological bone–ligament junction is a very complex structure composed of four zones: ligament, fibrocartilage, calcified fibrocartilage and bone (Spalazzi et al., 2008a). This transition zone is important because it allows the distribution of mechanical stresses to a wide area. Using a sheep model, Schiavone et al. demonstrated that synthetic prosthesis and augmentation devices are still separated from bone and tendon by fibrous tissue that does not have the physiological characteristics of an insertion junction after 9 months (Schiavone Panni et al., 1993). This exposes the ligament to abnormal stresses secondary to a nonperfect distribution. Comparatively, the patellar tendon autograft has a physiological junction with the four distinct layers formed by 6 months after surgery. As for a semitendinous autograft, the integration of the graft at the tendon–bone interface is not ideal because it fails to fully integrate with the bone through an anatomic enthesis and may be associated with postoperative laxity (Spalazzi et al., 2008b). To try to solve this problem, a rabbit model was used to test ACL semitendinous grafts enhanced with BMP-2 gene transfer (Martinek et al., 2002). The authors noted matrix formation with transition from bone to mineralized and nonmineralized cartilage, but they also found that stiffness and load to failure were significantly enhanced.

Collagen infiltration into the prosthesis during healing completely separates fibres and leads to the breakdown of the textile structure. Tightly braided structures do not allow penetration of collagen, while looser and porous knitted and braided ones permit this collagen infiltration, which has been shown to cause fibres to swell, separate and thus contribute to the overall weakness (Poddevin et al., 1995b). Collagen itself is immature, not even organized nor uniformly oriented, so it would appear that this is insufficient to provide any real mechanical support to the synthetic ligament (Guidoin, 1994). This uncontrolled healing leads to loss of integrity in the textile structure. Some degree of encapsulation of the implant was also observed, mainly in the over-the-top technique, but this did not increase with the duration of implantation.

There is also abrasion of the textile structure, which can be divided into two types. The first and more important one is desquamation, or the ‘surface peeling’ and flattening of the fibres (Poddevin et al., 1995b). This is frequent around the femoral condyle in the over-the-top technique and out of the tibial osseous tunnel in the intra-articular zone, where there is contact between yarns and bone (Poddevin et al., 1995c). Its level of severity depends on the type of weave; the tighter the weave, the more abrasion is observed. Poddevin et al. found that this is the main reason for prosthesis failure. To prevent this, some models added protection near these points and surgeons were told to smooth the osteocartilagenous edges of tunnels (Poddevin et al., 1997).

The second mechanism is intra-articular abrasion in torsion and flexion at the yarn–yarn interface. This develops after thousands of cycles. The fatigue of the implant leads to axial breaking and fibres fraying. Every structure composed of textiles, especially the more tightly woven ones, is sensitive to this type of failure. The flattened fibres observed could be explained by previous manufacturing processes such as texturizing and heat setting in addition to compressive forces.

Clinically, the patients with chronic synovitis reactions present with a swollen, warm and painful knee. An analysis of the synovial fluid to rule out acute infection shows no bacteria, but it does show a marked increase in the white blood cell count, mainly lymphocytes. Klein and Jensen described three types of effusion: an acute one, usually 6–13 months following surgery; a chronic one found in the long-term follow-up when patients complain of intermittent moderate swelling mainly after activities, attributed by authors to recurrent instability; and a discrete but persistent joint swelling without any definite pain (Klein and Jensen, 1992). Marois et al. studied three different types of fibres and showed that only mild hyperplasia was present in the synovial lining of the knee joint in close contact with the material, but away from the implant, the synovial tissue remained normal. This mostly mild foreign body inflammatory reaction is in a chronic state after a month (Marois et al., 1995). Finally, there are the effects of the wear particles of these synthetic ligaments. These particles are produced progressively by friction or by a bolus following a rupture of the graft (Figure 7.21). They accumulate in the periarticular synovial folds, mainly in the retrotibial and retrofemoral (Olson et al., 1988) areas. The degree of synovial hypertrophy and foreign body response, with macrophage infiltration and foreign body giant cells, is proportional to the accumulation of those particles (Olson et al., 1988).

In a study conducted by Murray, all patients had degenerative changes on radiographic examination of their ACL-grafted knee, which were not symmetric with the contralateral side (100% against 39%) (Murray and Macnicol, 2004). They concluded that the LK ligament was not effective in preventing osteoarthritis. They were not the only ones to observe progressive degenerative arthritis in their patients. Could the inflammatory reaction to the artificial ligament eventually produce osteoarthritis? In opposition to this idea, Daniels found an increased incidence of degenerative changes in ACL-reconstructed knees compared with conservatively treated ruptures, irrespective of meniscal injury and regardless of the type of graft used (Daniel et al., 1994). Could this just be explained by the initial trauma and the delay before surgery?

Meanwhile, Olson et al. tried to use a rabbit model to explain the role of the artificial ligament in the pathogenesis of osteoarthritis, which is a well-known wear mechanism (Olson et al., 1988). The wear particles induce the production of significant levels of neutral proteinases (collagenases and gelatinases) by synovial cells and chondrocyte-activating factors. The substrate of those enzymes is actually the molecular architecture of the articular cartilage. Consequently, it mediates a biochemical breakdown of articular cartilage and the ultrastructural components of the articular matrix that give hyaline cartilage its biochemical properties. Moreover, Olson found that interleukin-1 (IL-1) production might be another mechanism that adversely affects the joint because it binds to chondrocytes and induces a decrease in matrix

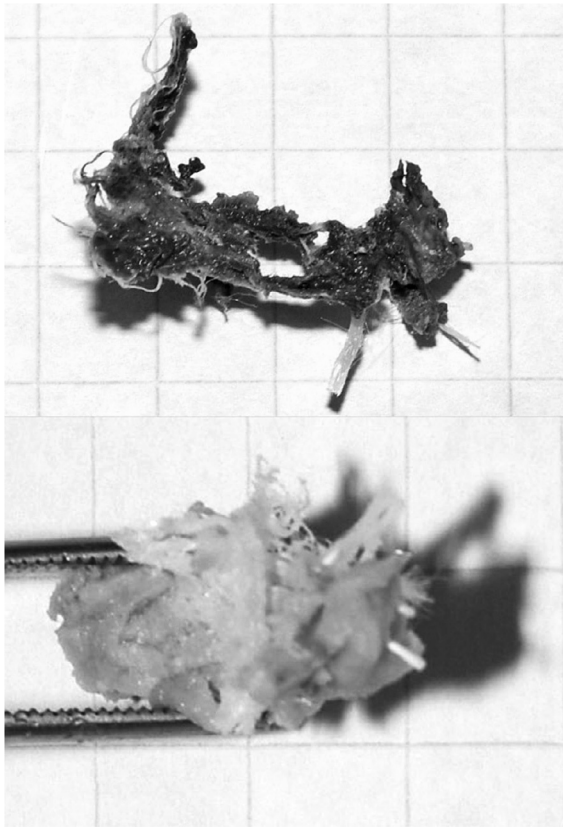

Figure 7.21 Macroscopic particles found in the knee joint of an explanted prosthesis following failure.

synthesis. The cartilage degenerative wear particles produced further enhance these reactions and could then play a role in the pathogenesis of osteoarthritis.

The type of material, size of particle and dose are important factors to take into consideration in this process. First of all, a dose-dependent response was noted. All the ligaments tested led to the production of enzymes. Xenografts and carbon are the biggest producers, probably because they generate the largest and smallest particles, respectively. The reaction to xenografts could be explained by traces of glutaraldehyde, a product used to decrease immunogenicity and increase the ligament's strength. All of the other ligaments tested were similar according to these parameters. They concluded that these artificial devices are used to prevent osteoarthritis, but they may actually be inducing it. On top of it all, as with any nonviable substance in the human body, ACL prostheses are susceptible to bacterial seeding from bacteraemia (Paulos et al., 1992). The poor clinical results and high complication rates easily explain why the orthopaedic community is somehow dissatisfied with the synthetic ligaments on the market.

7.11 Augmentation devices

The idea of an augment implant is to create a hybrid device. It is meant to protect the biological graft during the vulnerable period when the graft undergoes a phase of degeneration and loss of strength before being incorporated (Kumar and Maffulli, 1999). The Kennedy Ligament Augmentation Device® (LAD) (3 M, St-Paul, MN) implant was introduced by Kennedy in 1979 and is made of braided polypropylene (Figure 7.22). It was initially attractive because it was found to share the load and to be stronger and stiffer than the biological ACL (Kennedy, 1983). A cadaveric study showed that the LAD carries approximately 45% of the load with a semitendinous graft and 28% with a patellar tendon graft (Hanley et al., 1989). The counterpart is that it may stress-shield the autogenous tissue, preventing it from developing adequate tensile strength (Schepsis and Greenleaf, 1990). It happens when the device is fixed at both ends. Hunter recommended its use for autogenous grafts smaller than 9 mm to protect against plastic deformity, when a bone plug was broken during harvesting, and in patients with hyperlaxity to prevent stretching during the healing phase (Hunter, 1995).

Multiple studies in the early 1990s demonstrated good results in knee function in the short term and a rate of complications similar to that for autograft reconstruction, but others could not demonstrate any increase in stability (Hunter and Van Kampen, 1993; Hunter and Mittun, 1991; Noyes and Barber, 1992; Bartlett, 1991; Barrett and Field, 1993).

A prospective randomized study of 64 patients followed for more than 2 years showed no differences in residual laxity and functional stability between the group with the LAD and the one without it (Moyen et al., 1992). A problem arose at the suture interface between the graft and the LAD and was identified as the weakest link of the composite (Mascarenhas and MacDonald, 2008).

The examination of explanted devices noted significant yarn–yarn abrasion at the distal end of the implant and at anchorage sites, as well as yarn–bone abrasion at the exit of the tunnels (Poddevin et al., 1995a). Moreover, the device appears to initiate an inflammatory reaction in the knee, causing effusion and synovitis, and delaying

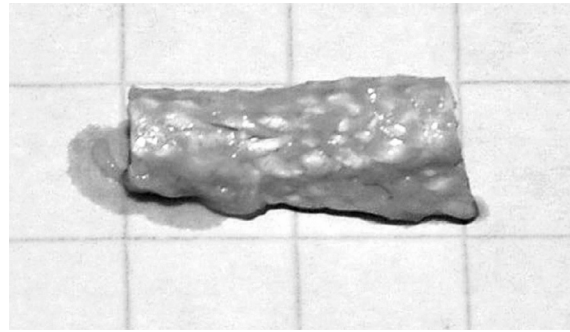

Figure 7.22 Example of an explanted Kennedy Ligament Augmentation Device® made of braided polypropylene.

maturation of the autogenous graft, and it may be associated with an increased risk of infection. Its routine use is no longer recommended (Kumar and Maffulli, 1999).

7.12 Tissue engineering and scaffolds

Tissue engineering is defined as the application of biological, chemical and engineering principles toward the repair, restoration or regeneration of living tissues, using three approaches: the use of three-dimensional, porous matrices that promote tissue regeneration and facilitate the transport of nutrients and metabolites; the use of isolated cells that have been expanded *in vitro*; and the use of molecular and mechanical regulatory factors, or a combination of any of these (Cooper et al., 2005). This emerging field has broad applicability and may provide solutions to a variety of orthopaedic disorders, including fracture nonunion, cartilage injury and tendon or ligament insufficiency (Petrigliano et al., 2006). The principle is to provide a temporary site for cell attachment, proliferation and mechanical stability while the new tissue is regenerating. Compared to the transplantation of cells alone, it offers the potential advantage of immediate functionality (Vunjak-Novakovic et al., 2004). Strategies have ranged from bridging torn ACL ends with a bioconductive graft to off-the-shelf, long-term bioresorbable grafts designed for total replacement (Noyes et al., 1984; Altman et al., 2008). Development can occur *in vivo* or *ex vivo*. *In vivo*, a scaffold is implanted into the host and encourages tissue ingrowth and neoligament formation. Conversely, *ex vivo* systems use a bioreactor that applies exogenous signals to stimulate cells for the subsequent host implantation of a readily functional ligament. The ideal ACL replacement scaffold should be biodegradable, porous and biocompatible; should exhibit sufficient mechanical strength; and should be able to promote the formation of ligamentous tissue in an organized fashion with rapid cellular infiltration but without initiating a severe inflammatory response. Differences between scaffolds can generally be categorized into one or more of six domains: bulk material, three-dimensional architecture and porosity, surface chemistry, mechanical properties, initial scaffold environment (osmolarity and pH), and late scaffold environment (degradation characteristics) (Sahoo et al., 2006; Altman et al., 2002a; Cooper et al., 2003).

Three-dimensional porous scaffolds promote new tissue formation by providing a surface and void volume that promote the attachment, migration, proliferation and desired differentiation of connective tissue progenitors throughout the region where new tissue is needed. It should be biodegradable because persistence of a scaffold or implant precludes the formation of new tissue in the space that it occupies. In addition, following the integration of a rigid nondegradable implant, the adjacent tissue is often mechanically protected (stress shielding), changing local mechanical signals and resulting in the loss of desired local tissue. The scaffold should degrade at a rate proportional to the development of the new tissue to avoid failure. The rate of decrease in mechanics must not exceed the rate of increase in tissue load-carrying capabilities. Three features of the degradation process appear to influence performance: the rate at which the matrix loses its mechanical properties, the rate at which the matrix is

removed from the site, and the nature and concentration of the soluble products that are released into the site as the material is broken down. These characteristics are hard to control and vary widely. The degradation products then have to be further degraded or cleared. The effects of these products on graft cells depend on multiple factors. The degradation products of polylactides and polyglycolides are not ideal for tissue regeneration. To match the degradation rate with tissue in-growth, a polyethylene oxide-based gel was developed that contains both cell adhesion molecules and other peptides that are released as the gel is degraded. Finally, the mechanical properties of the scaffold are determined both by the material properties of the bulk material and its structure.

Several groups have tried to develop a scaffold using natural polymers such as collagen and silk or synthetic polymers such as polylactic acid (PLA) or composite materials (Altman et al., 2002a; Cooper et al., 2003). Collagen and PLA are the most often used; however, none of them has achieved more than 20% of the ultimate tensile strength of human ACLs (Ge et al., 2006). Collagen is usually derived from bovine submucosa and intestine or rat tails. It has to be processed to remove foreign antigens, improve its mechanical strength, and sometimes to slow down the degradation rate by crosslinking. The advantages of collagen include its compatibility with synthetic polymers and the fact that it can easily be modified, hemostatic, synergic with bioactive components and nontoxic. There are concerns over the use of collagen in ligament tissue engineering, however. It does not offer the mechanical integrity required to support the dynamic loading of the ACL at all time points and has a relatively quick *in vivo* degradation (Majima et al., 2005; Funakhoshi et al., 2005). High cost, variability, hydrophilicity, complex handling properties, potential disease transmission associated with the use of bovine collagen products and the leaching of chemical crosslinking agents are other disadvantages (Vunjak-Novakovic et al., 2004).

Another option is bioresorbable silk. The silk matrix is an appropriate three-dimensional culture environment for cell attachment and spreading after being processed to extract the allergen component, sericin. The development of a twisted fibre architecture gives the scaffold excellent mechanical properties similar to those found in the ACL. It is inexpensive and noncytotoxic and it has good biocompatibility and a slow proteolytic degradation time. In fact, it degrades completely after 2 years. The most promising silk is from the *Bombyx mori* silkworm (Laurencin and Freeman, 2005; Altman et al., 2002a). It is the largest and most stable source that has been commercialized for a long time. It can be coated with growth factors to enhance cell attachment and proliferation.

PLA and polyglycolic acid (PGA) are the two main synthetic polymers. Poly-lactide-co-glyclide (PLGA) and poly-L-lactic acid (PLLA) are isoforms of these products. They are hydrolytically degraded materials. The process starts immediately upon implantation and is not dependent on the ability of the body to infiltrate the graft with remodelling tissue (Agrawal and Athanasiou, 1997). PGA has the highest tensile strength but degrades rapidly, and loss of strength is also thought to be too rapid for the PLGA. The best option might be PLLA; several observations of favourable PLLA device interactions in animal and human clinical studies have been published. PLLA has the highest cell number, maintains its structural integrity, and exhibits high mechanical properties

over time. This polymer degrades in lactic acid and can take up to 2 years for full resorption. The advantages of synthetic polymers are their ease of processing and controlled degradation. However, the chemically and biologically inert polymeric materials are unlikely to induce cell adhesion and tissue formation. To overcome this drawback, natural polymers extracted from native ECM have been used to modify the synthetic materials to improve cell adhesion properties. Cooper pointed out that cell seeding yielded better results, positively influencing the healing response and the long-term success of those neoligaments (Cooper et al., 2007). According to Lu, PLLA braided scaffolds precoated with fibronectin were found to be the most suitable substrate for ACL tissue engineering (Lu et al., 2005). Fibronectin is in fact an important protein, which is upregulated during ligament healing and has been shown to improve cell attachment efficiency and affect long-term matrix production by ACL cells.

Architecture is very important in the design of a scaffold. Its structure determines the transport of nutrients, metabolites and regulatory molecules to and from the cells, whereas its mechanical properties determine mechanotransduction at cellular and tissue levels (Altman et al., 2008, 2002a). Porosity can modulate the functionality and cellular response of the implant (Cooper et al., 2005). It is known that a highly porous scaffold is desirable because it allows cell seeding or migration throughout the materials (Ge et al., 2006). To culture a high number of cells, a large surface area is required. For example, 150 μm of pore diameter is required for bone in-growth and 200–250 μm for soft tissue (Woo et al., 2004; Yahia, 1997; von Recum, 1986; Konikoff et al., 1974). These pore size ranges are required for tissue in-growth and capillary supply, and to improve the quality of anchorage in bone tunnels. The interconnectivity between pores also allows tissue in-growth into the interior of the matrix in this relatively initial avascular environment. Finally, yarn bundle size also needs to be considered, especially in a three-dimensional braiding system, which comprises a network of continuous filament and yarn bundles with fibrous architecture oriented in various directions (Cooper et al., 2005).

Other aspects to consider are the cell source, cellular response and cellular affinity for the scaffold. ACL fibroblasts were shown to respond to specific growth factors, dynamic mechanical stimulation and static tension, but they are known to have a low doubling rate, and a suitable source of autologous ACL fibroblasts is not yet available. This is why other sources, such as mesenchymal stem cells from bone marrow, are under investigation and seem to be an excellent cell source. They have the potential to differentiate into cells of multiple mesenchymal lineages (Petrigliano et al., 2006).

Regulatory factors are also important in the development of new tissue. Mechanical signals are important mediators in the differentiation of connective tissue progenitors; they enhance mass transport and directly stimulate the cells to achieve mechanically competent tissue formation. In fact, they induce cell alignment in the direction of the resulting force. Numerous efforts such as growth factor use, cell therapy and gene therapy have been employed for *in vivo* and *in vitro* models in an effort to enhance ligament healing. A group of authors even treated the LK ligament with radio frequency and noted an increase in cell proliferation and attachment (Sugihara et al., 2006). Meanwhile, there are still many factors that need to be considered, such as the dose and timing of applications during ligament healing, delivery vehicles and the possible combined

effects of multiple growth factors for positively synergistic outcomes. The attachment, survival, proliferation and differentiation of stem cells and progenitor cells can be optimized *in vitro* if implants are precoated with selected bioactive proteins. However, the main concerns are the cost and controlled release of those growth factors. The new generation of bioinductive biomaterial scaffolds are capable of delivering multiple growth factors or releasing these molecules in response to mechanical loading. Kimura et al. implanted in rabbits a plain-woven braided PLLA scaffold combined with a gelatin hydrogel for the controlled release of bFGF growth factors wrapped with a collagen membrane (Kimura et al., 2008). Their results suggest that the local controlled release of those growth factors could induce osseointegration and intrascaffold cell migration to increase the mechanical strength of the new ACL.

Cooper et al. are trying to develop scaffolds based on PLGA, which is already used for sutures and fixation devices and is biocompatible and biodegradable (Cooper et al., 2000). They predesign heterogeneity into the pore size and fibre orientation of their model, so that cell ingrowth is different depending on where it is located in the material. The intention is that stresses of the knee joint can be more appropriately withstood. For example, a particular region has properties to withstand abrasion on bony edges while the extremities are designed to enhance bone fixation into tunnels. Spalazzi et al. also thought about designing a scaffold with inhomogeneity at the ACL-to-bone interface in order to optimize integration with a controlled cell distribution (Spalazzi et al., 2008a). Multiphasic scaffold designs seem to represent a promising strategy for complex musculoskeletal tissues, as is the biological fixation of an ACL graft (Spalazzi et al., 2006). This kind of material could be used as a graft collar, a hollow cylinder through which ACL graft will be inserted or preincorporated into a degradable polymer-based ACL prosthesis.

These authors also developed a mechanoactive scaffold. The principle is to apply compression to a tendon graft to promote matrix remodelling, which would eventually lead to fibrocartilage formation by upregulation of fibrocartilage markers, because it has been shown by Berry et al. that the cellular response in terms of alignment and cellular metabolism was highly dependent on the applied strain profile (Berry et al., 2003). The precise mechanism is unclear but is thought to result from the influence of mechanical signal transduction pathways as well as differing rates of nutrients, metabolites and oxygen mass transfer induced by these stimuli (Altman et al., 2002b). This could potentially be used as a collar for an ACL graft at the bone–graft junction. Some preliminary studies have also shown that, in addition to tensile loading, other mechanical factors such as electromagnetic fields and ultrasound may play a role in regulating the differentiation of mesenchymal progenitor cells (Naruse et al., 2000; Aaron and Ciombor, 1996; Jadeja et al., 2007).

Tischer et al. developed a new scaffold based on acellular tendon allografts seeded with autologous cells (Tischer et al., 2007). The biomechanical properties of the tendon remained the same because this new method used for acellularity preserves the collagenous matrix. This process should also minimize adverse immunogenic reactions often encountered in allograft material. According to them, if animal experiments are successful, tissue-engineered constructs could be generated using a simple dermal biopsy and acellularized tendons as scaffolds.

To date, clinical studies have been infrequent and inconsistent, however. Jadeja et al. reviewed a composite carbon-fibre polyester scaffold used in ACL-deficient knees at their institutions (ABC® – Active Biosynthetic Composite Ligament) (Jadeja et al., 2007). It was introduced in 1985 and is made of 24 strands of interwoven carbon and polyester unit material with radial overbraiding and a loop at either end. The over-the-top technique was used. The early failure of their first cohort was attributed to technical errors. The second cohort showed a very low initial failure rate (0% in the first 3 years) but with an increasing incidence of failure (27.9%) noted after 5 years, mainly at the intra-articular tibial tunnel exit. Another study also using the same ABC® scaffold reported 90% satisfaction among 71 patients with a mean follow-up of 5 years. There were no failures and only two patients suffered from recurrent synovitis (Petrou et al., 2006).

The advantage of a tissue-engineered ligament is that it does not elicit a permanent foreign body reaction, because it is gradually reabsorbed and replaced by natural tissue. In contrast to the permanent synthetic prosthesis, which loses strength with time, the mechanical behaviour of tissue-engineering grafts should improve with time because of neoligament tissue development and remodelling (Ge et al., 2006). Potential problems associated with these implants are allogenicity and batch-to-batch variability, making consistent reproduction difficult (Mascarenhas and MacDonald, 2008). A study showed that the degree of in-growth of the implant was highly variable (Barry et al., 1995). This is a major concern and some authors recommend that until this issue is resolved, the reconstruction of ACL with scaffold should be discouraged. The ideal artificial ACL perfectly mimics all the characteristics of a normal ACL in terms of strength, compliance, elasticity and durability without any side effects. Moreover, it should be user-friendly for surgeons and compatible with the actual surgical equipment. Unfortunately, none of the synthetic grafts have met the qualifications needed for a lasting ACL substitute. Ge et al. listed five reasons why progress in that field is slow: (1) no scaffold has been able to handle the mechanical loadings of an ACL; (2) disruption of the blood supply undermines the regeneration potential; (3) the transitional zone between the bone and ligament is a challenge to recreate; (4) regeneration secondary to cytokine activation is difficult; and (5) the process has not yet been able to restore stretch-sensitive mechanoreceptors (Ge et al., 2006).

As we can see, tissue engineering is an emerging field, and there are still many problems to overcome. Despite extensive research, no materials have achieved the goal of a construct with the biomechanical, biofunctional and biostable properties of a native ACL. It will be interesting to observe what the new generation of scaffolds will bring.

7.13 Xenografts

Few studies in the past 10 years have mentioned xenografting due to its high level of complications and bad publicity. Recently, Stone et al. transplanted immunochemically modified porcine patellar tendon using the two-bone tunnels technique in 10 patients with ACL-deficient knees and followed them up for 24 months without

any immunosuppressive treatment. At the time of publication, five of them were still in place (Stone et al., 2007). Only one was removed because of a bone plug loosening at 15 months. No one had any knee effusion and everyone went back to their previous level of activity with a stable knee. They were able to demonstrate the process of the ligamentization of the xenograft with the explanted implants (two sports accidents). They concluded that this modified porcine implant could be considered an option for patients with a ruptured ACL.

With a goat model, some authors developed an artificial biological ligament with a porcine tendon treated with epoxy-crosslinking fixation (Wang et al., 2008). This process produces a passive-degrading material only when tissue regeneration is necessary. The diversified minimization of the antigen process to reduce immunogenicity, the mechanical enhancement modification of proteins and a surface activating process with adhesion to enrich seed cells and growth factors were also applied to the materiel. The appearance is similar to normal tendon. At 52 weeks, no trace of ligament material was found; the regenerated host-ligament collagen fibres were arranged in an orderly fashion but still differed from a normal cruciate ligament. The integration at the bone–ligament interface also seemed adequate. According to the authors, the ligament showed good biocompatibility and acceptable biomechanical properties in spite of the multiple treatments. They believe this could become a good option as an augmentation device for an ACL-deficient knee because its final loading strength was only 30–40% of the original one. Perhaps new studies should combine the technologies developed with scaffolds to produce a new generation of ACL implants.

7.14 Conclusion

The long-term results of ACL reconstruction are disappointing in spite of 30 years of effort, and given that scientists are still looking for the optimal biomaterial and graft structure to meet the demanding and complex characteristics of the native ACL, one question remains: Do we still need an artificial substitute to replace or reinforce a broken or torn ACL? The scientific community vacillates back and forth with different types of implants, trying not to fail in the same ways that the their predecessors did. Is tissue engineering the answer? Only the future will tell. But for now, even if not perfect, studies show that bone–patellar tendon–bone or hamstring autografts are the way to go – and for the long haul! An ACL prosthesis that lasts as long as the patient lives and that can be implanted using arthroscopic techniques with minimal postoperative pain and rapid recovery without complication is the dream of every surgeon.

References

Aaron, R.K., Ciombor, D.M., 1996. Acceleration of experimental endochondral ossification by biophysical simulation of the progenitor cell pool. J. Orthop. Res. 14, 582–589.

Adachi, N., Ochi, M., Uchio, Y., Iwasa, J., Kuriwaka, M., Ito, Y., 2004. Reconstruction of the anterior cruciate ligament. Single- versus double-bundle multistranded hamstring tendons. J. Bone Joint Surg. Br. 86B, 515–520.

Aglietti, P., Giron, F., Buzzi, R., Biddau, F., Sasso, F., 2004. Anterior cruciate ligament reconstruction: bone-patellar tendon-bone compared with double semitendinosus and gracilis tendon grafts. A prospective, randomized clinical trial. J. Bone Joint Surg. Am. 86, 2143–2155.

Agrawal, C.M., Athanasiou, K.A., 1997. Technique to control pH in vicinity of biodegrading PLA-PGA implants. J. Biomed. Mater. Res. 38, 105–114.

Allum, R.L., 2001. The anterior cruciate ligament-current concepts. Knee 8, 1–3.

Altman, G.H., Horan, R.L., Lu, H.H., Moreau, J., Martin, I., Richmond, J.C., Kaplan, D.L., 2002a. Silk matrix for tissue-engineered anterior cruciate ligaments. Biomaterials 23, 4131–4141.

Altman, G.H., Horan, R.L., Martin, I., Farhadi, J., Stark, P.R., Vollach, V., Richmond, J.C., Vuniak-Novakovic, G., Kaplan, D.L., 2002b. Cell differentiation by mechanical stress. FASEB J. 16, 270–272.

Altman, G.H., Horan, R.L., Weitzel, P., Richmond, J.C., 2008. The use of long-term bioresorbable scaffolds for anterior cruciate ligament repair. J. Am. Acad. Orthop. Surg. 16, 177–187.

Alwyn-Smith, S., 1918. The diagnosis and treatment of injuries to the crucial ligaments. Br. J. Surg. 6, 176.

Amiel, D., Kleiner, J.B., Roux, R.D., Harwood, F.L., Akeson, W.H., 1986. The phenomenon of 'ligamentization': anterior cruciate ligament reconstruction with autogenous patellar tendon. J. Orthop. Res. 4, 162–172.

Amiel, D., Billings, E., Akeson, W.H., 1989. Ligament structure, chemistry and physiology. In: Daniel, D., et al., (Eds.), Knee Ligaments: Structure, Function, Injury and Repair. Raven Press, New York, p. 34.

Amis, A.A., Dawkins, G.P., 1991. Functional anatomy of the anterior cruciate ligament. Fiber bundle actions related to ligament replacements and injuries. J. Bone Joint Surg. Br. 73, 260–267.

Amis, A.A., Bull, A.M.J., Lie, D.T.T., 2005. Biomechanics of rotational instability and anatomic anterior cruciate ligament reconstruction. Oper. Tech. Orthop. 15, 29–35.

Andersen, H.N., Bruun, C., Sondegârd-Peterson, P.E., 1992. Reconstruction of chronic insufficient anterior cruciate ligament in the knee using a synthetic Dacron prosthesis. A prospective study of 57 cases. Am. J. Sports Med. 20, 20–23.

Barrett, G.R., Field, L.D., 1993. Comparison of patella tendon versus patella tendon/Kennedy ligament augmentation device for anterior crudate ligament reconstruction: study of results, morbidity, and complications. Arthroscopy 9, 624–632.

Barry, M., Thomas, S.M., Rees, A., Shafigian, B., Mowbray, M.A., 1995. Histological changes associated with an artificial anterior cruciate ligament. J. Clin. Pathol. 48, 556–559.

Bartlett, J., 1991. Anterior cruciate ligament autografts and augmentation. In: Presented at the Combined Annual Meeting of the Australian and New Zealand Orthopaedic Associations. Christchurch, New Zealand, September.

Berry, C.C., Cacou, C., Lee, D.A., Bader, D.L., Shelton, J.C., 2003. Dermal fibroblasts respond to mechanical conditioning in a strain profile dependent manner. Biorheology 40, 337–345.

Beynnon, B.D., Fleming, B.C., Labovitch, R., Parsons, B., 2002. Chronic anterior cruciate ligament deficiency is associated with increased anterior translation of the tibia during the translation from non-weightbearing to weightbearing. J. Orthop. Res. 20, 332–337.

Bolton, C.W., Bruchman, W.C., 1985. The Gore-Tex expanded polytetrafluoroethylene prosthetic ligament. An in vitro and in vivo evaluation. Clin. Orthop. Relat. Res. 196, 202–213.

Borchers, J.R., Pedroza, A., Kaeding, C., 2009. Activity level and graft type as risk factors for anterior cruciate ligament graft failure, a case control study. Am. J. Sports Med. 37, 2362–2367.

Bryant, J.T., Cooke, T.D.V., 1988. A biomechanical function of the ACL: prevention of medial translation of the tibia. In: Feagin, J.A. (Ed.), The Crucial Ligaments. Diagnosis and Treatment of Ligamentous Injuries About the Knee. Livingstone, Edinburgh.

Chaudhari, A.M., Briant, P.L., Bevill, S.L., Koo, S., Andriacchi, T.P., 2008. Knee kinematics, cartilage morphology, and osteoarthritis after ACL injury. Med. Sci. Sports Exerc. 40, 215–222.

Cho, S., Muneta, T., Ito, S., Yagishita, K., Ichinose, S., 2004. Electron microscopic evaluation of two-bundle anatomically reconstructed anterior cruciate ligament graft. J. Orthop. Sci. 9, 296–301.

Cooper, J.A., Lu, H.H., Ko, F.K., Laurencin, C.T., 2000. Fiber-Based Tissue Engineered Scaffold for Ligament Replacement: Design Considerations and in vitro Evaluation. Society for Biomaterials, Mt. Laurel, NJ, 208.

Cooper, J.A., Sahota, J., Gorum, J., Carter, J., Ko, F.K., Doty, S., Laurencin, C.T., 2003. Evaluation of a Novel Tissue-Engineered Ligament: in vivo Studies. Society for Biomaterials, New Jersey, Spring 2003 Meeting, 162.

Cooper, J.A., Lu, H.H., Ko, F.K., Freeman, J.W., Laurencin, C.T., 2005. Fiber-based tissue-engineered scaffold for ligament replacement: design considerations and in vitro evaluation. Biomaterials 26, 1523–1532.

Cooper, J.A., Sahota, J.S., Gorum II, W.J., Carter, J., Doty, S.B., Laurencin, C.T., 2007. Biomimetic tissue-engineered anterior cruciate ligament replacement. Proc. Natl. Acad. Sci. U. S. A. 104, 3049–3054.

Corner, E.M., 1914. Notes of a case illustrative of an artificial anterior crucial ligament, demonstrating the action of that ligament. Proc. R. Soc. Med. 7, 120–121.

Daniel, D.M., Stone, M.L., Dobson, B.E., Fithian, D.C., Rossman, D.J., Kaufman, K.R., 1994. Fate of the ACL injured patient. A prospective outcome study. Am. J. Sports Med. 22, 632–644.

DeAngelis, J.P., Cote, M., Fulkerson, J.P., Caminiti, S., 2008. Central quadriceps tendon for anterior cruciate ligament reconstruction: long-term results. Arthroscopy 24 (6), e18–e20.

Dericks Jr., G., 1995. Ligament advanced reinforcement system anterior cruciate ligament reconstruction. Oper. Tech. Sports Med. 3, 187–205.

Dodds, J.A., Arnoczky, S.P., 1994. Anatomy of the anterior cruciate ligament: a blueprint for repair and reconstruction. Arthroscopy 10, 132–139.

Drogset, J.O., Grontvedt, T., Robak, O.R., Meister, A., Viser, A.T., Engebretsen, L., 2006. A sixteen-year follow-up of three operative techniques for the treatment of acute ruptures of the anterior cruciate ligament. J. Bone Joint Surg. Am. 88, 944–952.

Duri, Z.A., Aichroth, P.M., 1995. Partial anterior cruciate ligament tears: evaluation and a clinical review. Knee 2, 131–138.

Duthon, V.B., Barea, C., Abrassart, Fasel, J.H., Fritschy, Ménétrey, J., 2006. Anatomy of the anterior cruciate ligament. Knee Surg. Sports Traumatol. Arthrosc. 14, 204–213.

Ekdahl, M., Wang, J.H., Ronga, M., Fu, F.H., 2008. Graft healing in anterior cruciate ligament reconstruction. Knee Surg. Sports Traumatol. Arthrosc. 16, 935–947.

Ellison, A.E., Berg, E.E., 1985. Embryology, anatomy, and function of the anterior cruciate ligament. Orthop. Clin. North Am. 16, 3–14.

Esposito, I.J., Beard, D.J., Dodd, C.A.F., Shafighian, B., 1997. Rehabilitation following patellar tendon or ABC prosthetic ligament reconstruction for chronic ACL deficient knee. Knee 4, 81–86.

Fideler, B.M., Vangsness Jr., C.T., Lu, B., Orlando, C., Moore, T., 1995. Gamma irradiation: affects on biochemical properties of human bone–patellor tendon–bone allografts. Am. J. Sports Med. 23, 643–646.

Forssblad, M., Valentin, A., Engström, B., Werner, S., 2006. ACL reconstruction: patellar tendon versus hamstring grafts-economical aspects. Knee Surg. Sports Traumatol. Arthrosc. 14, 536–541.

Forster, M.C., Forster, I.W., 2005. Patellar tendon or four-strand hamstring? A systematic review of autografts for anterior cruciate ligament reconstruction. Knee 12, 225–230.

Frank, D.A., Altman, G.T., Re, P., 2007. Hybrid anterior cruciate ligament reconstruction: introduction of a new technique for anatomic anterior cruciate ligament reconstruction. Arthroscopy 23, 1354.e1–1354.e5.

Friedman, M.J., 1991. Prosthetic anterior cruciate ligament. Clin. Sports Med. 10, 499–513.

Fujikawa, K., Iseki, F., Tomatsu, T., Takeda, T., Seedhom, B.B., 1984. Microscopic and histologic findings after reconstruction of the anterior cruciate ligament by the Leeds-Keio artificial ligament. Knee 10, 35–40.

Funakhoshi, T., Majima, T., Iwasaki, N., Yamane, S., Masuko, T., Minami, A., Harada, K., Tamura, H., Tokura, S., Nishimura, S., 2005. Novel chitosan-based hyaluronan hybrid polymer fibers as a scaffold in ligament tissue engineering. J. Biomed. Mater. Res. 74, 338–346.

Ge, Z., Yang, F., Goh, J.C.H., Ramakrishna, S., Lee, E.H., 2006. Biomaterials and scaffolds for ligament tissue engineering. J. Biomed. Mater. Res. 77, 639–652.

Ghalayini, S.R.A., Helm, A.T., Bonshahi, A.Y., Lavender, A., Johnson, D.S., Smith, R.B., 2010. Arthroscopic anterior cruciate ligament surgery: results of autogenous patellar tendon graft versus the Leeds-Keio synthetic graft: five year follow-up of a prospective randomized control trial. Knee 17, 334–339.

Gillquist, J., Odensten, M., 1993. Reconstruction of old anterior cruciate ligament tears with a Dacron prosthesis. A prospective study. Am. J. Sports Med. 21, 358–366.

Girgis, F.G., Marshall, J.L., Monajem, A., 1975. The cruciate ligaments of the knee joint. Anatomical, functional and experimental analysis. Clin. Orthop. Relat. Res. 106, 216–231.

Goldblatt, J.P., Fitzsimmons, S.E., Balk, E., Richmond, J.C., 2005. Reconstruction of the anterior cruciate ligament: meta-analysis of patellar tendon versus hamstring tendon autograft. Arthroscopy 21, 791–803.

Good, L., Askew, M.J., Boom, A., Melby III, A., 1993. Kinematic in-vitro comparison between the normal knee and two techniques for reconstruction of the anterior cruciate ligament. Clin. Biomech. 8, 243–249.

Gordon, M.D., Steiner, M.E., 2004. Anterior cruciate ligament injuries. In: Garrick, J. (Ed.), Orthopaedic Knowledge Update in Sports Medicine III. AAOS, Rosemont, USA, pp. 169–170.

Gries, P.E., Steadman, J.R., 1996. Revision of failed prosthetic anterior cruciate ligament reconstruction. Clin. Orthop. Relat. Res. 323, 78–90.

Grood, E.S., Walz-Hasselfeld, K.A., Holden, J.P., Fr, Noyes, Levy, M.S., Butler, D.C., Jackson, D.W., Drez, D.J., 1992. The correlation between anterior-posterior translation and cross-sectional area of anterior cruciate ligament reconstructions. J. Orthop. Res. 10, 878–885.

Guidoin, R., 1994. Mechanisms of failure for anterior cuciate ligament prostheses implanted in humans. A Retrospective Analysis of 79 Surgically Excised Explants.

Guidoin, M.F., Marois, Y., Bejui, J., Poddevin, N., King, M.W., Guidoin, R., 2000. Analysis of retrieved polymer fiber based replacement for the ACL. Biomaterials 21, 2461–2474.

Hamido, F., Misfer, A.K., Al Harran, H., Khadrawe, T.A., Solinan, A., Talaat, A., Awad, A., Krairat, S., 2011. The use of the LARS artificial ligament to augment a short or undersized ACL handstrings tendon graft. Knee 18, 373–378.

Hanley, P., Lewis, J.L., Hunter, R.E., Kistukas, S., Kowalczyk, C., 1989. Load sharing and graft forces in anterior cruciate ligament reconstruction with the ligament augmentation device. Am. J. Sports Med.. 17, .

Hefzy, M.S., Grood, E.S., 1986. Sensitivity of insertion locations on length patterns of anterior cruciate ligament fibers. J. Biomech. Eng. 108, 73–82.

Huanag, J.M., Wang, Q., Shen, F., Wang, Z., Kang, Y., 2010. Cruciate ligament reconstruction using LARS artificial ligament under arthroscopy: 81 cases report. Chin. Med. J. 123, 160–164.

Hunter, R.E., 1995. Anterior cruciate ligament reconstruction with a composite graft bone-patellar tendon-bone/ligament augmentation device. Oper. Tech. Sports Med. 3 (3), 182–186.

Hunter, R., Mittun, P., 1991. ACL reconstruction with patellar-tendon LAD composite graft. In: Presented at the Annual Meeting of the Arthroscopy Association of North America. San Diego, CA, April.

Hunter, R.E., Van Kampen, C., 1993. A Composite Graft ACL Reconstruction: a Prospective Multi-Center Study. In: Presented at the Second AOSSM/JOSSM Trans-Pacific Meeting. Maui, HI, 20–25 March.

Indelicato, P.A., Talley, C., 1995. Allograft tissue in the reconstruction of the anterior cruciate ligament. J. Sports Traumatol. Relat. Res. 3, 185–191.

Indelicato, P.A., Pascale, M.S., Huegel, M.O., 1989. Early experience with the Gore-Tex polytetrafluoroethylene anterior cruciate ligament prosthesis. Am. J. Sports Med. 17, 55–62.

Jadeja, H., Yeoh, D., Lal, M., Mowbray, M., 2007. Patterns of failure with time of an artificial scaffold class ligament used for reconstruction of the human anterior cruciate ligament. Knee 14, 439–442.

Jansson, K.A., Harilainen, A., Sandelin, J., Karjalainen, P.T., Aronen, H.J., Tallroth, K., 1999. Bone tunnel enlargement after anterior cruciate ligament reconstruction with the hamstring autograft and endobouton fixation technique. A clinical, radiographic and magnetic resonance imaging study with 2 years of follow up. Knee Surg. Sports Traumatol. Arthrosc. 7, 290–295.

Jari, S., Shelbourne, K.D., 2002. Staged bilateral anterior cruciate ligament reconstruction with use of contralateral patellar tendon autograft: a case report. Am. J. Sports Med. 30, 437–440.

Jarvela, T., 2007. Double-bundle versus single-bundle anterior cruciate ligament reconstruction: a prospective, randomized clinical study. Knee Surg. Sports Traumatol. Arthrosc. 15, 500–507.

Javernick, M.A., Potter, B.K., Mack, A., Dekay, K.B., Murphy, K.P., 2006. Autologous hamstring anterior cruciate ligament reconstruction in patients older than 40. Am. J. Orthop. 35, 430–434.

Jones, A.P., Sidhom, S., Sefton, G., 2007. Long-term clinical review (10–20 years) after reconstruction of the anterior cruciate ligament using the Leeds-Keio synthetic ligament. J. Long Term Eff. Med. Implants 17, 59–69.

Kartus, J., Movin, T., Karlsson, J., 2001. Donor-site morbidity and anterior knee problems after anterior cruciate ligament reconstruction using autografts. Arthroscopy 17, 971–980.

Kennedy, J.C., 1983. Application of prosthetics to anterior cruciate ligament reconstruction and repair. Clin. Orthop. Relat. Res. 172, 125–128.
Kimura, Y., Hokugo, A., Takamoto, T., Talato, Y., Kurosawa, H., 2008. Regeneration of anterior cruciate ligament by biodegradable scaffold combined with local controlled release of basic fibroblast growth factor and collagen wrapping. Tissue Eng. 14, 47–57.
Klein, W., Jensen, K.U., 1992. Synovitis and artificial ligaments. Arthroscopy 8, 116–124.
Konikoff, J.J., Billings, W., Nelson, L.J., Hunter, J.M., 1974. Development of a single stage active tendon prosthesis. I. Distal end attachment. J. Bone Joint Surg. Am. 56, 848.
Konishi, Y., Fukubayashi, T., Takeshita, D., 2002. Possible mechanism of quadriceps femoris weakness in patients with ruptured anterior cruciate ligament. Med. Sci. Sports Exerc. 34, 1414–1418.
Kousa, P., Jarvinen, T.L., Vihavainen, M., et al., 2003. The fixation strength of six hamstring tendon graft fixation devices in anterior cruciate ligament reconstruction. Part I: femoral site. Am. J. Sports Med. 31 (2), 174–181.
Krych, A.J., Jackson, J.D., Hoskin, T.L., Dahm, D.L., 2008. A meta-analysis of patellar tendon autograft versus patellar tendon allograft in anterior cruciate ligament reconstruction. Arthroscopy. 24, 292–298.
Kuhn, M.A., Ross, G., 2007. Allografts in the treatment of anterior cruciate ligament injuries. Sports Med. Arthrosc. 15, 133–138.
Kumar, K., Maffulli, N., 1999. The ligament augmentation device: an historical perspective. Arthroscopy 15, 422–432.
Laurencin, C.T., Freeman, J.W., 2005. Ligament tissue engineering: an evolutionary materials science approach. Biomaterials 26, 7530–7536.
Lavoie, P., Fletcher, J., Duval, N., 2000a. Patient satisfaction needs as related to knee stability and objective findings after ACL reconstruction using the LARS artificial ligament. Knee 1, 157–163.
Lavoie, P., Fletcher, J., Duval, N., 2000b. Patient satisfaction needs as related to knee stability and objective findings after ACL reconstruction. Knee 7, 157–163.
Lee, C.A., Meyer, J.V., Shilt, J.S., Poehling, G.G., 2004. Allograft maturation in anterior cruciate ligament reconstruction. Arthroscopy 20, 2046–2049.
Lohmander, L.S., Ostenberg, A., Englund, M., Roos, H., 2004. High prevalence of knee osteoarthritis, pain, and functional limitations in female soccer players twelve years after anterior cruciate ligament injury. Arthritis Rheum. 50, 3145–3152.
Lu, H.H., Cooper, J.A., Manuel, S., et al., 2005. Anterior cruciate ligament regeneration using braided biodegradable scaffolds: in vitro optimization studies. Biomaterials 26, 4805–4816.
Majima, T., Funakosi, T., Iwasaki, N., et al., 2005. Alginate and chitosan polyion complex hybrid fibers for scaffolds in ligament and tendon tissue engineering. J. Orthop. Sci. 10, 302–307.
Mannel, H., Marin, F., Claes, L., Durselen, L., 2004. Anterior cruciate ligament rupture translates the axes of motion within the knee. Clin. Biomech. 19, 130–135.
Marois, Y., Cronier, B., Guidoin, R., Delagoutte, J.P., Belanger, A.Y., Marois, M., Poddevin, N., King, M.W., 1995. Synovial healing response to synthetic ligamentous fibers implanted in the joint of the rat. Actualité En Biomatériaux 3, 339–348.
Martinek, V., Latterman, C., Usas, A., Abramowitch, S., Woo, S.L., Fu, F.H., Huard, J., 2002. Enhancement of tendon-bone integration of anterior cruciate ligament grafts with bone morphogenetic protein-2 gene transfer: a histological and biomechanical study. J. Bone Joint Surg. Am. 84, 1123–1131.

Marumo, K., Saito, M., Yamagishi, T., Fujii, K., 2005. The 'ligamentization' process in human anterior cruciate ligament reconstruction with autogenous patellar and hamstring tendons: a biochemical study. Am. J. Sports Med. 33, 1166–1173.

Mascarenhas, R., MacDonald, P.B., 2008. Anterior cruciate ligament reconstruction: a look at prosthetics – past, present and possible future. McGill J. Med. 11, 29–37.

McCarthy, D.M., Tolin, B.S., Schwendeman, L., 1993. Prosthetic replacement for anterior cruciate ligament. In: Jackson, D.W., Arnoczky, S.P., Woo, S.L.Y. (Eds.), The Anterior Cruciate Ligament: Current and Future Concepts. Raven, New York: NY, pp. 343–356.

Meunier, A., Odensten, M., Good, L., 2007. Long-term results after primary repair or non-surgical treatment of anterior cruciate ligament rupture: a randomized study with a 15-year follow-up. Scand. J. Med. Sci. Sports 17, 230–237.

Mody, B.S., Howard, L., Harding, M.L., Parmar, H.V., Learmonth, D.J., 1993. The ABC Carbon and polyester prosthetic ligament for ACL-deficient knees. Early results in 31 cases. J. Bone Joint Surg. Br. 75, 818–821.

Moore, S.L., 2002. Imaging the anterior cruciate ligament. Orthop. Clin. North Am. 33, 663–674.

Moyen, B.J., Jenny, J.Y., Mandrino, A.H., Lerat, J.L., 1992. Comparison of reconstruction of the anterior cruciate ligament with and without a Kennedy ligament augmentation device. A randomized prospective study. J. Bone Joint Surg. Am. 74, 1313–1319.

Mroz, T.E., Joyce, M.J.J., Steinmetz, M.P., Lieberman, I.H., Wang, J.C., 2008. Musculoskeletal allograft risks and recalls in the United States. J. Am. Acad. Orthop. Surg. 16, 559–565.

Munshi, M., Davidson, M., MacDonald, P.B., Froese, W., Sutherland, K., 2000. The efficacy of magnetic resonance imaging in acute knee injuries. Clin. J. Sport Med. 10, 34–39.

Murray, A.W., Macnicol, M.F., 2004. 10–16 year results of Leeds-Keio anterior cruciate ligament reconstruction. Knee 11, 9–14.

Naruse, K., Mikuni-Takagaki, Y., Azuma, Y., Ito, M., Ota, T., Kameyama, K., Itoman, M., 2000. Anabolic response of mouse bone-marrow-derived stromal cell clone ST2 cells to low-intensity pulsed ultrasound. Biochem. Biophys. Res. Commun. 268, 216–220.

Nau, T., Lavoie, P., Duval, N., 2002. A new generation of artificial ligament in reconstruction of the anterior cruciate ligament. Two-year follow-up of a randomised trial. J. Bone Joint Surg. Br. 84, 356–360.

Noyes, F.R., Barber, S.D., 1992. The effect of a ligament augmentation device on allograft reconstructions for chronic ruptures of the anterior cruciate ligament. J. Bone Joint Surg. Am. 74, 960–973.

Noyes, F.R., Butler, D.L., Grood, E.S., Zernicke, R.F., Hefzy, M.S., 1984. Biomechanical analysis of human ligament grafts used in knee ligament repairs and reconstructions. J. Bone Joint Surg. 66, 344–352.

O'Brien, T.K., McLeod, A., Cooke, W.D., et al., 1991. Successes and failure following 5 years of clinical experience with the Surgicraft ABC prosthetic anterior cruciate ligament. In: Williams, K.R., Toni, A., Middleton, J., Pallotti, G. (Eds.), Interfaces in Medicine and Mechanics – 2. Elsevier, Barking.

Olson, E.J., Kang, J.D., Fu, F.H., Georgescu, H.I., Mason, G.C., Evans, C.H., 1988. The biochemical and histological effects of artificial ligament wear particles: in vitro and in vivo studies. Am. J. Sports Med. 16, 558–570.

Oni, O.O.A., 1998. Mechanism of injury in anterior cruciate ligament disruption. Knee 5, 81–86.

Patel, J.V., Church, J.S., Hall, A.J., 2000. Central third bone-patellar tendon-bone anterior cruciate ligament reconstruction: a 5-year follow-up. J. Arthroscopy 16, 67–70.

Pattee, G.A., Friedman, M.J., 1992. The history of intra-articular anterior cruciate ligament reconstruction. Oper. Tech. Orthop. 2, 44–48.
Paulos, L.E., Rosenberg, T.D., Grewe, S.R., Tearse, D.S., Beck, C.L., 1992. The Gore-Tex anterior cruciate ligament prosthesis: a long term follow-up. Am. J. Sports Med. 20, 246–252.
Petersen, W., Laprell, H., 2000. Insertion of autologous tendon grafts to the bone: a histological and immunohistochemical study of hamstring and patellar tendon grafts. Knee Surg. Sports Traumatol. Arthrosc. 8, 26–31.
Petersen, W., Tillmann, B., 1999. Structure and vascularisation of the cruciate ligaments of the human knee joint. Anat. Embryol. 200, 325–334.
Petersen, W., Zantop, T., 2006. Anatomy of the anterior cruciate ligament with regard to its two bundles. Clin. Orthop. Relat. Res. 454, 35–47.
Petrigliano, F.A., McAllister, D.R., Wu, B.M., 2006. Tissue engineering for anterior cruciate ligament reconstruction: a review of current strategies. Arthroscopy 22, 441–451.
Petrou, G., Chardouvelis, C., Kouzoupis, A., Dermon, A., Petrou, H., Tilkeridis, C., Gavros, M., 2006. Recontruction of the anterior cruciate ligament using the polyester ABC ligament scaffold: a minimum follow-up of four years. J. Bone Joint Surg. Br. 88, 893–899.
Poddevin, N., Marois, Y., Cronier, B., Delagoutte, J.P., Mainard, D., Belanger, A.Y., King, M. W., Guidoin, R., 1995a. Rupture of current prostheses. A retrospective analysis of 89 surgically excised explants. Actualités En Biomatériaux 3, 313–326.
Poddevin, N., Marois, Y., Cronier, B., Delagoutte, J.P., Belanger, A.Y., King, M.W., Guidoin, R., 1995b. Prothèse du ligament croisé antérieur: importance de la structure textile pour assurer la biofonctionalité, la biocompatibilité et la biodurabilité. Actualité En Biomatériaux 3, 327–337.
Poddevin, N., Marois, Y., Cronier, B., Delagoutte, J.P., Maynard, D., Jaeger, J.H., Belanger, A. Y., King, M.W., Guidoin, R., 1995c. Macroscopic, histologic and ultrastructural study of 89 prostheses of anterior cruciate ligament excised because of prosthesis failure. Rev. Chir. Orthop. Reparatrice Appar. Mot. 81 (5), 410–418.
Poddevin, N., Kin, M.W., Guidoin, R.G., 1997. Failure mechanisms of anterior cruciate ligament prostheses: in vitro wear study. J. Biomed. Mater. Res. 38, 370–831.
Prodromos, C., Joyce, B., Shi, K., 2007. A meta-analysis of stability of autografts compared to allografts after anterior cruciate ligament reconstruction. Knee Surg. Sports Traumatol. Arthrosc. 15, 851–856.
Purchase, R., Mason, R., Hsu, V., Rogers, K., Gaughan, J.P., Torg, J., 2007. Fourteen-year prospective results of a high-density polyethylene prosthetic anterior cruciate ligament reconstruction. J. Long Term Eff. Med. Implants 17, 13–19.
Rading, J., Peterson, L., 1995. Clinical experience with the Leeds-Keio artificial ligament in anterior cruciate ligament reconstruction. A prospective two-year follow-up study. Am. J. Sports Med. 23, 316–319.
Rihn, J.A., Irrgang, J.J., Chhabra, A., Fu, F.H., Harner, C.D., 2006. Does irradiation affect the clinical outcome of patellar tendon allograft ACL reconstruction? Knee Surg. Sports Traumatol. Arthrosc. 14, 885–896.
Rodeo, S.A., Suzuki, K., Deng, X.H., Wozney, J., Warren, E.F., 1999. Use of recombinant human bone morphogenetic protein-2 to enhance tendon healing in a bone tunnel. Am. J. Sports Med. 27, 476–488.
Roe, J., Pinczewski, L.A., Russell, V.J., Salmon, L.J., Kawamata, T., Chew, M., 2005. A 7-year follow-up of patellar tendon and hamstring tendon grafts for arthroscopic anterior cruciate ligament reconstruction: differences and similarities. Am. J. Sports Med. 33, 1337–1345.
Rubenstein, D.L., Sarin, G., Subbio, C., Miller, L.S., 1998. Revision of failed Gore-Tex anterior cruciate ligament reconstruction. Oper. Tech Sports Med. 6 (2), 97–101.

Saddemi, S.R., Frogameni, A.D., Fenton, P.J., Hartman, J., Hartman, W., 1993. Comparison of perioperative morbidity of anterior cruciate ligament autografts versus allografts. Arthroscopy 9, 519–524.

Sahoo, S., Ouyang, H., Goh, J.C., Tay, T.E., Toh, S.L., 2006. Characterization of a novel polymeric scaffold for potential application in tendon/ligament tissue engineering. Tissue Eng. 12, 91–99.

Sajovic, M., Vengust, R., Komadina, R., Tavcar, R., Skaza, K., 2006. A prospective randomized comparison of semitendinous and gracilis tendon versus patellar tendon autografts for anterior cruciate ligament reconstruction: five-year follow-up. Am. J. Sports Med. 34, 1933–1940.

Salehpour, A., Butler, D.L., Proch, F.S., Schwartz, H.E., Feder, S.M., Doxey, C.M., Radcliffe, A., 1995. Dose-dependent response of gamma irradiation on mechanical properties and related biochemical composition of goat bone-patellar tendon-bone allografts. J. Orthop. Res. 13, 898–906.

Savarese, A., Lunghi, E., Budassi, P., Agosti, A., 1993. Remarks on the complications following ACL reconstruction using synthetic ligaments. Ital. J. Orthop. Traumatol. 19, 79–86.

Scavenius, M., Hansen, S., Bak, K., Norring, K., Jensen, K.H., Jorgensen, U., 1999. Isolated total ruptures of the anterior cruciate ligament – a clinical study with long-term follow-up at 7 years. Scand. J. Med. Sci. Sports 9, 114–119.

Schepsis, A.A., Greenleaf, J., 1990. Prosthetic materials for anterior cruciate ligament reconstruction. Orthop. Rev. 19, 984–991.

Schiavone Panni, A., Denti, M., Franzee, S., Monteleone, M., 1993. The bone-ligament junction: a comparison between biological and artificial ACL reconstruction. Knee Surg. Sports Traumatol. Arthrosc. 1, 9–12.

Schutte, M.J., Dabezies, E.J., Zimny, M.L., Happel, L.T., 1987. Neural anatomy of the human anterior cruciate ligament. J. Bone Joint Surg. Am. 69, 243–247.

Seedhom, B.B., 1988. Concepts and mechanical aspects of the Leeds-Keio ligament. In: Presented at the Fifth International Symposium on Cruciate Ligament Reconstruction of the Knee, Palm Springs, Calif.

Shelbourne, K.D., Nitz, P., 1990. Accelerated rehabilitation after anterior cruciate ligament reconstruction. Am. J. Sports Med. 18, 292–299.

Shelbourne, K.D., Vanadurongwan, B., Gray, T., 2007. Primary anterior cruciate ligament reconstruction using contralateral patellar tendon autograft. Clin. Sports Med. 26, 549–565.

Shiavi, R., Limbird, T., Borra, H., Edmondstone, M.A., 1991. Electromyography profiles of knee joint musculature during pivoting: changes induced by anterior cruciate ligament deficiency. J. Electromyogr. Kinesiol. 1, 49–57.

Sledge, S.L., Steadman, J.R., Silliman, J.F., et al., 1992. Five-year results with the Gore-Tex anterior cruciate ligament prosthesis. Am. J. Knee Surg. 5, 65–70.

Sonnery-Cottet, B., Chambat, P., 2006. Anatomic double bundle: a new concept in anterior cruciate ligament reconstruction using the quadriceps tendon. Arthroscopy 22, 1249.e1–1249.e4.

Spalazzi, J.P., Doty, S.B., Moffat, K.L., Levine, W.N., Lu, H.H., 2006. Development of controlled matrix heterogeneity on a triphasic scaffold for orthopedic interface tissue engineering. Tissue Eng. 12, 3497–3508.

Spalazzi, J.P., Dagher, E., Doty, S.B., Guo, X.E., Rodeo, S.A., Lu, H.H., 2008a. In vivo evaluation of a multiphased scaffold designed for orthopaedic interface tissue engineering and soft tissue-to-bone integration. J. Biomed. Mater. Res. 86, 1–12.

Spalazzi, J.P., Vyner, M.C., Jacobs, M.T., Moffat, K.L., Lu, H.H., 2008b. Mechanoactive scaffold induces tendon remodeling and expression of fibrocartilage markers. Clin. Orthop. Relat. Res. 466, 1938–1948.
Steadmann, J.R., Seeman, M.D., Hutton, K.S., 1995. Revision ligament reconstruction of failed prosthetic anterior cruciate reconstruction. Instr. Course Lect. 44, 417–429.
Stone, K.R., Abdel-Motal, U.M., Walgenbach, A.W., Turek, T.J., Galili, U., 2007. Replacement of human anterior cruciate ligaments with pig ligaments: a model for Anti-Non-Gal antibody response in long-term xenotransplantation. Transplantation 83, 211–219.
Strocchi, R., De Pasquale, V., Gubellini, Facchiri, A., Maracci, M., Buda, R., Zaffagnini, S., Ruggeri, A., 1992. The human anterior cruciate ligament: histological and ultrastructural observations. J. Anat. 180, 515–519.
Sugihara, A., Fujikawa, K., Watanabe, H., Murakami, H., Kikuchi, T., Tsukazai, S., Aloki, Y., Matsu Naga, M., Nemoto, K., 2006. Anterior cruciate reconstruction with bioactive Leeds-Keio ligament (LK II): preliminary report. J. Long Term Eff. Med. Implants 16, 41–49.
Sun, K., Tian, S., Zhang, J., Xia, C., Zhang, C., Yu, T., 2009. Anterior cruciate ligament reconstruction with BPTP autograft, irradiated versus non-irradiated allograft: a prospective randomized clinical study. Knee Surg. Sports Traumatol. Arthrosc. 17, 464–474.
Talbot, M., Berry, G., Fernandes, J., Ranger, P., 2004. Knee dislocation: experience at the Hopital du Sacre-Cœurde Montreal. Can. J. Surg. 47, 20–24.
Tarachand, V., 1990. A retrospective study of the ABC ligament for chronic instability of the knee. MCh(Orth)Thesis, University of Liverpool.
Tischer, T., Vogt, S., Aryee, S., et al., 2007. Tissue engineering of the anterior cruciate ligament: a new method using acellularized tendon allografts and autologous fibroblasts. Arch. Orthop. Trauma Surg. 127, 735–741.
Tsai, K.J., Chiang, H., Jiang, C.C., 2004. Magnetic resonance imaging of anterior cruciate ligament rupture. BMC Musculoskeletal Disord 5, 21.
von Recum, A.F., 1986. Handbook of Biomaterials Evaluation: Scientific, Technical and Clinical Testing of Implant Materials. Macmillan, New York.
Vunjak-Novakovic, G., Altman, G., Horan, R., Kaplan, D.L., 2004. Tissue engineering of ligaments. Annu. Rev. Biomed. Eng. 6, 131–156.
Wang, K., Zhu, L., et al., 2008. Artificial biological ligament: it making, testing, and experimental study on animals. Microsurgery 28 (1), 44–53.
West, R.V., Harner, C.D., 2005. Graft selection in anterior cruciate ligament reconstruction. J. Am. Acad. Orthop. Surg. 13, 197–207.
Wilk, R.M., Richmond, J.C., 1993. Dacron ligament reconstruction for chronic anterior cruciate ligament insufficiency. Am. J. Sports Med. 21, 374–380.
Williams, G.N., Snyder-Mackel, L., Barrance, P., Axe, M.J., Buchanan, T.S., 2005. Neuromuscular function after anterior cruciate ligament reconstruction with autologous semitendinosus-gracilis graft. J. Electromyogr. Kinesiol. 15, 170–180.
Woo, S.L.-Y., Buckwalter, J.A., 1988. Injury and repair of the musculoskeletal soft tissues. J. Orthop. Res. 6, 907–931.
Woo, S.L.Y., Jia, F., Zou, L., Gabriel, M.T., 2004. Functional tissue engineering for ligament healing: potential of antisense gene therapy. Ann. Biomed. Eng. 32, 342–351.
Yagi, M., Wong, E.K., Kanamori, A., Debski, R.E., Fu, F.H., Woo, S.L., 2002. Biomechanical analysis of an anatomic anterior cruciate ligament reconstruction. Am. J. Sports Med. 30, 660–666.
Yahia, L., 1997. Ligaments and Ligamentoplasties. Springer, Berlin, Heidelberg.

Yamazaki, S., Yasuda, K., Tomita, F., et al., 2002. The effect of graft-tunnel diameter disparity on intraosseous healing of the flexor tendon graft in anterior cruciate ligament reconstruction. Am. J. Sports Med. 30 (4), 498–505.

Yamazaki, S., Yasuda, K., Tomita, F., Minami, A., Tohyama, H., 2006. The effect of intraosseous graft length on tendon-bone healing in anterior cruciate ligament reconstruction using flexor tendon. Knee Surg. Sports Traumatol. Arthrosc. 14, 1086–1093.

Zantop, T., Brucker, P.U., Vidal, A., Zelle, B.A., Fu, F.H., 2007. Intraarticular rupture pattern of the ACL. Clin. Orthop. Relat. Res. 454, 48–53.

Zelle, B.A., Beasley, L.S., Fu, F.H., 2005a. The envelope of function in anterior cruciate ligament injuries. Oper. Tech. Orthop. 15, 86–88.

Zelle, B.A., Latterman, C., Chhabra, A., Fu, F.H., Huard, J., 2005b. Biological considerations of tendon graft incorporation within the bone tunnel. Oper. Tech. Orthop. 15, 36–42.

Index

Note: Page numbers followed by *f* indicate figures and *t* indicate tables.

C